Determination of Volatile Metabolites of Fecal Contaminants in Water Samples by Differential Mobility Spectrometry

Dissertation

zur Erlangung des akademischen Grades eines
Doktors der Naturwissenschaften
– Dr. rer. nat. –

vorgelegt von

Lena Ganda Saptalena

geboren in Bandung, Indonesien

Fakultät für Chemie
der
Universität Duisburg-Essen

2014

Die vorliegende Arbeit wurde im Zeitraum von März 2009 bis Januar 2014 im Arbeitskreis von PD Dr. Ursula Telgheder an der Fakultät für Chemie der Universität Duisburg-Essen durchgeführt.

Tag der Disputation: 10.04.2014

Gutachter: PD Dr. Ursula Telgheder
Prof. Dr. Karl Molt

Vorsitzender: Prof. Dr. Christian Mayer

Kurzfassung

Escherichia coli und Coliforme werden traditionell als Indikatororganismen für fäkale Kontamination in Wasser verwendet. Aufgrund des anhaltenden Ausbruchs von *E. coli*, besteht dringender Bedarf, alternative Methoden zu entwickeln, die die Bakterien zeitnah und präzise detektieren und identifizieren können. Bisher verfügbare Standardmethoden benötigen einen hohen Zeitaufwand ($18 - 48\ h$).

In dieser Studie wurde ein empfindliches und schnelles Verfahren für den Nachweis von coliformen und *E. coli* Bakterien entwickelt. Das Verfahren ist eine Kombination aus einer enzymatischen und einer analytischenMethode. Die enzymatische Methode basiert auf der modernen Taxonomie von Coliformen und *E. coli*, in dem das Vorhandensein / Nichtvorhandensein von Coliformen und *E. coli* Bakterien werden über die Anwesenheit / Abwesenheit der Enzyme B-Galaktosidase bzw. B-Glucuronidase bestimmt.

Die Analysemethode basiert auf der Kopplung von GC mit Differential Mobility Spectrometry betrieben werden. Anhand der Fingerprintanalyse ausgewählter flüchtiger Metaboliten wurde die Leistungsfähigkeit der Analysentechnik überprüft. Aus dem Head-space von Standard-Lösungen wurden ausgewählte Substanzen (2,5-Dimethyltetrahydrofuran, Dimethyldisulfid, 2-Heptanon, 2,5-Dimethylpyrazin, Benzaldehyd, Dimethyltrisulfid, 2-Nonanon, Nonanal, Decanal, 2-Undecanon, Indol und 2-Tridecanon), die als Metaboliten von *E. coli* in der Literatur beschrieben werden, bestimmt. 2-Undecanon, Indol und 2-Tridecanon konnten aufgrund der relativ geringen Flüchtigkeit nicht detektiert werden.

Weiterhin wurden die experimentellen Parameter optimiert. Die Hochfrequenz-(RF-) Spannung beeinflusst die Peaktrennung und Signalintensität. Je höher die RF-Spannung, desto besser werden die Signale getrennt. Allerdings nimmt die Signalintensität ab; $1200V$ (entspricht $24\ kV\ /\ cm$) wurde als die optimale HF-Spannung für die Detektion der oben genannten Verbindungen festgelegt.

Ein wichtiger experimenteller Parameter ist die Wahl des geeigneten Nährmediums. Folgende Nährmedia wurden verwendet: Colilert-18®, Glucose-Brühe, M9-Medium, tryptische Sojabrühe (TSB) und Tryptophan Brühe. Als optimal stellte sich Colilert-18 ®-Medium heraus, da bei dessen Verwendung für *E. coli* spezifisch o-Nitrophenol (ONP)

freigesetzt wird, welches mit GC-DMS empfindlich nachweisbar ist. Die Validierung erfolgte mit Gaschromatographie - Massenspektrometrie (GC-MS)-Analyse.

Um die Analysenzeit zu verkürzen, wurden *E. coli* DSM 30083 Bakterien in Colilert-18® unter verschiedenen Inkubationszeiten gezüchtet. Nach 2,5 Stundenerfolgte die Spaltung von ONPG durch das Enzym B-Galactosidase. Nach dieser Zeit war es möglich, o-Nitrophenol aufgrund der hohen Nachweisempfindlichkeit mittels GC-DMS zu detektieren. Das Signal erscheint bei einer Retentionszeit von $t_r = 184.9\ s$ und Kompensationsspannungen von $C_{v,1} = -2.82\ V$ (im positiven Modus) und $C_{v,2} = -4.09\ V$ (im negativen Modus).

Die Nachweis- und Bestimmungsgrenzen für die Bestimmung von o-Nitrophenol wurde mit dem Kalibrierverfahren nach DIN 32645 zu 45 ng (pos. Mode) und 49 ng (neg. Mode) berechnet.

Da die gebildete Menge von der Konzentration der *E. coli* Bakterien in den Proben abhängt, wurde eine Korrelation zwischen der *E. coli*-Konzentration und der Signalintensität für o-Nitrophenol bestimmt. Nach 2,5 h Inkubationszeit wurden $\mathbf{3.37 \times 10^7}$ bzw $\mathbf{3.21 \times 10^7} E.coli - Zellen\ /\ ml$ erhalten.

Um die Leistungsfähigkeit der entwickelten Methode zu untersuchen, wurden für die Differenzierung von *E. coli* von anderen *E. coli* und von anderen Bakterien 5 Arten von Bakterien in Colilert-18® für $3\ Stunden$ gezüchtet und die gasförmigen Metabolitemittels GC-DMS analysiert.

Als Bakterien wurden (1) *E. coli* DSM 30083, (2) *E. coli* DSM 1576, (3) *E. coli* RV, (4) *K. pneumoniae* (ein coliform Bakterien), und *P. aeruginosa* (ein nicht-coliforme Bakterien) ausgewählt. Basierend auf der Anwesenheit / Abwesenheit von ONP konnte *E. coli* und *K. pneumoniae* von *P. aeruginosa* unterschieden werden.

Basierend auf der Intensität des ONP-Signals und der endgültigen Zellkonzentration konnte *E. coli* von *K. Pneumonie* unterschieden werden. Mit der entwickelten Methode ist es jedoch nicht möglich, den Unterschied zwischen einzelnen *E. coli*-Stämmen zu unterscheiden.

Um die Wirkung von saisonalen Einflüssen im Feld zu überprüfen (z. B. Änderung der Wassertemperatur) wurde die Inkubationstemperatur variiert. Wie erwartet, wurde bei einer Temperatur von $36\ °C$ ein maximales Zellwachstum beobachtet.

Abschließend wurde ein Algorithmus zur Detektion und Identifizierung von *E. coli* und Coliformen dargestellt. Mit der entwickelten Methode können die Zielorganismen erheblich schneller als mit bestehenden Methoden identifiziert werden. Somit ist ein hohes Potenzial für den Einsatz vor Ort gegeben. Einschränkend ist die relativ hohe Nachweisgrenze, die durch Verwendung von Mikroextraktionstechniken als Anreicherungsmethode verbessert werden könnte.

Summary

Escherichia coli and coliform are traditionally used as indicator organisms for fecal contamination in water. Due to persistence outbreak of *E. coli,* there is an urgent need to develop a method that could detect the bacteria in timely and accurate manners. The main limitation of standard and alternative methods is the time to obtain the result ($18 - 48\ h$). An analysis time exceeding one day is often too slow for authorities to take a rapid response in case of an outbreak. There are emerging analytical methods which are relatively faster, but most existing analytical methods have some technical limitations, such as the need for vacuum, the need for oven, and the size of the analytical instruments which are not practical for on-site applications.

In this study, a method for rapid detection and identification of coliform and *E. coli* bacteria was developed. The method is a combination of **enzymatic** and **analytical** methods. The **enzymatic** method was built upon the modern taxonomy of coliform and *E.* coli, in which the presence/ absence of **coliform** and ***E. coli*** is characterized by the presence/absence of **β-galactosidase** and **β-glucuronidase** enzymes, respectively. As *E. coli* is also a type of coliform, the presence of *E. coli* is indicated by the presence of both enzymes. The **analytical** method employed the use of microAnalyzer™ (a miniaturized Gas Chromatography – Differential Mobility Spectrometry (GC-DMS) system), which is an advanced gas detector that requires a low power consumption, has a built-in GC system, compact, portable, and could be operated using ambient pressure. Differential mobility spectrometry (DMS) is an ambient pressure ion-separation technique that characterizes chemical substances using differences in the gas phase mobility of ions in alternating strong and weak electric fields that are generated using a high frequency asymmetric waveform.

In this study, at first the performance of GC-DMS in the detection of volatile metabolite compounds released by *E. coli* was investigated through "finger-print" recognition analysis. Twelve compounds known to be metabolites of *E. coli* (2,5-dimethyltetrahydrofuran, dimethyl disulfide, 2-heptanone, 2,5-dimethylpyrazine, benzaldehyde, dimethyl trisulfide, 2-nonanone, nonanal, decanal, 2-undecanone, indole, and 2-tridecanone) were prepared from standard solutions and the headspace gases were analyzed by GC-DMS. It was found that the last three compounds (which have relatively low volatility) could not be detected by the GC-DMS. This study, however, revealed the effect of radio-frequency (RF) voltage on the

peak separation and signal intensity: the higher the RF voltage, the better the separation among the peaks, but the poorer the signals intensity; $1200\ V$ (corresponds to $24\ kV/cm$) was found to be an optimum RF voltage for the aforementioned compounds.

As the type and composition of metabolites released by bacteria are determined by many factors (such as the type of growth medium, the temperature of growth, and cell age), the study was continued by the determination of suitable growth medium, i.e. a medium which could stimulate *E. coli* in producing either unique "finger-print" compounds or unique biomarker compounds, which could be detected by the miniaturized GC-DMS. Five media commonly used to grow *E. coli* were examined: **Colilert-18®, glucose broth, M9-medium, tryptic soy broth (TSB)** and **tryptophan broth**. It was found that unlike all other four media, **Colilert-18®** medium stimulated *E. coli* growth in a way that it produced a unique biomarker, namely *o*-nitrophenol (**ONP**), and this biomarker was detectable by the GC-DMS. The finding was confirmed by gas chromatography – mass spectrometry (GC-MS) analysis. Colilert-18® contains ortho-Nitrophenyl-β-galactoside (**ONPG**) and 4-methylumbelliferyl-β-D-glucoronide (**MUG**) substrates. In the presence of ONPG substrate, **β- Galactosidase** enzyme in ***E. coli* and coliform** is activated and helped the hydrolysis of ONPG into β-D-Galactose and ***o*-nitrophenol**. In standard Colilert-18® test, due to its appearance, *o*-nitrophenol (which is a yellow crystalline solid) is usually used as a chromogenic indicator which confirms the absence/ presence of coliform. In the presence of the **MUG** substrate, **β-Glucuronidase** enzyme in *E. coli* is supposed to be activated and helped the hydrolysis of MUG into β-D-Glucuronate and **methylumbelliferone**. However, headspace analysis of *E. coli* metabolites by GC-DMS and GC-MS analysis performed in this work only detected and identified the presence of ***o*-nitrophenol**, not of **methylumbelliferone**, due to the poor volatility of methylumbelliferone**.** Therefore, up to this particular point, the developed method was able to detect and identify coliforms including *E. coli*, but not able to distinguish *E. coli* from other coliforms. To distinguish *E. coli* from non - *E. coli*, a standard Colilert-18® test which involved the viewing of the sample under a $365\ nm$, $6\ Watt$ fluorescent UV lamp was needed; the presence of *E. coli* was indicated by a blue fluorescence effect.

The time to perform standard Colilert-18® test is usually between 18 and $24\ h$, which is the main limitation of the method. To shorten the analysis time, *E. coli* DSM 30083 bacteria were grown in Colilert-18® under **various incubation periods**. It was found that the cleavage

opening (the cleaving of ONPG by β-galactosidase enzyme) took approximately $2.5\ h$, as indicated by the presence of *o*-nitrophenol which could be detected by the GC-DMS after *E. coli* was incubated for just $2.5\ h$. This means, the analysis time is 7 to 9 times faster than the standard Colilert-18® test. This is because the GC-DMS could detect a very low amount of *o*-nitrophenol despite the subtle or insignificant color change of the chromogenic indicator in the sample. Signal peak of *o*-nitrophenol was detected by the GC-DMS at both positive and negative ion channels of the DMS detector. The signal appeared at a retention time of $t_r = 184.9\ s$ and compensation voltages of $C_{v,1} = -2.82\ V$ (in the positive mode) and $C_{v,2} = -4.09\ V$ (in the negative mode). GC-DMS system has three-dimensional data; it consists of: (1) retention time and (2) compensation voltage(s) which are unique to compounds' identity, and (3) signal intensity. Unlike similar spectrometry methods, the difference in retention times of compound signals in GC-DMS could be very small (a matter of seconds instead of minutes), and compounds could still be differentiated based on their unique compensation voltages. Overall, the work in this section showed that compared to the already shortened incubation period ($2.5\ h$), the GC-DMS retention time ($184.9\ s$) is much shorter. Hence, the analysis time using GC-DMS does not affect much the overall analysis time, which is excellent.

Detection limit of *o*-nitrophenol was determined by calibrating mass of *o*-nitrophenol standard against signal intensity using DIN 32645 method. Detection limits of $\mathbf{45.11\ nanogram}$ and $\mathbf{48.85\ nanogram}$ of *o*-nitrophenol were obtained for the positive and negative modes of the detector, respectively. As the amount of *o*-nitrophenol is a dependent variable (the amount of *o*-nitrophenol in the headspace depends on the concentration of *E. coli* in the samples), concentration of *E. coli* was calibrated against signal intensity. When *E. coli* was incubated for $2.5\ h$, detection limits of **initial** concentration of *E. coli* (concentration level before *E. coli* was incubated) of $\mathbf{3.37 \times 10^7}$and $\mathbf{3.21 \times 10^7 cells/ml}$ were obtained for the positive and negative modes, respectively. As *E. coli* growth curve showed the increase of final concentration of *E. coli* with respect to incubation period, it is concluded that the limit of initial concentration could be decreased if the incubation period is increased.

To investigate the performance of the developed method in the differentiation of *E. coli* from other *E. coli* and from other bacteria, 5 types of bacteria were grown in Colilert-18® for

$3\ h$ and the metabolite gases were analyzed by GC-DMS. These bacteria were (1) ***E. coli* DSM 30083**, (2) ***E. coli* DSM 1576**, (3) ***E. coli* RV**, (4) ***K. pneumonia*** (a coliform bacteria), and ***P. aeruginosa*** (a non-coliform bacteria). Based on the presence/absence of ONP, *E. coli* and *K. pneumoniae* could be distinguished from *P. aeruginosa*. Based on the intensity of ONP and the final cell concentration, *E. coli* could be distinguished from *K. pneumonia*. The method, however, could not distinguish the difference of *E. coli* from one strain to another.

To anticipate the effect of seasonal variation in practical application, e.g. change in water temperature, the effect of sample preheating temperature (i.e. incubation temperature) variation was investigated. It was found that the sample should be incubated at $36\ ℃$ to accommodate maximum cell growth and signal intensity.

From the overall finding, an algorithm to detect and identify *E. coli* and coliform was presented. Overall, the developed method was significantly faster than existing methods, was able to differentiate target organisms from non-target organisms, and is potential for on-site application. The main limitation is the relatively high detection limit, which could be improved by improving the sample enrichment technique using membrane filtration technique, and by improving the sample extraction and introduction methods. Nevertheless, to the author's knowledge, the method developed in this work is the first reported application of miniaturized (portable) GC-DMS technology for headspace analysis of volatile metabolite biomarkers in conjugation to enzymatic approach using a defined substrate media and the first one which is applied for the detection and identification of fecal contaminant in water samples.

Acknowledgments

My greatest thank goes to my research supervisor, PD Dr. Ursula Telgheder, for her invaluable support, guidance, patience, and time she has been giving me. Her extraordinary support guided me throughout the period of my study. I would also like to sincerely thank Prof. Dr. Torsten C. Schmidt (the chairman of IAC, UDE) for all opportunities and support he has been giving me, which has enabled me to do PhD at the IAC.

I would like to sincerely thank my dissertation committee, PD Dr. Ursula Telgheder, Prof. Dr. Karl Molt and Prof. Dr. Christian Mayer, for their time and feedback on the dissertation and the final examination. I am very thankful to them that my final examination went smooth.

I am very thankful to Dr. Andriy Kuklya and Dr. Klaus Kerpen for their great help and support especially during the analytical part of my work in the IMS lab, which covered not just fruitful insight into the scientific aspect, but also technical (troubleshooting) aspect of the experimental work. I am very thankful to Mr. Robert Marks who has given me kind assistance in the experimental work. I would also like to extend my thanks to everyone in the IAC working group, past and present (especially Mr. Gerd Fischer, Mrs. Lydia Vassen, Mr. Robert Knierim, Mrs. Claudia Ulrich, Mr. Holger Lutze, Mr. Joerg Eltfeld, Mrs Xolelwa Lamani, Mr. Ahmed Deeb, and Mr. Alexander Ewert for their help in administrative matter, daily life, and/or experimental work), and indeed everyone in the department, for their help and support. I would also like to acknowledge Mr. Schumann (the Schumann Analytics) for the consultation in using the microAnalyzer™ instrument and the IGOR software.

I would like to sincerely thank many people in the Biofilm Center, UDE, especially Prof. Dr. Hans-Curt Flemming for allowing me to use the microbiology lab and providing me the necessary infrastructure for the microbiological aspect of my research, Dr. Jost Wingender for his very important and fruitful comments and expertise guidance during the work, and Mrs. Astrid Dannehl for her kind support, especially for the practical aspect of my experiment in the lab, without with I would not have been able to do the experimental work.

I am extremely thankful to Prof. Dr.-Ing. Ramchandra Bhandari for his unwavering support that enables me to finish my master and PhD degrees. Without his incredible help and supports in many aspects of my life, things would just have gone the way of so many other unaccomplished good intentions.

I would like to thank Prof. Dr. Hartmut Gaese, Prof. Dr. Lars Ribbe, Prof. Dr. Michael Sturm, Prof. Dr. Jackson Roehrig, Dr. Nicole Kretschmer, Mrs. Karola Schmelzer, Mrs. Simone Sandholz, Mr. Andreas Bohler, Dr. Maxime Souvignet, Mr. Joern Trappe, and Mrs. Ina Keggenhof for their kind support during the period of my master course at ITT FH-Köln.

I would like to thank Mr. Qomarul Arifin, Mr. Nurul Huda, Mr. Hideyuki Yamazawa, Mr. Ikuhiro Kato, Mrs. Mutia Leflina Anshar, Mr. Baha Siahaan, and Mr. Dedy Sulin for their support during my work in PT Keihin Indonesia. I would like to thank Prof. Dr. I Gede Wenten (the Membrane Research Center, PPAU Bioteknologi ITB, Indonesia), as well as Mr. Ketut Wiguna and Mrs. Indah Susanthi, for their support and encouragement during the early career of my life. I would also like to thank many people in the Institut Teknologi Bandung, Indonesia, especially my academic supervisors, Prof. Dr. Yazid Bindar and Dr. Isdiriayani Nurdin, who have helped me to pursue my advanced degrees in Germany. I am also thankful to Prof. Tjandra Setiadi who gave me an opportunity to work in his project shortly after I graduated from the university.

The *Bundesministerium für Bildung und Forschung* (BMBF) is gratefully acknowledged for their financial support in form of International Postgraduate Studies in Water Technologies (IPSWaT) scholarships, which enable me to attain master and doctoral degrees in Germany. I would like to especially thank the IPSWaT scholarship managers (past and present): Dr. Cornelia Parisius, Mrs. Sara Sabzian, Prof. Dr. Ulrike Schaub, and Mrs. Gabriella Al-Khinli.

I would like to thank my friends, especially Dessy, Sveta, Beatrix, Fauzan, Hanim, Dadang, Noni, Hesty, Osmond, Mbak Yul, Gita, and Mbak Eva for their kind support and cheerful companion during the PhD period. Finally, unlimited thanks and love are given to my mum, my dad, my sister (Lani) and my brothers (Agung and Wisnu) in Indonesia for their love and support throughout my life journey.

Essen, 29.01.2014

Lena Ganda Saptalena

Table of Contents

List of Abbreviations

AFNOR	*Association Française de Normalisation*
APHA	*American Public Health Association*
API	*Analytical Profile Index*
ATCC	*American Type Culture Collection*
CV	*Compensation Voltage*
DAPI	*4′,6′-diamidino-2-phenylindole*
DC	*Direct Current*
DIN	*Deutsches Institut für Normung*
DMS	*Differential Mobility Spectrometry*
DNA	*Deoxyribonucleic acid*
DSM	*Deutsche Sammlung von Mikroorganismen*
DSMZ	*Deutsche Sammlung von Mikroorganismen und Zellkulturen*
ECA	*Enterobacterial Common Antigen*
E. coli	*Escherichia coli*
EC	*European Commission*
ECDC	*European Centre for Disease Prevention and Control*
EEC	*European Economic Community*
EFSA	*European Food Safety Authority*
ELISA	*Enzyme-linked Immunosorbent Assay*
Ent.	*Enterobacter*
Esch.	*Escherichia*
EU	*European Union*
FAIMS	*Field Asymmetric waveform Ion Mobility Spectrometry*
FISH	*Fluorescent In Situ Hybridization*
FC	*Fecal coliform*

GC	*Gas Chromatography*
GC-DMS	*Gas Chromatography – Differential Mobility Spectrometry*
GC-FID	*Gas Chromatography – Flame Ionization Detector*
GC-MS	*Gas Chromatography – Mass Spectrometry*
IBDG	*indoxyl-β-D-glucuronide*
IEA	*Immuno-enzyme Assay*
IFA	*Immunofluorescence Assay*
IMS	*Ion Mobility Spectrometry*
IMS	*Immunomagnetic Separation*
ISH	*In Situ Hybridization*
ISO	*International Organization for Standardization*
ISO/DIS	*International Organization for Standardization/ Draft International Standard*
K. oxytoca	*Klebsiella oxytoca*
K. pneumoniae	*Klebsiella pneumoniae*
LOD	*Limit of detection*
LOQ	*Limit of quantitation*
MCC-IMS	*Multi Capillary Column Coupled Ion Mobility Spectrometry*
MF	*Membrane Filter*
MI agar	*MUGal-IBDG (4-methylumbelliferyl-β-D-galactopyranoside - indoxyl-β-D-glucuronide) agar*
MPN	*Most Probable Number*
MS	*Mass Spectrometry*
MTBE	*Methyl Tertiary Butyl Ether*
m-TEC agar	*modified Thermotolerant Escherichia Coli agar*
MTF	*Multiple-Tube Fermentation*
MUG / MUGlu	*4-methylumbelliferyl-β-D-glucoronide*

MUGal	*4-methylumbelliferyl-β-D-galactopyranoside*
NB	*Nutrient Broth*
ONP	*o-Nitrophenol*
ONPG	*Ortho-Nitrophenyl-β-D-galactopyranoside*
PCR	*Polymerase Chain Reaction*
PNPG	*Para-Nitrophenyl-β-D-galactopyranoside*
RF	*Radio Frequency*
RNA	*Ribonucleic Acid*
rRNA	*Ribosomal Ribonucleic Acid*
Rt, RT	*Retention Time*
RV (in E. coli RV)	*Ring-Versuch*
Ser.	*Serratia*
SPC	*Solid-phase Cytometry*
spp. (in Pantoea spp.)	*Several species*
STEC	*Shiga toxin-producing E. coli*
STP	*Standard Temperature and Pressure*
TC	*Total Coliform*
tRNA	*Transfer Ribonucleic Acid*
TSA	*Tryptic Soy Agar*
TSB	*Tryptic Soy Broth*
TTC	*Triphenyl Tetrazolium Chloride*
US EPA	*United States Environmental Protection Agency*
UV	*Ultraviolet*
WHO	*World Health Organization*
X-Glu	*5-bromo-4-chloro-3-indolyl-β-D-glucuronide*
X-Gal	*5-bromo-4-chloro-3-indolyl-β-D-galactopyranoside*

List of Symbols

α	*Alpha-function (relative variation of K_0 depending on E/N)*[*)]
	[*)] *In Chapter 4, "α" refers to 'significance level' (a statistical parameter)*
b	*Intercept of calibration curve*
C_v	*Compensation voltage (V)*
d	*Drift length (cm)*
DC	*Direct current*
E	*Electric field strength (V/cm)*
f	*Degree of freedom*
K	*Mobility coefficient*[*)]
	[*)] *In Chapter 4, "k" refers to "relative uncertainty of the quantitation limit"*
K_H	*Mobility coefficient under high field condition*
K_L	*Mobility coefficient under low field condition*
K_0	*Reduced mobility*
$K_{H,inv}$	*Inverse Henry's constant (atm.m^3/mol)*
m	*gradient of calibration curve*
N	*Gas density (kg/m^3)* [*)]
	[*)] *In Chapter 4, "N" refers to "number of calibration measurement"*
$\widehat{N}$	*number of parallel calibration measurement*
p	*Pressure (atm)*
RF	*Radio frequency*
s_{x0}	*standard deviation of the method*
s_y	*rest standard deviation*
t	*Drift time (s)*
T	*Temperature (K)*
t_c	*Oscillation period (s)*
$t_{f,\alpha}$	*Student's t-value*

t_r	*Retention time (s)*
V_d	*Drift velocity for ions (m/s)*
V_{rf}	*RF voltage (V)*
x	*predictor variable/ independent variable/ regressor*
$\bar{x}$	*arithmetic mean value of* x_i
x_{LOD}	*limit of detection (German: "Die Nachweisgrenze")*
x_{LOQ}	*limit of quantitation (German: "Die Bestimmungsgrenze")*
y	*criterion variable/ response variable/ dependent variable*
$\bar{y}$	*arithmetic mean value of* y_i

List of Figures

List of Tables

1 General introduction

Partly reproduced from:

> *"Saptalena LG, Kerpen K, Kuklya A, Telgheder U. "Rapid detection of synthetic biomarkers of Escherichia coli in water using microAnalyzer: A field dependence study". International Journal for Ion Mobility Spectrometry **2012**;15:47"*

1.1 Background and motivation

Current practices of irrigation in many countries take a special care on water quality as shown by the establishment of national or regional water quality guidelines for irrigation. Despite the advanced approaches in the prevention of contamination of irrigation water by waterborne pathogens, severe outbreaks associated with the consumption of agricultural products still occur, even in the developed countries. As a recent example, an outbreak of Shiga toxin-producing *E. coli* (STEC) O104:H4 had occurred in Europe between May and July 2011, with the vast majority of cases reported by Germany. As per 8 July 2011, 44 out of 3774 infected people died because of the infections [1].

While the contamination path of microbial pathogens into agricultural products can be very complex, a continuous and real-time monitoring of the microbial quality of water used to irrigate the crops is an important and good agriculture practice. The detection of the source of an outbreak in a timely manner is necessary. To date, however, due to limited resources the monitoring practices of irrigation water quality in many countries are usually done only on a monthly or quarterly basis. In addition to that, the existing methods for the environmental monitoring of bacteria in water sample are typically labor- and time-consuming, especially because they usually involve culturing. Classical methods such as the membrane filtration (MF) and multiple-tube fermentation (MTF) methods or enzymatic method such as Colilert-18® needs at least 18 h to produce the results [2].

Studies over the past three decades have shown consistent evidence that various bacteria release different volatile organic compounds that can be profiled and used for their speciation [3, 4]. Several chemical detectors and assays are presently being refined for use in the identification of volatile byproducts of bacterial metabolism which are sufficiently

sensitive for analysis of volatile constituents in human breath as well as analysis of headspace above clinical cultures [4]. Some examples include: gas chromatography - flame ionization detection (GC-FID) analysis of volatile metabolites released by common lung pathogens, gas chromatography - mass spectrometry (GC-MS) analysis of volatile metabolites released by *Pseudomonas aeruginosa* and *E. coli*, gas chromatography - differential mobility spectrometry (GC-DMS) analysis of volatile metabolites released by *E. coli* and some other bacteria, and multi capillary column coupled ion mobility spectrometry (MCC-IMS) analysis of volatile metabolites released by *E. coli* [4-9].

The key challenges in using these methods are the technical complexities, such as the size of the analytical instruments, the need for vacuum, the need for oven and the high energy requirement which make them not suitable for field monitoring [4, 10]. In addition to that, these methods still require overnight culturing and, therefore, are time-consuming. There is a need in providing the method which could detect and identify volatile compounds released by bacteria in a rapid, sensitive, and simple ways, preferably based on a small and inexpensive detector [4, 10]. An example of such device is microAnalyzer™, which is a small, portable, oven-less gas detector, comprises of an integrated miniaturized GC-DMS system [11]. The DMS technology is developed based on a planar high-field asymmetric waveform ion mobility spectrometry (FAIMS) technique. The technology was first introduced in the literature by Buryakov et al. in 1993 [12]. To date the DMS technology has been applied in many areas, such as the detection of explosives [13], fire debris [14], environmental contaminants [15, 16], and bioorganisms [4, 17]. In those applications, DMS shows promise for on-site analysis because it is small, low cost, and sensitive [14].

In this study the miniaturized GC-DMS was used for the detection and identification of several fecal contaminants bacteria. This spectrometric method was combined with an enzymatic method, i.e. Colilert-18®.

1.2 Objectives

The general objectives of this study were to provide a method that could rapidly detect, identify, and quantify coliform and *E. coli* contaminants in environmental water samples using a combined approach (conjugation of spectrometric method using miniaturized GC-

DMS and enzymatic method using defined substrate media) and to optimize the method such that it could be practical for on-site, real-time monitoring of the microbial quality of the water samples. For those purposes the following specific objectives were formulated: (1) to review the existing methods available for the detection of coliform and *E. coli* and to review their advantages and limitations; (2) to investigate the performance of the miniaturized GC-DMS in the detection and characterization of typical volatile metabolite compounds released by the bacteria and to optimize the parameters affecting the performance; (3) to determine the suitable media for growing the bacteria and to characterize the volatile metabolite compounds released by the bacteria when they were grown in different media; (4) to determine the optimum incubation time needed for the production of volatile metabolite compounds which could be detected and characterized by the miniaturized GC-DMS; (5) to investigate the performance of the developed method in the differentiation of coliform and non-coliform bacteria; and (6) to develop an algorithm which could be used as an early warning system for the detection and identification of coliform and *E. coli* in practical application.

1.3 Fecal contamination indicators

Freshwaters contaminated by fecal discharges may transport a variety of pathogenic microorganisms. To protect public health, the detection of all waterborne diseases transported by such microorganisms is necessary. Various indicators of fecal contamination are usually used to detect fecal pollutions in many types of waters. Total coliforms (TC) and fecal coliforms (FC) are two major groups of fecal contaminants often used as the indicators. The TC group, however, do not necessarily indicate a health risk, because their presence may result from regrowth in the distribution system or from environmental sources [18-20]. The FC group or some other thermotolerant coliforms also represent a poor indicator of fecal contamination because some FC group members (such as species of the genera *Klebsiella* and *Enterobacter*) pose lack significance to human health [20]. *E. coli* is the only thermotolerant coliform which always originates from the intestine of human and warm-blooded animals and thus it is considered to be the preferred fecal contamination indicator due to its significance to human health [21, 22].

1.3.1 Definition of coliform and *E. coli* bacteria

The coliform group includes a broad diversity in terms of genus and species, whether or not they belong to the Enterobacteriaceae family [2]. There is no universal definition of coliform bacteria; it differs slightly depending on the country or on the organization in charge of the microbiological monitoring regulations. In *Standard Methods for the Examination of Water and Wastewater*, coliform bacteria are defined as:

- all aerobic and facultative anaerobic, Gram-negative, non-spore-forming, rod-shaped bacteria that ferment lactose with gas and acid formation within $48\ \mathrm{h}$ at $35\ ^{\circ}\mathrm{C}$ (multiple-tube fermentation technique); or
- all aerobic and many facultative anaerobic, Gram-negative, non-spore-forming, rod-shaped bacteria that developed a red colony with a metallic sheen within $24\ \mathrm{h}$ at $35\ ^{\circ}\mathrm{C}$ on an Endo-type medium containing lactose (membrane filter technique) [23].

AFNOR (1990) defines total coliforms (TC), including the thermotolerant coliforms and specifically *E. coli,* as:

- total coliforms (TC) are rod-shaped, non-spore-forming, Gram-negative, oxidase-negative, aerobic or facultative anaerobic bacteria that are able to grow in the presence of bile salts or other replacement surface active agents having an analogous growth inhibitory effect and that ferment lactose with gas and acid (or aldehyde) production within $48\ \mathrm{h}$ at $37 \pm 1\ ^{\circ}\mathrm{C}$
- thermotolerant coliforms have the same fermentation properties as total coliforms (TC) but at a temperature of $44 \pm 0.5\ ^{\circ}\mathrm{C}$
- *E. coli* is a thermotolerant coliform which, among other things, produces indole from tryptophane at a temperature of $44 \pm 0.5\ ^{\circ}\mathrm{C}$, gives a positive methyl red test result, is unable to produce acetyl–methyl carbinol and does not use citrate as its sole carbon source [2, 24].

The above traditional definitions of coliform and *E. coli* have been recently modified because, according to some studies, not all coliform bacteria can ferment lactose [25, 26]. Furthermore, some *E. coli* strains neither ferment lactose nor produce indole [26]. Advances

in molecular methods and sequencing have recently redesigned coliform taxonomy based on their enzymatic activities. In brief, the taxonomy can be described as [2, 23, 25, 27-30]:

- coliform bacteria are characterized by the presence of β-galactosidase enzyme
- *E. coli* is a coliform species which is also characterized by the presence of β-glucuronidase.

From the above classification it is clear that coliform bacteria are characterized by the presence of β-galactosidase enzyme, whereas *E. coli* is characterized by the presence of both β-galactosidase and β-glucuronidase enzymes. β-galactosidase is an enzyme which allows the hydrolysis of ortho-nitrophenil-β-galactopyranoside (ONPG) to the yellow-coloured *o*-nitrophenol. β-glucuronidase is an enzyme which catalyzes the hydrolysis of β-glucopyranosiduronic derivatives (such as -methyl-umbelliferyl-β-D-glucuronide (MUG)) into their corresponding aglycons and D-glucuronic acid.

1.3.2 Regulations and guidelines for monitoring of fecal contaminants

The use of the coliform group as an indicator of fecal contamination is usually subject to strict governmental regulations and their regulated level is usually varied according to the type of water uses. Regulations and guidelines for drinking water are usually stricter than for other uses. The German Drinking Water Directive, for example, limits the total coliform, *E. coli*, and *Enterococci* to $0/100$ ml [31]. The WHO (1994) and the US EPA (1990) also limit the total coliform and *E. coli* to $0/100$ ml [32, 33].

Unlike for drinking water, the guidelines for other types of waters, especially for irrigation water, are usually less strict. Around 70% of the water withdrawals at global level go for irrigation (UN Water, 2012) [34]. Because of its high consumption, agriculture can usually accept lower quality water than domestic and industrial users. Rising demands for good quality water for domestic and industrial uses in countries with highly developed economies have already created the necessity to reuse wastewater. Many developing countries are now facing a similar situation, especially in arid and semi-arid regions where limited water availability is already a severe constraint on development [35]. Reusing wastewater for irrigation has then become an option. The reuse of wastewater for agricultural practices is not an entirely new concept. Law (1968) cited 99 references on the use of sewage as an

agricultural water resource [35, 36]. Due to the public health hazard it may pose, some countries have developed standards for its safe use. In Germany, the quality requirement for irrigation water is regulated by the DIN 19650 (Table 1). These quality requirements refer to the hygienic/microbiological aspects of irrigation water in agriculture, gardening, landscaping as well as in parks and sport facilities. The hygienic safety of irrigation water is divided into 4 qualification classes which have to be verified for each intended use (refer to the excerpt of the DIN 19650 in Table 1) [37, 38].

1.3.3 Methods for the detection of fecal contaminants

There are several approved methods for the detection and identification of coliform and *E. coli* in water. In Germany, the method for detection and enumeration of coliform and specifically, *E. coli*, is regulated by the DIN ISO 9308-**1**:2012 (for water intended for human consumption, disinfected pool water and other waters with low bacterial numbers) [39] and DIN ISO 9308-**2**:2012 (for all other types of water except marine water; when used for the enumeration of *E. coli* in marine water, a $1 \rightarrow 10$ dilution in sterile water is required) [40]. The DIN ISO 9308-**1**:2012 method is based on membrane filtration (MF) technique, subsequent culture on a differential agar medium and calculation of the number of target organisms in the sample [39], whereas the DIN ISO 9308-**2**:2012 method is based on the growth of target organisms in a liquid medium and calculation of the Most Probable Number (MPN) of organisms by referencing to MPN tables [40]. In France, AFNOR has approved the multiple-tube fermentation (MTF) technique and the MF technique [2, 24]. In the USA (which is also adopted in Canada), the US EPA has also approved the MTF technique, the MF technique, and the presence/absence test (including the ONPG-MUG test).

Rompré et al. (2002) have reviewed these methods and other existing methods and grouped them into three categories: classical methods, enzymatic methods, and molecular methods [2]. The following sections summarize the review. Additional information from more recent studies is also discussed. In addition to the three categories, an additional category (namely spectrometric method), which is also the core of this research, is added. A specific section of the spectrometric method, i.e. the differential mobility spectrometry method, is presented and elaborated in a separate section.

Table 1. Hygienic/ microbiological qualification classes of irrigation water and their application according to DIN 19650, 1999 [37, 38]

Qualification class	Application	Faecel streptococci colonies/ 100 ml (according to the German Drinking Water Ordinance "TrinkwV" or EU Guidelines for Bathing Water [1])	*Escherichia coli* colonies/ 100 ml (according to the German Drinking Water Ordinance "TrinkwV" or EU Guidelines for Bathing Water [1])	Salmonellae colonies/ 1000 ml (according to DIN 38414-13)	Potentially infectious stages of human and pet parasites[2] in 1000 ml
1 (Drinking water)	All crops in greenhouses and on open land without restriction	Not detectable	Not detectable	Not detectable	Not detectable
2 [3]	Crops on open land and in greenhouses for raw consumption, schools sport fields, public parks	≤ 100 [4]	≤ 200 [4]	Not detectable	Not detectable
3 [3]	• Crops in greenhouses not intended for consumption • Crops on open land for raw consumption up to the fruiting stage or for vegetables up to 2 weeks prior to harvesting • Fruits and vegetables for conservation • Greenland or forage plants up to 2 weeks before cut or grazing • All other crops on open land without restriction • Other sport fields [5]	≤ 400	≤ 2000	Not detectable	Not detectable

Table 1 (*continued*). Hygienic / microbiological qualification classes of irrigation water and their application according to DIN 19 650, 1999 [37, 38]

Qualification class	Application	Faecel streptococci colonies/ 100 ml (according to the German Drinking Water Ordinance "TrinkwV" or EU Guidelines for Bathing Water [1)])	*Escherichia coli* colonies/ 100 ml (according to the German Drinking Water Ordinance "TrinkwV" or EU Guidelines for Bathing Water [1)])	Salmonellae colonies / 1000 ml (according to DIN 38414-13)	Potentially infectious stages of human and pet parasites[2)] in 1000 ml
4 [3), 5)]	• Wine and fruit cultures for rotection against frost • Forest, polder and wetlands • Sugar-beets, starch potatoes, oil fruits and nonfood plants for industrial processing and seeds up to two weeks prior to harvesting • Grain up to the germination phase (not intended for raw consumption) • Feed for conservation up to 2 weeks prior to harvesting	Wastewater which has undergone at least one biological treatment			• For intestinal nematodes: no standard recommendations are possible • For Taenia stages: not detectable

[1)] Microbiological surveys according to the methods applied for bathing water.

[2)] As far as it is necessary for the protection of the health of humans and animals, an examination of the irrigation water for intestinal nematodes (Ascaris and Trichuris species as well as hookworms) and/or life stages of tapeworms (especially Taenia) may be accommodated according to WHO recommendation.

[3)] If a wetting of the parts of the crop products which are appropriate for consumption is excluded, a restriction according to the hygienic / microbiological qualification classes may be dropped.

[4)] Guide value, below which measured values should lie, according to the German Drinking Water Ordinance TrinkwV § 2 Para 3 "as far as the state-of-the-art and a justifiable expenditure allow, taking into consideration each individual case".

[5)] In case of spray irrigation, it has to be ensured through protective measures that employees and the public are not at risk.

1.3.3.1 Classical methods

1.3.3.1.1 Multiple-tube fermentation technique

The MTF technique for the enumeration of coliform has been used for over 90 years as a water quality monitoring method. The method consists of inoculating a series of tubes with appropriate decimal dilutions of the water samples [2, 41]. The schematic outline of the procedure is given in Figure 1. The results of the MTF technique are expressed in terms of the MPN of microorganisms present. This number is a statistical estimate of the mean number of coliform in the sample [2, 23].

There are some advantages and disadvantages of the MTF technique. The technique is easy to implement and can be performed by a technician with basic microbiological training. It is relatively inexpensive as it requires unsophisticated laboratory equipment. It is especially useful when the conditions do not allow the use of the MF technique, such as turbid or colored waters. However, the technique is extremely time-consuming, requiring 48 h for presumptive results and necessitates a subculture stage for confirmation which could take up to a further 48 h. It can become very tedious and labor intensive since many dilutions have to be processed for each water sample. Some factors may also significantly affect the coliform bacteria detection, especially during the presumptive phase. Beside the interference by high numbers of non-coliform bacteria, the inhibitory nature of the media used in this technique has also been identified as factors contributing to underestimates of coliform abundance. Therefore, this technique lacks precision in qualitative and quantitative terms [2, 41, 42].

1.3.3.1.2 Membrane filter technique

The MF technique is fully accepted and approved as a procedure for monitoring drinking water microbial quality in many countries. This method consists of filtering a water sample on a sterile filter with a 0.45-μm pore size which retains bacteria, incubating this filter on selective media and enumerating typical colonies on the filter [2]. Many media and incubation conditions for the MF method have been tested for optimal recovery of coliforms from water samples [43, 44]. Among these, the most widely used for drinking water analysis are the Tergitol-TTC medium in Europe [24] and the m-Endo-type media in North America [23].

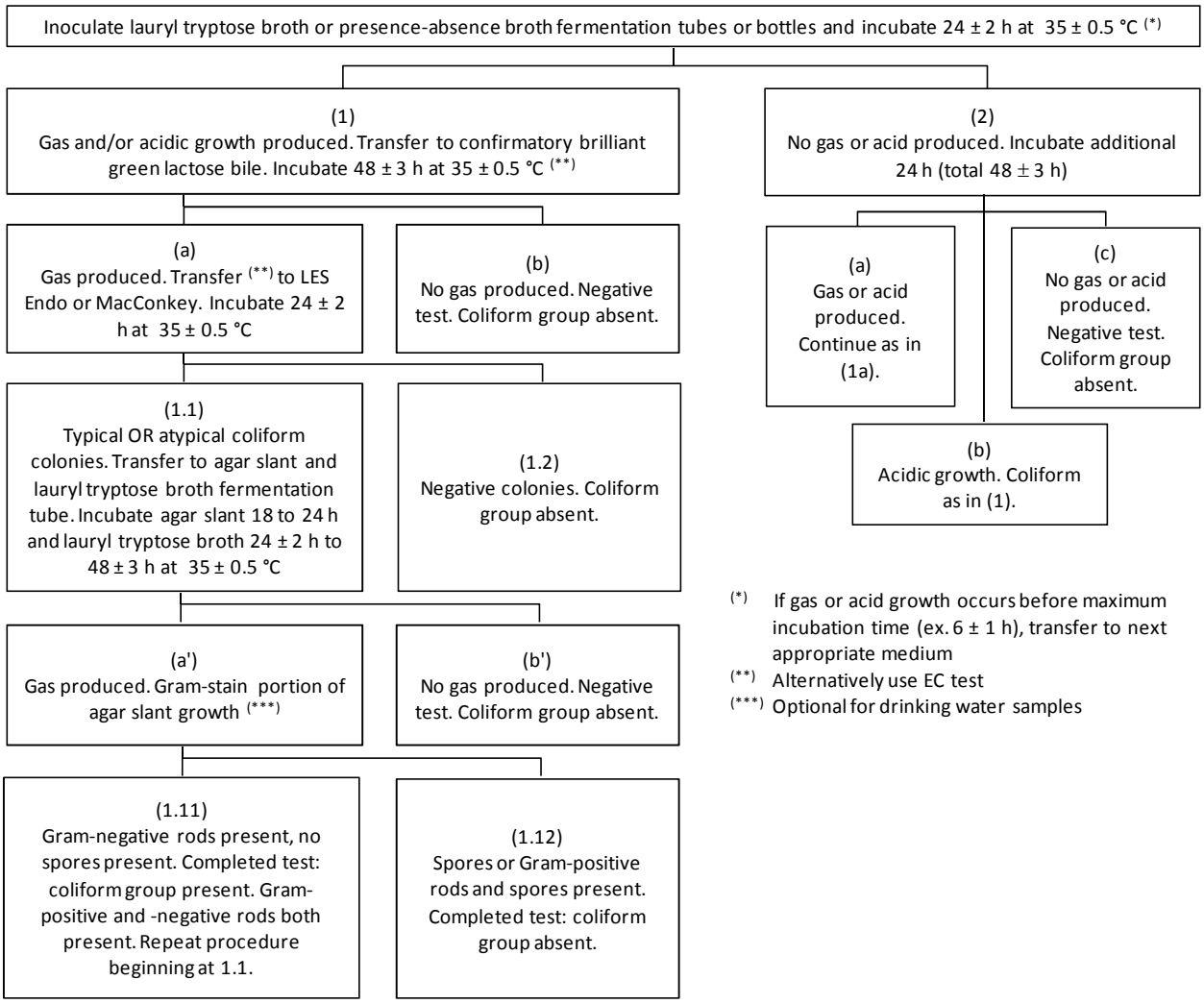

Figure 1. Schematic outline of coliform detection according to the Multiple-Tube Fermentation technique [41]

Coliform bacteria form yellow-orange colonies on Tergitol-TTC media (incubation 24 and 48 h at 37 and 44 °C for total coliform (TC) and fecal coliform (FC), respectively). When grown on an Endo-type medium containing lactose (incubation 24 h at 35 °C for TC), coliform bacteria form red colonies with a metallic sheen [2].

There are several advantages and disadvantages of the MF technique. Compared to other techniques such as MTF, MF enables the examination of larger volumes of water, which leads to greater sensitivity and reliability. MF also offers a quantitative enumeration comparatively to the semi-quantitative information given by MTF. MF is relatively simple to use and many samples can be processed in a day with limited laboratory equipment by a technician with basic microbiological training. However, MF is not sufficiently specific; a

confirmation stage is needed, which could take further 24 h after the first incubation period on selective media. The presence of high numbers of background heterotrophic bacteria was shown to decrease coliform recovery by MF [45, 46]. MF cannot recover stressed or injured coliform. Some improvements in the method have increased the detection of injured coliform bacteria, including the development of m-T7 medium formulated specifically for the recovery of stressed coliform in drinking water [47]. However, m-T7 may not be as efficient when stressing agents other than chlorine are involved [43] and other authors found that the m-T7 medium performed no better than the m-Endo medium in enumerating *E. coli* and *C. freundii* cells exposed to ozone [48]. Calabrese and Bissonnette (1990) reported an increase in coliform recovery on m-Endo and m-T7 media, as well as an increase in *E. coli* recovery on an m-FC medium when these media were supplemented with catalase, sodium pyruvate [49], or both [2, 50].

1.3.3.2 Enzymatic methods

The use of microbial enzyme profiles to detect indicator bacteria is an attractive alternative to classical methods, because enzymatic reactions are rapid and sensitive [2]. The use of the β-D-glucuronidase and β-D-galactosidase enzymes activities for the detection and enumeration of *E. coli* and TC, respectively, have been investigated by many studies for many years now and some of these studies are summarized here.

The activitity of β-D-galactosidase has been used mostly for enumerating the coliform group within the Enterobacteriaceae family. β-D-galactosidase catalyzes the breakdown of lactose into galactose and glucose. β-D-glucuronidase, on the other hand, has been used more specifically for enumerating *E. coli* coliform. β-D-glucuronidase catalyzes the hydrolysis of β-D-glucopyranosiduronic derivatives into their corresponding aglycons (non sugar compounds) and D-glucuronic acid. Although this bacterial enzyme was discovered first in *E. coli*, its relative specificity for identifying this microorganism was not apparent until Kilian and Bulow (1976) surveyed the Enterobacteriaceae and reported that glucuronidase activity was mostly limited to *E. coli* [2, 30]. The prevalence of this enzyme and its utility in the detection of *E. coli* in water were later reviewed by Feng and Hartman (1982) [29]. β-D-glucuronidase-positive reactions were observed in $94–96\%$ of the *E. coli* isolates tested [29, 30, 51, 52]. Other authors found a higher proportion of β-D-glucuronidase-negative *E. coli* (a

median of 15% from *E. coli* isolated from human fecal samples) [53]. In contrast, β-D-glucuronidase activity is less common in other Enterobacteriaceae genus, such as *Shigella* (44 to 58%), Salmonella (20 to 29%) and Yersinia strains and in Flavobacteria [29, 30, 54, 55].

1.3.3.2.1 Chromogenic and fluorogenic subtrates used in enzymatic methods

To detect the presence or absence of the activity of specific microbial enzymes, some chromogenic and fluorogenic substrates (which upon cleavage by a specific enzyme produce colour and fluorescence effect, respectively) have been used as indicators. Some authors have reviewed the use of chromogenic and fluorogenic substrates to detect the presence or activity of specific enzymes in aquatic systems [28], in bacterial diagnostics [56], and in foods [54].

To detect the presence of β-D-glucuronidase in *E. coli*, fluorogenic substrate 4-methylumbelliferyl-β-D-glucuronide (MUGlu) [29, 57] was used. Other authors used the following chromogenic substrates: indoxyl-β-D-glucuronide (IBDG) [58], the phenolphthalein-mono-β-D-glucuronide complex [59] and 5-bromo-4-chloro-3-indolyl-β-D-glucuronide (X-Glu) [60].

To detect the presence of β-D-galactosidase in coliforms, some authors used the following chromogenic substrates: o-nitrophenyl-β-D-galactopyranoside (ONPG), p-nitrophenyl-β-D-galactopyranoside (PNPG), and 6-bromo-2-naphtyl-β-D-galactopyranoside [61]. Other authors used chromogenic substrate 5-bromo-4-chloro-3-indolyl-β-D-galactopyranoside (X-Gal) and fluorogenic substrate 4-methylumbelliferyl-β-D-galactopyranoside (MUGal) [62].

Those authors noted that the use of these substrates has led to improved accuracy and faster detection. Methods for detection or enumeration may be performed in a single medium, thus bypassing the need for a time-consuming isolation procedure prior to identification [2].

The enzymatic methods are often combined with the classical methods or with other emerging methods. Such combinations are summarized below.

1.3.3.2.2 Presence/ absence techniques and enumeration by MTF technique using enzymatic methods

To overcome some limitations of the classical MTF and MF techniques, defined substrate methods were developed based on the enzymatic properties of coliforms. Unlike the classical methods, which eliminate the growth of non-coliform bacteria with inhibitory chemicals, the defined substrate methods are based on the principle that only the target microbes (Total Coliforms and *E. coli*) are fed and no substrates are provided for other bacteria. A defined substrate is used as a vital nutrient source for the target microbe(s). During the process of substrate utilization, a chromogen or a fluorochrome is released from the defined substrate, indicating the presence of the target microorganisms.

Over the years, the enzymatic methods have been combined with classical methods to improve specificity and to decrease analysis time. The incorporation of MUGlu into lauryl tryptose broth used as the medium for the multi-tube fermentation (MTF) technique was an example of such combined method and was first proposed for rapid detection and immediate confirmation of *E. coli* in food and water samples by Feng and Hartman (1982) [29]. The presence of methylumbelliferone due to the hydrolysis of MUGlu (positive samples) was detected by exposure to long-wave UV light and visualization of blue-white fluorescence. Some authors have suggested using a spectrofluorometer [63] or a spectrophotometer [64, 65] to decrease the threshold of fluorescence detection and thus reduce the incubation time [2]. Edberg and Edberg (1988) proposed using a combined substrate technology with the substrate ONPG for the constitutive enzyme β-galactosidase present in all coliforms and the substrate MUGlu for the specific detection of *E. coli* [66]. The defined substrate method was basically constituted as a presence/absence test. The tubes, which are colorless after samples addition, are incubated at $35\ ^{\circ}\mathrm{C}$. Any yellow color in the test tube (indicating the hydrolysis of ONPG) was taken as positive for TC. Any yellow tube is exposed to longwave UV light, and blue-white fluorescence demonstrates the presence of *E. coli*. No additional confirmatory tests need to be performed [2]. The first experiments by Edberg and Edberg (1988) demonstrated that examination of environmental isolates of TC and *E. coli* showed sensitivity equal to that of classical methods (up to $1\ \mathrm{CFU}/100\ \mathrm{ml}$) with potentially greater specificity [66]. Data also confirmed the ability to detect injured coliforms with a maximum response time of $24\ \mathrm{h}$. Rice et al. (1990, 1991) used numerous pure strains

of *E. coli* to determine the detection efficiency of the defined-substrate technology with β-D-glucuronidase and showed positive results (95.5% β-D-glucuronidase-positive isolates in 24 h and 99.5% positive after 28 h of incubation). None of the non-*E. coli* isolates were positive [2, 67, 68].

Several commercial tests were then developed based on the defined substrate technology: Colilert (IDEXX Laboratories, Portland, ME, USA), Colisure (Millipore corporation, Bedford, MA, USA), and Coli-Quick (Hach, Loveland, CO, USA). Most of these are available for presence/absence response and for enumeration by the MTF technique. The most widely used among them is the Colilert test, which utilizes the defined-substrate technique with ONPG and MUGlu. Several authors have reported numerous comparisons between these commercial tests and the classical MTF and MF techniques in the enumeration of TC and *E. coli* in various types of waters [66, 69-79]. The main conclusions of these studies is that these tests were effective for the detection of the coliforms from various types of waters, usually as sensitive as the MTF technique for the detection of *E. coli* and sometimes more sensitive for the detection of TC. Another commercial test, Quanti-Tray (QT) (IDEXX), which is an extended MPN version of the Colilert test (an MPN version with a limited number of tubes was also commercialized at an early stage), was also compared with MF technique by Fricker et al. (1997) [80] and Eckner (1998) [81]. These authors concluded that there was no significant difference for the enumeration of *E. coli* between the QT and MF techniques, except that the recovery of TC was greater with QT than with MF. McFeters et al. (1997) compared the Colisure test with standard reference methods for detecting bacteria subject to chlorine stress: with Colisure, recovery of chlorine-injured TC and *E. coli* improved over standard methods, resulting in a more realistic estimate of the actual population of indicator bacteria in public water supplies [82, 83].

In conclusions, tests based on the defined-substrate technology using chromogenic and fluorogenic substrates are applicable for the detection and enumeration of coliforms and *E. coli* in drinking water. These tests are easy to use and give a more rapid and more realistic estimate (especially in the presence of chlorine residual) of indicators of bacteriological contamination of waters than classical presence/absence or MTF media. These methods might be more expensive in terms of consumables than the classical methods when the

latter require no additional confirmation steps. When confirmation steps are required, the costs incurred in both methods are equivalent. In all cases, enzymatic methods require less manpower and therefore their cost in terms of commercial value is lower [2].

1.3.3.2.3 MF technique conjugated to enzymatic detection of coliforms

Beside the conjugation to MTF technique, enzymatic methods have also been conjugated to MF technique. Several studies have reported such conjugations using MUGlu medium in the detection of *E. coli* [57] or MI agar containing MUGal and IBDG in detection of TC and *E. coli* [58]. The method was shown to be sensitive, selective, specific and rapid (results available in 24 h) [84]. Gaudet et al. (1996) and Ciebin et al. (1995) associated MUGlu or X-Glu with classical m-TEC and lauryl tryptose agar and compared these modified media with the classical media. The modified agar media usually showed higher or similar recovery of TC and *E. coli* [2, 85, 86].

Different commercial agar media are now available for the detection of TC and *E. coli*. They include classical agar media used for *E. coli* and coliform enumeration modified with specific chromogenic and/or fluorogenic substrates for the detection of β-D-glucuronidase and/or β-D-galactosidase: Chromocult Coliform Agar (Merck, Darmstadt, Germany), Fluorocult *E. coli* Direct Agar (Merck) and m-ColiBlue24 broth (Hach) [87]. The use of these plate count methods, including chromogenic and/or fluorogenic substrates, allows far more rapid, easier, and more accurate estimates of coliform and *E. coli* abundance in drinking waters than the utilization of classical media. They can be used by any laboratory able to use conventional culture methods. However, they are more expensive and do not satisfactorily solve the problems linked to the presence of non-culturable indicator bacteria [2].

1.3.3.2.4 Direct determination of enzymatic activity by fluorimetry

The combinations of enzymatic methods to classical MTF and MF techniques which have been described above still often require 18 to 24 h to complete because they involve overnight culturing. More studies have been directed to reduce the analysis time, so that the tests could be completed within a working day's schedule. One example is by direct determination of enzymatic activity by fluorimetry.

George et al. (2000) finalized a protocol based on the fluorogenic substrates MUGal and MUGlu for a direct enzymatic detection of FC in freshwaters in $30\ \mathrm{min}$. The enumeration of the bacteria was done using epifluorescence microscopy [88]. Similar rapid assays which involved direct determination of enzymatic activity by fluorimetry without any cultivation steps were done on freshwater [89] and seawater [90]. An automated analyzer (Colifast CA-100 (Colifast Systems, Oslo, Norway)) has also been developed on the basis of this method. The detection of 1 culturable TC takes around $11\ \mathrm{h}$ [2].

1.3.3.2.5 Detection of coliforms by enzymatic methods using solid-phase cytometry

Several studies to further reduce the analysis time and to lower the detection limit in the detection of coliforms have been reported. These studies include the conjugation of enzymatic methods to solid-phase cytometry (SPC). In SPC, the principles of epifluorescence microscopy and flow cytometry are combined [91, 92]. Van Poucke and Nelis (1999) evaluated instrumental detection of fluorescent signals for decreasing the time analysis of an enzymatic membrane filtration test [93]. They used a laser-scanning device (ScanRDI1-Chemunex, Ivrysur-Seine, Paris, France) which detects and enumerates low numbers of fluorescently labeled cells by means of a solid phase cytometry technique. This method allowed the detection of *E. coli* and TC within $3.5\ \mathrm{h}$, in principle also including metabolically active but nonculturable cells [94]. This method, when applied for the detection of *E. coli* and TC in naturally contaminated and uncontaminated well water, surface water and tap water samples, has indicated more than 90% *E. coli* and more than 92% TC agreement and equivalence with reference methods including mFC agar (*E. coli*), m-Endo agar (TC) and Chromocult Coliform agar (*E. coli* and TC) [93-95]. The detection of fluorescent coliforms by SPC is fast, but the method requires a solid phase cytometer [2].

1.3.3.3 Molecular methods

Molecular methods have been developed to increase the rapidity of analysis. They are able to achieve a high degree of sensitivity and specificity without the need for complex cultivation and additional confirmation steps. Consequently, some of these methods permit the detection of specific culturable and/or non-culturable bacteria within hours instead of days which is required by the traditional methods [2].

1.3.3.3.1 Immunological methods

Over the last 20 years, efforts have been made to use immunological methods for the detection of water quality indicators in drinking water. Among these efforts are enzyme-linked immunosorbent assay (ELISA) and immunofluorescence assay (IFA) or immuno-enzyme assay (IEA).

ELISA is a rapid, simple and quite sensitive test, which allows the detection of less than 10^{-9} g of antigenic-protein [2]. This method is very useful for testing monoclonal antibodies or detecting spiked microorganisms. However, assay limitations are often associated with the specificity of the antibody used, the concentration of both antibody and antigen and the type of reaction solution used [96]. Its application to the detection of specific cells from a natural contaminated sample is also limited [97]. There are several studies reporting the application of immunological methods through ELISA assays in the detection of Enterobacteriacea [98-101]. A recent example is the work of Kuo et al. (2010) who developed a combination of ELISA and polymerase chain reaction (PCR) to rapidly detect representative coliforms in water samples. The detection time was 4 h and the limit of detection (LOD) was 5 CFU$/100$ ml for total coliforms [99].

IFA allows the identification and enumeration of a single specific cell in a natural sample. Assays can be performed by a direct or an indirect procedure. The indirect procedure involves the addition of a fluorochrome-labeled antibody. Enumeration of fluorescently labeled cells can rapidly be achieved by using epifluorescence microscopy or solid-phase cytometry after filtration of the water sample or by flow cytometry. Several studies have reported the application of immunological method through IFA assays in the detection of Enterobacteriaceae [102, 103]. The method is rapid and simple [96]. However, the method is difficult to apply on water quality monitoring if the number of targeted cells in the samples are very low. Analyses performed on large volumes of filtered water samples are limited, depending on the particles content. In addition to that, due to a problem of cross-reactivity with other bacterial strains, the use of immunological methods for the detection of coliforms and *E. coli* had not yet been successful [2, 102].

1.3.3.3.2 Nucleic acid-based methods

Nucleic acid-based methods offer taxonomic information of bacteria at different levels, such as classes, genera, species or subspecies. Some of them can be performed without the need for a complex cultivation step, thereby permitting the detection of specific bacteria within hours, instead of few days required with the cultivation-based methods. There are several nucleic acid-based methods for the detection and identification of bacteria. The most frequently used are the polymerase chain reaction (PCR) and the in situ hybridization (ISH) methods.

PCR has been applied for the detection of coliform, *E. coli,* and related microorganisms such as pathogenic *Salmonella* spp. in water sample [104-108]. The method has several advantages and limitations. The specificity is poor [104]. The usual PCR analysis time also takes a few days. Some authors have developed PCR protocols for a more rapid detection of low concentrations of *E. coli* in water samples [104, 108]. Nested PCR protocols were used for the detection of *E. coli* [108]. This technique permits a more rapid detection (6 to 8 h) than the usual PCR, since confirmation of the correct sequence amplification by probe hybridization is no longer necessary. There are also some studies which offer real-time quantitative PCR approach; it consists of monitoring the fluorescently PCR products as they are amplified [109]. The sensitivity of PCR is also known very high; however, it is difficult to use PCR for the quantification of microorganisms, especially when applied to the detection of those cells in a natural sample that are viable or metabolically active without being culturable. [2].

In situ hybridization (ISH) is a type of hybridization that uses a labeled complementary DNA or RNA strand (i.e., probe) to localize a specific DNA or RNA sequence in a portion or section of tissues or cells. Early work on in situ hybridization relied on radioactive probes to reveal and detect the probetarget hybrid [110]. Nowadays, several oligonucleotide probes are commercially available. To find the continuous target sequence unique to a specific microorganism, researchers rely on computer-aided sequence comparison available in the Ribosomal Database Project (RDP) [111], in GenBank for DNA [112], or in the ARB software package (Max Planck Institute, Bremen, Germany). Current work on rRNA in situ

hybridization uses fluorescent-labeled nucleotide probes almost exclusively to detect hybridization (FISH).

The FISH technique for detection of microorganisms has several advantages and limitations. Compared to other ISH techniques, it is more sensitive, faster, and easier to use [113]. Depending on the concentration of targeted cells in the sample and to increase resolution, FISH detection can be performed by means of flow or solid-phase cytometry. Flow cytometry enables quantification of the fluorescence intensities for each target-probe hybrid [114]. FISH is also highly specific at a cellular level. However, when applied to the detection of nutrient starved bacterial cells disseminated in drinking waters, it induces weak fluorescent hybridization signals [115, 116]. To increase the intensity, fluorescence amplification systems are attractive alternatives [116, 117]. FISH technique cannot be applied to the detection of nonphylogenetically identified microorganisms such as coliforms. In this case, work can be done on Enterobacteriaceae, the nearest phylogenetically identified group [2].

1.4 Spectrometric methods for the detection of fecal contaminant bacteria

Physicochemical and analytical methods for detection and identification of bacteria are constantly being investigated. The developments are mainly focused on vibrational spectroscopy- and mass spectrometry-based techniques [118-123]. Unlike classical or molecular methods, detection and identification of bacteria in spectrometry methods are mostly done via the detection and identification of volatile by-products of bacterial metabolism.

Studies reported on spectrometry methods for bacterial detection and identification were usually done on the following approaches: (i) through analysis of bacteria biomarkers (which are detected via headspace analysis of bacteria metabolites or via analysis of pyrolysis products of bacteria), or (ii) through bacteria 'fingerprints' recognition. In the next section, spectrometric methods which have been used for detection and identification of bacteria are described.

1.4.1 Gas chromatography - mass spectrometry

Gas chromatographic techniques have been employed for the detection or identification of microorganisms since around 50 years ago. In 1963, Oyama proposed a technique involving

a chromatographic characterization of the pyrolysis products of bacteria or substances of biological origin to determine the possible existence of life on Mars [124]. To date, GC-MS have been applied for the detection and identification of various bacteria. Labows et al. (1980) had performed GC-MS analysis of headspace volatiles metabolites released by different species and strains of *Pseudomonas* bacteria [8]. All strains of *Pseudomonas aeruginosa* produced a distinctive series of odd-carbon methyl ketones, particularly 2-nonanone and 2-undecanone, and 2-aminoacetophenone, in addition to two sulfur compounds, dimethyldisulfide and dimethyltrisulfide. GC-MS has also been used for the identification of *C. difficile*, an enteric pathogen, based on different short-chain fatty acids metabolically produced by *C. difficile* as compared to other *Clostridia* [125].

In the detection of *E.* coli, Yu et al. (2000) have used GC-MS to characterize volatile compounds released by *E. coli* O157:H7 and their absorption by strawberry fruit. As shown in Table 2, 12 compounds were released both by the pathogenic and non-pathogenic *E. coli*, (only the compositions were different) [6].

Table 2. Volatile compounds produced by *E. coli* and detected by GC-MS (Yu et al. 2000) [6]

Compounds	Retention time (min)	*E. coli* O157:H7 (ng)[a]		*E. coli* (ng)[a]
		ATCC 43895	ATCC 35150	ATCC 15597
2,5-dimethyltetrahydrofuran	13.36 and 14.01[b]	216 ± 124 NS[c]	152 ± 17	152 ± 70
dimethyl disulfide	16.54	54 ± 56 NS	25 ± 7	12 ± 6
2-heptanone	28.32	60 ± 19 A	52 ± 4A	8 ± 1 B
2,5-dimethylpyrazine	30.27	297 ± 31 NS	515 ± 31	389 ± 326
benzaldehyde	35.12	398 ± 127 NS	483 ± 67	130 ± 6
dimethyl trisulfide	36.4	112 ± 133 NS	23 ± 1	29 ± 2
2-nonanone	46.31	147 ± 46 A	133 ± 18 A	9 ± 12 B
nonanal	47.43	109 ± 36 NS	71 ± 34	72 ± 52
decanal	55.86	58 ± 16 NS	53 ± 22	34 ± 6
undecanone	62.7	41 ± 9 NS	33 ± 6	31 ± 1
indole	63.55	20248 ± 1622 NS	19249 ± 473	19427 ± 4238
unknown	75.76	83 ± 15 B	72 ± 7 B	132 ± 4 A
2-tridecanone	77.22	24 ± 7 B	19 ± 2 B	44 ± 1 A

[a] Amount of compound ± standard deviation emitted per 5 plates of culture medium. [b] Two isomers of compound detected. [c] Means within *E. coli* strains followed by different letters are significantly different by least-squares difference (LSD) at $P = 0.05$ or are not significantly different (NS). [d] Plate count agar means significantly differs (*) from *E. coli* mean across strains by a single degree of freedom contrast at $P = 0.05$ within the analysis of variance or does not differ (NS).

Koek et al. (2006) developed an analytical method consisted of an oximation and silylation derivatization reaction and subsequent analysis by gas chromatography coupled to mass spectrometry for the analysis of microbial metabolomes. The method was validated using different microorganisms, i.e. *Bacillus subtilis, Propionibacterium freudenreichii*, and *Escherichia coli*. Many metabolite classes could be analyzed with the method: alcohols, aldehydes, amino acids, amines, fatty acids, (phospho-) organic acids, sugars, sugar acids, (acyl-) sugar amines, sugar phosphate, purines, pyrimidines, and aromatic compounds [126].

1.4.2 Gas chromatography - flame ionization detection

GC-FID using automated headspace concentration has been applied in the analysis of several common lung pathogens. It reveals a number of characteristic and highly conserved dominant components. The volatile compounds released by *Proteus mirabilis, Klebsiella pneumoniae, Pseudomonas aeruginosa* and *Staphylococcus aureus* which were grown in tryptic soy broth for $24\ \mathrm{h}$ consisted mainly of isobutanol, isopentanol, isopentyl acetate, 1-undecene and methyl ketones [7].

1.4.3 Ion mobility spectrometry

IMS is an analytical vapor detection technique which is developed based on the detection of ionized compounds which are passed through electrical field and are characterized by their corrected drift times or ion mobilities [127]. Snyder et al. (1991) reported the detection of *E. coli* using IMS based on the presence/absence of hydrolysis of ONPG into ONP (*o*-nitrophenol). They found that in the absence of *E. coli*, hydrolysis of ONPG into ONP did not occur and vice versa [127, 128]. Headspace analysis of ONPG with and without *E. coli* is shown in Figure 2.

Lawrence (1998) also earlier investigated the use of laboratory IMS in the differentiation of normal and bacteria-infected red oak wood. By applying thermal desorption to the wood samples, the latter type of wood displayed two additional intense lower mobility (longer drift time) peaks than in the ion mobility spectrum of the former wood type [127].

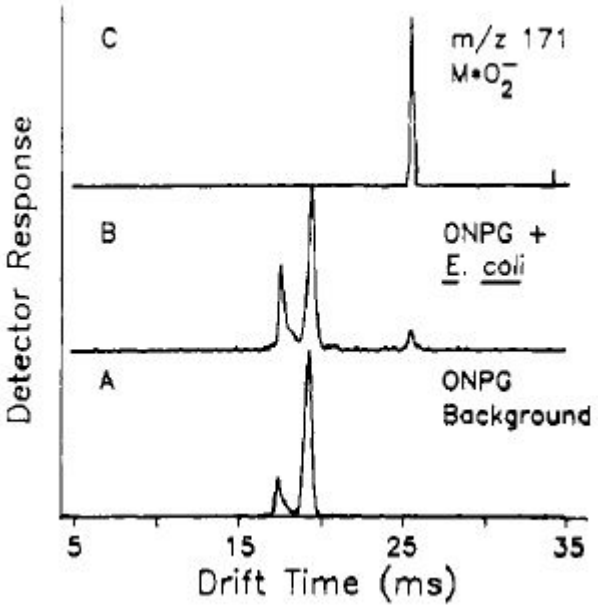

Figure 2. IMS/MS analysis of headspace vapors from ONPG with and without *E. coli* by Snyder et al. (1991) [127].

1.4.4 Multi capillary column coupled ion mobility spectrometry

MCC-IMS have been used for the detection of metabolic volatile organic compound in human breath [129, 130] and also for the characterization of volatile compounds released by *E. coli* [5]. The latter study reported that *E. coli* strain BL21 pLB4 revealed four analytes as a part of their metabolism byproducts: ethanol, propanone (acetone), heptan-2-one, and nonan-2-one.

1.4.5 Gas chromatography - differential mobility spectrometry

Unlike MS which is a vacuum-based technique, DMS is a gaseous phase ionic separation technique operating at ambient pressure, where the separation of ions is achieved by exploiting the difference in the ion mobilities between alternating high and low electric fields within the DMS drift cell [131-135]. During the last decade DMS has been primarily employed for detecting volatile organic compounds (VOCs). The low power consumption, compactness of DMS, coupled to ambient pressure operation with minimal maintenance makes it an attractive alternative to MS for VOC analysis where portability is required. Recently, DMS has been successfully coupled with GC for the analysis of human breath, bacterial odours and for jet fuel analysis [131-137].

Application of GC-DMS for detection and characterization of bacteria have been gaining interest in recent years. Shnayderman et al. (2005) used headspace analysis to characterize *E. coli, B. subtilis, B. thuringiensis*, and *M. smegmatis* using GC-DMS [4]. Krebs et al. (2006) used GC-DMS for species-specific detection of *Bacillus* spores, including *B. anthracis*, the causative agent of anthrax. Using a combination of FAIMS (a synonym for DMS) and pyrolysis technique, the method was able to differentiate *B. anthracis* from other *Bacillus* [138]. Discrimination of bacteria using Py-GC-DMS to differentiate several strains of *Bacillus* was also done by Cheung et al. (2009) [118].

Prasad et al. (2007) used pyrolysis GC-DMS (py-GC-DMS) to differentiate *E. coli, P. aeruginosa, S. warneri* and *M. luteus* grown in different temperature (23, 30, and 37 °C) [132]. The authors found that the volatile compounds released by the bacteria are temperature-dependent, which implies that characterization of bacteria according to their volatile compounds should be done in a controlled envinroment (e.g. a certain temperature). Study about the use of GC-DMS for *E. coli* detection has also been reported by Saptalena et al. (2012) [10]. Theory of DMS is elaborated in the next section.

1.5 Theory of differential mobility spectrometry

Differential mobility spectrometry (DMS) is an ambient pressure ion-separation technique that characterizes chemical substances using differences in the gas phase mobility of ions in alternating strong and weak electric fields that are generated using a high frequency asymmetric waveform [139]. DMS is also known by several other names. DMS should not be confused with differential mobility analysis (DMA), which is a form of conventional ion mobility spectrometry (conventional IMS). Although the DMS technology is derived from IMS, these are two different technologies. The differences are explained in the next section. DMS is also sometimes referred to as differential ion mobility spectrometry (which is frequently shortened as differential IMS). DMS has a planar micro-fabricated design. Parallel to DMS, there is another field-dependent mobility analyzer which uses field asymmetric waveform principle. This analyzer is known as FAIMS (field asymmetric waveform ion mobility spectrometry) ([140], p.33). Unlike DMS, FAIMS has a cylindrical design (besides a different instrumental technique) [141].

The DMS technology has come from the former USSR. It was firstly developed in the early 1980s within the military and security establishment as a means for explosive detection in the field. The first DMS technology was patented by Mixail P. Gorshkov. The research was continued by Buryakov and Nazarov, who spearheaded the miniaturization of DMS at NMSU and later at Sionex. In 1993 Buryakov et al. introduced the first basic concept of DMS in the literature [12].

To date DMS has been applied in many areas, such as the detection of explosives [13], fire debris [14], environmental contaminants [15, 16], and bioorganisms [4, 17]. In those applications, DMS shows promise for on-site analysis because it is small, low cost, and sensitive [14].

1.5.1 DMS vs IMS

DMS can be compared with conventional ion mobility spectrometry (IMS) since both techniques are based on the motion of ions induced by electric fields at atmospheric pressure ($760\ \mathrm{Torr}$) [142]. A conventional IMS is a chamber housing a series of metal plates to which incrementally decreasing (or increasing) dc voltages are applied (i.e., forming a drift tube) [142-144]. The electric field produced by this set of electrodes is designed to be as uniform as possible. Ions are gated into the drift tube using a shutter grid assembly and are subsequently separated because of differences in their drift velocities. The ion drift velocity is proportional to the field strength at low electric fields (e.g., $200\ \mathrm{V/cm}$). Thus, the ion mobility, K, which is determined from this experiment, is independent of the strength of the applied electric field [142].

In contrast to IMS, the gaseous ion separation in DMS occurs as ions are conveyed by a drift gas that is orthogonal to the applied electric field. Ion-shutter, drift rings, or aperture grids employed in IMS are not needed in DMS [139]. Conventional IMS operates at low electric fields (less than $1\ \mathrm{kV/cm}$), whereas DMS operates at much stronger electric fields (greater than $10\ \mathrm{kV/cm}$). At this higher electric field, there is a nonlinear dependence of ion mobility on the electric field strengths [139, 142]. This nonlinear dependence of the ion mobility on the electric field strength is the basis for the development of DMS technology.

In DMS, a continuous stream of ions is separated as they are carried by a drift gas between closely spaced electrodes. Ions will cluster with other neutral species in the drift gas. The field dependence of the ion mobility arises from changes in the composition of these clusters with respect to the local temperature of the ion [145]. When the stronger electric field acts on the ion, it travels faster and the local temperature increases as a result of the increased number of collisions with the drift gas. As the ion heats up it will de-cluster and increase in mobility. Under low-strength fields, the ion velocity is decreased and the ion cools so that it reforms clusters with the neutral gas molecules and returns to a mobility characteristic of low-strength fields [139]. Dimer ions exhibit the reverse behaviour. The ionic charge is not as accessible to the neutral gas molecules as with monomeric ions. Under high field conditions and an increased local temperature the ion mobility decreases compared to the low-field mobility. This decrease in mobility is caused by the increased number of collisions and expanded cross-sections of the hotter dimer ions.

1.5.2 Fundamentals of DMS

Unless mentioned specifically, the fundamental concept of DMS presented in this section is written based on studies by Buryakov et al. (1993) [12], Borsdorf and Eiceman (2006) [146], and Shvartsburg (2009) [140].

It is known that when ions in a drift gas are subjected to an electric field then directed flow of these ions occurs along the field lines with a velocity (V_d) equal to:

$$V_d = KE \tag{1}$$

where E is the electric field intensity and K is the coefficient of ion mobility. The value of K (and hence the velocity) are different for various ion species. It is usually normalized to temperature and pressure and reported as reduced mobility (K_0) in order to compare spectra obtained using different experimental conditions. Such corrections however do not and cannot compensate or adjust for any changes in ion identity which may arise, particularly at extremes of temperature or moisture. Values for K_0 are calculated according to the conventional equation:

$$K_0 = \left(\frac{d}{t * E}\right) * \left(\frac{p}{760}\right) * \left(\frac{273}{T}\right) [=](cm^2/Vs) \quad (2)$$

where $d =$ drift length (cm), $t =$ drift time (s), $E =$ field strength (V/cm), $p =$ pressure (torr), and $T =$ temperature (K). At high electric field (greater than $10\ \mathrm{kV/cm}$), as applied in DMS, there is a nonlinear dependence of ion mobility (K) on the electric field strengths (E), and the K value is better represented by K_H, a nonconstant, high-field, mobility term [139, 142]:

$$K_H = K_L \left[1 + \alpha\left(\frac{E}{N}\right)\right] \quad (3)$$

where K_H and K_L (or K_0) are the mobility coefficients under high and low field conditions, respectively, and α are characteristics of ions. The dependence of α on electric field (E) and gas density (N) are shown by nomenclature $\alpha\left(\frac{E}{N}\right)$. Figure 3 shows three possible examples of the dependence of the ratio of mobility coefficients on the electric field strength with 3 types of alpha values.

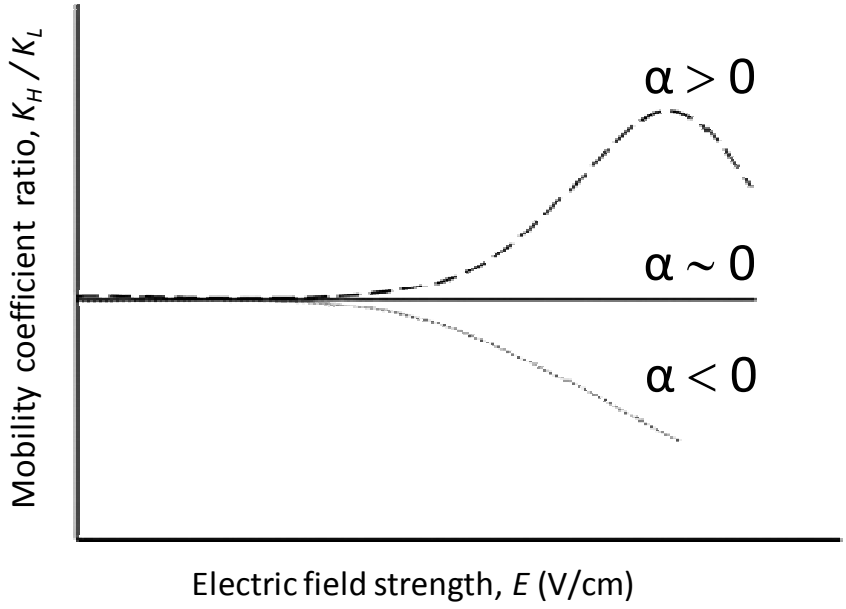

Figure 3. A schematic of three possible examples of dependence of mobility coefficients on electric field strength [139]

In DMS, ions are passed in a flow of gas through a narrow gap defined by two electrodes (Figure 4, top frame) and exposed to a high-frequency, asymmetric electric field created with a waveform (Figure 4, bottom frame) applied to one electrode; the other electrode is grounded.

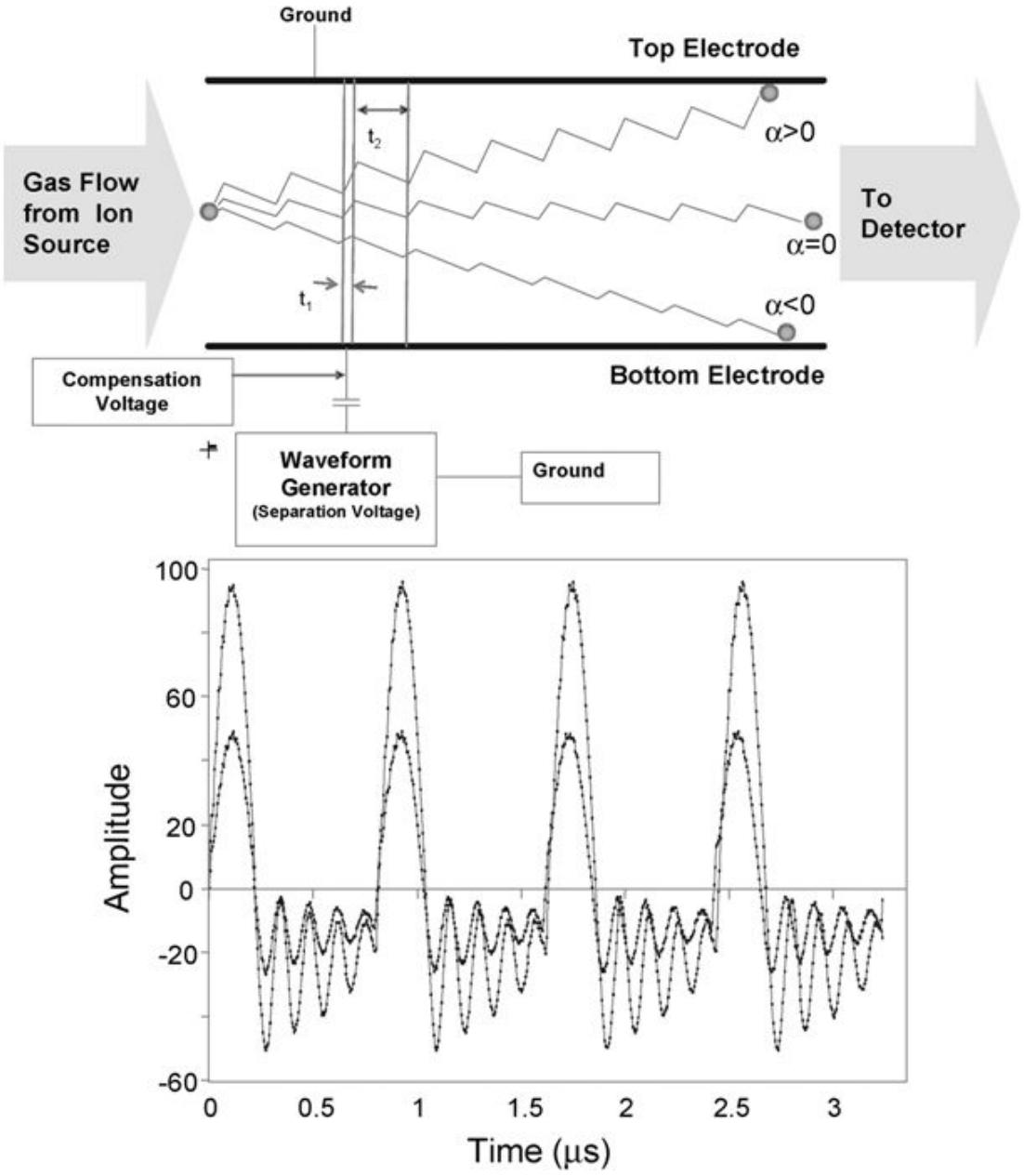

Figure 4. Scheme of DMS analyzer. Top: principle of ion characterization. Bottom: actual asymmetric waveforms for two levels of voltage (superimposed for comparison) [146]

The mixtures of ions that are moving with the stream of gas carrier are affected by the following asymmetric periodic electric field $E(t)$applied perpendicularly to ion motion:

$$\frac{1}{t_c}\int_0^T E(t)\mathrm{d}t = \langle E(t)\rangle = 0 \tag{4}$$

$$\langle E^{2n+1}(t)\rangle \neq 0 \tag{5}$$

where t_c is the field oscillation period and n is an integer not less than 1. These conditions conform to the shape of an asymmetric curve with period $T = t_1 + t_2$ whose absolute value during the positive semi-period $t_1(E_{max})$ is much greater than that at the negative semi-period $t_2(E_{min})$, if $t_1 \ll t_2$ (Figure 5). The effect of this field is to make the ions oscillate in the transverse direction with period T during their motion in the gas carrier stream. The velocity of each ion during the semi-period depends on amplitudes E_{max} and E_{min} and $\alpha(E)$. Therefore, besides the quick oscillation with period T, ions will be slowly displaced along electric field lines if their $\alpha(E)$ functions differ. The sign and magnitude of the average transverse displacement of the ions during total period T depends on the form of the function $K(E)$, that is on the sign and magnitude of $\alpha(E)$. Thus, using a high-frequency asymmetric electric field it is possible to separate ions having different $\alpha(E)$ values.

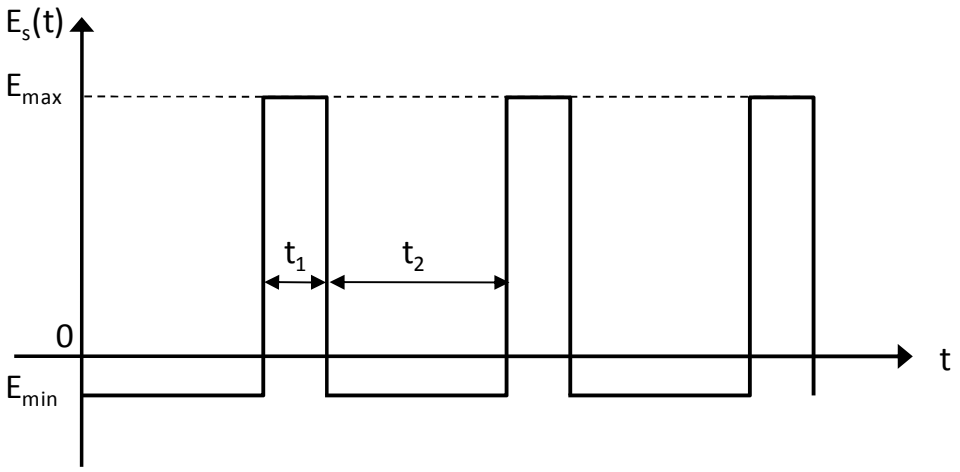

Figure 5. Function form of *$E_s(t)$* (excitation wave form) [12]

1.5.3 RF voltage and DC compensation voltage

As mentioned in the previous section, in DMS a high asymmetric electric field is applied perpendicular to the direction of the gas flow that carries the ions. This field is referred to as a radio frequency (RF) voltage. The field is designed to satisfy the condition $E_1 t_1 = E_2 t_2$, so integrals above and below the time axis (in Figure 5) are equal. If mobility of an ion is independent of E, then $K(E_1) = K(E_2)$ and displacement of ions during the high and low portions of the applied field will be equal and opposite $(K(E_1)E_1 t_1 = -K(E_2)E_2 t_2)$. In this instance, the sum in displacement of the ions during one period of the separation field will be zero.

Ions with a field dependence on mobility, i.e. $K(E_1) \neq K(E_2)$, will be displaced on the y-axis during a period of the separation field $(K(E_1)E_1 t_1 + K(E_2)E_2 t_2) \neq 0$ and the direction of displacement governed by the sign of mobility dependence. If there is a positive dependent of mobility on electric field, then ions will be displaced a distance $(K(E_1)E_1 t_1 + K(E_2)E_2 t_2) = \Delta K E_1 t_1$. The extent of displacement depends on field amplitude (E_1), field waveform (ratio t_1/t_2), and ion mobility dependence (ΔK). Ions with negative mobility dependence will be displaced in a direction opposite that of ions with positive field dependence. All ions that collide with either electrode are neutralized and swept from the analyzer.

An ion which is displaced from the centre of the analyzer can be restored or compensated to the centre of the gap when a DC potential (the compensation field, C) is superimposed on the asymmetric waveform. Ions restored to the gap center will be passed through to the detector. Compensation voltages will be characteristic for ions with differing ΔK. A scan of compensation voltage provides a complete measure of ion species in the analyzer as shown in Figure 6. The compensation voltage is therefore swept over a range of voltages and the spectra obtained display the compensation voltage versus the intensity of ion current.

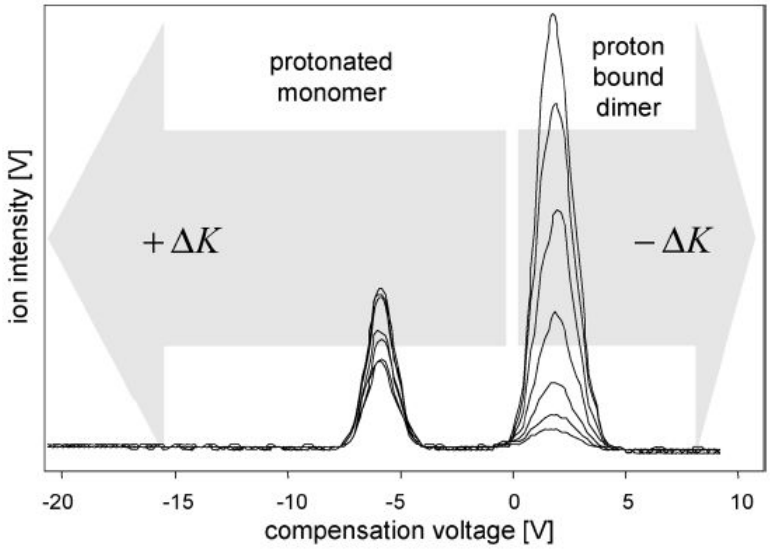

Figure 6. A DMS spectrum showing the relationship between compensation voltage and ΔK. The reference point is $0\ V$ and increasing displacement from $0\ V$ is understood as increased positive or negative dependence on electric field [146]

1.5.4 Ionization theory in DMS

DMS technology relies upon ionization chemistry to detect the presence of a given chemical species. The ionization sources may be either radioactive (generally ^{63}Ni) or nonradioactive (e.g. UV). Once the sample is ionized, the objective of the technology is to separate and differentiate one ion species from another. After separation, the sensor detects and quantifies one species from another. Finally, the detection and quantification are presented as actionable data [147].

Production of ions from ^{63}Ni begins with the emission of high energy electrons as shown in Eq. 6:

$$^{63}_{28}Ni \xrightarrow{yields} \beta^- + {}^{63}_{29}Cu \tag{6}$$

The radioactive half-life of ^{63}Ni is approximately 100 years and the beta particles have a distribution of energies with a mean of $17\ \mathrm{keV}$ with a maximum of $67\ \mathrm{keV}$. Electrons emitted from the foil collide with the molecules of the supporting atmosphere and in the instance of air or nitrogen, produce ions of N_2^+ as shown in Eq. 7:

$$N_2 + \beta^- \xrightarrow{yields} N_2^+ + \beta' + e^- \quad (7)$$

The electrons produced in Eq. (7) will eventually reach thermal energies and become attached to oxygen forming negative ions in air. This initial reaction (Eq. 7) is followed by further reactions producing positive ions in ambient gas and these ions, termed reactant ions, are used in the chemical ionization of sample [146, 148]. In a clean air atmosphere, the positive reactant ions formed through Eqs. (8) to (12) terminate in water clusters of a gas phase proton with the structure $(H_2O)_nH^+$:

$$N_2^+ + 2N_2 \xrightarrow{yields} N_4^+ + N_2 \quad (8)$$

$$N_4^+ + H_2O \xrightarrow{yields} 2N_2 + H_2O^+ \quad (9)$$

$$H_2O^+ + H_2O \xrightarrow{yields} H_3O^+ + OH \quad (10)$$

$$H_3O^+ + H_2O + N_2 \xrightarrow{yields} H^+(H_2O)_2 + N_2 \quad (11)$$

$$H^+(H_2O)_2 + H_2O + N_2 \xrightarrow{yields} H^+(H_2O)_3 + N_2 \quad (12)$$

The number of water molecules (n) depends upon gas temperature and the level of moisture of the gas atmosphere internal to the region of the analyzer with the ion source [146, 149-153]. The gases of portable analyzers are scrubbed over molecular sieves in a recirculated flow system so the number of water molecules is kept comparatively constant.

Collisions between molecules (M) from a sample and the reactant ions can lead to the formation of an adduct ion $(MH^+(H_2O)_n)$ that may proceed with stabilization by loss of water to the formation of product ions, (MH^+) as shown in Eq. (13). The adduct ion is often not shown in such reactions which might appear mistakenly to be concerted mechanisms:

$$M + H^+(H_2O)_n \xrightarrow{yields} MH^+(H_2O)_{n-x} + xH_2O \quad (13)$$

Nonetheless, the reaction in Eq. (13) will be favorable if the gas-phase proton affinity of the sample molecule is larger than that of water ($691\,\frac{kJ}{mol}$).

Depending on the physicochemical properties of the substances and their concentration and on the experimental conditions, additional product ions can also be formed as shown in Eqs. (14–16).

$$MH^+ + nL \xrightarrow{yields} MH^+ \cdot L_n \qquad \text{Cluster formation} \qquad (14)$$

$$MH^+ + M \xrightarrow{yields} M_2H^+ \qquad \text{Dimerization} \qquad (15)$$

$$M_2H^+ + nL \xrightarrow{yields} M_2H^+ \cdot L_n \qquad \text{Formation of clustered proton bound dimers} \qquad (16)$$

In addition to positive reactant ions, negative ions are also being formed in an ion source principally through the attachment of a thermalized electron to molecular oxygen. The dominant reaction pathway provides $(H_2O)_nO_2^-$ as reactant ions in addition to various adducts such as $(H_2O)_nO_2O_2^-$ and $(H_2O)_n(CO_2)O_2^-$ [146, 154-158].

Negative product ions are formed from neutral sample molecules (MX) due to charge transfer reactions and include dissociative electron attachments (Eq. (17)) and associative electron attachments according to Eq. (18).

$$(MX) + (H_2O)_nO_2^- \xrightarrow{yields} M + X^- + nH_2O + O_2 \qquad (17)$$

$$(MX) + (H_2O)_nO_2^- \xrightarrow{yields} (MX)O_2^- + nH_2O \qquad (18)$$

Though these reactions are written with a single step, suggesting concerted mechanisms, the association between MX and O_2^- results first in the formation of an adduct ion MXO_2^-. Later, the adduct ion can undergo reactions in Eqs. (17) and (18) or other reactions such as proton abstraction according to Eq. (19):

$$M + (H_2O)_nO_2^- \xrightarrow{yields} (M-1)^- + neutrals \quad (19)$$

Cluster or hydrated ions for these product ions are also known with the structures $M^-(H_2O)_n$ and $(M-1)^-(H_2O)_n$. As with positive ion reactions, favorable molecular properties, in this instance, electron affinity, promote ionization and affect relative response factors. Thus, compounds such as aromatic hydrocarbons, carboxylic acids, nitro-alkanes, or nitro-aromatic compounds and halocarbons exhibit favorable response with negative ion chemistry and alkanes, alkenes, and others show poor response in negative polarity [146].

In DMS, the change in concentration can be characterized with changes in peak intensities for the reactant ions, protonated monomer and proton bound dimer. Decreases in reactant ion peak intensity quantitatively follows increases in $[M]$ with corresponding increases in peak intensities first for the protonated monomer and then for the proton-bound dimer as shown in Eqs. (20) and (21):

$$(H_2O)_nH^+ + M \xrightarrow{yields} MH^+ + nH_2O \quad (20)$$

$$(M)(H_2O)_mH^+ + M \xrightarrow{yields} (M)_2H^+ + mH_2O \quad (21)$$

As $[M]$ decreases, the proton-bound dimer peak intensity increases with decreases in peak intensities for the protonated monomer and the reactant ions. Eventually, the proton-bound dimer is no longer detected and this is followed by loss of MH^+ intensity and full restoration of the reactant ion peak. Such changes can occur on millisecond or second timescales and is ultimately limited by mass flow rates into the ion source. Typical intensity of reactant and product ions depending on the vapor concentration for an analyte can be illustrated by Figure 7.

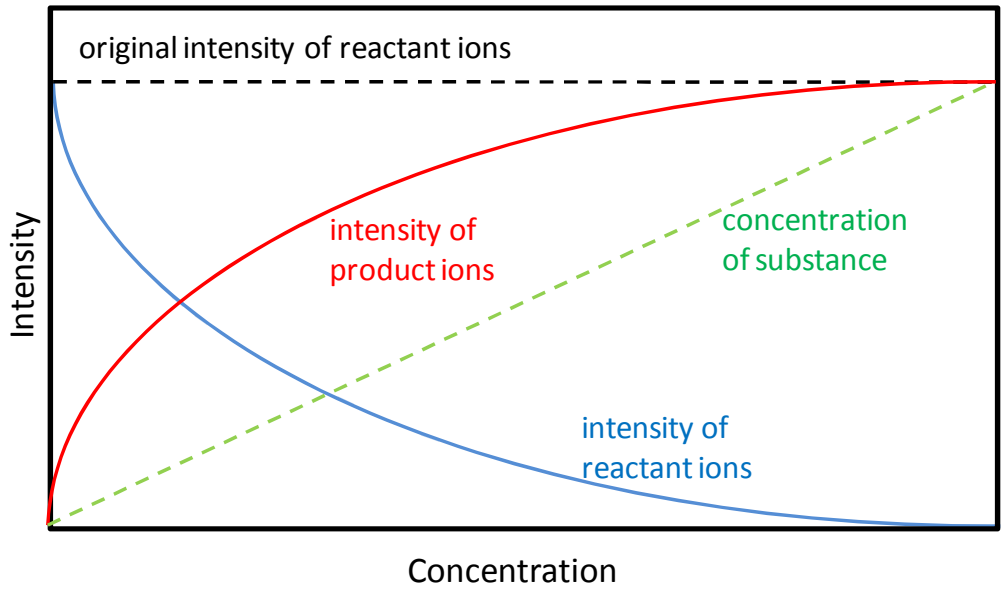

Figure 7. Intensity of reactant and product ions depending on the vapor concentration for an analyte [159]

1.6 Outline

To achieve the research objectives detailed in section 1.2, the thesis has been organized into seven chapters.

Chapter 1 presents the background, motivation, and objectives of the work. A literature review is also given in this chapter. The literature review is started with the definition of fecal contaminant bacteria, followed by the regulations for monitoring their level in the environmental water body, and with the review of existing methods for their detection. Spectrometric methods for the detection of the bacteria are the main part of the study. Therefore, it is given a bigger portion than other methods and given in a separate section. The main spectrometric method used in this study was DMS, a new technique within the ion mobility spectrometry field. Additionally, MS was also applied for validation of compounds identity. Therefore, a theory of DMS is described in more detail and given in the separate section.

Chapter 2 deals with the evaluation of the GC-DMS response on the detection of synthetic biomarkers of *E. coli* using 12 standard compounds. The GC-DMS spectra of the standard compounds (prepared as single compound and as mixture of compounds in water) at a

certain RF voltage are presented and analyzed. A dispersion voltage study to determine the dependence of compensation voltage on RF voltage was also done and presented in this chapter.

Chapter 3 deals with the determination of the effect of growth media on the type and composition of volatile metabolites released by the *E. coli*. Five different culture media (Colilert-18®, Tryptic Soy Broth (TSB), glucose broth, tryptophan broth, and M-9) were used to grow the bacteria. Headspace analysis and characterization of the volatile metabolite compounds were done using GC-DMS and GC-MS.

Chapter 4 describes the investigation of ONPG cleaving time by *E. coli* bacteria which were grown in Colilert-18®. In the presence of *E. coli*, the ONPG substrate in Colilert-18 is cleaved/ hydrolyzed by β-galactosidase enzyme in *E. coli* into β-D-Galactose and *o*-nitrophenol. To investigate the cleaving period, *E. coli* was incubated under various incubation periods and the presence of *o*-nitrophenol was checked from time to time via headspace analysis using GC-MS and GC-DMS. The determination of the cleaving period is important in shortening the overall analysis time.

Chapter 5 presents the performance of the GC-DMS in the differentiation of bacteria through the analysis of the biomarkers released by the different bacteria. In this work, different types of coliform and non-coliform bacteria (*E. coli DSM 30083, E. coli DSM 1576, E. coli* RV, *Klebsiella pneumonia, and Pseudomonas aeruginosa*) were used. The biomarkers released by the bacteria were characterized by GC-DMS. A validation was also done using GC-MS.

Chapter 6 describes an early warning system developed for the detection of coliform and *E. coli* bacteria in water samples.

Chapter 7 covers the general conclusions and outlook. Recommendations on how to improve the developed method are outlined in this chapter.

2 Detection of synthetic biomarkers of *E. coli* in water samples by Differential Mobility Spectrometry: A dispersion voltage study

Partly reproduced from:

> *Saptalena LG, Kerpen K, Kuklya A, Telgheder U (**2012**). Rapid detection of synthetic biomarkers of Escherichia coli in water using microAnalyzer: A field dependence study. International Journal for Ion Mobility Spectrometry 2012;15:47*

2.1 Introduction

In order to develop an analytical method for the detection of biomarkers of *E. coli* in water samples by DMS, the optimization of the experimental parameters (e.g. the GC ramp rate, the sensor temperature, the radio frequency voltage (V_{rf}), and the compensation voltage (C_v) scanning range) are necessary. The concept of RF voltage and compensation voltage are quite unique in the spectrometry fields and, therefore, will be discussed in this chapter in more detail.

In DMS studies, the study of the effect of RF voltage on the detection of chemical compounds is known as a dispersion voltage study or a field dependence study. There are a couple of ways to do the dispersion voltage study. The first way is by programming the DMS in such a way so that the RF voltage is varied automatically by a set amount, each time a full C_v scan is performed. The plot generated from the scanning method is called as a dispersion plot. Another way to do the dispersion voltage study is by changing the RF voltage manually, allowing an incremental variation of RF voltages, each time a full C_v scan is performed.

Examples of dispersion voltage studies or field dependence studies have been reported by Krylov et al. (2002), Krylova et al. (2003), and Rearden (2006) [137, 145, 160]. Krylov et al. (2002) performed the field dependence study on several ketone compounds, from acetone to decanone (C_3H_6O to $C_{10}H_{20}$O) [145]. Krylova et al. (2003) performed the field dependence study on organophosphorus compounds (dimethylmethyl phosphonate (DMMP), trimethyl phosphate (TMP), diethylmethyl phosphonate (DEMP), etc.) [160]. Rearden (2006) performed the field dependence study on several major components of

gasoline such as benzene, *m*-xylene, *p*-xylene, toluene, collectively referred to as BTX, and methyl *tert*-butyl ether (MTBE) [137]. The dispersion voltage study on volatile metabolite compounds released by *E. coli* bacteria was first reported by Saptalena et al. (2012) [10] and will be described in this chapter in more detail.

In this work, to understand the response of GC-DMS in analyzing volatile metabolite compounds released by *E. coli* bacteria, 12 standard compounds were used to characterize the DMS response. These compounds were selected based on the study reported by Yu et al. (2000) [6] in which 12 compounds were found to be released by pathogenic *E. coli* O157:H7 ATCC (American Type Culture Collection) 35150 and nonpathogenic *E. coli* ATCC 15597 which were grown in Brain and Heart Infusion (BHI) broth. The type of compounds released by the pathogenic *E. coli* were the same with those released by the nonpathogenic one, but different in composition, with indole being the major compound released by both types of *E. coli*. The detection was done using GC-MS.

In this work, individuals and mixtures of the 12 compounds were prepared in water from reference standards. The headspace gases were then analyzed using GC-DMS. Differential mobility spectra showed monomer peaks of each analyte at a given RF voltage were recorded. Dispersion voltage study determining the dependence of signal intensities and compensation voltages of each analyte on the applied RF voltages were then performed and recorded for positive and negative modes.

2.2 Materials and Methods

2.2.1 Reagents and samples preparation

Twelve chemicals were purchased from various suppliers in Germany and were used without further purification: dimethyl disulfide (99%), 2,5-dimethyltetrahydrofuran (96% mix of cis and trans), 2,5-dimethylpyrazine (≥98%), benzaldehyde (≥98%) and indole (≥99%) were purchased from Aldrich; decanal (≥98%), 2-undecanone (99%), and 2-tridecanone (99%) were purchased from Sigma; 2-heptanone (≥98%) and 3-nonanone (≥97%) were purchased from Merck; dimethyl trisulfide (≥98%) was purchased from Fluka; and nonanal (95%) was purchased from Acros. Standard solutions of individual and mixture of compounds (10 g/l per compound) were prepared in water in order to simulate the headspace analysis of

volatile compounds released by *E. coli* in water. Working solutions of individual analytes and mixtures of analytes were prepared by diluting the standard solutions to $1\ \mathrm{mg/ml}$. Ultra-pure water ($18.2\ \mathrm{M\Omega}$, Millipore) was used for the preparation of the solutions. The samples (each $10\ \mathrm{ml}$) were placed in 20-mL vials and were preheated at $37\ ^{\circ}\mathrm{C}$ for $15\ \mathrm{min}$ prior to the headspace sampling.

2.2.2 Instrumentation and operational setting

GC-DMS analysis was carried out on a miniaturized GC-DMS system (microAnalyzer™, Sionex Corporation). The dimension of the instrument is $250\text{-mm} \times 82\text{-mm} \times 118\text{-mm}$ and the weight is $1.4\ kg$. Unlike the earlier models of DMS (SVAC-V, SVAC-G, and SVAC-E), the microAnalyzer™ is equipped with a built-in GC column.

The main parts of the instrument are an ambient air sampling system, a pre-concentrator, a gas chromatographic separation module, a differential-mobility detection system (microDMx), and a moisture control unit. The instrument is designed to be operated with a flow of air at ambient pressure [161].

There are three stages in the operation of the system: sampling, loading (chromatographic separation), and analyzing (DMS detection). The flow diagram of each stage is given in Figure 8. The instrumentation and operating condition of each stage are described below.

2.2.2.1 Sampling stage

In the sampling stage (Figure 8, top frame) a sample pump draws the sample in through a check valve and a pre-concentration trap (usually with a flow rate between 50 and $100\ \mathrm{ml/min}$) for $30\ s$ (by default). A transport flow pump maintains a constant transport gas flow through a molesieve filter and a manifold. The transport flow pump flow rate is usually $300\ \mathrm{ml/min}$ (by default) and the pressure is between 1 and $10\ \mathrm{psi}$ [161].

In this work, the flow rate of the sample collection was $80\ \mathrm{ml/min}$, the sample collection period was kept $30\ s$, the transport flow pump flow rate was $300\ \mathrm{ml/min}$, and the sample pump voltage was $10\ \mathrm{V}$. The trap material was Carbopack-B ($60/80$ mesh) and the molesieve filter type was HCRMS (hydrocarbon/moisture trap).

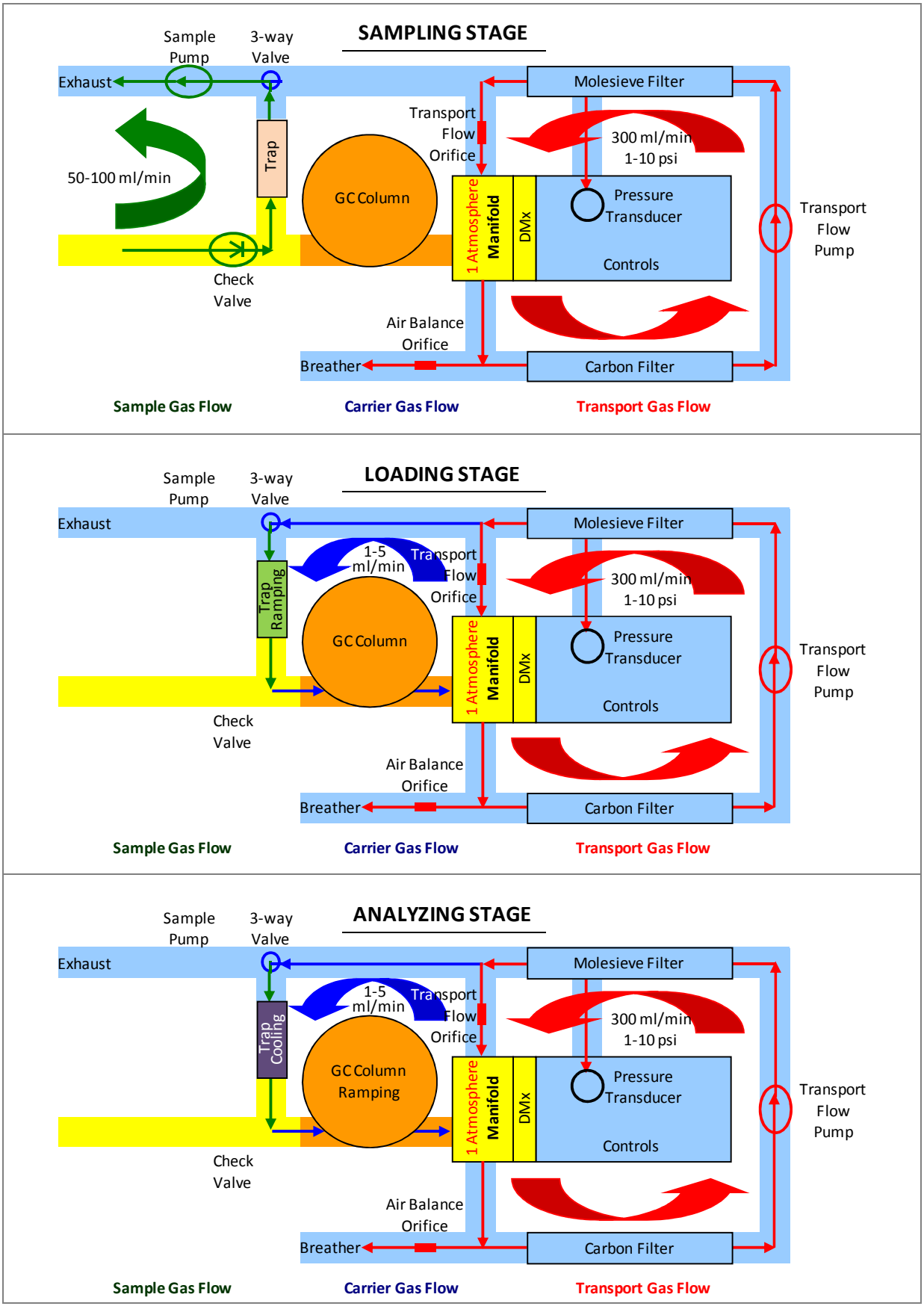

Figure 8. Flow diagrams of three operation stages of the miniaturized GC-DMS (modified from Sionex [161])

The sample gas inlet of the miniaturized GC-DMS is an internally threaded hole, and the connection to the sample gas inlet is made by 1.6-mm outside diameter stainless steel instrument grade tubing and 1.6-mm internal thread nut and ferrule.

In this work, to characterize the standard compounds in a controlled environment (i.e. using nitrogen gas instead of ambient air), the sample introduction system was slightly modified. The schematic drawing of the instrument after modification is shown in Figure 9. A stainless steel T-joint (Swagelok® Tee) was placed on the sample inlet. One fitting of the T-joint (Figure 9, point C) was connected to the original sample inlet (Figure 9, point A), whereas the opposite fitting (Figure 9, point E) was connected to a 1-m Teflon tube which was connected to a $0.5\ \text{bar}$, grade-5 nitrogen. The third fitting (Figure 9, point D) was capped with a septum and served as the new sample injection inlet. A $500\text{-}\mu\text{l}$ gas-tight syringe (Hamilton, Europe) was used to collect the headspace samples ($500\ \mu\text{l}$ per analysis) from the sample vials and to inject them into the miniaturized GC-DMS through the new fitting (Figure 9, point D).

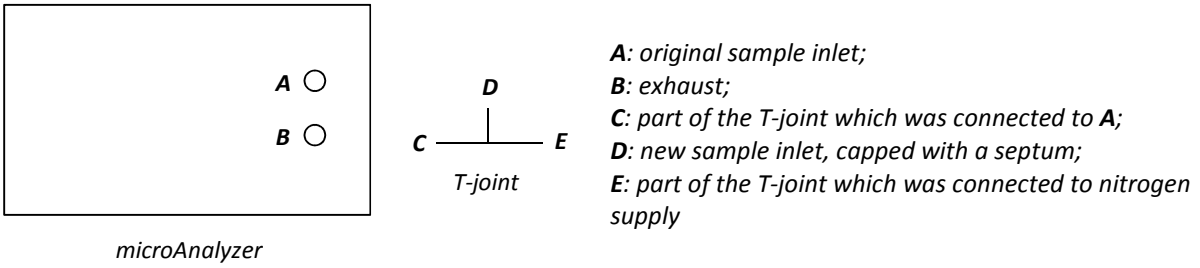

Figure 9. Schematic diagram of the modified sample introduction system

2.2.2.2 Loading stage (chromatographic separation)

After the $30\ s$ sampling, a 3-way valve can be programmed to allow the flow of the transport gas ($1\text{-}5\ \text{ml/min}$) through the pre-concentration trap and the GC column. During this loading stage (Figure 8, middle frame) the pre-concentration trap is heated to allow the desorption of the chemicals of interest from the trap to the GC column [161].

In this work, the temperature of the pre-concentration trap was programmed as follow: starting at the 30^{th} seconds of the whole stages, the initial temperature was set at $40\ ^\circ\text{C}$, and then it was increased to $200\ ^\circ\text{C}$ in $1\ s$, to $300\ ^\circ\text{C}$ in $4\ s$, and then was held at $300\ ^\circ\text{C}$ for $100\ s$. The sample was then passed through the GC column to allow a nominal pre-separation of analytes. The GC was equipped with a $10\text{-m} \times 0.25\text{-mm} \times 0.25\text{-}\mu\text{m}$ DB-XLB column (Agilent Technologies). The GC column temperature was programmed as follow: the

initial temperature was set at 60 °C and held for 60 s, increased 1 °C /s to 140 °C, and then held at 140 °C for 200 s.

2.2.2.3 Analyzing stage (microDMx detection)

In this stage, the trap is cooled and the chemicals of interest are introduced into the microDMx sensor based on their individual retention times (Figure 8, bottom frame). In the microDMx, an oscillating asymmetric RF electric field (1 MHz and ranging from 500 to 1500 V, which is equivalent to 10-30 kV/cm) and a DC compensating electric field are applied across two parallel plates that are 0.5 mm apart. The microDMx setting in this stage is explained in the following sections (2.2.2.3.1 and 2.2.2.3.2) according to the objectives of each section.

2.2.2.3.1 Analysis of GC-DMS spectra of the standard compounds

Prior to do a dispersion voltage study, headspace analysis of standard solution of each compound was performed to locate their retention time. For each analyte of the 12 compounds, 10 ml of 1 g/l of solution (equivalent to 1000 ppm) was prepared separately in ultra pure water (18.2 MΩ, Millipore) and placed in a 20-ml vial. The headspace gases were analyzed using the miniaturized GC-DMS. Before the headspace gases were injected, 100 blank spectra were collected and each analyte was measured in triplicate.

To locate the retention time of each individual compound at a given RF voltage, the setting of the microDMx was set as follow: the sensor temperature was set at 80 °C, the RF voltage was set at 1100 V (corresponds to 22 kV/cm), and the compensation voltage scanning range was set at full scanning range, i.e. from -40 to +15 V.

2.2.2.3.2 Dispersion voltage study

To determine the effect of RF voltage on signal separation and intensity, dispersion voltage study on mixtures of the 12 compounds was performed using incremental method. For each analysis, mixture of the 12 compounds with equimolar concentration (each 1 g/l or 1000 ppm) in water was used as sample. For the dispersion voltage study, the following microDMx setting was used: the sensor temperature was set at 80 °C, the RF voltage was varied from 900 (18 kV/cm) to 1400 V (28 kV/cm) with an increment of 100 V. The compensation voltage scanning range was set at first at a full scanning range (from -40 to

+15 V). After all compensation voltage values of each compound at all RF voltage variation were determined, the dispersion voltage study was repeated in a more narrow scanning range which covered all compensation voltage of all compounds, i.e. from -13 to +5 V.

2.2.3 Data Analysis

For each analysis, during the experiment the GC-DMS spectra corresponding to the detected positive and negative ions were recorded using Expert™ and the chromatographic data was automatically stored as Microsoft Office Excel workbook. The data collected using the Expert™ software was then processed using IGOR Pro 6. The IGOR Pro 6 was also used to generate the GC-DMS spectra and to generate various types of graphs.

In generating several retention time and compensation voltage graphs (such as shown in the Result and Discussion section, e.g. in Figure 10, Figure 11, and Figure 12), Gaussian curve fitting function was applied. For each graph, the original retention time profile is shown as a green curve, whereas the after-filtered profile (fitted using Gaussian function) is shown as a red curve. All data processing was done using the IGOR Pro 6.

2.3 Results and Discussion

2.3.1 Analysis of GC-DMS spectra of the standard compounds

Prior to do the incremental dispersion voltage study, a qualitative headspace analysis of standard solution of each compound was performed at a fixed RF voltage, i.e. 1100 V (equal to 22 $\mathrm{k}V/\mathrm{cm}$) to locate the retention time of each compound. The GC-DMS spectra for all compounds are given in Figure 10, Figure 11, and Figure 12 and are presented based on the sequence of their retention time:

- GC-DMS spectra of the first 4 compounds (2,5-dimethyltetrahydrofuran, $\boldsymbol{t_r = 50.70\ s}$; dimethyl disulfide, $\boldsymbol{t_r = 52.85\ s}$; 2-heptanone, $\boldsymbol{t_r = 62.02\ s}$; and 2,5-dimethylpyrazine, $\boldsymbol{t_r = 66.56\ s}$) are given in Figure 10;
- GC-DMS spectra of the next 4 compounds (benzaldehyde, $\boldsymbol{t_r = 76.24\ s}$; dimethyl trisulfide, $\boldsymbol{t_r = 77.05\ s}$; 2-nonanone, $\boldsymbol{t_r = 104.17\ s}$; and nonanal, $\boldsymbol{t_r = 112.70\ s}$) are given in Figure 11;

- GC-DMS spectra of the last 4 compounds (decanal, $\boldsymbol{t_r = 178.09\ s}$; undecanone, $\boldsymbol{t_r = 193.26\ s}$; indole, $\boldsymbol{t_r = 200.34\ s}$; and 2-tridecanone, $\boldsymbol{t_r = 303.55\ s}$) are given in Figure 12.

For each analyte, the retention time and the compensation voltage profiles are given on the left and right frame of the figures, respectively.

As seen in Figure 10 - Figure 12 (compensation voltage profiles on the right frames), at $1100\ V$ RF voltage, the reactant ion positive (RIP) is located at $C_v = -16.67\ V$. In addition to this RIP, in all compensation voltage profiles, there seems to be another unidentified peak, i.e. located at $C_v = -23.89\ V$. This is not the peak of analyte, rather an unknown background which resembles a secondary RIP. Example of this unknown peak is given in Figure 13 for the first 3 compounds (2,5-dimethyltetrahydrofuran, dimethyl disulfide, and 2-heptanone). The unknown peaks are highlighted in blue circles and the original spectra are marked with blue arrows. This peak appeared in every compensation voltage profile for all the 12 compounds and should not be confused with peak of analytes.

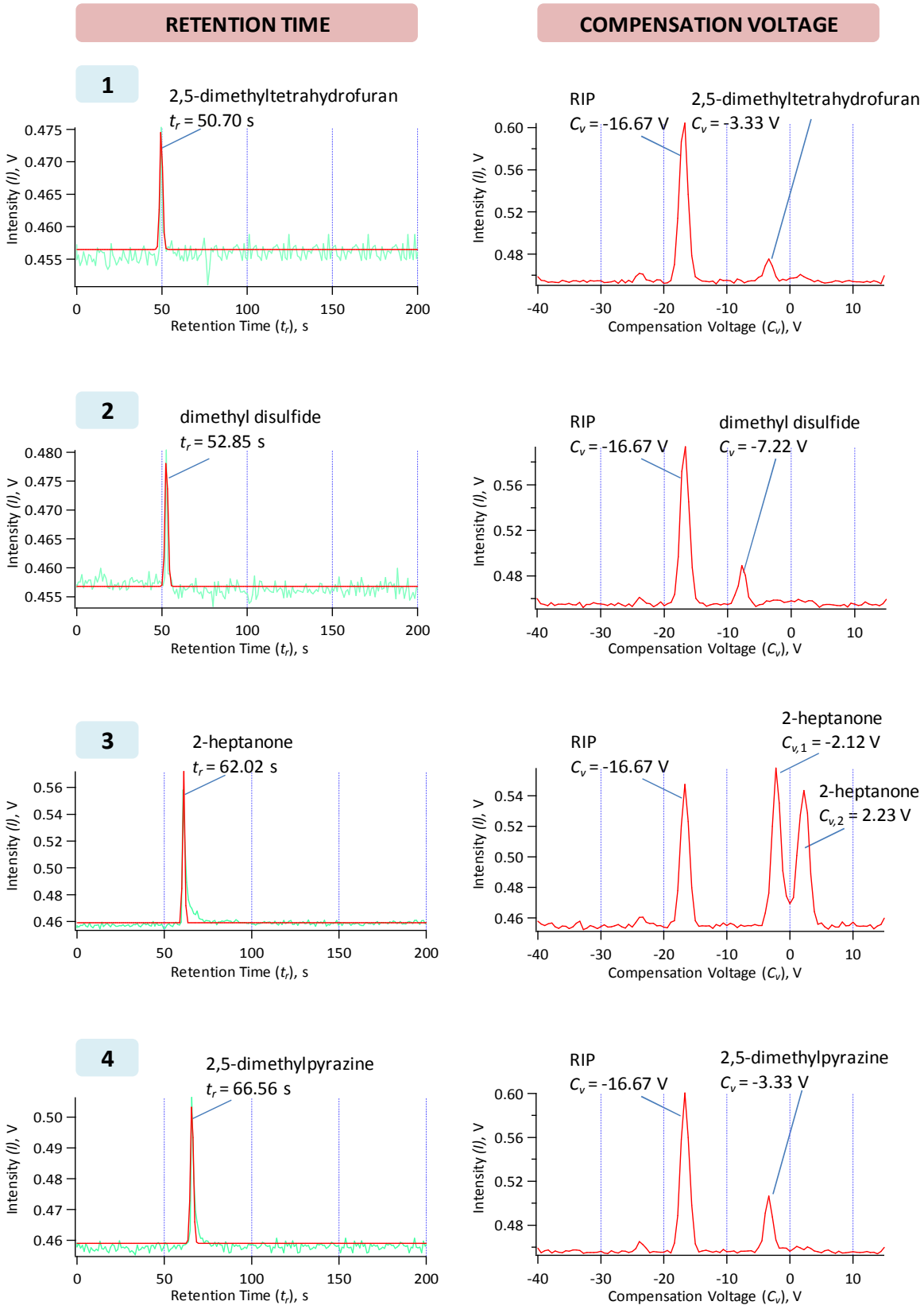

Figure 10. GC-DMS spectra of (1) 2,5-dimethyltetrahydrofuran, (2) dimethyl disulfide, (3) 2-heptanone, and (4) 2,5-dimethylpyrazine at $1100\ V$ RF voltage

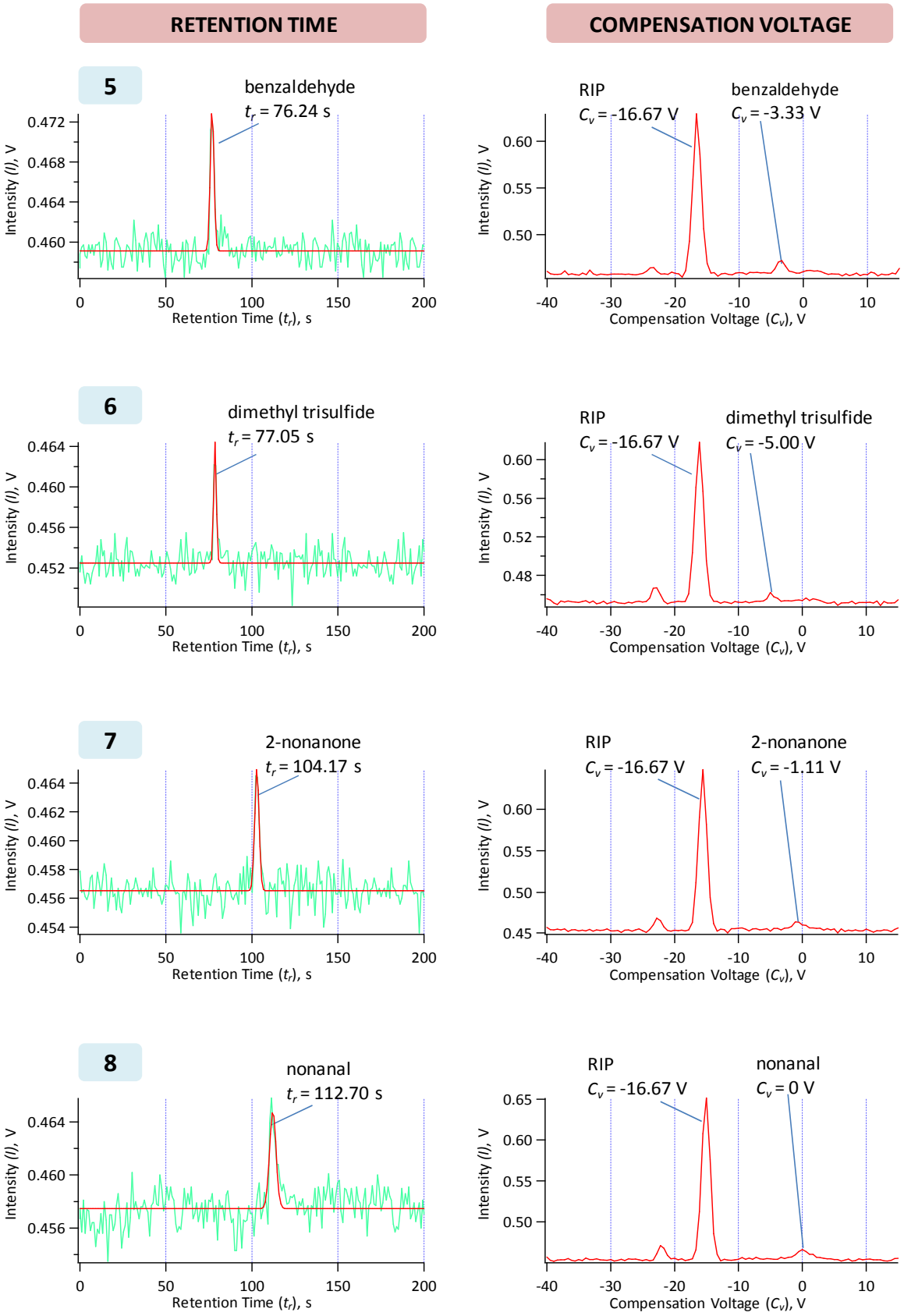

Figure 11. GC-DMS spectra of (5) benzaldehyde, (6) dimethyl trisulfide, (7) 2-nonanone, and (8) nonanal at $1100\ V$ RF voltage

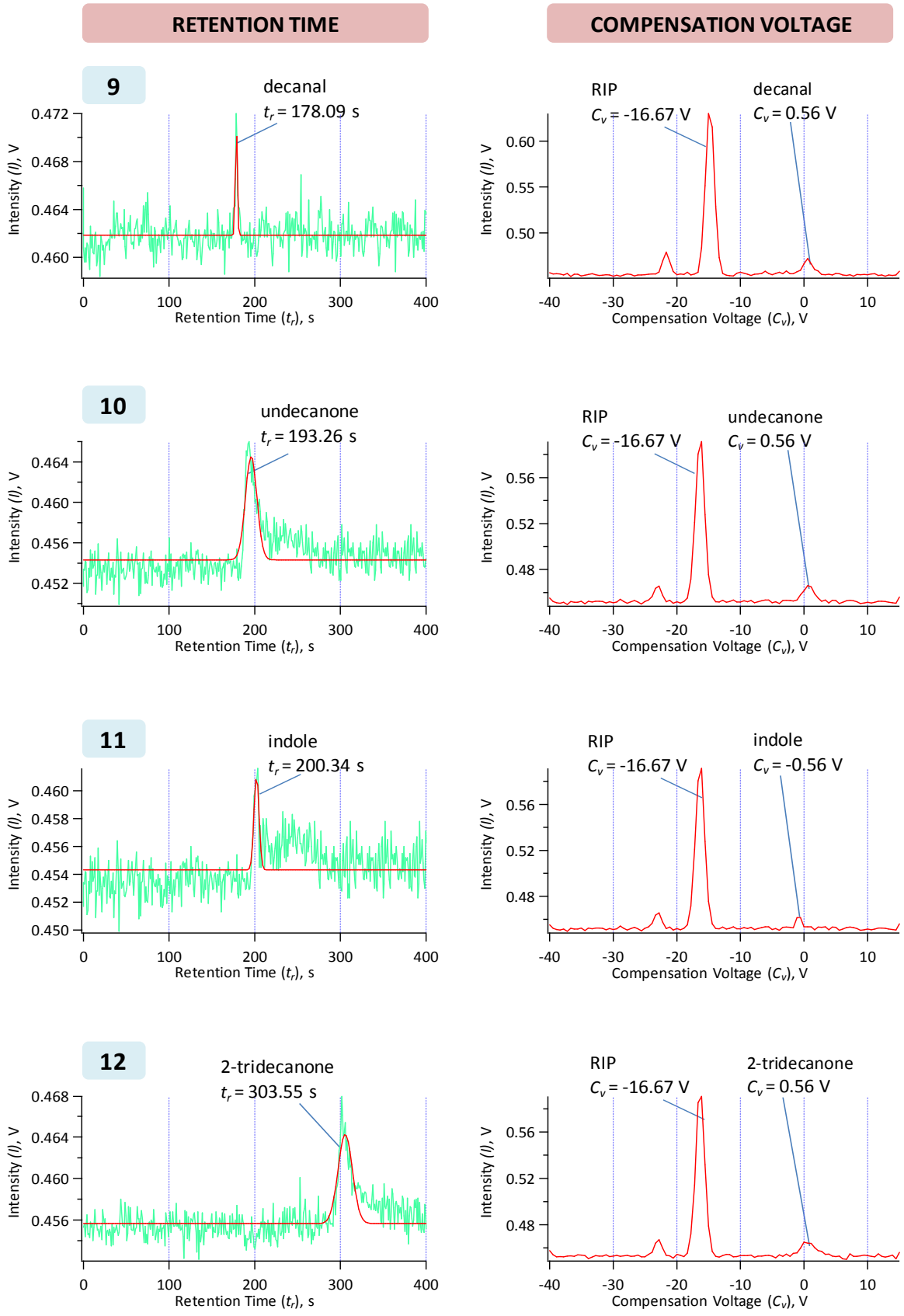

Figure 12. GC-DMS spectra of (9) decanal, (10) undecanone, (11) indole, and (12) 2-tridecanone at 1100 *V* RF voltage

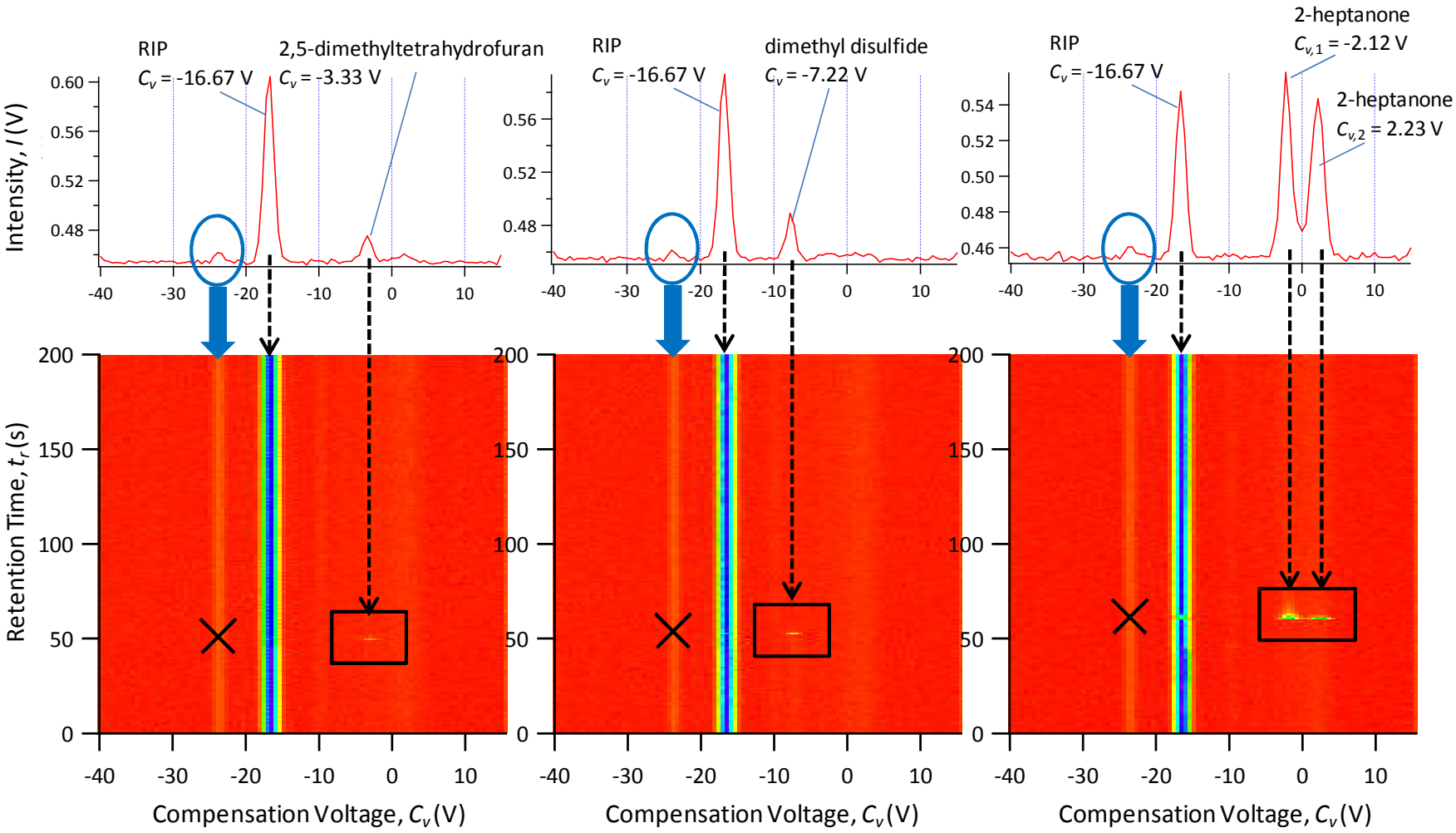

Figure 13. Illustration of the unknown background peaks

As also seen in Figure 10 - Figure 12 (compensation voltage profiles on the right frames), for each analyte, peak of monomer was observed at various compensation voltages. In case of 2-heptanone (compound no. 3), besides a monomer, a dimer peak was also observed. Although spectra of all compounds were recorded both on positive and negative modes, spectra of all peaks only appeared in the positive mode. The retention time and compensation voltage values of all compounds are summarized in Table 3.

Table 3. Observed GC-DMS retention time and compensation voltage of the standard compounds (representing synthetic biomarker compounds of *E. coli*) at $1100\ V$ RF voltage

No.	Compounds	Result from this study				Result from literature (Yu et al. 2000) [6]
		Compensation Voltage		Retention Time		Retention Time, t_r (min)
		$C_{v,1}$ (V)	$C_{v,2}$ (V)	t_r (s)	t_r (min)	
-	Reactant ion positive (RIP)	-16.67	-	-	-	-
1	2,5-dimethyltetrahydrofuran	-3.33	n/a	50.70	0.85	13.36; 14.01
2	dimethyl disulfide	-7.22	n/a	52.85	0.88	16.54
3	2-heptanone	-2.12	2.23	62.02	1.03	28.32
4	2,5-dimethylpyrazine	-3.33	n/a	66.56	1.11	30.27
5	benzaldehyde	-3.33	n/a	76.24	1.27	35.12
6	dimethyl trisulfide	-5.00	n/a	77.05	1.28	36.40
7	2-nonanone	-1.11	n/a	104.17	1.74	46.31
8	nonanal	0.00	n/a	112.70	1.88	47.43
9	decanal	0.56	n/a	178.09	2.97	55.86
10	2-undecanone	0.56	n/a	193.26	3.22	62.70
11	indole	-0.56	n/a	200.34	3.34	63.55
12	2-tridecanone	0.56	n/a	303.55	5.06	77.22

As can be seen in Table 3 and Figure 10 - Figure 12, the retention time of each compound is relatively short, with the first 2 compounds appeared within $1\ min$ and the last compound (the 12th compound) appeared shortly after $5\ min$. Some compounds (i.e. compound no. 1 and 2 and compound no. 5 and 6) have very close retention times with each other, i.e. one compound appeared within $3\ s$ after the other. The peaks of such compounds would usually overlap with each other. However, as the compounds have different compensation voltages, the peaks are located apart and easily distinguished from each other. As a comparison, result

from another study (Yu et al. (2000) [6]) is also presented in Table 3. The sequence of the appearance of the compounds in this study is the same to the other study, but the retention times of the compounds in this study is much shorter, with the latest compound appeared at $5.06\ min$, compared to $77.22\ min$ in the other study. This is due to the use of much shorter GC column (i.e. a $10\text{-m} \times 0.25\text{-mm}$ DB-XLB column, as opposed to the other study, which used a $60\text{-m} \times 0.32\text{-mm}$ fused silica DB-5 column). Therefore, the additional dimensional data in DMS operation (i.e. the compensation voltage data) allows a much shorter analysis time.

In reviewing peaks of all 12 compounds in Figure 10 - Figure 12, in which the RF voltage was set at a fixed value, i.e. $V_{rf} = 1100\ V$, peaks of ions with short retention time tend to appear at negative C_v, whereas peaks of ions with longer retention time tend to centered around zero C_v. To understand the dependence of compensation voltage on RF voltage, a dispersion voltage study is needed. The result is presented in the next section.

2.3.2 Dispersion voltage study

Dispersion voltage study was performed to determine the effect of RF voltage on compensation voltage and to determine the optimum RF voltage and compensation voltage range for the mixture of the 12 compounds. The RF voltage (V_{rf}) was varied from 900 to $1400\ V$ (18 to $28\ kV/cm$) with an increment of $100\ V$. The spectra of the analytes at $V_{rf} = 1100\ V$ to $V_{rf} = 1400\ V$ (22 to $28\ kV/cm$) are given in Figure 14 (left frame), whereas the peak location of each analyte at every RF voltage variation is plotted and shown in the right frame. Each analysis was conducted for $500\ s$ and signal for each compound in the analytes was observed within $200\ s$, except for undecanone, indole, and 2-tridecanone, which were undetected even though the spectra was recorded until $500\ s$.

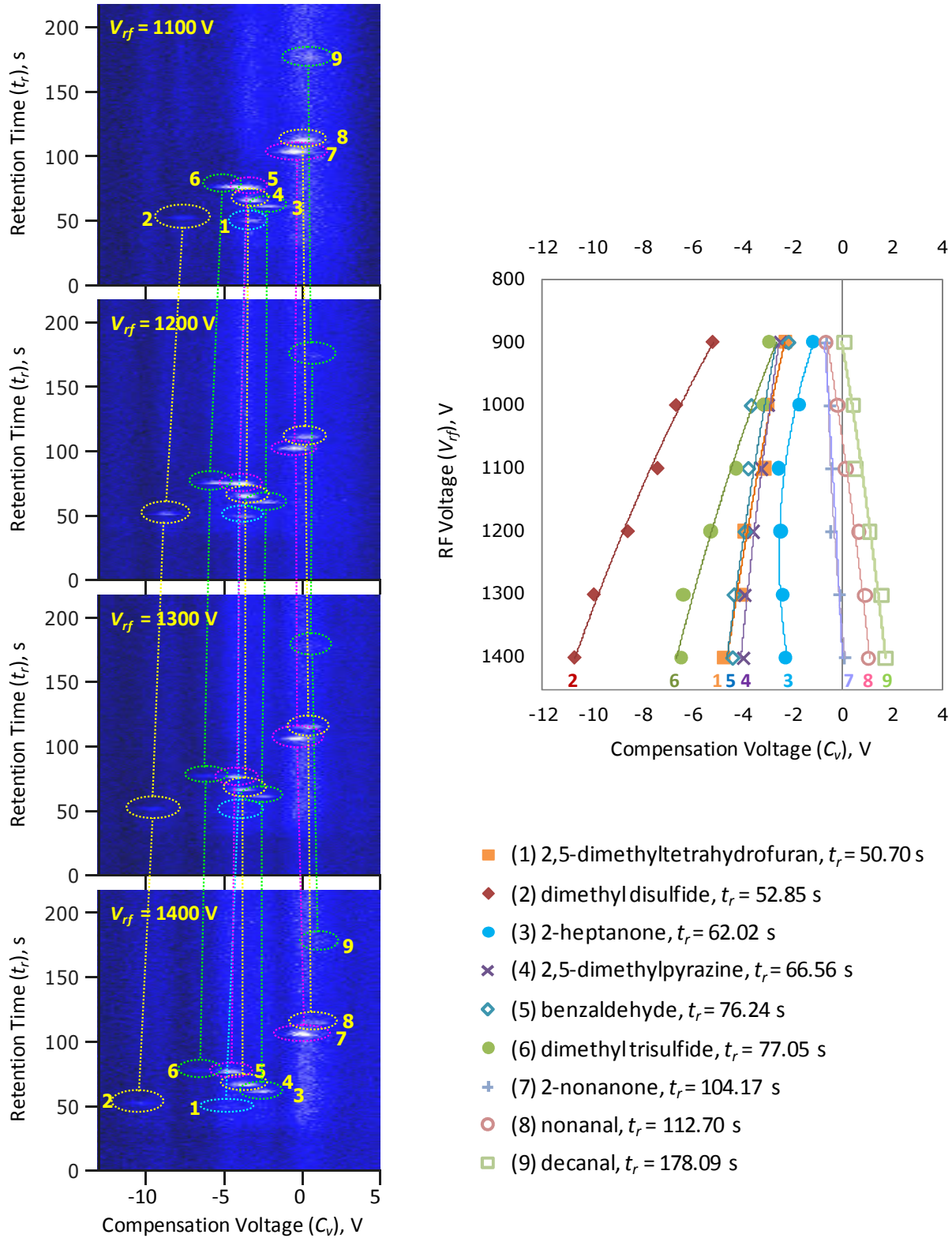

Figure 14. Dependence of the compensation voltages of synthetic biomarker compounds of *E. coli* on RF voltages showing the broadening of the distance among each peak at increasing RF voltage

As presented in the earlier section, the retention time of undecanone, indole, and 2-tridecanone which were prepared as a single compound in water are $193.26\ s$, $200.34\ s$, and $303.55\ s$, respectively. There are a couple of reasons why these signals were not observed in the spectra of mixture of compounds. First, due to the modification of the sample introduction system, the concentration of the headspace sample entering the system was actually much lower than that inside the sample vials due to the dilution by nitrogen gas. As explained in the Materials and Methods (instrumentation and operational setting section), instead of collecting $80\ ml/min$ analyte directly from the environment, the sample pump collected $80\ ml/min$ nitrogen gas, whereas 500 µl analyte was spiked/injected into the stream of nitrogen gas using a gas-tight syringe to avoid contaminants. By operating the sample pump for $30\ s$ per analysis, the sample pump only collected 500 µl headspace of analyte (from a $20-ml$ vial containing $10\ ml$ of $1\ mg/ml$ mixture of analyte solution), in addition to $40\ ml$ nitrogen.

The second reason is the low volatility of the undetected compounds. The inverse Henry's constant, $K_{H,inv}$, representing volatility of each compound [162] is given in Table 4 (except for compound $\#1, \#4, \#6, \#7$, and $\#12$ which were not available). As shown in Table 4, two of the undetected compounds (compound $\#10$ and $\#11$) have very low volatility compared to other compounds. Unfortunately there are no volatility data available for the third undetected compounds, 2-tridecanone. However, since the inverse Henry's constant represents the partial pressure of the gas-phase composition divided by the aqueous-phase composition, the vapor pressure of each compound (which represents both the total and partial pressure of each compound if the compound is prepared as a single compound) might as well explain the non-existence of the last three compounds signals. The vapor pressure data of the single compound is also given in Table 4. Overall, although the concentrations of the compounds prepared in the aqueous solution were equimolar, compounds with lower volatility would have lower concentrations in the headspace and in this case the instrument was not sensitive enough to detect the compounds.

Table 4. Detection of synthetic *E. coli* biomarkers signals by microAnalyzer™

No	Compounds	Molecular Structure	Vapor Pressure, P ($mmHg$ at 25 °C)	Molecular Weight, Mr ($\frac{gr}{mol}$)	Inverse Henry's constant, $K_{H,inv}$ ($\frac{atm.m^3}{mol}$at $T = 298.15K$ and $\rho_{H_2O} = 997\ \frac{kg}{m^3}$)	Signal	Retention Time, t_r (s)
1	2,5-dimethyl-tetrahydrofuran	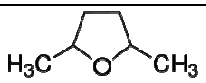	62.10	100.16	n/a	+	50.70
2	dimethyl disulfide	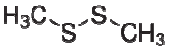	0.75	94.20	1.21×10^{-3}	+	52.85
3	2-heptanone	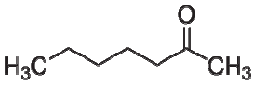	2.13	114.19	1.69×10^{-4}	+	62.02
4	2,5-dimethyl-pyrazine	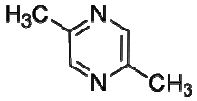	3.75	108.14	n/a	+	66.56
5	benzaldehyde	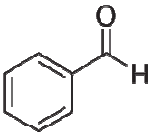	3.75	106.12	2.67×10^{-5}	+	76.24
6	dimethyl trisulfide	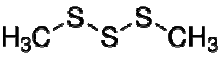	1.07	126.26	n/a	+	77.05
7	2-nonanone	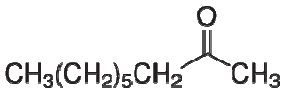	0.65	142.24	n/a	+	104.17
8	nonanal	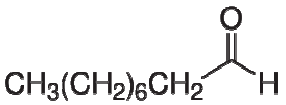	0.26	142.24	7.3×10^{-4}	+	112.70
9	decanal	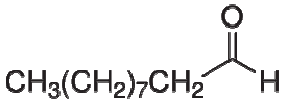	0.15	156.27	5.87×10^{-5}	+	178.09
10	2-undecanone	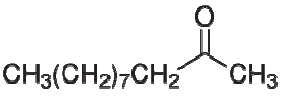	0.04	170.30	6.36×10^{-5}	-	-
11	Indole	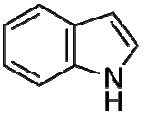	0.01	117.15	5.3×10^{-7}	-	-
12	2-tridecanone	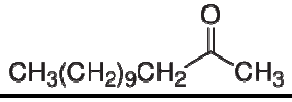	0.02	198.35	n/a	-	-

The dependence of the compensation voltage (and hence the peak separation) on RF voltage is also shown in the previous figure (Figure 14). As shown by this figure, the peak separation is improved at increasing RF voltage (as shown by the broadening of the distance between

each peak with the increase in RF voltage, or shown by the higher difference of compensation voltage between each peak with the increase in RF voltage). This is because at higher RF voltage the amplitude of the "zigzag" motion of the ions is increasing, and therefore the compensation voltages required by each ion to keep their net movement centered along the longitudinal axis of the ion filter region are also higher. As a result, the peaks were shifted farther from each other. In conclusions, the peak separation is best achieved at the highest RF voltage.

Although the peak separation is best achieved at the highest RF voltage, at higher RF voltage the peaks have lower intensity, as shown in Figure 15. This is because, at higher RF voltage, the amplitude of the "zigzag" motion of the ions is increasing, and, therefore, the possibility for each ion to touch the parallel plates is also increasing. Ions that touch the parallel plates are neutralized and passed through the electrometers without being detected.

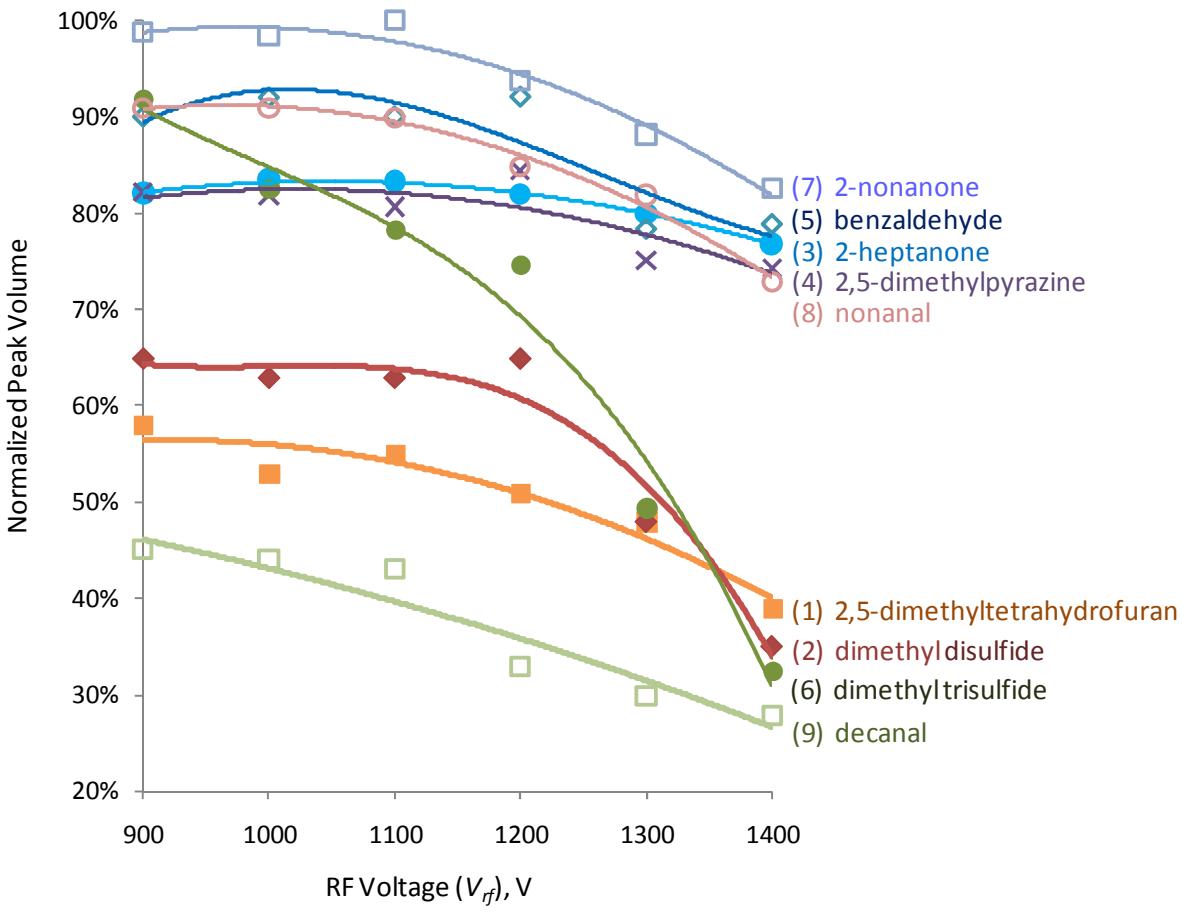

Figure 15. Dependence of intensity (expressed as normalized peak volume) of mixtures of compounds on RF voltage

Similar result on dispersion voltage study has been reported by Rearden [137]. In dispersion voltage study on benzene, MTBE, toluene, m-xylene, and p-xylene using GC-DMS at dispersion voltages of $900\,V$, $1100\,V$, $1200\,V$, $1300\,V$, and $1500\,V$, similar trend was reported by the author: peaks of analytes tend to shift towards more broadening range of compensation voltages at higher RF voltages, while the intensities simultaneously decreasing.

Since the increase in RF voltage gives a higher degree of peaks separation but lower signals intensity, the RF voltage should be optimized. For the 12 compounds being analyzed in this study, as can be seen in Figure 14 (right frame), a significant broadening of the distance among each peak is seen at $V_{rf} = 1200\,V$ ($24\,kV/cm$), as shown by the shift of compounds no. 3 and 6 from compounds no. $1, 4$, and 5, and by the shift of compound no. 7 from compound no. 8. At $V_{rf} > 1200\,V$, the peak separation does not change much (peaks of compounds no. $1, 4$, and 5 are still located next to each other and so does the peak of compounds no. 8 and 9). Therefore, $V_{rf} = 1200\,V$ ($24\,kV/cm$) is optimum.

In this work, no real *E. coli* samples were used because, to do a dispersion voltage study, it is necessary to use standard compounds which could be used further as references. Although only qualitative investigation have been carried out and no real *E. coli* samples were used in this stage, this particular work demonstrates the potential application of the miniaturized GC-DMS for the detection of several *E. coli* biomarkers. However, since some compounds (undecanone, indole, and 2-tridecanone) could not be detected, this method is not suitable to detect *E. coli* which produced such compounds (i.e. *E. coli* which were grown in BHI broth medium [6]).

Several studies have shown that the types of volatile compounds released by bacteria are medium dependent. Depending on their culturing mediums, besides releasing the 12 compounds discussed in this chapter, *E. coli* could also release other kinds of compounds. For example, *E. coli* grown on LB broth and LB agar produced ketone compounds [4, 5]; *E. coli* grown on Minimal medium produced hexane, benzaldehyde, butan-1-ol, ethanol, acetone, and several ketone compounds (hexan-2-one, heptan-2-one, and nonan-2-one) [5]; *E. coli* grown on tryptic soy broth (TSB) produced ethanol, 1-propanol, 3-methyl-1-butanol, octanol, 9-decene-1-ol, decanol, indole, dodecanol, cis-7-tetradecene-1-ol, and tetradecanol

[5, 163]; and *E. coli* grown on Colilert-18® produced *o*-nitrophenol [127]. To improve the performance of the miniaturized GC-DMS in detecting *E. coli*, a suitable cultivation medium need to be determined. A suitable medium is one that could grow *E. coli* in such a way that the *E. coli* would produce unique biomarkers and the biomarkers are easily detected and identified by the miniaturized GC-DMS. For this purpose, the next chapter will deal with the determination of the suitable cultivation medium.

2.4 Conclusions

The miniaturized GC-DMS was simple to use and could be used to detect several standard compounds (2,5-dimethyltetrahydrofuran, dimethyl disulfide, 2-heptanone, 2,5-dimethylpyrazine, benzaldehyde, dimethyl trisulfide, 2-nonanone, nonanal, decanal, undecanone, indole, and 2-tridecanone) within a relatively short time (below $6\,min$). Dispersion voltage study on the 12 compounds showed that the higher the RF voltage, the better the separation among the peaks, but the poorer the signals intensity. RF voltage which gave optimum peaks separation and signal intensity for the 12 compounds was $1200\,V$ (corresponds to $24\,kV/cm$).

When the 12 standard compounds used in this study (known also as *E. coli* metabolites that were grown in BHI broth in another study) were prepared as single compounds, headspace analysis of those compounds could result in the signal spectra of monomer peaks of each compound and, in case of 2-heptanone, both the monomer and dimer peaks. Compounds with lower molecular masses tend to have shorter retention time and negative compensation voltages, whereas compounds with higher molecular masses tend to have longer retention time and around-zero compensation voltage. However, when prepared as mixture of compounds, headspace analysis of the 12 compounds could only result in monomer peaks of compounds with relatively high volatility. Several compounds with low volatility (undecanone, indole, and 2-tridecanone) could not be detected.

Since several compounds (including indole, which is an important *E. coli* biomarker) could not be detected and the rest of the compounds are not specific enough for identification of *E. coli* and since the types of volatile compounds produced by *E. coli* are medium dependent,

a suitable cultivation medium need to be determined. For this purpose, the next chapter will deal with the determination of the suitable cultivation medium.

3 Determination of suitable cultivation medium based on the biomarkers released by *Escherichia coli* in the different media and their detection by GC-DMS and GC-MS

3.1 Introduction

As bacteria grow and proliferate, they release a variety of volatile compounds that can be profiled and used for their identification and speciation [4]. The identification could be done through the presence/absence of biomarker compounds (i.e. compounds that are seen as the indicators of the bacteria presence/absence) [123, 135] and through comparisons of chromatograms as fingerprints (pattern recognition) [132, 133]. Concerns over reliability of bacterial taxonomy with chemical analysis by instrumentation exist in both approaches (biomarker and fingerprint analysis) [132]. These are usually associated with variations, particularly in temperature of growth [132, 164], cell age [165], and food sources [4, 132, 166]. In the absence of rigorous control of these variations, fingerprint methods are disqualified since libraries are rendered unreliable from changes in the chemical components of bacteria [132].

As discussed in Chapter 2, under the applied experimental design, it was not possible to detect several standard compounds (indole, undecanone, and 2-tridecanone) in the mixture of 12 compounds being examined due to the low volatility of several compounds. The 12 compounds are known as metabolites produced by *E. coli* bacteria grown in BHI broth reported in another study [6]. Since indole is an important biomarker (as mentioned in the classical taxonomy of *E. coli* [2, 24, 41]), it is necessary to determine a suitable cultivation medium which could produce other unique and detectable volatile biomarker(s).

In reviewing different types of culture media for coliform and *E. coli* growth and different types of coliform and *E. coli* identification and quantification methods, it was found that, since some studies reported that not all coliform bacteria can ferment lactose [25, 26] and some *E. coli* strains neither ferment lactose nor produce indole [26], the classical taxonomy of coliform and *E. coli* need to be revised. Advances in molecular methods and sequencing

have recently redesigned coliform taxonomy based on their enzymatic activities. In brief, the taxonomy can be described as [2, 23, 25, 27-30]:

- **coliform** bacteria are characterized by the presence of **β-galactosidase** enzyme
- ***E. coli*** bacteria are characterized by the presence of **β-glucuronidase** enzyme

Since *E. coli* is also a species of coliform, *E. coli* is characterized by the presence of both β-galactosidase and β-glucuronidase enzymes.

To detect and enumerate coliform and *E. coli* through the presence of β-galactosidase and β-glucuronidase enzymes, several commercial test kits have been developed. Colilert-18® is among the most widely used commercial test kit. It employs chromogenic and fluorogenic substrates to produce color and fluorescence effects, respectively, upon cleavage by the above mentioned enzymes in the bacteria [2].

In Colilert-18® method, the detection of coliform and *E. coli* bacteria is confirmed based on the following enzymatic reactions through the use of chromogenic substrate, O-Nitrophenyl-β-D-galactopyranoside (ONPG), and fluorogenic substrate, 4-methylumbelliferyl-β-D-glucoronide (MUG) [27]:

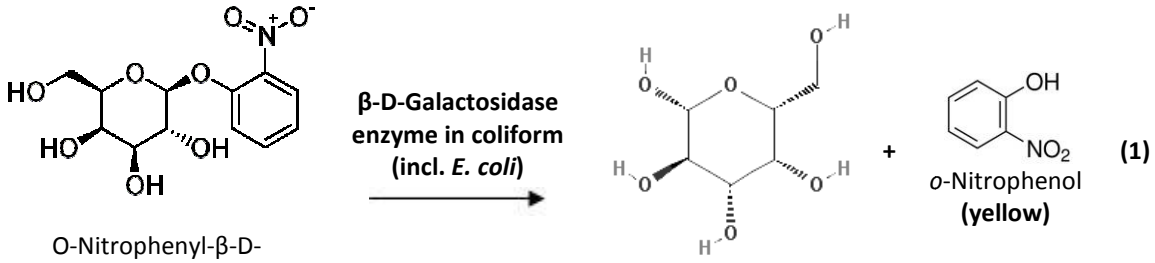

O-Nitrophenyl-β-D-galactopyranoside (ONPG)

β-D-Galactose

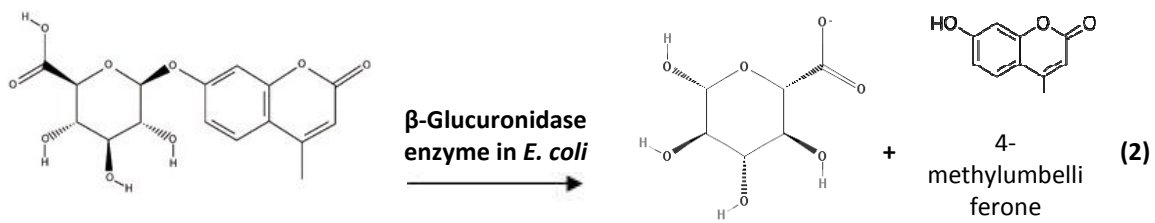

4-methylumbelliferyl-β-D-glucoronide (MUG)

β-D-Glucuronate

In reaction (1), in the presence of ONPG substrate, the β-D-Galactosidase in coliform bacteria (including *E. coli*) would hydrolyse the ONPG, producing a yellow substance, ***o*-nitrophenol**. In reaction (2), in the presence of MUG substrate, the β–glucuronidase in *E. coli* would break the bonds of MUG, producing a fluorogenic compound, **4-methylumbelliferone**, which can be visualized or detected by irradiation with UV light [27]. These changes could be distinguished after $18\,h$ and used as indicators of the absence/presence of coliform and *E. coli* in water sample. As such, *o*-nitrophenol and 4-methylumbelliferone could be used as biomarkers of coliform and *E. coli* grown in a specific controlled environment.

This chapter deals with the detection and identification of coliform and *E. coli* using the miniaturized GC-DMS based on the presence/absence of *o*-nitrophenol and 4-methylumbelliferone as biomarkers. Although *o*-nitrophenol and 4-methylumbelliferone were the only target compounds, the bacteria might release other compounds as well. Therefore, all detected compounds released by the bacteria need to be identified. The identification was done at first using GC-MS. As mentioned in Chapter 1, one of the main disadvantages of the GC-DMS is the non-existence of compounds library which could be used for compounds identification. For this purpose, GC-MS was used for initial compounds identification. After the compounds identity is known, standard solutions of the compounds were prepared and analyzed by the GC-DMS. The retention time and compensation voltage of the compounds released by bacteria and detected by the GC-DMS were then compared to the retention time and compensation voltage of the compounds prepared from the standard solutions and detected by the GC-DMS. Colilert-18® was used as the medium to grow the bacteria. As a comparison to other media, besides Colilert-18®, four other media known to be selective for *E. coli* growth (namely tryptophan broth, Tryptic Soy Broth (TSB), glucose broth, and M9-medium) were also used and investigated and the result is also presented in this chapter.

3.2 Experimental Section

3.2.1 Reagents and Samples

3.2.1.1 Chemicals

o-Nitrophenol (98%), 4-methylumbelliferone ($\geq 98\%$), and indole ($\geq 99\%$) were purchased from Sigma-Aldrich (Steinheim, Germany) and used as received.

3.2.1.2 Bacteria

Escherichia coli DSM 30083 was obtained from the *Deutsche Sammlung von Mikroorganismen und Zellkulturen* (DSMZ) GmbH, Braunschweig, Germany. Prior to use, the bacteria was grown on NB agar and incubated overnight at $37\ ^{\circ}C$.

3.2.1.3 Growth Media

The following growth media were used and were prepared freshly. Except for Colilert-18® (which was prepared according to manufacturer instruction), all other media were prepared according to recipes from *Handbook of Microbiological Media* by Atlas et al. (2010) [167].

- **Colilert-18®**: 4 packages of Colilert-18® (IDEXX, cat. nr. WPO2OI-18) were used in this experiment. Each package was dissolved in $100\ ml$ of sterile deionized water as per manufacturer instruction.
- **Tryptic Soy Broth (TSB)**: $4.5\ g$ of a premixed powder of TSB (Merck, 1.05459.0500) was dissolved in $150\ ml$ of deionized water and autoclaved for $15\ min$ at $15\ psi$ pressure and at $121\ ^{\circ}C$.
- **Glucose broth**: $1\ g$ of meat peptone (Oxoid, LP0034), $0.3\ g$ of meat extract (Oxoid, LP0029), and $0.5\ g$ of NaCl (Prolabo, 27810.295) were dissolved in $100\ ml$ deionized water. The pH was adjusted to 7.2, the volume was brought to $142.5\ ml$, and then autoclaved. Shortly before use, $7.5\ ml$ of sterile M9-glucose-solution was added to it.
- **M9-medium**: the following compounds were firstly dissolved in $100\ ml$ of deionized water: $0.7\ g$ of $Na_2HPO_4{\cdot}2H_2O$ (Riedel-de Haën, 30412), $0.3\ g$ of KH_2PO_4 (Fluka, 60218), $0.1\ g$ of NH_4Cl (Riedel-de Haën, 31107), and $0.05\ g$ of NaCl (Prolabo, 27810.295). The solution was then brought into $132\ ml$ using deionized water and

was autoclaved. The following solutions were then prepared and autoclaved separately: $10\ g$ of D(+)-Glucose (Oxoid, LP0071) in $50\ ml$ of deionized water, $2.465\ g$ of $MgSO_4 \cdot 7H_2O$ (Fluka, 63142) in $10\ ml$ of deionized water, and $0.2\ g$ of $CaCl_2 \cdot 2H_2O$ (Fluka, 21101) in $10\ ml$ of deionized water. Shortly before use, $15\ ml$ of the $D(+)$ −Glucose solution, $1.5\ ml$ of the $MgSO_4 \cdot 7H_2O$ solution, and $1.5\ ml$ of the $CaCl_2 \cdot 2H_2O$ solution were added into the first solution.

- **Tryptophan broth**: $2.4\ g$ of DEV-tryptophan (Merck, 1.10694.0500) was dissolved in $150\ ml$ of deionized water, adjusted into pH 7.2, and was autoclaved.

Each growth medium was then distributed into 20-ml headspace vials. The volume of the medium in each headspace vial was $10\ ml$. Some of these growth media were later inoculated by the bacteria; some others were kept as blank samples. For each analysis, the samples were made in triplicates.

3.2.2 Instrumentation

3.2.2.1 GC-DMS

The experimental setup consisted of a miniaturized GC-DMS (microAnalyzer™ from the Sionex, USA) connected to a $0.5\ bar$ nitrogen gas supply. The operational principle of the instrument has been described (in Chapter 2). The instrumentation setting for *the sampling and loading stages* used in the earlier work was applied in this work without modifications and can be summarized as follow: the suction pump was operated for $30\ s$, the flow rate of the suction pump was $80\ ml/min$, and the flow rate of the transport gas (the recirculation air) was $300\ ml/min$. Headspace sample ($500\ \mu l$ per analysis) was injected manually into the stream of nitrogen gas entering the sample inlet using a $500\mu l$-gas-tight syringe. In the loading stage, the temperature of the pre-concentration trap was programmed as follow: the intial temperature was set at $40\ °C$, and then it was increased to $200\ °C$ in $1\ s$, to $300\ °C$ in $4\ s$, and then was held at $300\ °C$ for $100\ s$. The sample was then passed through the GC column. The GC column temperature was programmed as follow: the initial temperature was set at $60\ °C$ and held for $60\ s$, increased $1\ °C/s$ to $140\ °C$, and then held at $140\ °C$ for $200\ s$.

In the analyzing stage (DMS detection), the operating parameters were set as follow: the RF voltage was set at $1100\,V$, the sensor temperature was set at $80\,°C$, the compensation voltage scanning range was set between -13 and $+5\,V$, and the retention time was recorded until $500\,s$. Response of the ion channels were recorded in both positive and negative modes.

3.2.2.2 GC-MS

The experimental setup consisted of a GC-17A GC-MS system (Shimadzu) equipped with an Rtx-440 (30-m×0.25-m×0.25-μm) fused silica column at a flow rate of $1.4\,ml/min$ of helium. The oven temperature was programmed as follow: the initial temperature was set at $40\ ℃$ and was held for $1\,min$, followed by a $10\ ℃\ /min$ increase to a final temperature of $250\ ℃$ which was held constant for $5\,min$. The injector and interface temperatures were held isothermally at $200\ ℃$ and $250\ ℃$, respectively. The sample ($500\ \mu l$) was injected into the column manually from a $500\ \mu l$ gas-tight syringe (Hamilton, USA) and the detector was set with a scan interval of $0.15\,s$ and m/z range of $45-350$.

3.2.3 Procedure

3.2.3.1 Sample preparation

3.2.3.1.1 Preparation of standard compounds

One liter of $10\,mg/ml$ of *o*-nitrophenol, 4-methylumbelliferone, and indole in water were prepared separately in ultra pure water ($18.2\,M\Omega$, Millipore). Each was then diluted and prepared as $1\,mg/ml$ of standard solution. For each analysis, $10\,ml$ of each standard solution was prepared as a working solution, was placed in a 20-ml vial, and was covered with an air-tight septum.

3.2.3.1.2 Preparation of bacterial samples

Colonies of *E. coli* DSM 30083 which were previously grown overnight on NB agar were used to inoculate each growth medium (which was prepared as $10\,ml$ medium in the 20-ml autoclaved headspace vials as described in Section 3.2.1.3). The initial concentration of bacteria cells in each sample vial was 5×10^7 cells/ml. To achieve this exact concentration, the liquid cultures were prepared as follow (the following data was recorded when preparing

sample for inoculation in Colilert-18® medium; other liquid cultures were prepared in the same way):

- Colonies that were grown on NB agar were transferred into an RG tube containing $10\ ml$ deionized water until the water became a cloudy suspension. The cloudy suspension usually contained between 10^8 to $10^{10}\ cells/ml$ bacteria (the exact concentration is known after the cell counting).
- The tube was then placed on a vortex and shaken at $900\ rpm$ for $10\ s$.
- Another three RG tubes were prepared, each contained $9\ ml$ deionized water.
- A series of dilution was then prepared: the cloudy suspension from the first RG tube was diluted 3 times in the other three tubes, so that the cell concentration in each tube became 10^{-1}, 10^{-2}, and 10^{-3} of the first suspension, respectively.
- The cell concentration in the second and last series of tubes dilution (the one with 10^{-2} and 10^{-3} concentrations of the original suspension) was then counted using a Thoma counting chamber.
- In case of bacteria to be prepared in the Colilert-18® solution, it was found that the concentration of the first RG tube suspension was $1.08 \times 10^{10} cells/ml$. Therefore, $46\ \mu l$ of aliquot was taken from this tube and transferred into each $10\text{-}ml$ Colilert-18® solution so that the initial cell concentration in the vial was each $5 \times 10^7\ cells/ml$.
- All other liquid cultures in tryptophan broth, M9, glucose broth, and TSB broth were prepared analytically in the same way.

All samples in the headspace vials were capped with autoclaved septa and aluminum caps. These samples of liquid cultures (consist of bacteria and growth media) and the blank samples (consist of only growth media) were incubated and shaken at $36\ ℃$ in a water bath GTL 1083 for $24\ h$, except those which were incubated in Colilert-18®, which were incubated for $18\ h$ according to the manufacturer's instruction. All samples were made in triplicate.

3.2.3.2 Headspace analysis of bacterial samples using GC-MS

For each analysis, after the $24\ h$ of incubation, from each sample of liquid cultures and blank media, $500\ \mu l$ of headspace sample was collected using a 500-μl gas-tight syringe and injected into the GC sample inlet manually. The sample was then immediately stored in the dark at $4\ ℃$ to preserve the cell concentration (to stop the growth of the bacteria). The cell concentration was then counted using Thoma cell counting chambers.

For each analysis with GC-MS, the analysis took $22\ min$. With a preheating and post cooling, the total analysis time was approximately $1 - 1.5\ h$. All analysis were made in triplicate.

3.2.3.3 Headspace analysis of bacterial samples using GC-DMS

For each analysis, after the $24\ h$ of incubation, from each sample of liquid cultures and blank media, $500\ \mu l$ of headspace sample was collected using a 500-μl gas-tight syringe and injected into the miniaturized GC-DMS sample inlet manually. The sample was then immediately stored in the dark at $4\ ℃$ to preserve the cell concentration (to stop the growth of the bacteria). The cell concentration was then counted using Thoma cell counting chambers.

For each analysis with GC-DMS, the analysis took $500\ s$. With a preheating and post cooling, the total analysis time was approximately $15 - 30\ min$. All analysis was made in triplicate.

3.2.3.4 Headspace analysis of standard compounds using GC-DMS

Prior to the headspace analysis of the standard compounds (standard solutions of *o*-nitrophenol, 4-methylumbelliferone, and indole) using GC-DMS, each sample was preheated for $15\ min$ at $36\ ℃$ and shaken using a magnetic stirrer. Headspace sample ($500\ \mu l$ per analysis) was then collected using a 500-μl gas-tight syringe and injected into the miniaturized GC-DMS sample inlet manually. Before the headspace gases of the standard compounds were injected, at least 100 blank spectra were collected and each analyte was measured in triplicate.

3.2.3.5 Cell counting

The bacterial cells concentration were counted using Thoma cell counting chamber (with 0.1-mm depth) after the $24\ h$ of incubation and after each run of analysis. For each cell

counting process, 20 areas were selected (marked with the yellow and pink circles) and the total sum of the bacteria was averaged. The procedure was duplicated and the final concentration was averaged from both counting.

Since the initial concentration of bacteria in each sample vial was $5 \times 10^7\ cells/ml$ and the bacterial concentration were usually multiplied logarithmically after the incubation, prior to the cells counting a series of dilution were made and the procedure was done in the same way as that in the previous section (Section 3.2.3.1.2 Preparation of bacterial samples).

3.2.3.6 Detection of methylumbelliferone

To detect the absence/presence of methylumbelliferone in the bacterial samples, from each sample vial $1\ ml$ of aliquot was collected and viewed under a $365\ nm$, 6-$Watt$ fluorescent UV lamp. A positive reaction of 4-methylumbelliferone is indicated by a blue fluorescence effect.

3.2.4 Data Analysis

3.2.4.1 GC-DMS data

For each analysis, the GC-DMS spectra corresponding to the detected positive and negative ions were recorded using Expert^{TM} and the chromatographic data was automatically stored as Microsoft Office Excel workbook. IGOR Pro 6 was then used to generate the GC-DMS spectra, to process the data, and to generate graphs.

In generating the retention time and compensation voltage graphs, IGOR Pro 6 was used. In some of the graphs, the data were processed using the Gaussian curve fitting functions when necessary. Both the raw data and the processed data are presented in the same frames.

3.2.4.2 GC-MS data

For each analysis, the GC-MS spectra were recorded using GCMS "LabSolutions" Version 2.30 (Shimadzu Corporation) and the chromatographic data was automatically stored as $*.qgd$ data file. The "PostRun" version of the software was then used to analyze the data and to generate graphs.

In identifying peaks, besides applying manual observation (by comparing the visually observed peaks from the blank samples and peaks from the spiked samples), auto-integration was also applied. Fifty highest peaks from each spectrum were auto-integrated and the identified peaks were listed in the fragment table. Using "similarity search" function which is connected to the NIST library database, the peaks were then identified.

In presenting the spectra, each spectrum in the figure was also smoothed. The smoothing was done using the Savitzky-Golay filter.

3.3 Results and Discussion

As mentioned earlier, five different media were used to grow *E. coli* bacteria: Colilert-18®, glucose broth, M9-medium, tryptophan broth, and tryptic soy broth (TSB). To characterize the volatile metabolite compounds released by the bacteria cultivated in the different media, GC-MS and GC-DMS analysis were done.

3.3.1 Detection of volatile metabolites of *E. coli* grown in Colilert-18®

3.3.1.1 GC-MS spectra

For each experiment, $10\,ml$ of Colilert-18® was spiked with *E. coli* so that the initial concentration of the cells was $5 \times 10^7\ cells/ml$. The samples were incubated for $18\ h$ and the headspace gases were then analyzed by GC-MS and GC-DMS.

GC-MS spectra corresponding to the volatile metabolites compounds released by *E. coli* grown in Colilert-18® are given in Figure 16 $a - e$:

- **Part (a)** shows the full time ($21\ min$) spectra obtained from the GC-MS analysis. Here the *Total Ion Chromatogram (TIC)* is presented. To distinguish between spectra produced by the bacteria and by the media itself, both spectra from the blank sample (i.e. medium only) and from the spiked sample (i.e. medium and *E. coli*) are presented in the same frame. Spectrum of the blank sample is shown as a black line, whereas spectrum of the spiked sample is shown as a red line.

- To have a closer look on the peaks, the spectra in **part (a)** were further divided into 3 sections of time interval and each is presented in **part (b)**, **(c)**, and **(d)**. **Part (b)** shows

the spectra of the blank and the spiked samples from retention time: $t_r = 3.5\ min$ to $t_r = 10\ min$; **part (c)** shows the spectra of the blank and the spiked samples from retention time: $t_r = 10\ min$ to $t_r = 15\ min$; and **part (d)** shows the spectra of the blank and the spiked samples from retention time: $t_r = 15\ min$ to $t_r = 21\ min$.

As can be seen in Figure 16 b (first section, $t_r < 10\ min$), several peaks appeared. However, by comparing the spectrum from the medium and the spectrum from the spiked medium, none of these peaks were produced by *E. coli* alone.

a. Colilert: with and without *E. coli* | Total Ion Chromatogram | Full Time

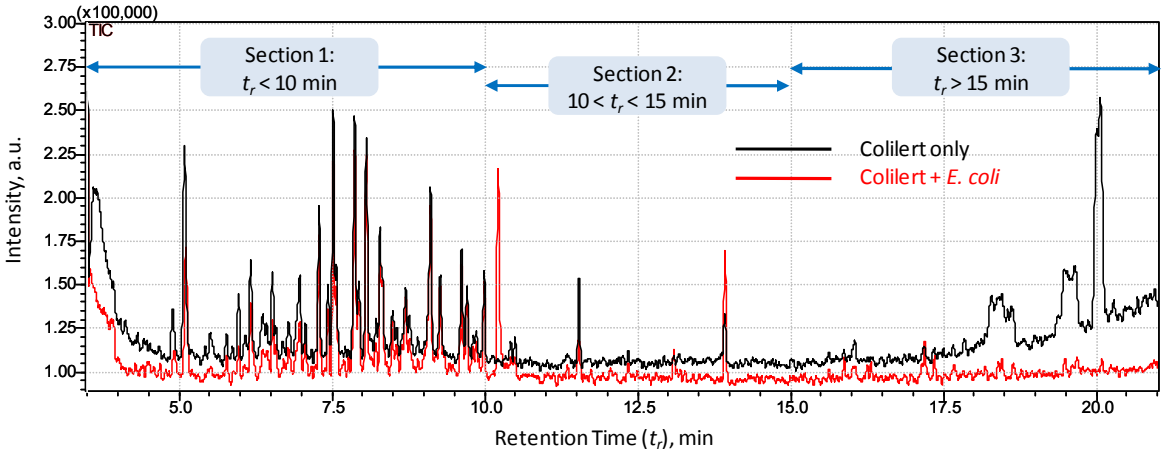

b. Colilert: with and without *E. coli* | Total Ion Chromatogram | Section 1: t_r < 10 min

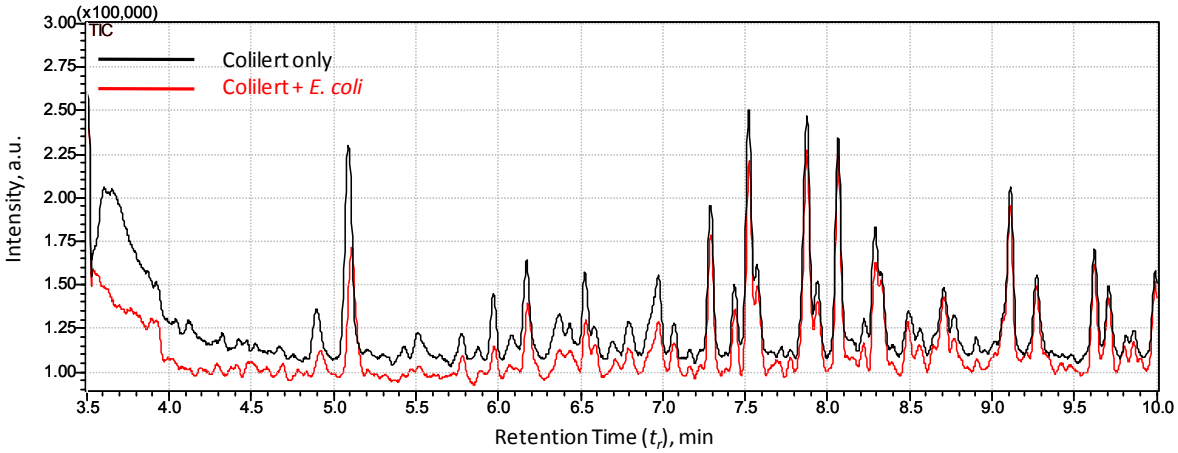

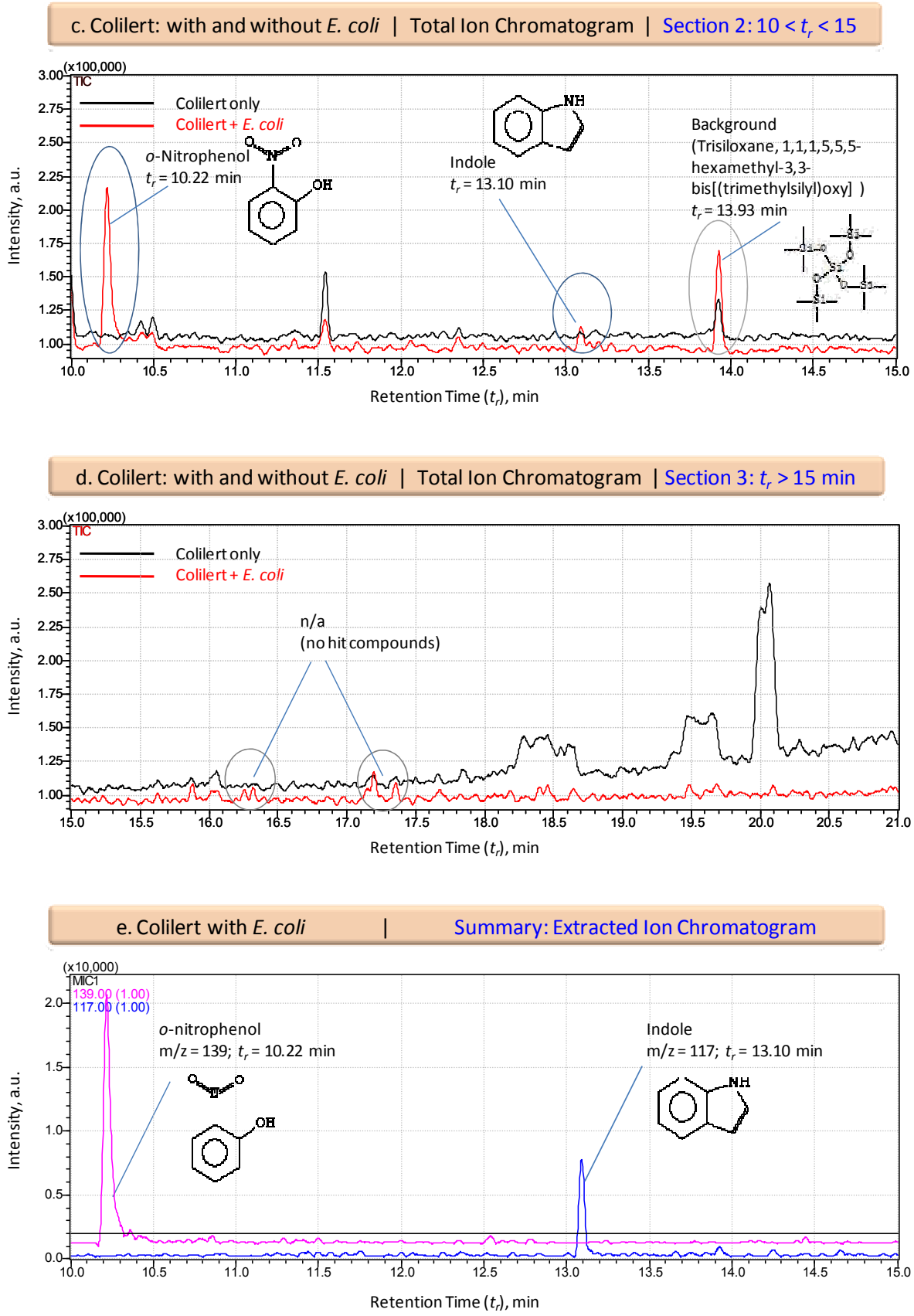

Figure 16 a-e. GC-MS spectra of volatile metabolites of *E. coli* incubated for 18 h in Colilert-18®

In the second section (Figure 16 c, from $t_r = 10\,min$ to $t_r = 15\,min$), several peaks appeared:

- at $t_r = 10.22\,min$, a peak uniquely produced by the spiked sample appeared. This peak, with mass/charge ratio, $\frac{m}{z} = 139$, is identified as ***o*-nitrophenol**.
- at $t_r = 13.10\,min$, another peak uniquely produced by the spiked sample appeared. This peak, with $\frac{m}{z} = 117$, is identified as **indole**.
- at $t_r = 13.93\,min$, another peak appeared to be produced by both the medium and the spiked medium, but the intensity in the spiked medium is higher than that in the medium. This peak, with $\frac{m}{z} = 384$, is identified as **Trisiloxane, 1,1,1,5,5,5-hexamethyl-3,3-bis[(trimethylsilyl)oxy]**. However, it came neither from the medium nor from the bacteria itself. Prior to do the GC-MS analysis with analytes, the GC-MS was allowed to collect up to 25 blank spectra, and Trisiloxane appeared to be produced by the column itself. Besides Trisiloxane, these compounds were also occasionally produced by the blank spectra:
  - $t_r = 11.55\,min, \frac{m}{z} = 342$: 2H-1,4-Benzodiazepin-2-one, 7-chloro-1,3-dihydro-5-phenyl-1-(trimethylsilyl)
  - $t_r = 16.05\,min, \frac{m}{z} = 174$: acetic acid, 3-[1,3]dioxolan-2-ylpropyl ester

In the third section (Figure 16 d, from $t_r = 15\,min$ to $t_r = 21\,min$), several peaks also appeared, but they were either produced by the background itself or unknown (NIST library database showed no hit compounds similar to those peaks).

The *Total Ion Chromatogram* of the spiked sample from Figure 16 a was then substracted by its background and the *Extracted Ion Chromatogram* is presented in Figure 16 e. From this GC-MS analysis, it appeared that the compounds produced uniquely by *E. coli* grown in Colilert-18® were only *o*-nitrophenol ($\frac{m}{z} = 139$, at $t_r = 10.22\,min$) and indole ($\frac{m}{z} = 117$, at $t_r = 13.10\,min$).

3.3.1.2 GC-DMS spectra

GC-DMS spectra of the blank medium, i.e. Colilert-18® which was incubated for $2.5\ h$, but was not spiked with *E. coli*, is given in Figure 17. The left and the right frames of Figure 17 show the response of the positive and the negative ion channels of the DMS detector, respectively. The RF voltage was set at $V_{rf} = 1100\ V$.

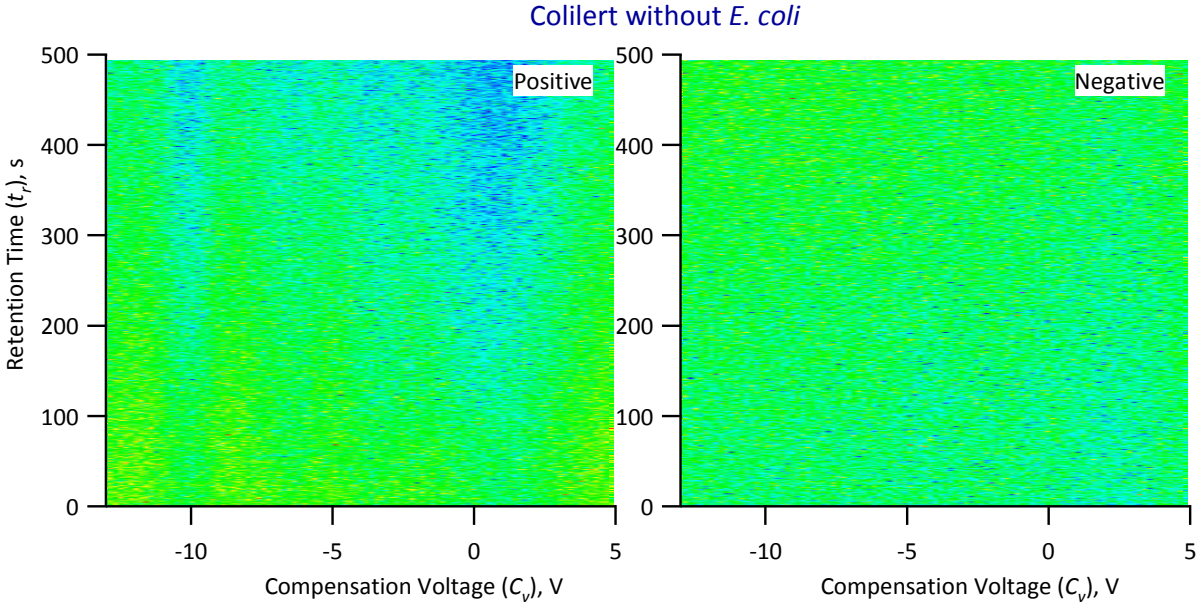

Figure 17. GC-DMS spectra of headspace gases from Colilert-18® (without *E. coli*) after $2.5\ h$ of incubation

GC-DMS spectra of the spiked medium, i.e. Colilert-18® which was spiked with *E. coli* and then incubated for $2.5\ h$, are given in Figure 18 and Figure 19, each represents the response of the detector in the positive and negative ion channels, respectively.

Each figure in Figure 18 and Figure 19 consists of 4 frames. The top left frame shows the 2D spectra, showing axis of retention time and compensation voltage. As can be seen in both the positive (Figure 18) and negative (Figure 19) modes, a peak appeared at retention time, $t_r = 195.28\ s$, which was not exist in Figure 17. This peak, upon a validation with GC-MS and confirmation with GC-DMS of the standard compound, was confirmed as *o*-nitrophenol ($mol.weight = 139\ g/mol$).

In the positive mode, this peak appeared at compensation voltage, $C_{v,1} = -2.82V$(Figure 18, bottom left frame), whereas in the negative mode, this peak appeared at $C_{v,2} = -4.09V$ (Figure 19, bottom left frame).

The retention time profiles at $C_{v,1}$ and $C_{v,2}$ are presented in each figure, at the right top frame. Here, both retention time profiles of the blank medium (i.e. Colilert-18® only) and the spiked medium (Colilert-18® containing *E. coli*) are given as blue and red curves, respectively. As can be seen here, at $t_r = 195.28\ s$, the peak only appeared in the spiked sample.

For an overall view, the $3D$ spectra showing retention time, compensation voltage, and intensity of the spiked sample are shown in the bottom right frames of both figures.

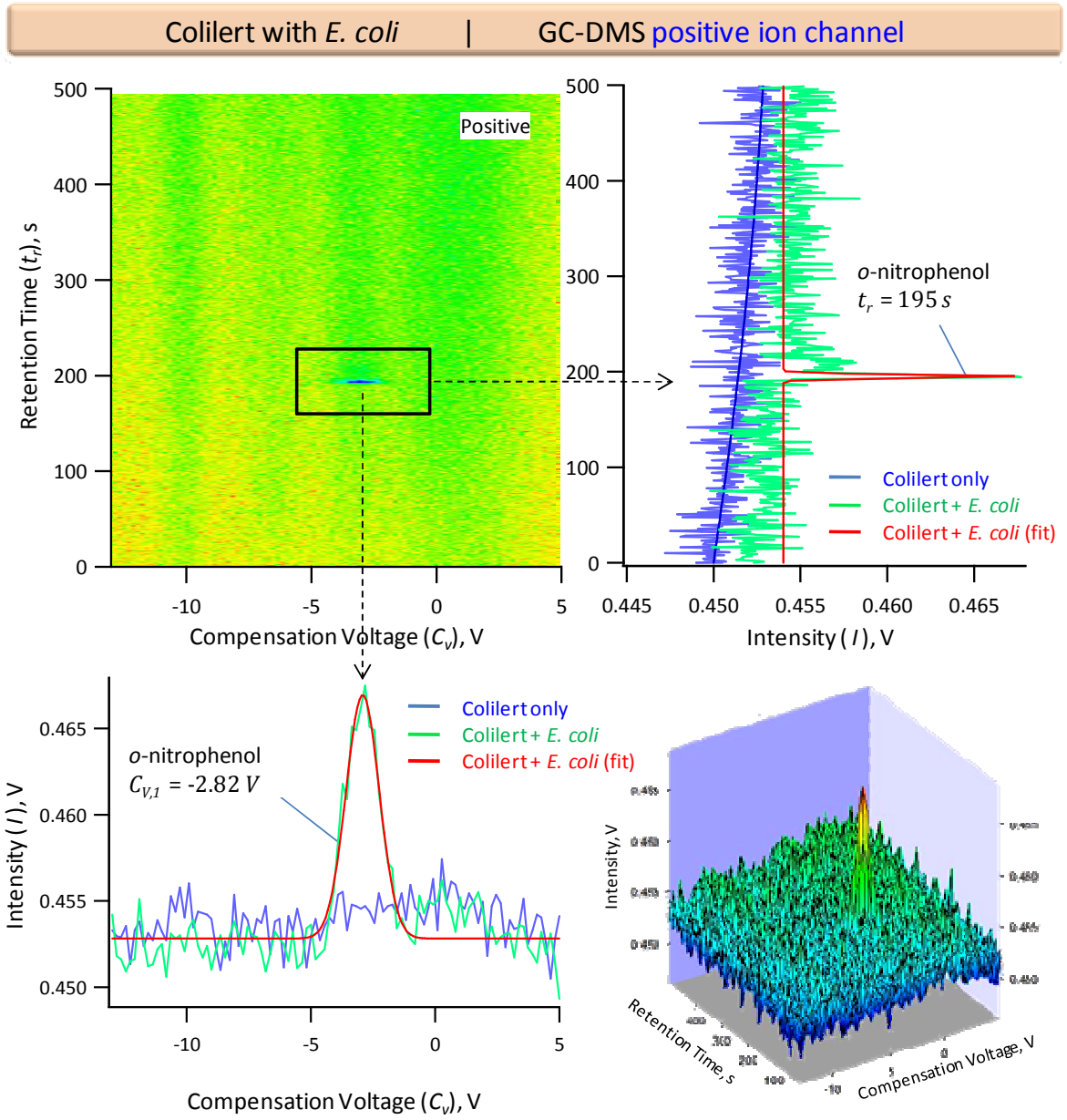

Figure 18. GC-DMS spectra (positive ion channel) of Colilert-18® spiked with *E. coli* after 18 h of incubation; top left: 2D spectra; bottom right: 3D spectra; top right: Retention Time profile, with and without *E. coli*; bottom left: Compensation Voltage profile, with and without *E. coli*

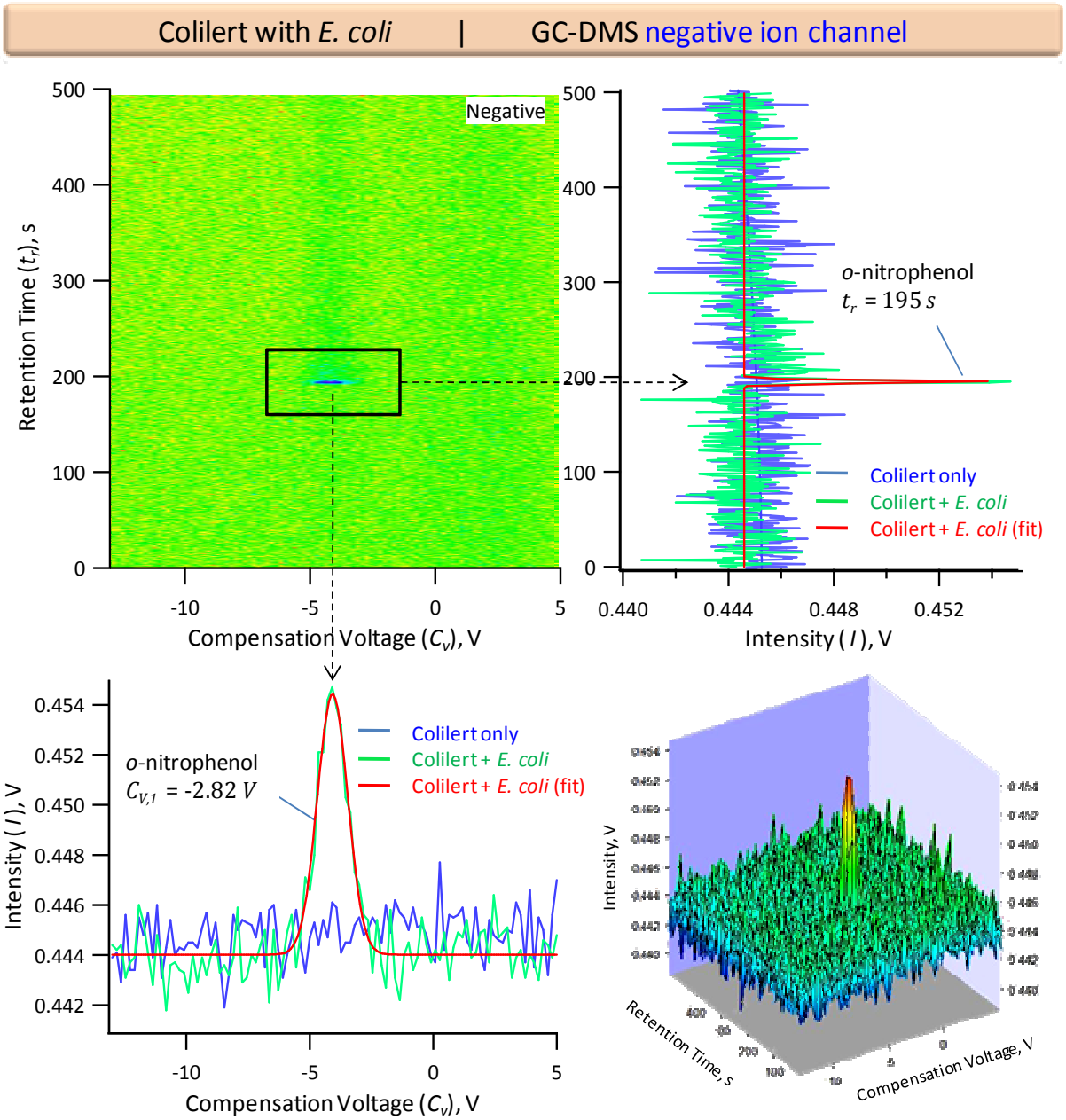

Figure 19. GC-DMS spectra (negative ion channel) of Colilert-18® spiked with *E. coli* after $18\ h$ of incubation; top left: $2D$ spectra; bottom right: $3D$ spectra; top right: Retention Time profile, with and without *E. coli*; bottom left: Compensation Voltage profile, with and without *E. coli*

Unlike in GC-MS, the spectra obtained from the GC-DMS analysis of *E. coli* sample did not contain indole. Also, neither in GC-MS nor in GC-DMS analysis the 4-methlyumbelliferone was detected. However, upon the viewing under $365\ nm$, $6\text{-}Watt$ fluorescent UV lamp, $1\ ml$ of aliquot of the spiked sample showed a positive reaction of 4-methlyumbelliferone (a blue fluorescence effect was observed). As explained in the introduction part, the enzymatic

reaction of *E. coli* cultivated in Colilert-18® was expected to produce both *o*-nitrophenol and 4-methlyumbelliferone.

To evaluate the absence of both peaks in the GC-DMS analysis of the bacterial sample, GC-DMS analysis of indole and 4-methlyumbelliferone were done using standard compounds (each $1\ mg/ml$). No peaks of 4-methylumbelliferone were detected by the GC-DMS (the spectra of 4-methylumbelliferone was the same with the spectra of pure water, i.e. only reactant ion peak appeared). When the concentration of the standard solution of 4-methylumbelliferone was increased with a concentration factor of 10 to 1000, the peak was still absence. The absence of the peak is likely attributed to the physicochemical properties of 4-methylumbelliferone which is a non-volatile compound. The physicochemical properties of 4-methylumbelliferone, indole, and *o*-nitrophenol are summarized in Table 5.

Table 5. Properties of the standard compounds [168]

Compounds	Structure	Molecular Weight, Mr $(\frac{gr}{mol})$	Inverse Henry's constant, $K_{H,inv}$ $(\frac{atm.m^3}{mol}$at $T = 298.15K$ and $\rho_{H_2O} = 997\ \frac{kg}{m^3})$	Vapor Pressure, P $(mmHg)$
o-nitrophenol $(C_6H_5NO_3)$	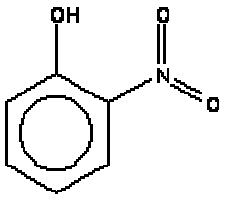	139.11	1.63×10^{-5}	1 (at 49.3 °C)
Indole (C_8H_7N)	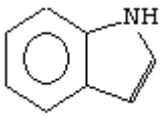	117.15	5.3×10^{-7}	0.0122 (at 25 °C)
4-methylumbelliferone $(C_{10}H_8O_3)$	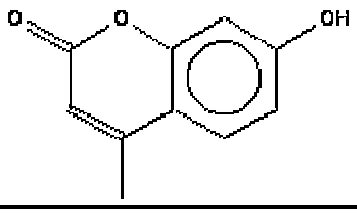	176.17	n/a	n/a

The GC-DMS spectrum of indole compound is given in Figure 20. The figure consists of 4 frames. The top left frame shows the image spectra of the positive ion channel. At $t_r = 200.34\ s$, a peak appeared. In the spectra of solution which only contained pure water, this peak was absence. Therefore, although this peak originated from indole solution is rather not sharp, it is concluded to be indole.

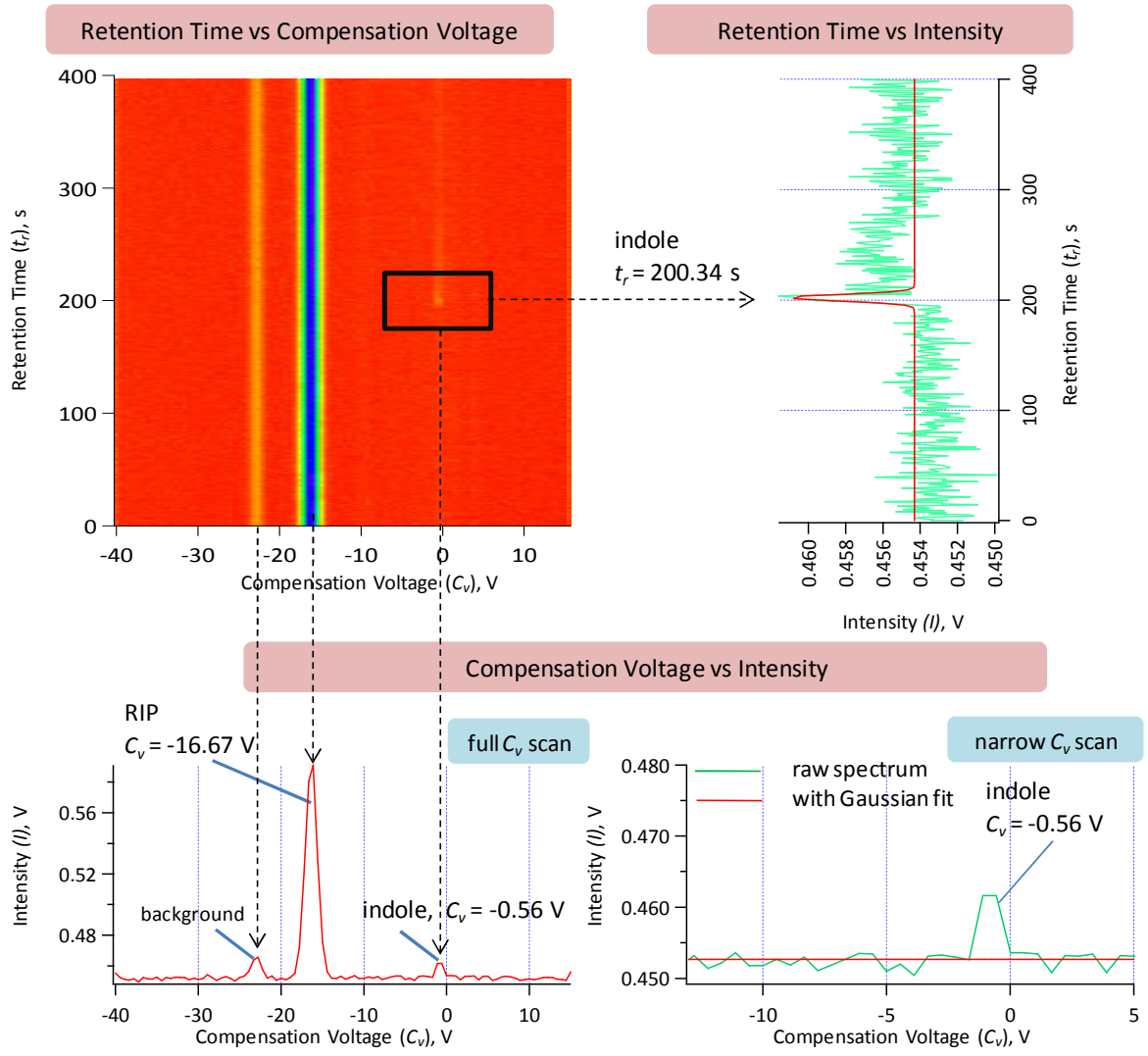

Figure 20. GC-DMS spectra of standard solution of indole at RF voltage, $V_{rf} = 1100\ V$

The absence of indole signal in the bacterial metabolite is likely attributed to the low volatility of indole, as indicated by its low inverse Henry's constant given in Table 5, i.e.

$K_{H,inv,Indole} = 5.3 \times 10^{-7} \frac{atm.m^3}{mol}$. On the other hand, the inverse Henry's constant of *o*-nitrophenol is 2 digits magnitude higher than indole. However, since using the same type of sample indole was able to be detected by GC-MS (although in a much lower amount than *o*-nitrophenol), it is possible that indole was poorly ionized by the DMS.

3.3.2 Detection of volatile metabolites of *E. coli* grown in glucose broth

3.3.2.1 GC-MS spectra

For each experiment, $10\,ml$ of glucose broth was spiked with *E. coli* so that the initial concentration of the cells was $5 \times 10^7\ cells/ml$. The samples were incubated for $24\ h$ and the headspace gases were then analyzed by GC-MS and GC-DMS. GC-MS spectra corresponding to the volatile metabolites compounds released by *E. coli* grown in glucose broth are given in Figure 21 $a - e$. The data presentation method for glucose broth and all other following medium is the same with the one for Colilert-18® so the description for each method (e.g. what is part a, b, c, etc.) will be skipped.

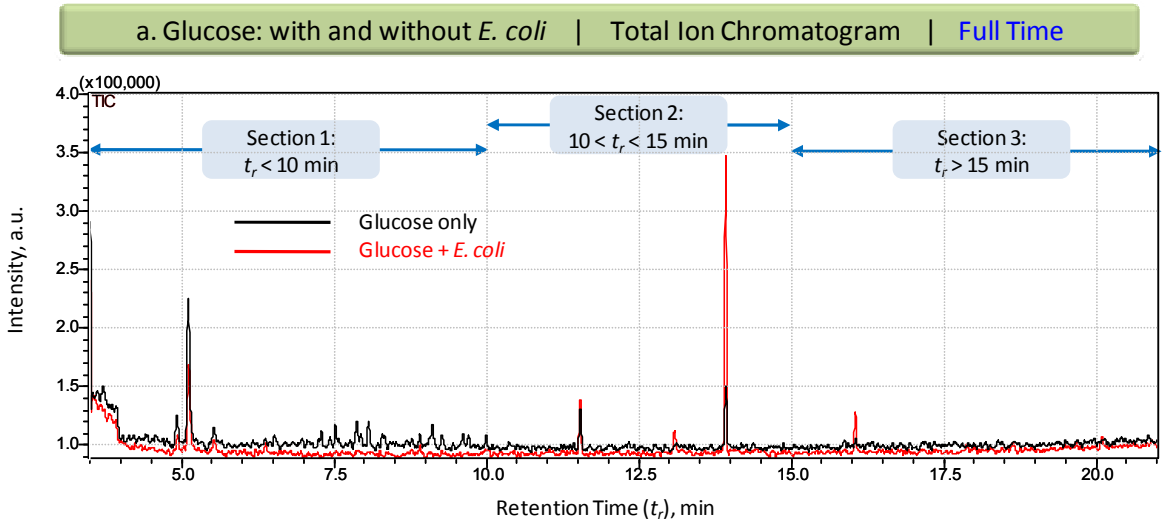

b. Glucose: with and without *E. coli* | Total Ion Chromatogram | Section 1: t_r < 10 min

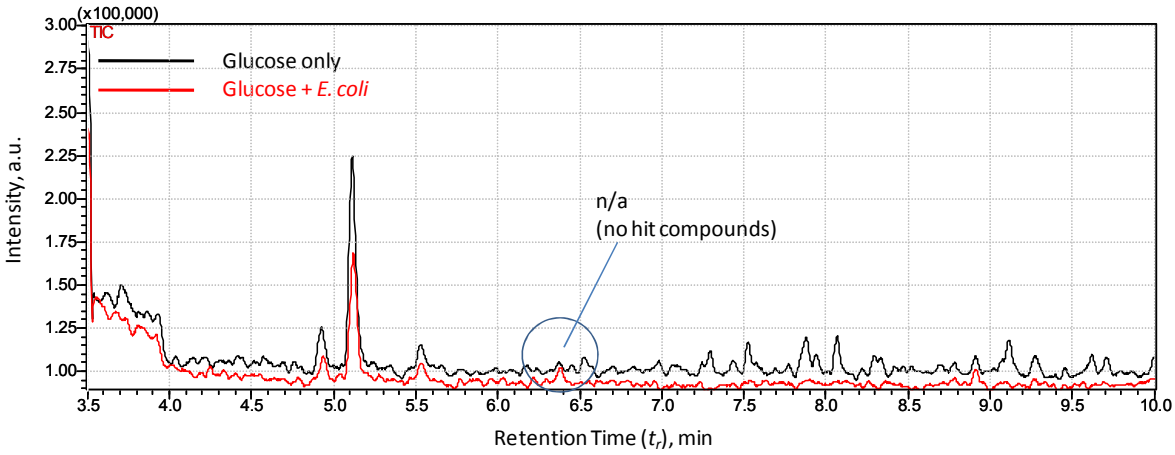

c. Glucose: with and without *E. coli* | Total Ion Chromatogram | Section 2: 10 < t_r < 15

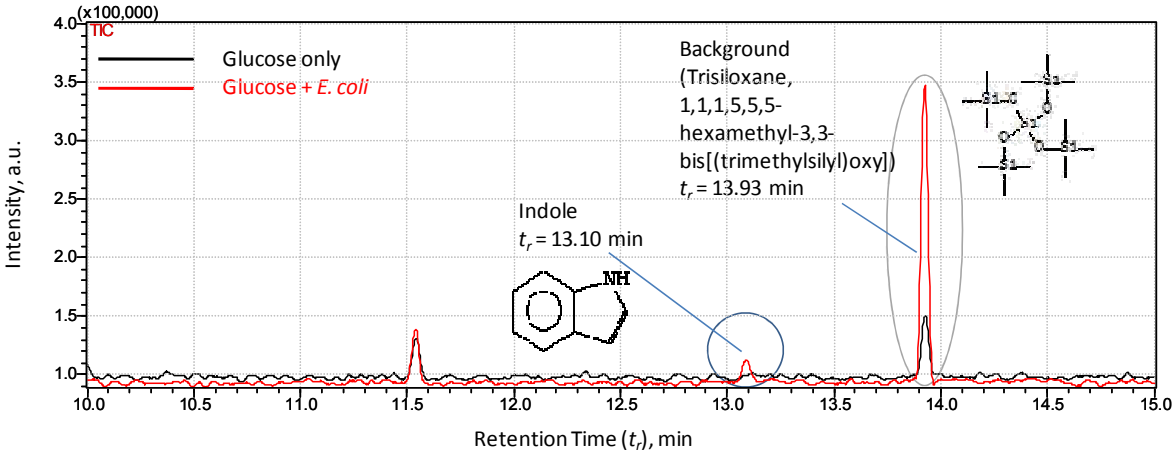

d. Glucose: with and without *E. coli* | Total Ion Chromatogram | Section 3: t_r > 15 min

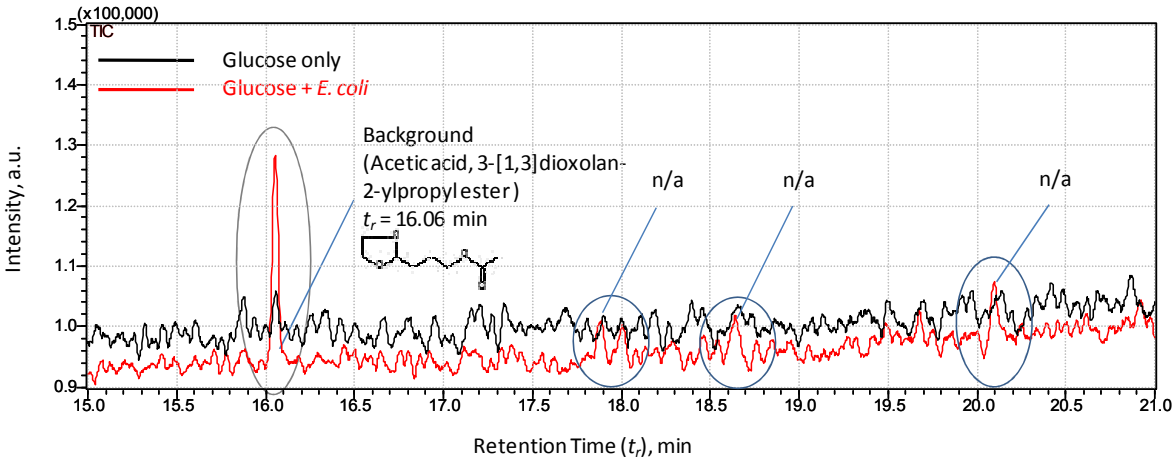

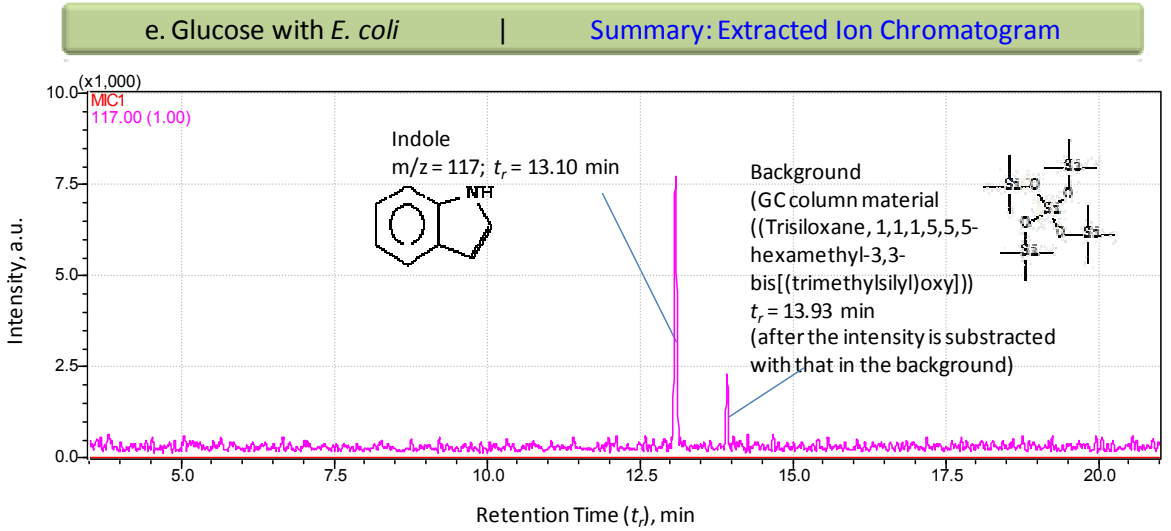

Figure 21 a-e. GC-MS spectra of volatile metabolites of *E. coli* incubated for 24 h in glucose broth

As can be seen in Figure 21 $a-e$, several peaks were detected (but only indole can be detected in the spiked sample **and** absent in the blank sample):

- at $t_r = 6.38\,min$, a peak which seems stronger in the spiked sample than in the blank sample appeared; however, the compound identity could not be identified.
- at $t_r = 10.22\,min$ (where *o*-nitrophenol produced by *E. coli* grown in Colilert-18®), no peak appeared.
- at $t_r = 13.10\,min$, peak of **indole** ($\frac{m}{z} = 117$) appeared.
- at $t_r = 13.93\,min$, like the one in Colilert-18® experiment, peak of **Trisiloxane, 1,1,1,5,5,5-hexamethyl-3,3-bis[(trimethylsilyl)oxy]** ($\frac{m}{z} = 384$) which came from the GC column itself appeared.
- at $t_r = 16.05\,min$, peak of **acetic acid, 3-[1,3]dioxolan-2-ylpropyl ester** ($\frac{m}{z} = 174$) appeared; however, this peak appeared to be produced by the blank media as well.

Upon the background subtraction of the *Total Ion Chromatogram* of the spiked sample in Figure 21 $a-d$, the *Extracted Ion Chromatogram* is presented in Figure 21 e. The extracted ion chromatogram shows only indole and Trisiloxane, 1,1,1,5,5,5-hexamethyl-3,3-bis[(trimethylsilyl)oxy], with indole released by *E. coli*, whereas the later came from the GC column itself.

3.3.2.2 GC-DMS spectra

GC-DMS retention time and compensation voltage profiles obtained from the detection of headspace gases collected from blank glucose broth (without *E. coli*) and from the spiked glucose broth (with *E. coli*) after $24\ h$ of incubation are shown in Figure 22. The retention time profiles are taken at compensation voltage of $C_v = -0.56\ V$, whereas the compensation voltage profiles are taken at retention time of $t_r = 200.34\ s$ as per reference of standard solution of indole in Figure 20. As shown in Figure 22, no peaks of analyte was detected when *E. coli* was grown in glucose broth and analyzed by GC-DMS.

Unlike in GC-MS where indole was detected, no indole or any other compounds was detected by the GC-DMS when *E. coli* was grown in glucose broth (Figure 22). The absence of indole has been explained in the previous section (3.3.1.2), whereas the absence of *o*-nitrophenol and 4-methylumbelliferone are attributed to the absence of ONPG and MUG in the glucose broth, respectively.

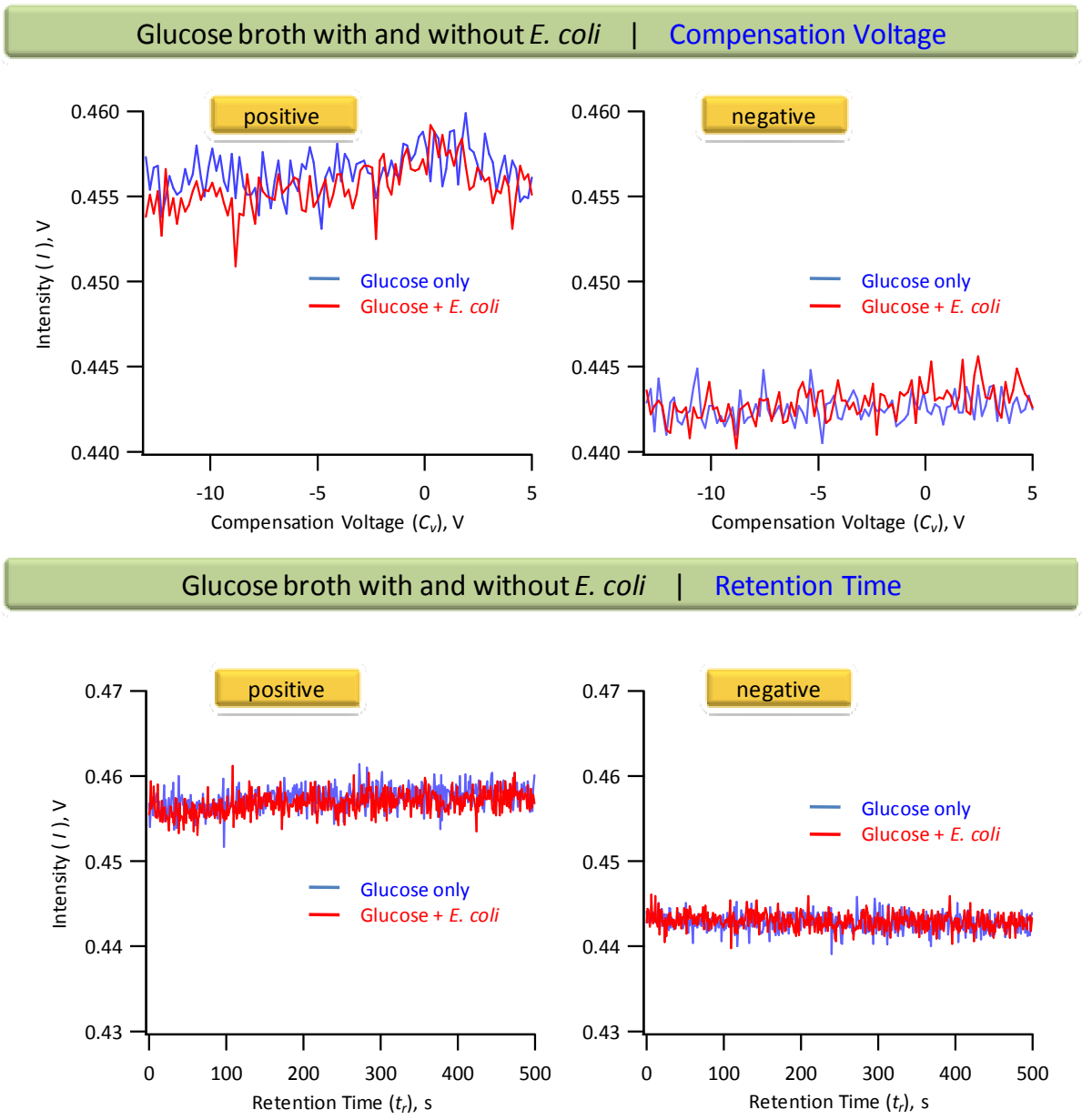

Figure 22. Retention Time and Compensation Voltage profiles of headspace gases from glucose broth (with and without *E. coli*) after $24\ h$ of incubation

3.3.3 Detection of volatile metabolites of *E. coli* grown in M9 medium

3.3.3.1 GC-MS spectra

For each experiment, $10\,ml$ of M9 medium was spiked with *E. coli* so that the initial concentration of the cells was $5 \times 10^7\ cells/ml$. The samples were incubated for $24\ h$ and the headspace gases were then analyzed by GC-MS and GC-DMS. GC-MS spectra corresponding to the volatile metabolites compounds released by *E. coli* grown in M9 medium are given in Figure 23 $a - e$.

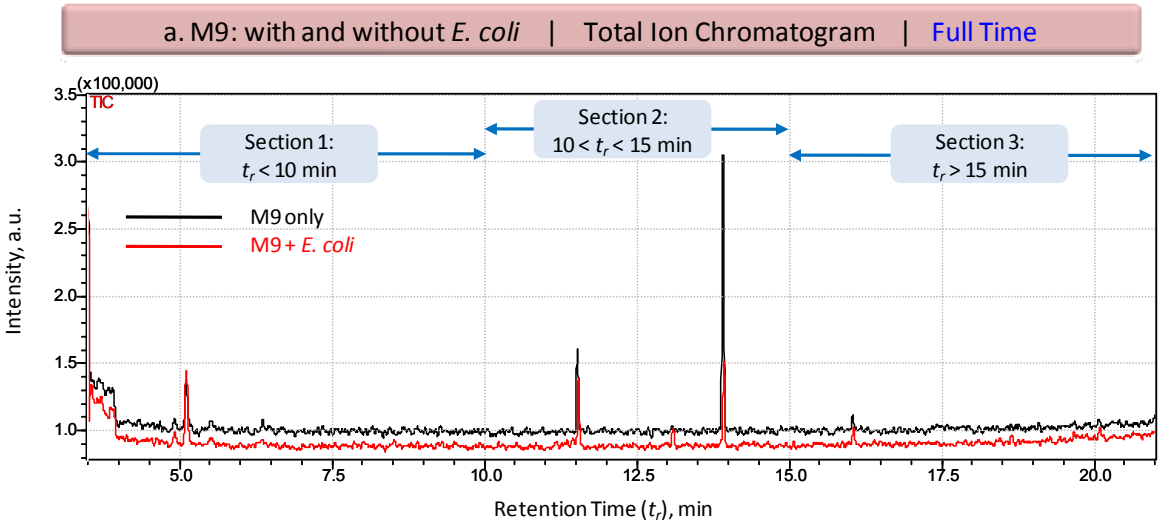

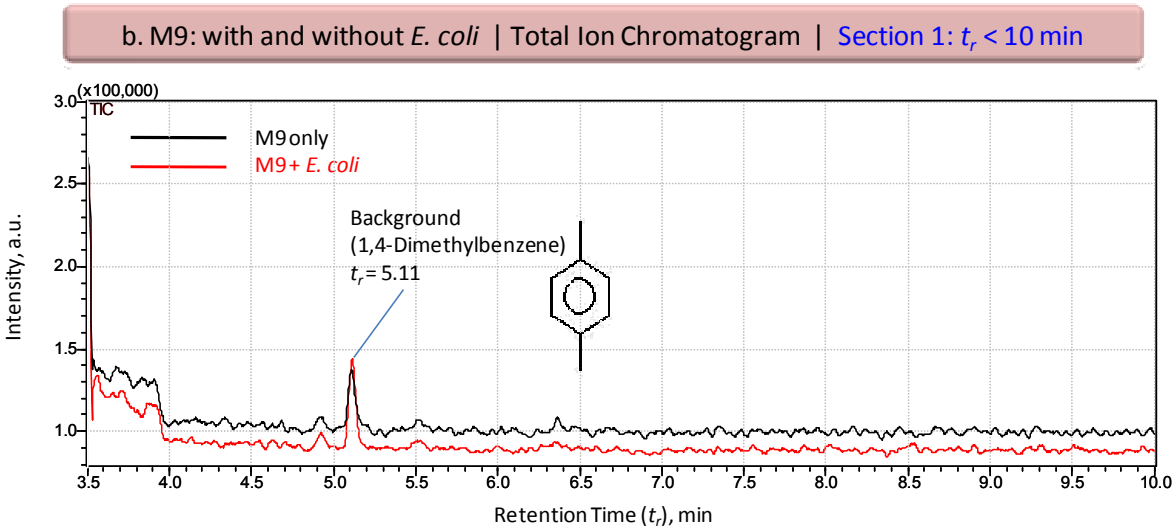

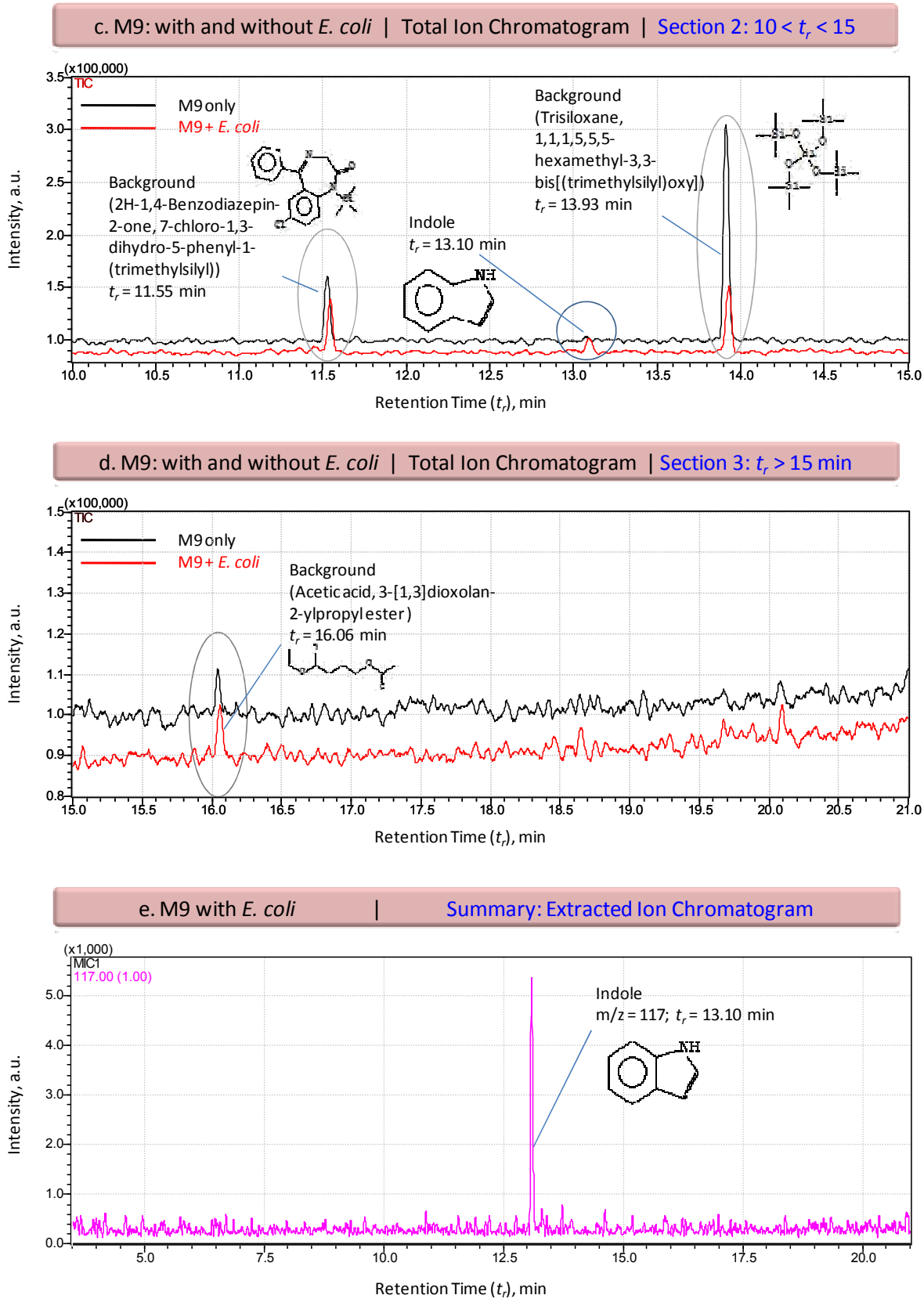

Figure 23 a-e. GC-MS spectra of volatile metabolites of *E. coli* incubated for 24 *h* in M9-medium

As can be seen in Figure 23 $a-e$, several peaks were detected (but only indole can be detected in the spiked sample **and** absent in the blank sample):

- at $t_r = 5.11\ min$, peak of 1,4-dimethylbenzene ($\frac{m}{z} = 106$) was detected, but this peak appeared in the background as well.
- at $t_r = 10.22\ min$ (where *o*-nitrophenol was previously appeared from *E. coli* grown in Colilert-18®), no peak appeared.
- at $t_r = 11.55$, peak of 2H-1,4-Benzodiazepin-2-one, 7-chloro-1,3-dihydro-5-phenyl-1-(trimethylsilyl) ($\frac{m}{z} = 342$) appeared both in the spiked and the blank samples
- at $t_r = 13.10\ min$, peak of **indole** ($\frac{m}{z} = 117$) appeared.
- at $t_r = 13.93\ min$, peak of Trisiloxane, 1,1,1,5,5,5-hexamethyl-3,3-bis[(trimethylsilyl)oxy] ($\frac{m}{z} = 384$) which came from the background itself appeared.
- at $t_r = 16.05\ min$, peak of acetic acid, 3-[1,3]dioxolan-2-ylpropyl ester ($\frac{m}{z} = 174$) which came from the background itself appeared.

Upon the background subtraction of the *Total Ion Chromatogram* of the spiked sample in Figure 23 $a-d$, the *Extracted Ion Chromatogram* is presented in Figure 23 e. The extracted ion chromatogram shows only indole produced by the bacteria alone.

3.3.3.2 GC-DMS spectra

GC-DMS retention time and compensation voltage profiles obtained from the detection of headspace gases collected from blank M9 (without *E. coli*) and from the spiked M9 (with *E. coli*) after $24\ h$ of incubation are shown in Figure 24.

As shown in Figure 24, when *E. coli* were grown in M9 medium, no peaks of indole, *o*-nitrophenol, and 4-methylumbelliferone were detected by the GC-DMS, due to the low volatility of indole and the absence of ONPG and MUG in the media.

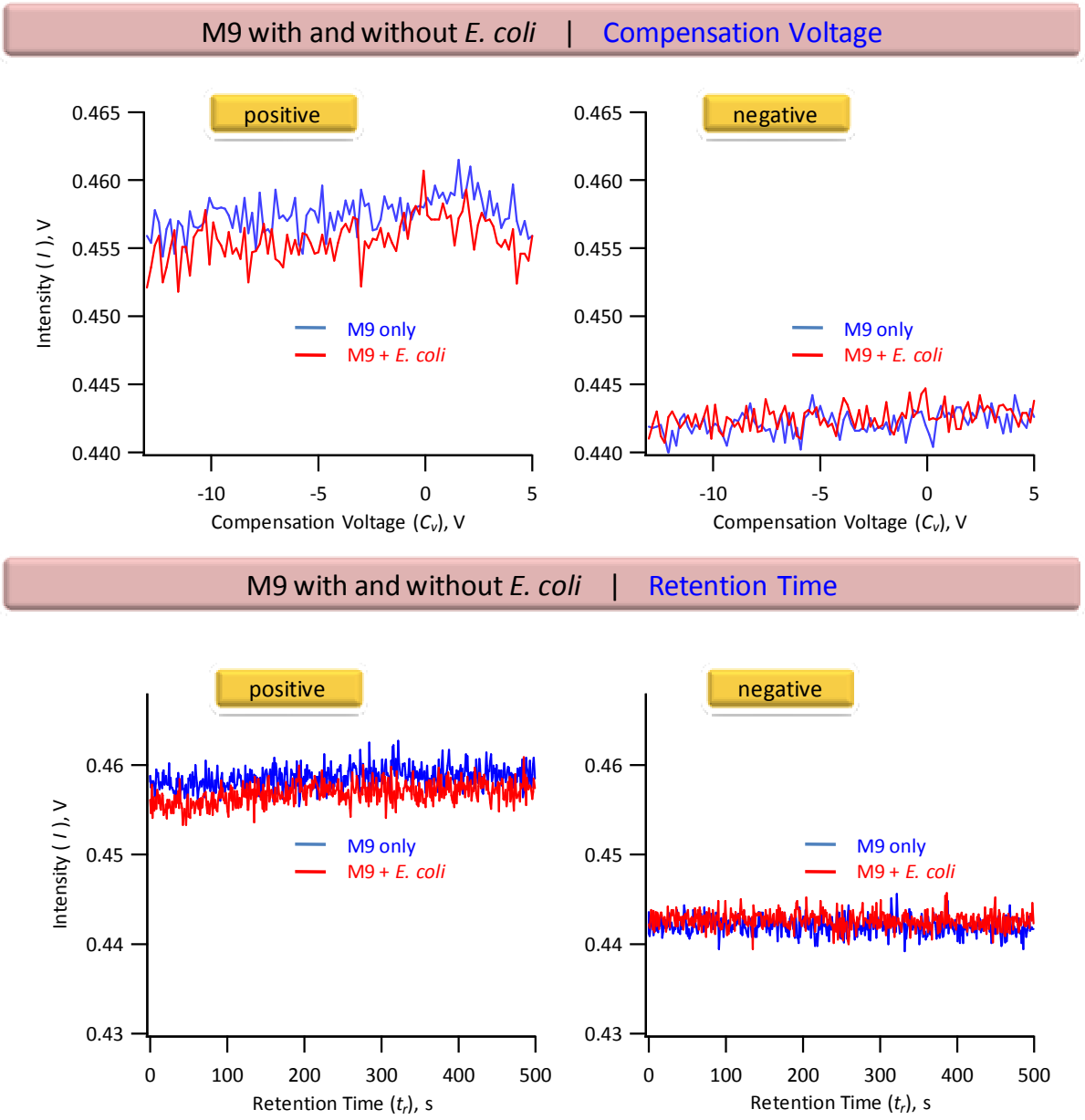

Figure 24. Retention Time and Compensation Voltage profiles of headspace gases from M9-medium (with and without *E. coli*) after $24\ h$ of incubation

3.3.4 Detection of volatile metabolites of *E. coli* grown in tryptophan broth

3.3.4.1 GC-MS spectra

For each experiment, $10\ ml$ of tryptophan broth was spiked with *E. coli* so that the initial concentration of the cells was $5 \times 10^7\ cells/ml$. The samples were incubated for $24\ h$ and the headspace gases were then analyzed by GC-MS and GC-DMS. GC-MS spectra

corresponding to the volatile metabolites compounds released by *E. coli* grown in M9 medium are given in Figure 25 $a - e$.

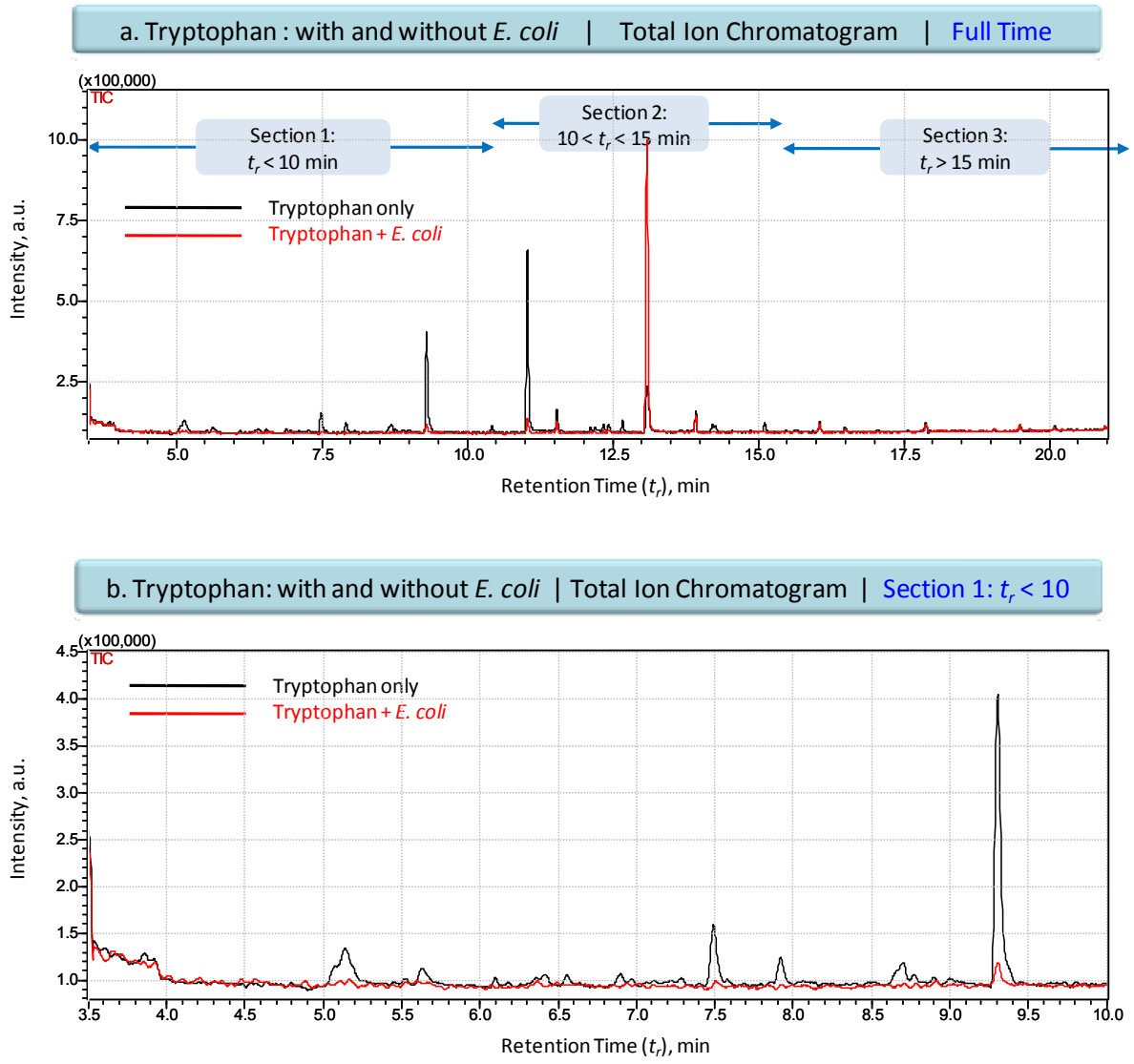

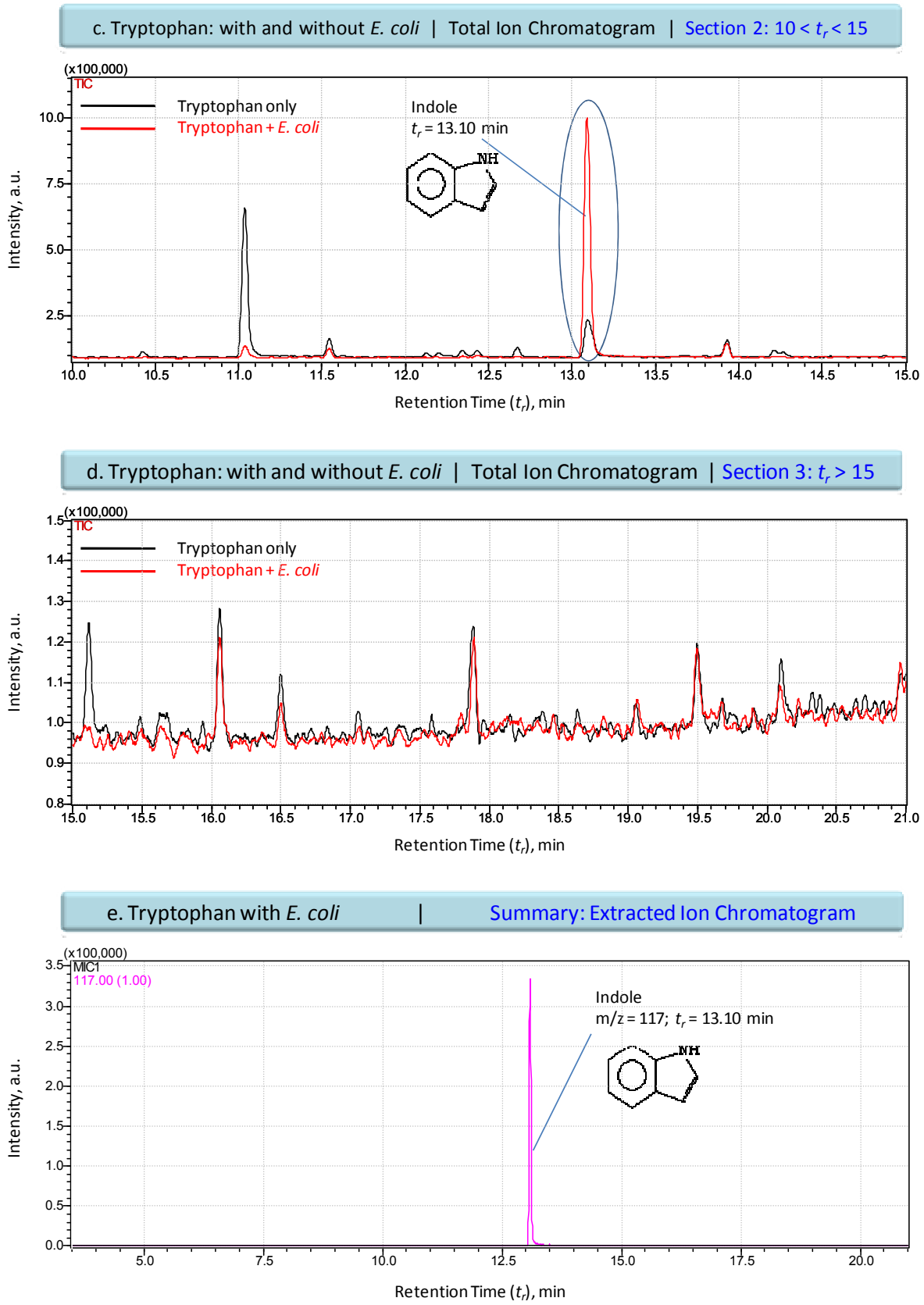

Figure 25 a-e. GC-MS spectra of volatile metabolites of *E. coli* incubated for $24\ h$ in tryptophan broth

As can be seen in Figure 25 $a - e$, several peaks were detected, but only indole came uniquely from the spiked sample and absent in the blank sample. In addition to that, the peak of indole appeared to be much higher than any other peaks. This will be discussed in more detail in the last section.

3.3.4.2 GC-DMS spectra

GC-DMS retention time and compensation voltage profiles obtained from the detection of headspace gases collected from blank tryptophan broth (without *E. coli*) and from the spiked tryptophan broth (with *E. coli*) after $24\ h$ of incubation are shown in Figure 26. As shown by the figure, when *E. coli* were grown in tryptophan broth, no peaks of compounds (including indole, *o*-nitrophenol, and 4-methylumbelliferone) were detected by the GC-DMS due to the low volatility of indole and the absence of ONPG and MUG in the media.

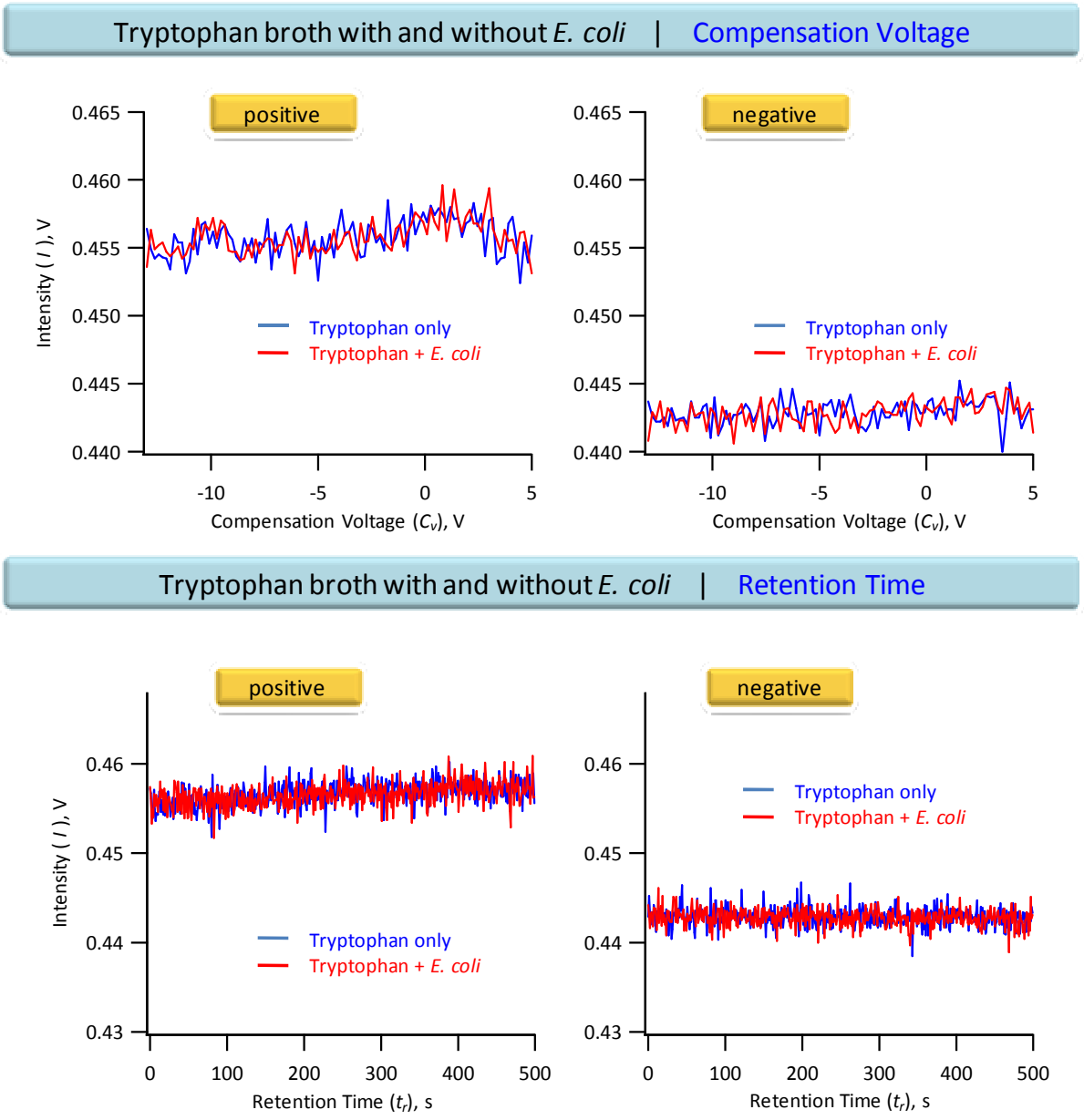

Figure 26. Retention Time and Compensation Voltage profiles of headspace gases from tryptophan broth (with and without *E. coli*) after $24\ h$ of incubation

3.3.5 Detection of volatile metabolites of *E. coli* grown in tryptic soy broth (TSB)

3.3.5.1 GC-MS spectra

Ten ml of Colilert-18® was spiked with *E. coli* so that the initial concentration of the cells was $5 \times 10^7\ cells/ml$. The sample was incubated for $18\ h$ and the headspace gases were then analyzed by GC-MS and GC-DMS.

GC-MS spectra corresponding to the volatile metabolites compounds released by *E. coli* grown in Colilert-18® are given in Figure 27 $a - e$:

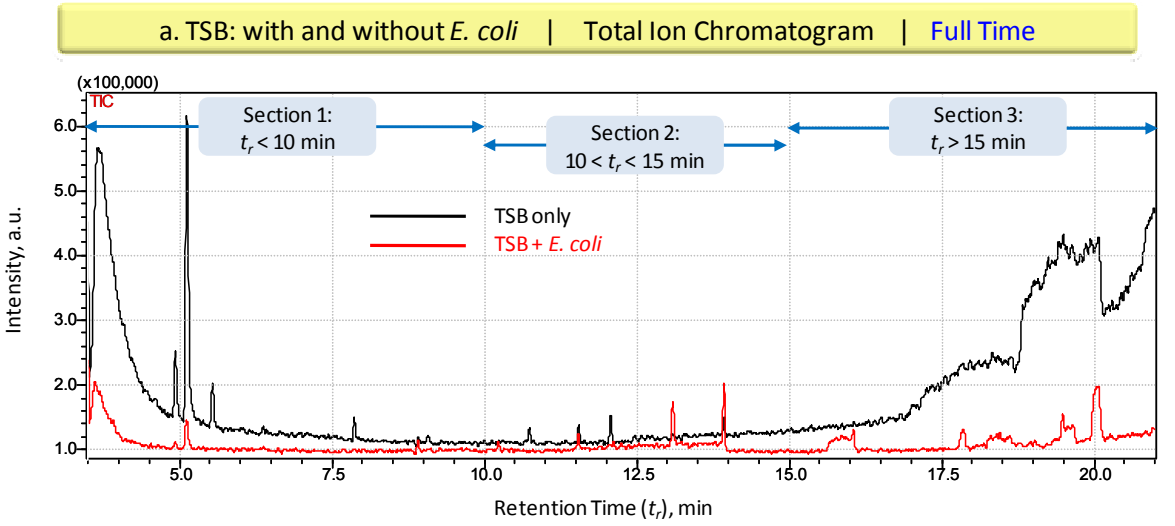

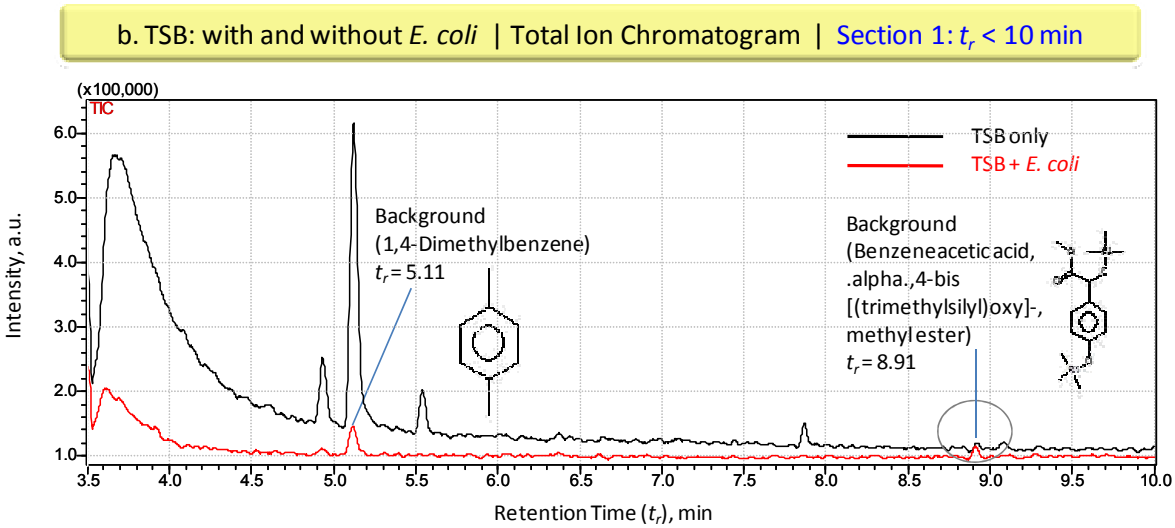

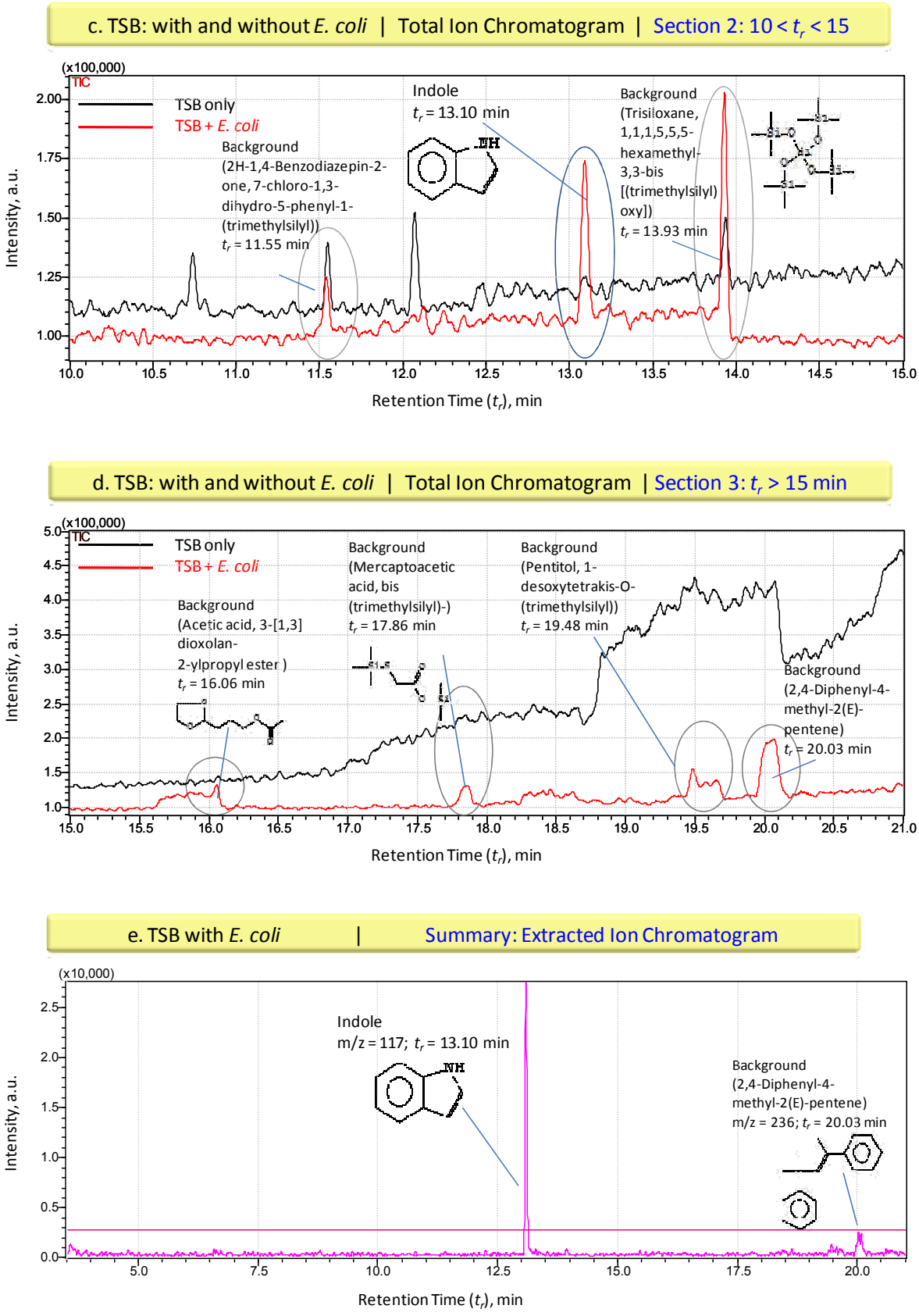

Figure 27 a-e. GC-MS spectra of volatile metabolites of *E. coli* incubated for 24 *h* in Tryptic Soy Broth (TSB)

3.3.5.2 GC-DMS spectra

GC-DMS retention time and compensation voltage profiles obtained from the detection of headspace gases collected from blank TSB (without *E. coli*) and from the spiked TSB (with *E. coli*) after $24\ h$ of incubation are shown in Figure 28.

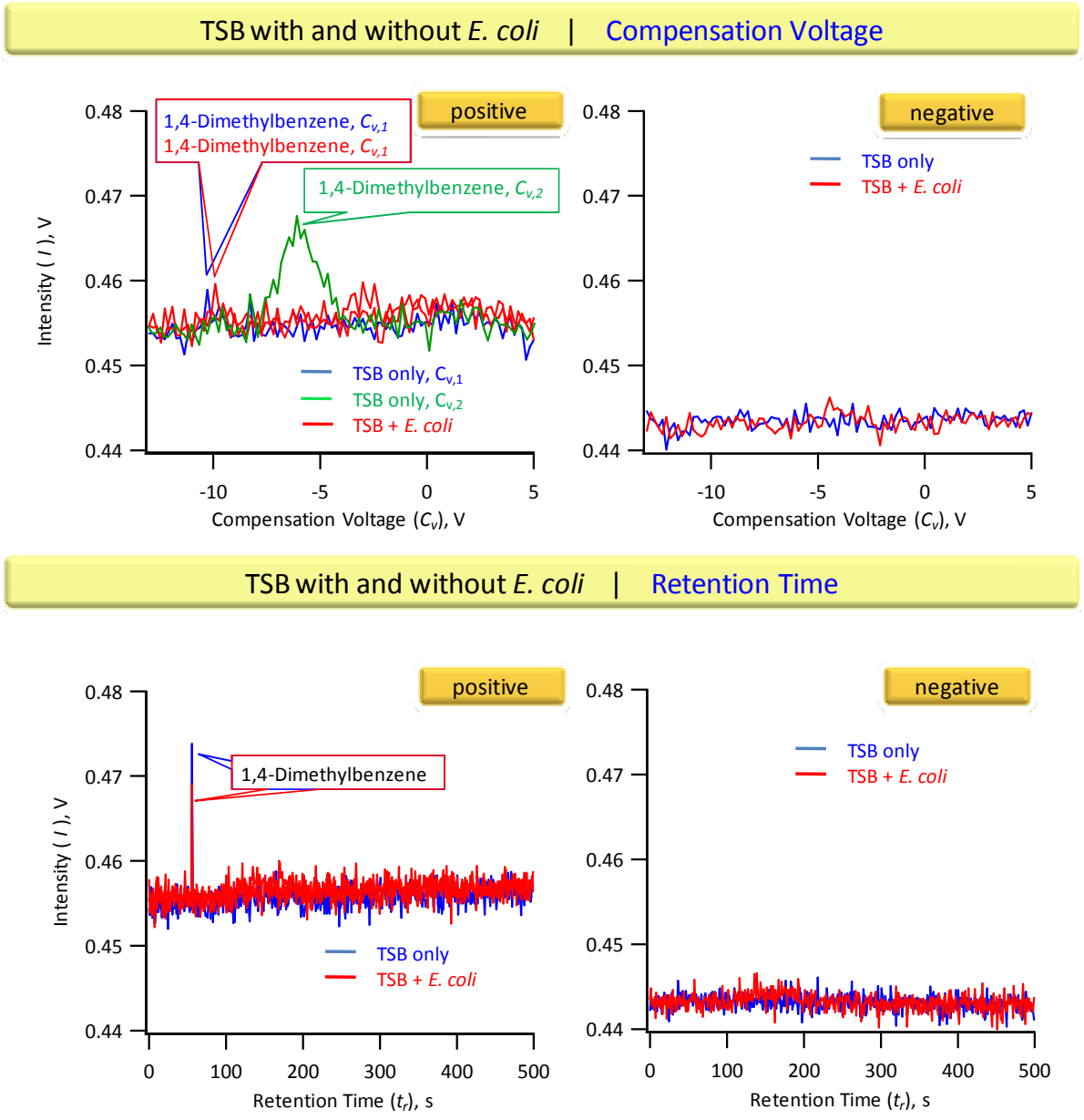

Figure 28. Retention Time and Compensation Voltage profiles of headspace gases from Tryptic Soy Broth (with and without E. coli) after $24\ h$ of incubation

As shown by Figure 28, 1,4-dimethylbenzene was detected in the positive mode. However, as also confirmed by the earlier GC-MS analysis in Figure 27 *b*, the 1,4-dimethylbenzene was produced by the media or the background itself, and not by the bacteria.

As an overall summary, a closer look at the intensity of each spectrum of volatile metabolite compounds released by *E. coli* grown in the different media and their detection by GC-DMS and GC-MS is given in Figure 29 and the intensity is presented as normalized peak area.

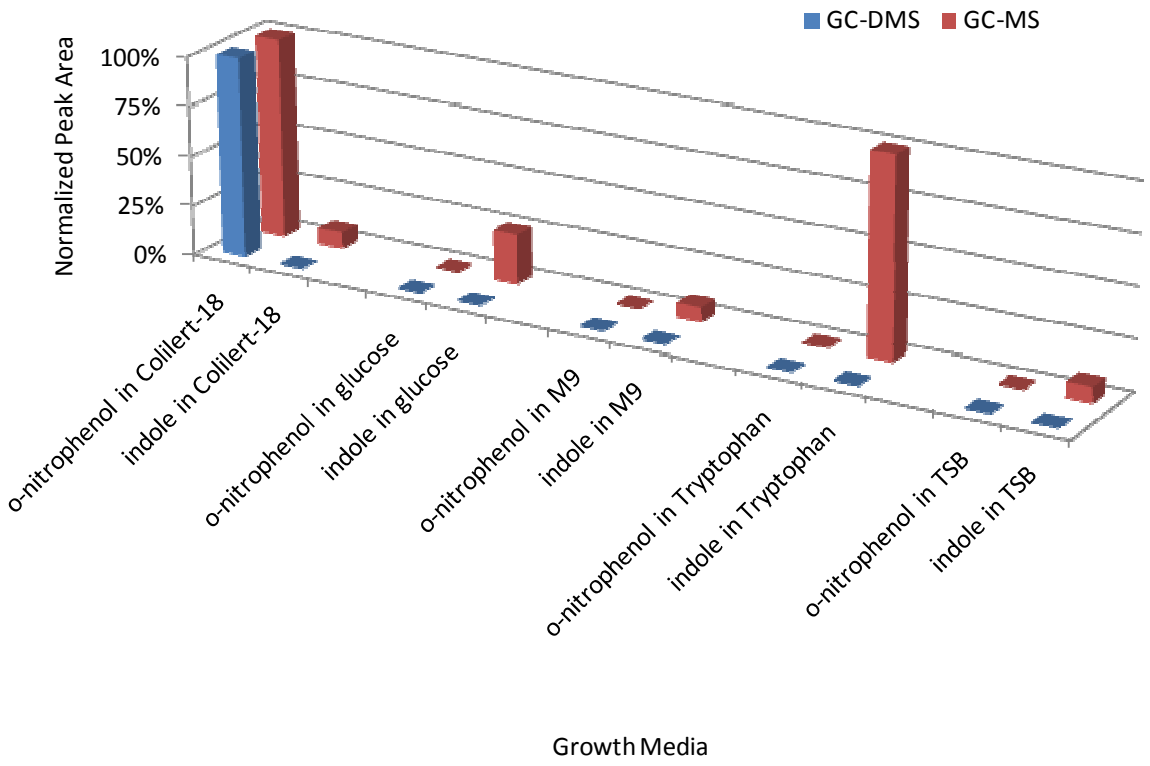

Figure 29. Normalized peak area of volatile metabolite compounds released by *E. coli* grown in different media and their detection by GC-DMS and GC-MS

In Figure 29 it is demonstrated that, in the detection of headspace gases of *E. coli* metabolites, the GC-MS (shown by the red bars) has a more sensitive detection towards certain compound with low volatility than the GC-DMS (shown by the blue bar). Indole compound was produced by *E. coli* grown in all different media, but the compound could only be detected by the GC-MS.

In addition to that, in comparison to other studies, the result from this study produced fewer compounds. In the earlier chapter it has been reviewed that *E. coli* grown on BHI broth such

as that reported by Yu et al. (2000) produced at least 12 different compounds including indole [6]; *E. coli* grown on LB agar such as that reported by Shnayderman et al. (2005) produced several ketone compounds [4, 5]; *E. coli* grown on Minimal medium such as that reported by Madula et al. (2009) produced hexane, benzaldehyde, butan-1-ol, ethanol, acetone, and several ketone compounds (hexan-2-one, heptan-2-one, and nonan-2-one) [5]; and *E. coli* grown on tryptic soy broth (TSB) such as that reported by Arnold et al. (1998) produced several alcohol compounds [5, 163].

The fewer type of compounds produced in this study (both in GC-MS and GC-DMS) is likely caused by the simplified approach used in the experiment, especially in the sample introduction method. As outlined in the material and methods, unlike in many other studies in which auto sampler and SPME fiber were used, only a simple gas-tight syringe was used in this study to inject the sample manually. The approach was simplified in accordance with the aim of the overall study to achieve a rapid and on-site detection of *E. coli*.

In addition to that, under the more recent coliform taxonomy, coliform and *E. coli* are characterized by the presence of β-galactosidase and β-glucuronidase enzymes [2, 23, 25, 27-30]. Therefore, when the analysis is done via GC-MS or GC-DMS, the relevant biomarkers are only *o*-nitrophenol and 4-methylumbelliferone.

In reviewing the GC-DMS result in Figure 29, *o*-nitrophenol was only produced when *E. coli* was grown in Colilert-18 (due to the presence of ONPG in this medium and the absence of ONPG in all other media). Therefore, among the five media being investigated, Colilert-18® is the only suitable media. However, since the analysis using GC-DMS could only detect *o*-nitrophenol, it could only confirm the presence/absence of coliform, not necessarily *E. coli*. The presence of *o*-nitrophenol only indicated the presence of coliform, but the absence of *o*-nitrophenol confirmed the absence both coliform and *E. coli*. To confirm the presence of *E. coli*, a fluorescent UV lamp is necessary.

3.4 Conclusions

On growing *E. coli* in five different media (Colilert-18®, glucose broth, M9-medium, tryptophan broth, and tryptic soy broth (TSB)), several compounds were detected by the GC-

MS and GC-DMS; however, some of these compounds were produced by the media themselves. Compounds that were produced uniquely by *E. coli* were only *o*-nitrophenol and indole.

When analyzed by the GC-MS, indole compound was produced by *E. coli* which was grown in every media, whereas *o*-nitrophenol was only produced by *E. coli* which was grown in Colilert-18® due to the absence of ONPG in all other media. However, when analyzed by the GC-DMS, no indole was detected in any media, whereas *o*-nitrophenol was able to be detected only in the Colilert-18® culture. Because of this and because *o*-nitrophenol is more unique than indole in determining the absence/presence of *E. coli* in water sample, the detection of *E. coli* by GC-DMS is best done when *E. coli* is grown in Colilert-18®. Further work needs to be done to determine the optimum incubation period and the detection limit of *o*-nitrophenol and *E. coli* grown in Colilert-18®. Such works are presented in the next chapter.

4 Determination of cleaving period of ONPG by β-D-galactosidase enzyme based on the detection of *o*-Nitrophenol by GC-DMS

4.1 Introduction

Classical methods to detect coliform and *E. coli*, such as the Multiple-tube Fermentation (MTF) and Membrane Filter (MF) methods require $24\ h$ to $48\ h$ to complete [24, 32]. For this reason, many advanced methods have been mainly focused on the shortening of the analysis time. Enzymatic method such as the detection of coliform and *E. coli* based on the presence/absence of β-D-glucuronidase and β-D-galactosidase activities, respectively, is an example of successful method because it is more rapid (i.e. $18 - 22\ h$) and sensitive than the classical method [2]. The method involves the use of chromogenic and fluorogenic substrates, namely ONPG (Ortho-Nitrophenyl-β-D-galactopyranoside) and MUGlu (4-methylumbelliferyl-β-D-glucoronide), which produce color and fluorescence effect upon cleavage by β-D-glucuronidase and β-D-galactosidase enzymes, which indicate the presence/absence of coliform and *E*. coli, respectively [2, 27].

The use of ONPG and MUGlu substrates in the detection and enumeration of coliform and *E. coli* was first introduced by Edberg and Edberg (1988) [66]. The authors demonstrated that examination of environmental isolates of total coliform and *E. coli* showed sensitivity equal to that of classical methods (up to $1\ CFU/100\ ml$) with potentially greater specificity [66]. Data also confirmed the ability to detect injured coliform with a maximum response time of $24\ h$. Rice et al. (1990, 1991) used numerous pure strains of *E. coli* to determine the detection efficiency of the defined-substrate technology with β-D-glucuronidase and showed positive results (95.5% β-D-glucuronidase-positive isolates in $24\ h$ and 99.5% positive after $28\ h$ of incubation). None of the non-*E. coli* isolates were positive [67, 68].

Many commercial methods that are widely used today, such as Colilert (IDEXX Laboratories, Portland, ME, USA), Colisure (Millipore corporation, Bedford, MA, USA), and Coli-Quick (Hach, Loveland, CO, USA), are developed based on this enzymatic method. Numerous comparisons among these commercial methods (or between the commercial methods with classical MTF and MF methods) have been reported [2]. Colilert-18®, which utilizes the defined substrate technique with ONPG and MUGlu is the most widely used method among

others and is included in the *Standard Method for the Examination of Water and Wastewater* [41]. However, the method still needs $18\ h$ to $22\ h$ to complete. To further shorten the analysis time, in this section the enzymatic method using Colilert-18® is investigated.

The main objectives of this chapter were to answer the following questions:

1. What is the detection limit of *E. coli*, i.e. what is the minimum cells concentration of *E. coli* that can be detected by the GC-DMS?

2. As mentioned in the previous chapter, the hydrolysis of ONPG by *E. coli* occurs as the following reaction:

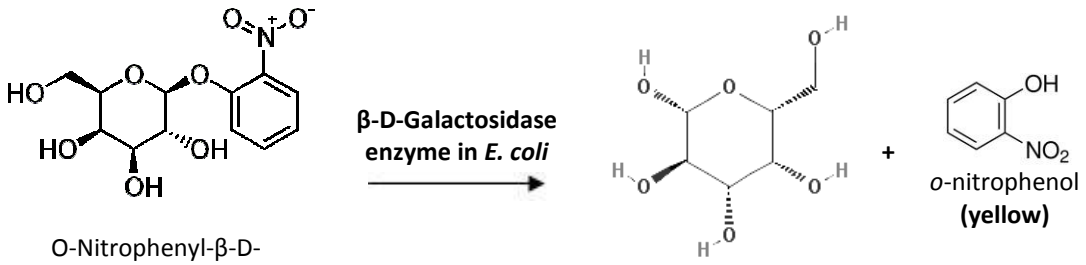

O-Nitrophenyl-β-D-galactopyranoside (ONPG)

β-D-Galactose

When *E. coli* is incubated in a rich ONPG environment, it does not immediately release *o*-nitrophenol. The β-D-galactosidase enzyme in *E. coli* needs a certain period of time in order to break the ONPG substrate into β-D-Galactose and *o*-nitrophenol (the so called cleavage opening process/ cleaving/ the splitting of a complex molecule into simpler molecules). How is the growth profile of *E. coli* from the initial incubation until a certain phase after the cleaving (in term of cells concentration and *o*-nitrophenol amount)?

3. As the overall objective of this study is to shorten the analysis time (by directly detecting the signal of *o*-nitrophenol instead of waiting for the clear visual appearance of *o*-nitrophenol), what is the minimum incubation period needed by *E. coli* to allow the enzymatic cleaving mentioned in #2?

4. What is the correlation between the bacteria cells concentration and the concentration of *o*-nitrophenol?

5. An XY scatter plot consists of cells concentration in the X-axis (as a predictor variable) and signal intensity of *o*-nitrophenol in the Y-axis (as a criterion variable) can be formulated from this study. Although *o*-nitrophenol acts rather as a secondary predictor variable (with cells concentration as a primary predictor variable), it would be necessary to know the sensitivity of the instrument itself in response to *o*-nitrophenol. Therefore, how is the relationship between *o*-nitrophenol concentration and its signal intensity? Also, what is the detection limit of *o*-nitrophenol?

To answers the above questions, the following works were done and the results are presented in this chapter:

- calibration of *o*-nitrophenol standard
- determination of the detection and quantitation limit of *o*-nitrophenol
- determination of the growth profile of *E. coli*
- determination of the cleavage opening period
- determination of the correlation between *E. coli* cells concentration and signal intensity
- determination of the detection and quantitation limits of *E. coli*

4.2 Experimental Section

4.2.1 Reagents and Samples

4.2.1.1 Chemicals

o-Nitrophenol (cat. nr. N19702, 98%) was purchased from Sigma-Aldrich (Steinheim, Germany) and used as received.

4.2.1.2 Bacteria

E. coli DSM 30083 was purchased from the *Deutsche Sammlung von Mikroorganismen und Zellkulturen GmbH* (Braunschweig, Germany). Prior to use, the bacteria was grown overnight on NB agar and incubated at $37\ ℃$.

4.2.1.3 Growth Media

Fourteen packages of Colilert-18® (IDEXX, cat. nr. WPO2OI-18) were used in this experiment. Eight packages were dissolved in sterile deionized water to make $8 \times 100\,ml$ Colilert-18® suspensions, the rest 6 packages were dissolved in $100\,ml$ of environmental water samples (to make $6 \times 100\,ml$ Colilert-18® suspensions). The $8 \times 100\,ml$ Colilert-18® suspensions were then distributed into 80 sample vials (to make $80 \times 10\,ml$ Colilert-18® suspensions). The capacity of each vial was $20\,ml$.

4.2.2 Instrumentation

4.2.2.1 GC-DMS

The experimental setup consisted of a miniaturized GC-DMS connected to a $0.5\,bar$ nitrogen gas supply. The operational principle of the microAnalyzer™ has been described in Chapter 2. The same experimental setup which was optimized and applied for the work in Chapter 3 was applied in this work without modifications.

To summarize, in this work, for each analysis, the sample pump ($80\,ml/min$) was run for $30\,s$ to collect $500\,\mu l$ headspace sample and $40\,ml$ nitrogen. A transport flow pump inside the instrument maintained a constant transport gas flow ($300\,ml/min$) through HCRMS (hydrocarbon/moisture trap) molesieve filters. After the $30\,s$ sampling, a 3-way valve was programmed to allow the flow of the transport gas ($1-5\,ml/min$) through the pre-concentration trap and the GC column. The temperature of the pre-concentration trap during the desorption of the chemical was programmed as follow: the initial temperature was set at $40\,°C$, and then it was increased to $200\,°C$ in $1\,s$, to $300\,°C$ in $4\,s$, and then was held at $300\,°C$ for $100\,s$. The sample was then passed through the GC column to allow a nominal preseparation of analytes. The GC was equipped with a 10-m×0.25-mm×0.25-µm DB-XLB column (Agilent Technologies). The GC column temperature was programmed as follow: the initial temperature was set at $60\,°C$ and held for $60\,s$, increased $1\,°C/s$ to $140\,°C$, and then held at $140\,°C$ for $200\,s$.

The DMS parameters were set as follow: the RF voltage was set at $1100\,V$; the scanning range of the GC-DMS spectra was recorded at the compensation voltage between $-13\,V$

and $+5\,V$ and at the retention time between $0\,s$ and $500\,s$. Response of the ion channels were recorded in both positive and negative modes.

4.2.2.2 GC-MS

For the confirmation of compounds identity, bacterial and blank samples were analyzed with a GC-17A GC-MS system (Shimadzu) equipped with an Rtx-440 (30-m×0.25-m×0.25-µm) fused silica column at a flow rate of $1.4\,ml/min$ of helium. The oven temperature was programmed as follow: the initial temperature was set at $40\ ℃$ and was held for $1\,min$, followed by $10\ ℃\ /min$ increase to a final temperature of $250\ ℃$ which was held constant for $5\,min$. The injector and interface temperature were held isothermally at $200\ ℃$ and $250\ ℃$, respectively. The sample ($500\ \mu l$) was injected manually into the column from gas-tight syringe, and the detector was set with a scan interval of $0.15\,s$ and m/z range of $45-350$.

4.2.3 Experiment and Data Analysis

4.2.3.1 Calibration of *o*-nitrophenol

Saturated vapors of *o*-nitrophenol (ONP) were prepared by placing $1\,g$ of ONP powder standard in $20\,ml$ capped vials. Different volumes of headspace gases samples were then collected from the sample vials and were then analyzed by the GC-DMS. The volumes of the headspace injection and the corresponding quantity of ONP are given in Table 6. The quantity was calculated using the following formula:

$$m = \frac{p_o v_o M}{(p_{atm} + p_o) V_m} \tag{1}$$

Where m is the weight of ONP, p_o is the vapor pressure of ONP (i.e. $0.113\,mmHg$ at $25\ ^oC$), v_o is the headspace injection volumes (listed in Table 6), M is the molar mass of ONP, $p_{atm}$is the atmospheric pressure, and V_m is molar volume of gas at STP (i.e. $22.414\,L/mol$). The calculation gives that for every $1\,\mu l$ of headspace injection volume, it contained $0.0082\,\mu g$ of ONP (or $8.2\,ng$ of ONP).

Table 6. Headspace sample injection volumes (and the corresponding weight of *o*-Nitrophenol) used in the calibration of *o*-Nitrophenol

No	Volume (μl)	Weight (μg)	Weight (ng)
1	5	0.0408	40.8
2	10	0.0816	81.6
3	20	0.1631	163.1
4	33	0.2691	269.1
5	50	0.4078	407.8
6	70	0.5709	570.9
7	90	0.7340	734.0
8	120	0.9787	978.7

The signal (intensity) data obtained from the GC-DMS analysis were recorded and then integrated over 3 dimensional axis (compensation voltage, retention time, and intensity). The result of the integration is presented as peak volume. Plots of the weight of *o*-nitrophenol against signal peak volume were produced for positive and negative modes (and given in Figure 30 and Figure 31, respectively). It was found that the peak volume was directly proportional to the quantity of *o*-nitrophenol. Therefore, a linear calibration function was derived. The calibration procedure was done using DIN 32645 (equivalent to ISO 11843) method and the procedure is explained below.

The linear regression curve which describes the dependency of the peak volume, y, on the weight of *o*-nitrophenol, x, followed a linear function:

$$y = mx + b \tag{2}$$

The gradient, m, was calculated from the ratio of square sums of xy, i.e Q_{xy}, and the square sums of xx, i.e. Q_{xx} :

$$m = \frac{Q_{xy}}{Q_{xx}} \tag{3}$$

The square sums of xy and xx are given by Eq. (4) and (5), respectively:

$$Q_{xy} = \sum_{i=1}^{N}(x_i y_i) - \frac{\sum_{i=1}^{N} x_i \sum_{i=1}^{N} y_i}{N} \tag{4}$$

$$Q_{xx} = \sum_{i=1}^{N} x_i^2 - \frac{(\sum_{i=1}^{N} x_i)^2}{N} \tag{5}$$

The intercept, b, was calculated from:

$$b = \bar{y} - m\bar{x} \tag{6}$$

Where $\bar{x}$ is the arithmetic mean value of the amount of *o*-nitrophenol and $\bar{y}$ is the arithmetic mean value of the peak volume:

$$\bar{x} = \frac{\sum_{i=1}^{N} x_i}{N} \tag{7}$$

$$\bar{y} = \frac{\sum_{i=1}^{N} y_i}{N} \tag{8}$$

The precision of the linear regression was defined by the rest standard deviation, s_y, which is the measure of the spread of the residue (the differences on y-axis between the measured value and the corresponding value on the regression curve):

$$s_y = \sqrt{\frac{Q_{yy} - \frac{Q_{xy}^2}{Q_{xx}}}{N-2}} \tag{9}$$

Q_{yy} was given by:

$$Q_{yy} = \sum_{i=1}^{N} y_i^2 - \frac{(\sum_{i=1}^{N} y_i)^2}{N} \tag{10}$$

The standard deviation of the method, s_{x0}, was calculated from the rest standard deviation, s_y:

$$s_{x0} = \frac{s_y}{m} \tag{11}$$

The upper and lower limits of the prediction band of the calibration curve were given by:

$$y_j^{u,l} = y_j \pm s_y t_{f,\alpha} \sqrt{\frac{1}{N} + \frac{1}{\widehat{N}} + \frac{\left(x_j - \bar{x}\right)^2}{Q_{xx}}} \tag{12}$$

where N is the number of calibration measurements, $\widehat{N}$ is the number of parallel calibration measurement, and $t_{f,\alpha}$ is the Student's t-value at f degrees of freedom ($f = N - 2$), at probability 95%, and at level of significance $\alpha = 0.05$ (type I error at one-sided question).

4.2.3.2 Determination of the limit of detection and quantitation of *o*-nitrophenol

The limit of detection, x_{LOD}, and limit of quantitation, x_{LOQ}, were estimated from the calibration curve using DIN 32645 method and the formula are given in Eq. (13) and (14), respectively:

$$x_{LOD} = \frac{s_y}{m} \cdot t_{f,\propto} \cdot \sqrt{\frac{1}{\widehat{N}} + \frac{1}{N} + \frac{\bar{x}^2}{Q_{xx}}} \tag{13}$$

$$x_{LOQ} = k\frac{s_y}{m} \cdot t_{f,\alpha} \cdot \sqrt{\frac{1}{\widehat{N}} + \frac{1}{N} + \frac{(kx_{LOD} - \bar{x})^2}{Q_{xx}}} \tag{14}$$

where k refers to $1/k$, i.e. the relative uncertainty of the result of the quantitation limit ($k = 3$ is often recommended). The value of $1/k$ is given by:

$$\frac{1}{k} = \frac{\Delta x_{LOQ}}{x_{LOQ}} \tag{15}$$

Δx_{LOQ} was calculated using:

$$\Delta x_{LOQ} = \frac{s_y}{m} \cdot t_{f,\alpha} \cdot \sqrt{\frac{1}{\widehat{N}} + \frac{1}{N} + \frac{(x - \bar{x})^2}{Q_{xx}}} \quad (16)$$

4.2.3.3 Preparation of bacteria

Two plates of *E. coli* colonies which were previously grown out of single colonies were inoculated into an RG tube containing $10\ ml$ of deionized water. The tube was shaken on a vortex mixer for $10\ s$ and then a series of dilution were made to prepare 3 suspensions (each $10\ ml$) with a concentration of $10, 100,$ and 1000 times lower than the original suspension. The cell concentrations in the diluted suspensions were determined using a Thoma counting chamber. The objective was to calculate the amount of inoculum needed to be inoculated into the growth media, Colilert-18® solution (in order to achieve a certain level of cells concentration). Samples of *E. coli* in Colilert-18® solution were placed inside $20\ ml$ headspace vials. The vials were capped with autoclaved aluminum caps and septa to retain the headspace compounds released by the bacteria.

4.2.3.4 Determination of growth curve and cleavage opening period

To determine *E. coli* growth curve and cleavage opening period, *E. coli* samples with initial concentration of $5 \times 10^7\ cells/ml$ were incubated for various incubation periods (Table 7). The incubation was done in a water bath GTL 1083 equipped with vials stake at $36\ ^oC$. During incubation, the vials were continuously shaken in the water bath.

At the end of each incubation period, headspace gases were collected using $500\ \mu l$ gas-tight syringe (for GC-DMS analysis) and the sample vials were placed in the dark at $4\ ^oC$ (for cells counting). GC-DMS spectra were recorded for both positive and negative modes at $RF = 1100\ V$. The spectra were then analyzed to investigate the presence/absence of *o*-nitrophenol.

Table 7. Variation of incubation periods applied in determination of *E. coli* growth curve and cleavage opening period

No	Initial cells concentration $(cells/ml)$	Incubation periods $(hours)$
1	5×10^7	0.5
2	5×10^7	1.0
3	5×10^7	1.5
4	5×10^7	2.0
5	5×10^7	2.5
6	5×10^7	3.0
7	5×10^7	3.5
8	5×10^7	4.0

Cells counting were done using Thoma counting chamber. The final cells concentration was recorded. For all analysis, the samples and procedures were made in triplicate. Plots of incubation period against final cells concentration were produced, resulting in a growth curve profile. The growth curve profile was analyzed; the lag phase and log phase of growth were distinguished from the trend.

To confirm the effect of cells concentration on the production of *o*-nitrophenol during lag phase (initial phase), *E. coli* samples with various initial concentrations (Table 8) were incubated for $\boldsymbol{0.5\ h}$.

Table 8. Variation of initial cells concentration applied in determination of cleavage opening period (incubation period = $\boldsymbol{0.5\ h}$)

No	Initial cells concentration $(cells/ml)$
1	5×10^6
2	5×10^7
3	5×10^8
4	5×10^9

4.2.3.5 Determination of correlation between *E. coli* concentration and signal intensity

To determine the correlation between *E. coli* concentration and signal intensity, a series of $10\ ml$ of *E. coli* samples with various initial concentrations were incubated for $\mathbf{2.5}\ \boldsymbol{h}$ (Table 9) at $36\ ^{o}C$ in the water bath GTL 1083 equipped with vials stake. Headspace samples were then collected with $500\ \mu l$ gas-tight syringe and were analyzed with GC-DMS. The responses (signal intensities) were recorded and then integrated into peak volume, for both positive and negative modes. The peak volumes were then plotted again the initial cells concentration. The plots were produced for both the positive and negative modes.

Table 9. Variation of initial cells concentration applied in determination of cleavage opening period (incubation period = $\mathbf{2.5}\ \boldsymbol{h}$)

No	Initial cells concentration $(cells/ml)$
1	3.0×10^7
2	3.5×10^7
3	4.0×10^7
4	5.0×10^7
5	6.0×10^7
6	7.0×10^7
7	8.0×10^7
8	9.3×10^7

The plots of final cells concentration against peak volume were found to be linear. Regression was done, and then the detection limit and quantitation limit of *E. coli* were estimated from the calibration curve using DIN 32645 method. The procedure is similar to the determination of detection and quantitation limit of *o*-nitrophenol.

4.2.3.6 Detection of *E. coli* in water sample collected from lake and river

Two types of water samples were collected from the environment:

- $3 \times 1L$ water samples were collected from the Baldeney Lake, Essen, and were labeled as X, Y, and Z.
- $3 \times 1L$ water samples were collected from the Ruhr river, Essen, and were also labeled as X, Y, and Z.

All samples were placed in $1L$ sterilized glass containers and were transported to the lab and were processed on the same day with the samples collection day. From each Z container, 100 ml of water samples were placed into separate distribution trays of Colilert®-18/Quanti-Tray/2000 system (IDEXX). The samples were then incubated at $36\ ^{o}C$ for $18\ h$. The Quanti-Tray analysis were performed in triplicate and the results were recorded as arithmetic mean values.

From each X and Y container, $2 \times 100\ ml$ Colilert-18® suspension were prepared (the water samples were mixed with Colilert-18® powders according to manufacturer's instruction); $4 \times 10\ ml$ samples were then collected from all X and Y containers and were then placed in $20\ ml$ sample vials. The samples were then incubated at $37\ ^{o}C$ for $2.5\ h$ and were then analyzed by GC-DMS.

4.3 Results and Discussion

4.3.1 Calibration of *o*-nitrophenol

To investigate the sensitivity of the GC-DMS towards *o*-nitrophenol, the correlation between the amount of *o*-nitrophenol and the signal intensity was investigated. This was done by calibrating a series of different amount of *o*-nitrophenol standard. The response (intensity) was recorded in the positive and negative modes. As GC-DMS consists of 3 dimensional data (compensation voltage, retention time, and intensity), the response was integrated over the 3 dimensional axis. The result of the intensity integration will be referred here as peak volume (instead of the usual peak area). The calibration curves obtained for the positive and negative modes are given in Figure 30 and Figure 31, respectively.

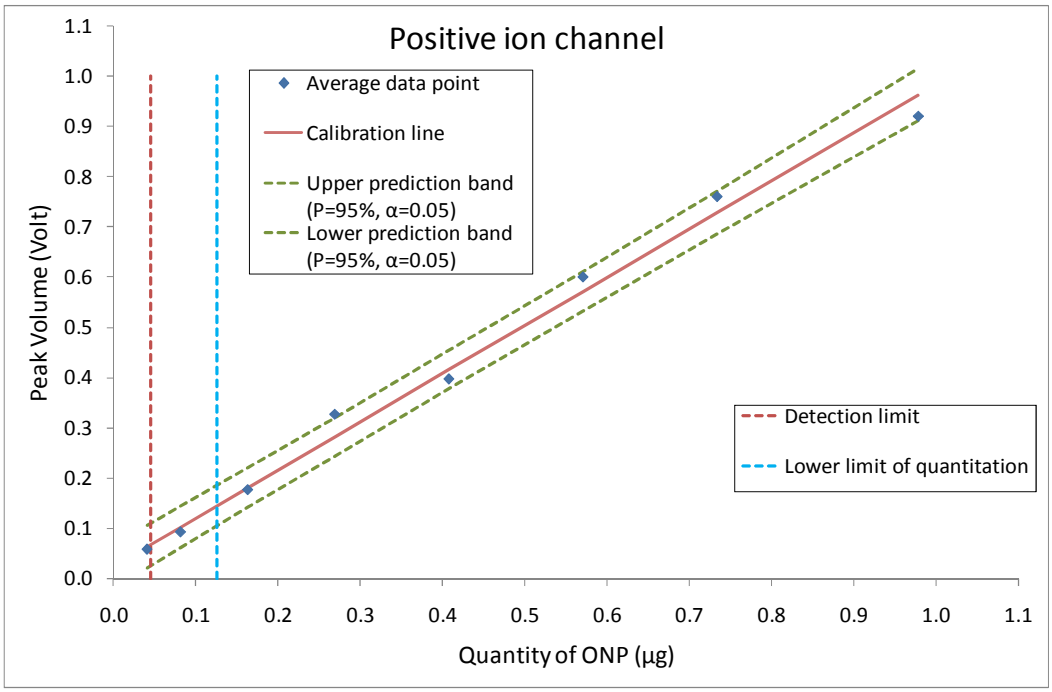

Figure 30. Response of the positive ion channels of the detector on headspace analysis of *o*-nitrophenol standard solutions

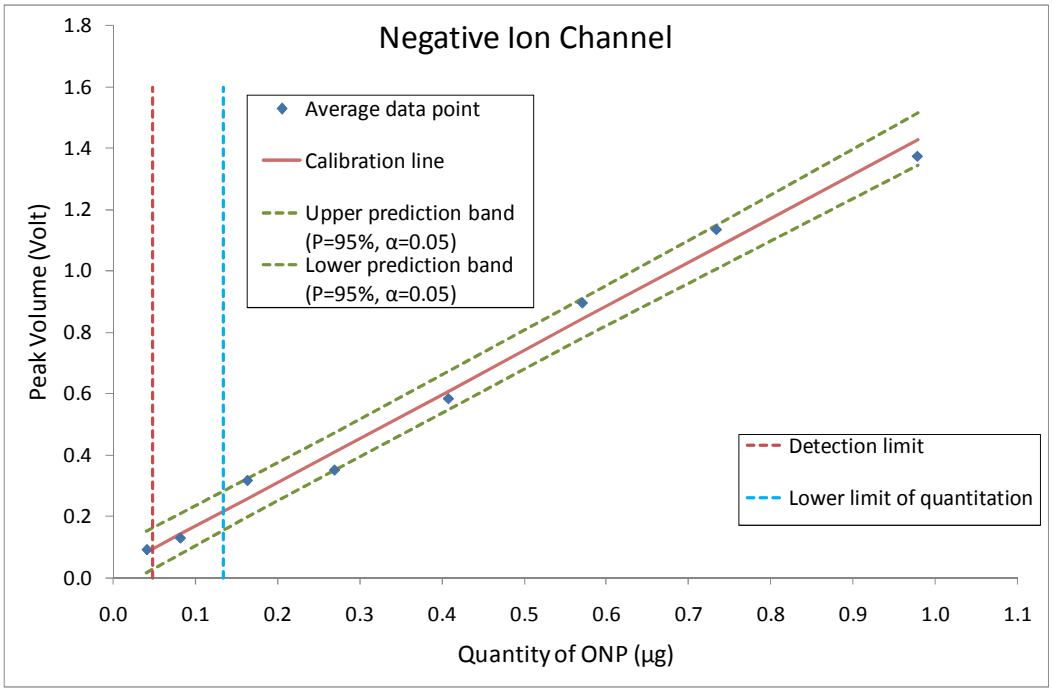

Figure 31. Response of the negative ion channels of the detector on headspace analysis of *o*-nitrophenol standard solutions

As can be seen in Figure 30, the correlation between the amount of *o*-nitrophenol and the peak volume for the positive ion channel is nearly linear in the range between $0.045\ \mu g$ and nearly $1\ \mu g$ of *o*-nitrophenol. The trend is similar for the negative mode, which is nearly linear in the range between $0.049\ \mu g$ and nearly $1\ \mu g$ of *o*-nitrophenol (Figure 31).

4.3.2 Detection limit and quantitation limit of *o*-nitrophenol

The detection limit and quantitation limit of *o*-nitrophenol were determined from the calibration curve using DIN 32645 method which were explained in section 4.2.3.5. Detection limits of $45.11\ ng$ and $48.85\ ng$ were obtained for the positive and negative modes, respectively. Lower limit of quantitations of $125.03\ ng$ and $134.67\ ng$ were obtained for the positive and negative modes, respectively. These results and the calibration parameters applied in the calculation are summarized in Table 10.

Table 10. Calibration parameters used in the calculation of detection and quantitation limits of *o*-Nitrophenol

Description	Symbol/ Equation	Value	
		Positive mode	Negative mode
Independent variable	x_i		
Response	y_i		
Calibration function	$y = mx + b$		
Gradient (slope)	m	0.9599	1.4348
Intercept	b	0.02	0.02
Number of calibration measurement	N	24	24
Number of paralel measurement	$\widehat{N}$	3	3
Rest standard deviation	s_y	0.0644	0.0499
Standard deviation of the method	s_{x0}	0.0660	0.0348
Upper (u) and lower (l) limits of the prediction band	$y_j^{u,l} = y_j \pm s_y t_{f,\alpha}\sqrt{\frac{1}{N}+\frac{1}{\widehat{N}}+\frac{(x_j-\bar{x})^2}{Q_{xx}}}$		
Degrees of freedom	$f = N - 2$	22	22
Probability value	P	95%	95%
Level of significance (type I error at one-sided question)	α	0.05	0.05
Student's t-value at $f = 13, P = 95\%, \alpha = 0.05$	$t_{f,\alpha}$	1.717	1.717
Detection limit	$x_{LOD} = \frac{s_y}{m} \cdot t_{f,\propto} \cdot \sqrt{\frac{1}{\widehat{N}}+\frac{1}{N}+\frac{\bar{x}^2}{Q_{xx}}}$	45.11 ng	48.85 ng
Lower limit of quantitation	$x_{LOQ} = k\frac{s_y}{m} \cdot t_{f,\alpha} \cdot \sqrt{\frac{1}{\widehat{N}}+\frac{1}{N}+\frac{(kx_{LOD}-\bar{x})^2}{Q_{xx}}}$	125.03 ng	134.67 ng

4.3.3 Determination of cleavage opening period

E. coli cells grow differently under different conditions. A typical growth curve usually follows a sigmoid function (having an "S" shape), e.g. as reported in the study of *E. coli* growth by Fujikawa et al. [169]. The phases of growth usually include a lag phase (initial phase, where *E. coli* either grow slowly or do not grow at all, adjust to new environment,

synthesize new enzymes, etc.), a log phase (an exponential phase, in which the slope of the growth curve is higher than the initial phase), and a stationary phase (in which the growth slows down).

The growth curve needs to be determined because studies show that β-galactosidase assay is best done when *E. coli* is entering the lag phase of growth [170-172]. Those studies suggested that this point takes place between 1 to $6\ h$ after *E. coli* is incubated (depending on the type of *E. coli* and the growing conditions).

To investigate the start of the log phase (which is indicated by the release of *o*-nitrophenol as a result of cleaving of ONPG by β-galactosidase enzyme in *E. coli*), *E. coli* samples with initial concentration of $5 \times 10^7\ cells/ml$ were incubated under various incubation periods, i.e. between 0 and $4\ h$ with $30\ min$ interval. Headspace gases were then collected from each sample at the end of each incubation period and subsequently analyzed by GC-DMS. The growth of *E. coli* with time is given in Figure 32 and the GC-DMS spectra are given in Figure 33.

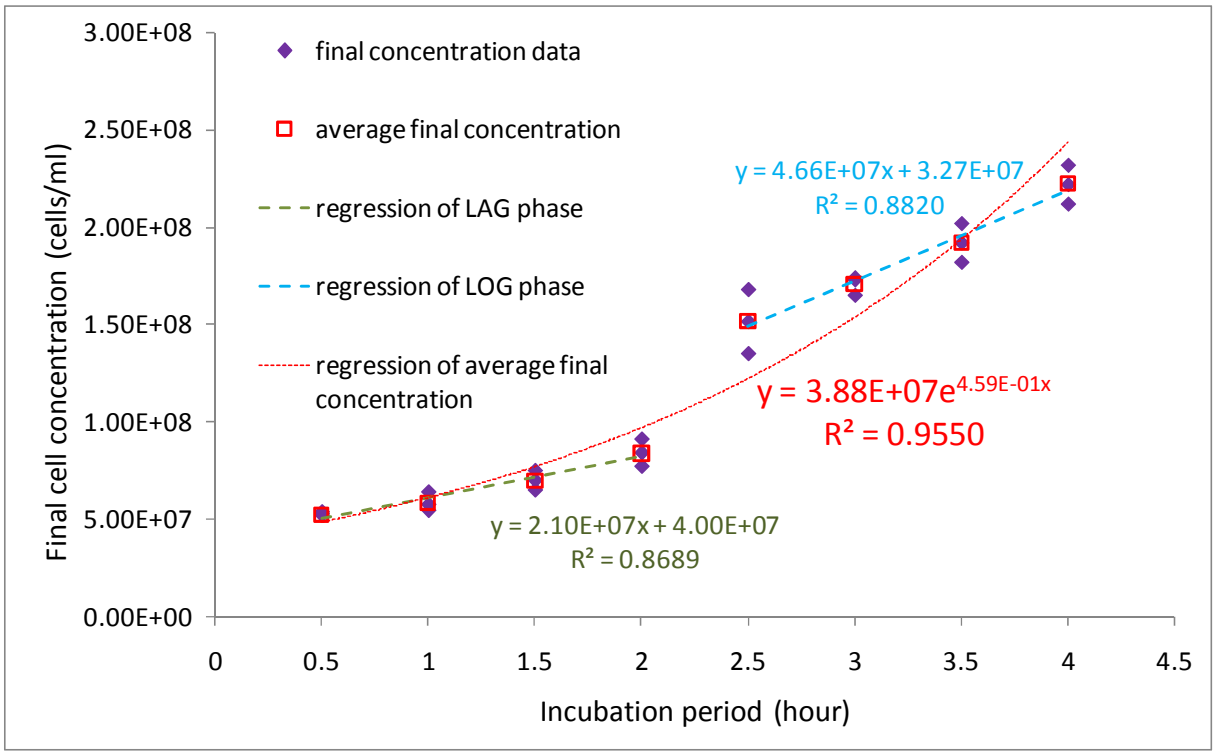

Figure 32. *E. coli* growth curve profile in the lag and log phases

The growth profile of *E. coli* in the first $4\ h$ consists of two phases, i.e. the lag and log phases. Regression lines were plotted for each phase and for the overall phase (Figure 32). From the slopes of the individual phases, it can be seen that the growth rate at the log phase is higher than that of the lag phase.

From the regression equation of the overall phase (Figure 32), the correlation between the final cell concentration and the incubation period is given by:

$$y = (3.88 \times 10^7)e^{0.459x} \tag{17}$$

The final cell concentration is determined not just by the incubation period, but also by the magnitude of the initial cell concentration as well, hence the 7 order or magnitude of the constant in the above equation (the initial cell concentration was $5 \times 10^7 cells/ml$). Taking into account the initial cell concentration into the equation, the correlation between the final cells concentration, the initial cell concentration, and the incubation period (for the first $4\ h$ of incubation) can be approached by the following exponential equation:

$$C_t = 0.776 C_0 e^{0.459 t_{inc}} \quad (18)$$

Where C_t is the final cells concentration, C_0 is the initial cells concentration, and t_{inc} is the incubation period.

A closer look at Figure 32 shows that the log phase is started approximately between $2 - 2.5\ h$ after the incubation. Therefore, the enzyme activation and the cleavage opening process (where β-galactosidase enzyme in *E. coli* cleaves the oxygen bridge in ONPG and splits the ONPG into β-galactose and *o*-nitrophenol) took in total between $2 - 2.5\ h$.

GC-DMS spectra in Figure 33 confirmed that no *o*-nitrophenol (ONP) signal was observed from headspace gases of *E. coli* samples which was incubated for $2\ h$. Six spectra are given in this figure:

- **Top frame (left)**: *E. coli* were incubated for $2\ h$ (no ONP was observed); the spectra of those incubated for $0.5\ h, 1\ h$, and $1.5\ h$ showed similar result, but not shown in this figure;
- **Top frame (right)**: *E. coli* were incubated for $2.5\ h$ (ONP was observed);
- **Middle frame**: *E. coli* were incubated for 3 and $3.5\ h$; both show ONP signals;
- **Bottom frame (left one)**: *E. coli* was incubated (in Colilert-18® solution, like all other aforementioned samples) for $4\ h$; ONP signal was observed;
- **Bottom frame (right one)**: Colilert-18® solution (contained no *E. coli*; given here for comparative purpose) was incubated for $4\ h$; no ONP signal was observed.

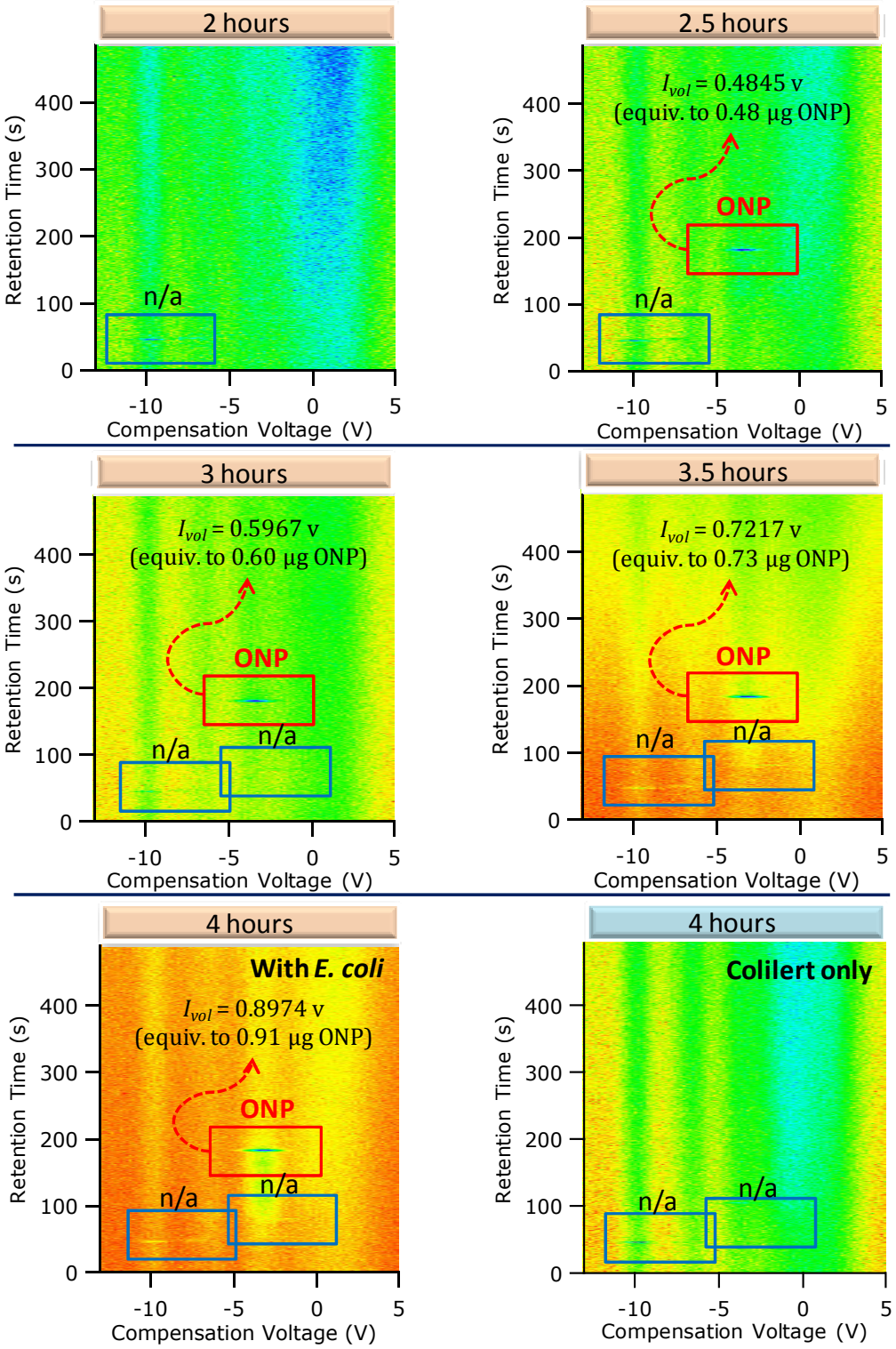

Figure 33. DMS spectra (positive mode) indicating the presence/absence of *o*-nitrophenol (ONP) in the headspace of *E. coli* DSM 30083 as a function of incubation period; n/a = unknown compounds. Remarks: the intensities of ONP are given as *peak volumes* (integrated signal intensities over 3-dimensional data) and the initial concentrations of *E. coli* were 5×10^7 $cells/ml$

As a remark, as seen in Figure 33, ONP was detected at a retention time of $t_r = 184.9\ s$ and a compensation voltage of $C_{v,1} = -2.82\ V$ (in the positive mode) and $C_{v,2} = -4.09\ V$ (in the negative mode). Besides ONP, a couple of other unknown compounds also appeared at:

- $t_{r,1} = 52\ s$; $C_{v,1,monomer} = -9.39\ V$; $C_{v,1,dimer} = -7\ V$
- $t_{r,2} = 80\ s$; $C_{v,2} = -2.3\ V$

Validation with GC-MS result shows no hit compounds for the identity of these unknown compounds. However, these compounds also appeared when *E. coli* was absent (as shown by the figure in the bottom frame (the one on the right, i.e. the blank medium)). Therefore, it can be assumed that these compounds were produced by the media itself.

The spectra shown in Figure 33 are spectra in positive mode. The ones in the negative mode showed similar result. Examples for complete spectra (positive and negative modes) are given in Figure 34. Here *E. coli* was incubated for $4\ h$.

As can be observed in Figure 33 (figure with the 6 spectra), the higher the incubation period, the stronger the intensity of the ONP signal (as a result of the increasing ONP concentration in the sample). More quantitative figures of the GC-DMS spectra are given in Figure 35 and Figure 36.

It should be noted that in Figure 33, the intensities of ONP are given as **peak volume** (integrated signal intensities over 3-dimensional data), whereas in Figure 35 and Figure 36, the intensities are given as intensities at a particular retention time (i.e. at $184.9\ s$). It should also be noted that the initial concentrations of *E. coli* (before incubation) were $5 \times 10^7\ cells/ml$.

Figure 35 and Figure 36 shows the intensity of ONP signal peak as a function of the incubation periods for both the positive and negative modes. The plots in both figures were fitted using Gaussian function. In Figure 35, the intensity scale is left as the original, whereas in Figure 36 the intensity scale is adjusted so that the baseline of all signals is at the same level (for comparative purpose). As can be seen in Figure 36, the higher the incubation period, the higher the intensity of ONP is. In addition to that, the intensity signal in negative mode tends to be higher than that in positive mode.

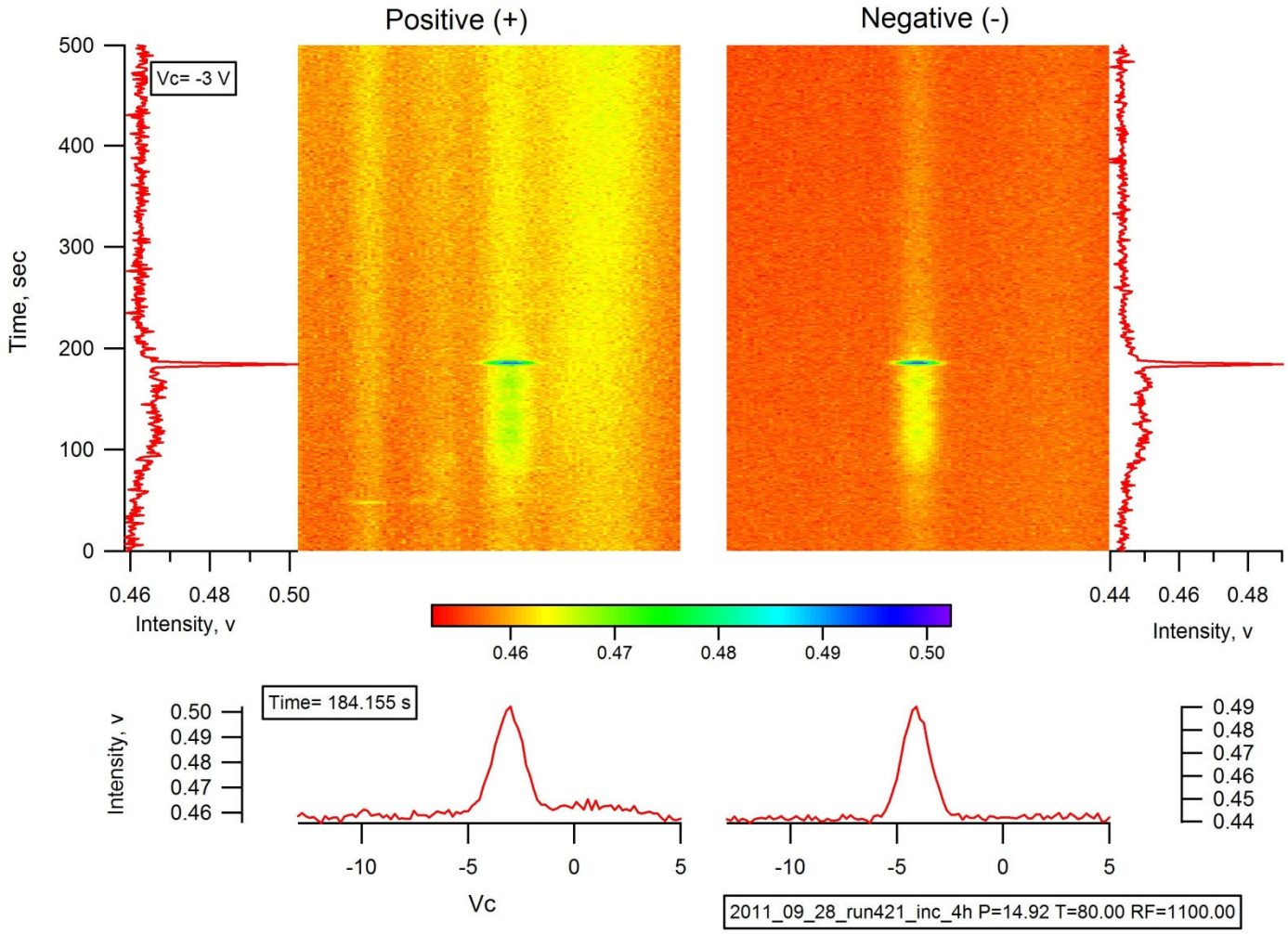

Figure 34. DMS spectra indicating the presence of *o*-nitrophenol (ONP) in the headspace of *E. coli* DSM 30083 which was incubated for 4 h

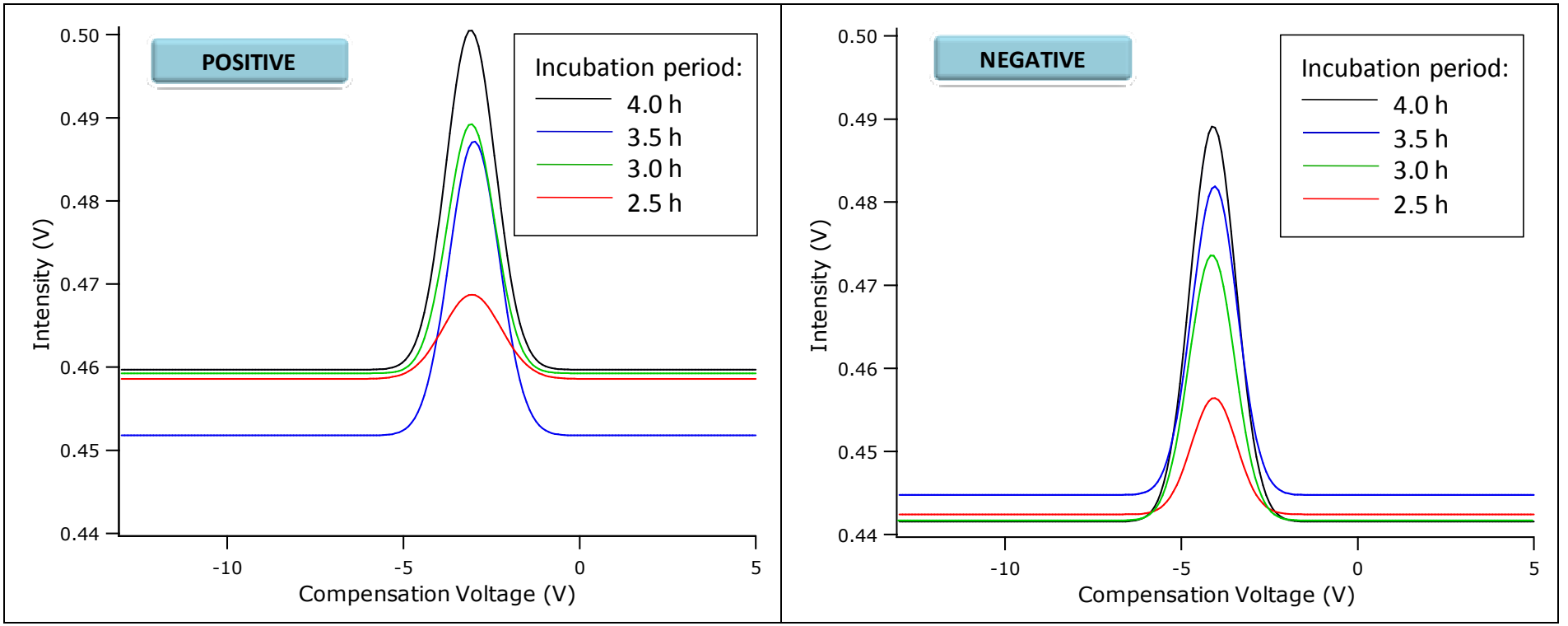

Figure 35. Intensity of *o*-nitrophenol as a function of incubation period of *E. coli* for both positive and negative ion channels; curves are fitted using Gaussian function; the intensity scale is raw (no baseline adjustment)

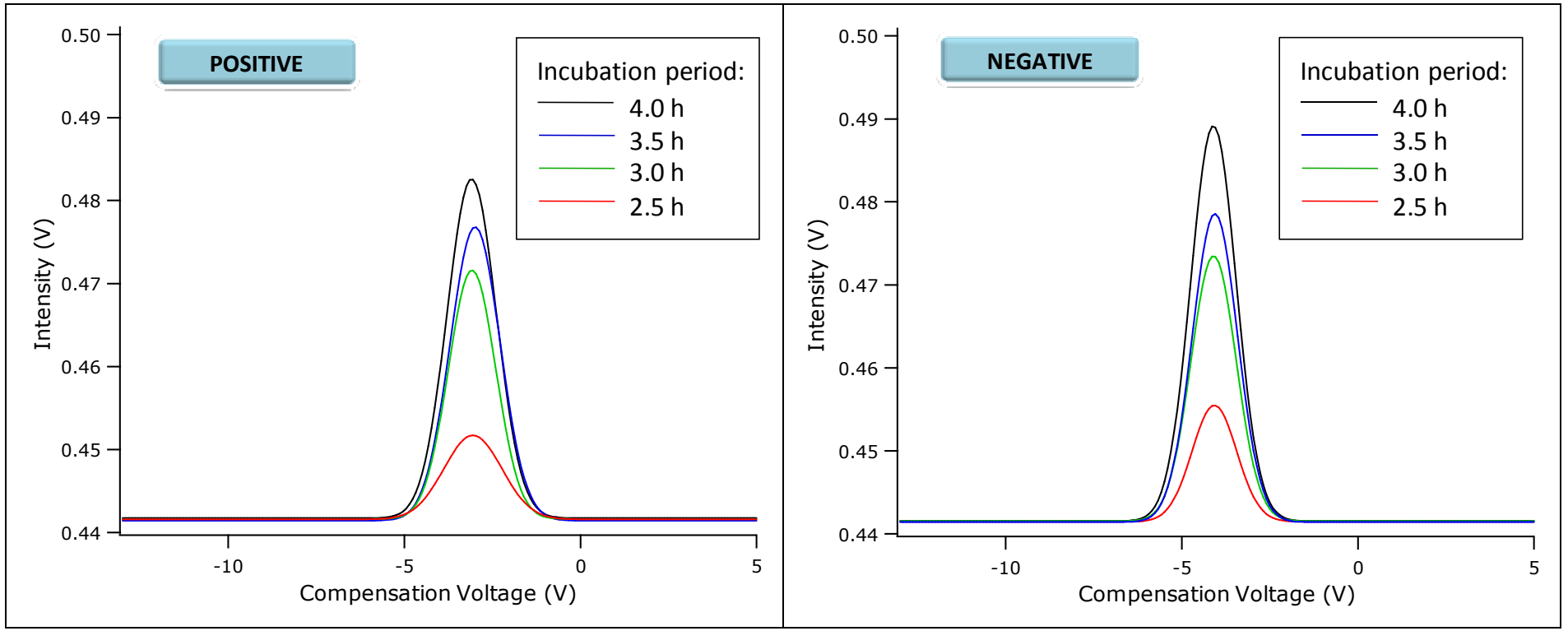

Figure 36. Intensity of *o*-nitrophenol as a function of incubation period of *E. coli* for both positive and negative ion channels*;* curves are fitted using Gaussian function; the intensity scale is shifted (baseline is adjusted at the same level, i.e. $0.442\ V$)

To further confirm the importance of sufficient incubation periods in ONPG cleaving, *E. coli* with various initial concentrations (ranging from 5×10^6 to 5×10^9 $cells/ml$, which is equivalent to 6.7 to 9.7 in logarithmic scale) were each incubated for $0.5\ h$ (within the lag phase period) and were then analyzed with GC-DMS. The initial and final cells concentration (before and after incubation) were then plotted and shown in Figure 37. As a comparison, *E. coli* with initial concentration of $5 \times 10^7 cells/ml$ and incubated for $2.5\ h$ is also shown in Figure 37.

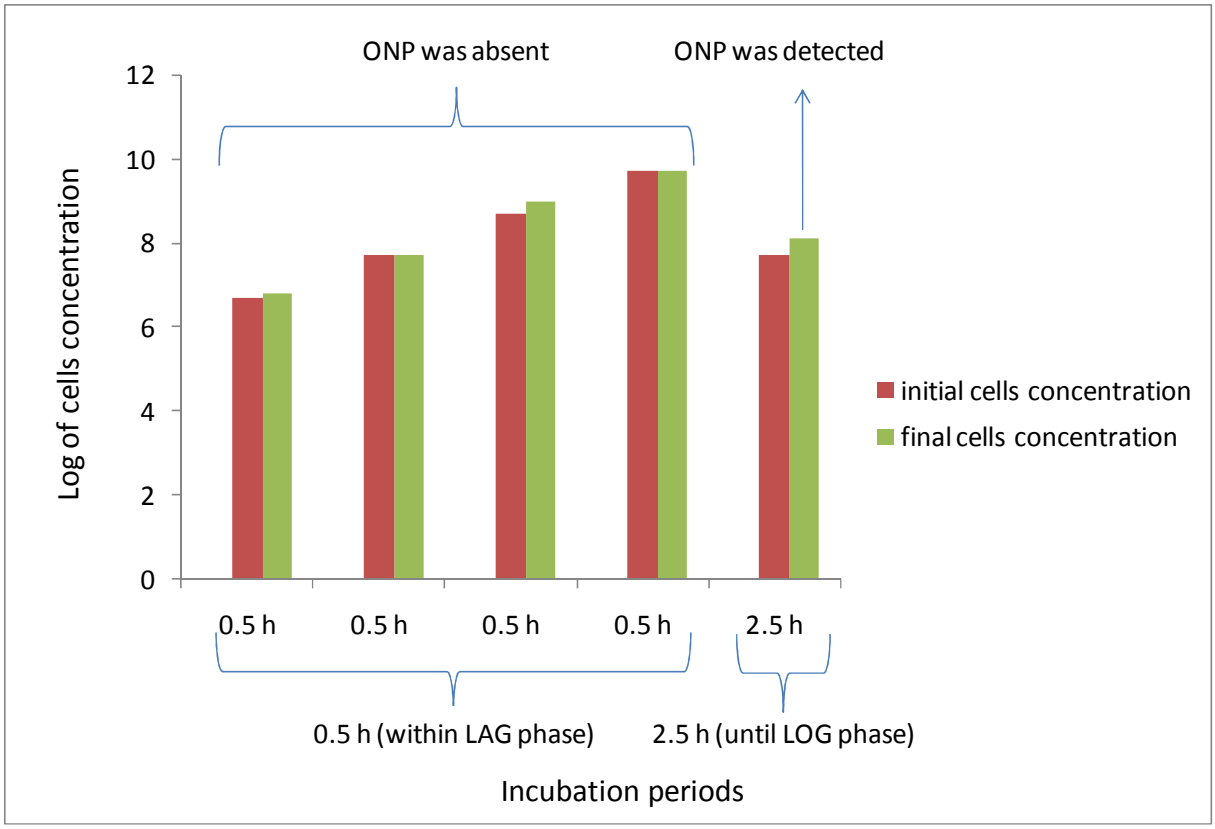

Figure 37. Presence/ absence of *o*-nitrophenol in relation to the cells concentration and incubation periods

As illustrated in Figure 37, no *o*-nitrophenol was detected when *E. coli* was incubated for $0.5\ h$, although some of the final concentrations were higher than the one incubated for $2.5\ h$ (due to the higher initial concentrations). This confirms the earlier result that the detection of *o*-nitrophenol does not determined by the cell concentration alone, but also by the incubation periods.

4.3.4 Correlation between cells concentration and signal intensity

In the first section of the results (section 4.3.1) the correlation between the amount of *o*-nitrophenol and signal intensity has been described. While it was necessary to investigate the sensitivity of GC-DMS against *o*-nitrophenol, the amount of *o*-nitrophenol itself is actually a dependent variable, i.e. it depends on the concentration of *E. coli* cells in the samples.

To see the relation between cells concentration and signal intensity, calibration was done. The results are presented in form of **initial** cells concentration against signal peak volume. The **initial** cells concentration refers to the concentration of *E. coli* **before incubation**. The incubation period was set at $2.5\ h$. The signal peak volume refers to the peak volume which was recorded as a response to **final concentration** (concentration of *E. coli* **after incubation**). The results of the calibration are given in Figure 38 and Figure 39, each for the positive and negative mode, respectively.

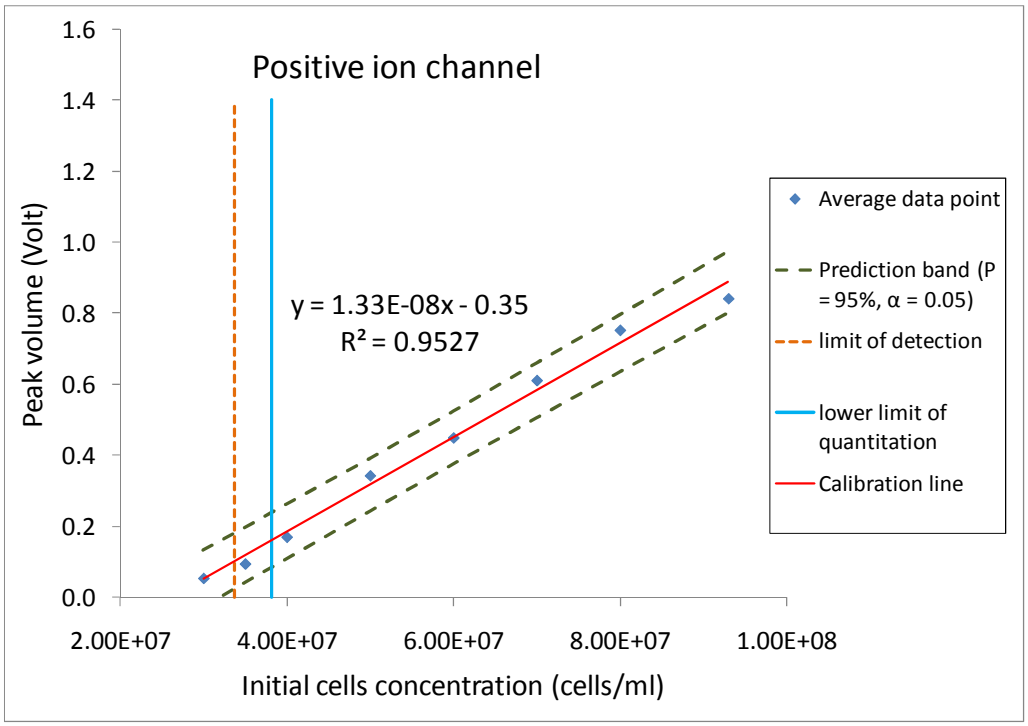

Figure 38. Response of the POSITIVE ion channels of the detector on various INITIAL cells concentration of *E. coli*; incubation period = $2.5\ h$

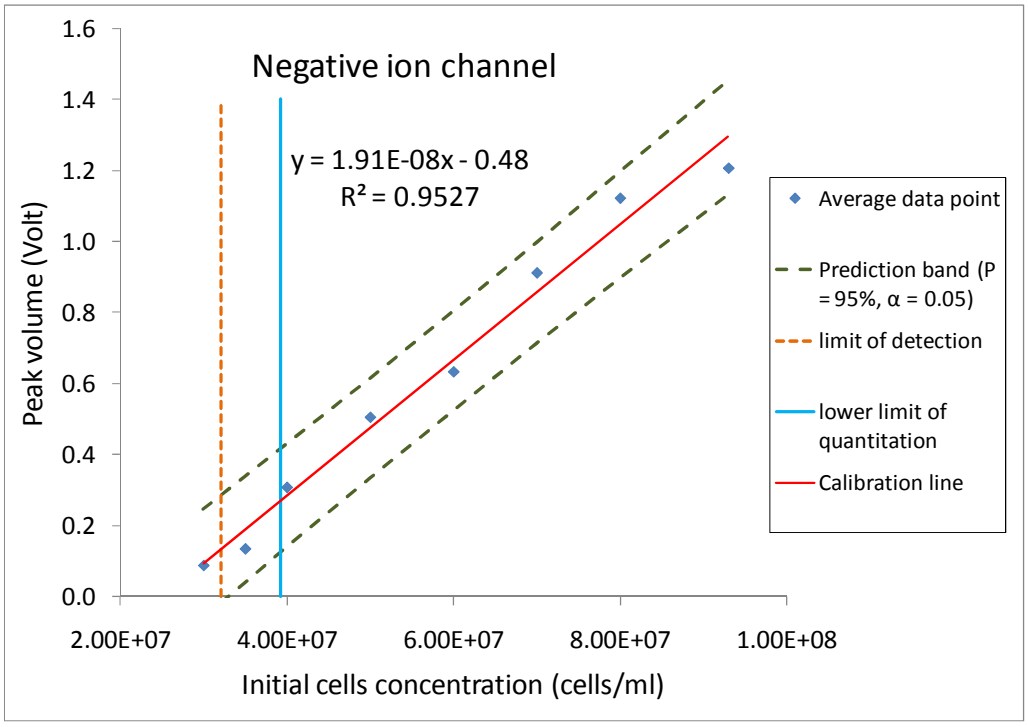

Figure 39. Response of the NEGATIVE ion channels of the detector on various INITIAL cells concentration of *E. coli*; incubation period = $2.5\ h$

From Figure 38, it can be inferred that the correlation between the signal intensity (peak volume) and the **initial** cells concentration in the positive mode is nearly linear in the concentration range between 3×10^7 and 8×10^7 $cells/ml$. Similar trend was observed for the negative mode (Figure 39).

4.3.5 Detection limit and quantitation limit of *E. coli*

The detection limit and quantitation limit were determined from the calibration curve using DIN 32645 method. Detection limits of $3.37 \times 10^7$and $3.21 \times 10^7 cells/ml$ were obtained for the positive and negative modes, respectively. Lower limit of quantitations of 3.72×10^7 and 3.92×10^7 $cells/ml$ were obtained for the positive and negative modes, respectively. The results and the statistical parameters are summarized in Table 11.

Table 11. Detection and quantitations limits for *E. coli* and the corresponding statistical parameters used in the calculation *(part* 1*)*

Description	**Symbol/ Equation**	**Value**	
		Positive mode	**Negative mode**
Independent variable	x_i		
Response	y_i		
Calibration function	$y = mx + b$		
Gradient (slope)	$m = \frac{Q_{xy}}{Q_{xx}}$	1.33×10^{-8}	1.91×10^{-8}
Intercept	$b = \bar{y} - m\bar{x}$	-0.35	-0.48
Number of calibration measurement	N	24	24
Number of paralel measurement	$\widehat{N}$	3	3
Rest standard deviation	$s_y = \sqrt{\frac{Q_{yy} - \frac{Q_{xy}^2}{Q_{xx}}}{N-2}}$	0.0707	0.1341
Standard deviation of the method	$s_{x0} = \frac{s_y}{m}$	5.33×10^6	7.03×10^6

Table 11b. Detection and quantitations limits for *E. coli* and the corresponding statistical parameters used in the calculation *(part 2 (continued))*

Description	Symbol/ Equation	Value	
		Positive mode	Negative mode
Upper (u) and lower (l) limits of the prediction band	$y_j^{u,l} = y_j \pm s_y t_{f,\alpha} \sqrt{\frac{1}{N} + \frac{1}{\hat{N}} + \frac{(x_j - \bar{x})^2}{Q_{xx}}}$		
Degrees of freedom	$f = N - 2$	22	22
Probability value	P	95%	95%
Level of significance (type I error at one-sided question)	α	0.05	0.05
Student's t-value at $f = 13, P = 95\%, \alpha = 0.05$	$t_{f,\alpha}$	1.717	1.717
Detection limit	$x_{LOD} = \frac{s_y}{m} \cdot t_{f,\propto} \cdot \sqrt{\frac{1}{\hat{N}} + \frac{1}{N} + \frac{\bar{x}^2}{Q_{xx}}}$	3.37×10^7 $cells/ml$	3.21×10^7 $cells/ml$
Lower limit of quantitation	$x_{LOQ} = k\frac{s_y}{m} \cdot t_{f,\alpha} \cdot \sqrt{\frac{1}{\hat{N}} + \frac{1}{N} + \frac{(kx_{LOD} - \bar{x})^2}{Q_{xx}}}$	3.72×10^7 $cells/ml$	3.92×10^7 $cells/ml$

4.3.6 Detection of coliform and *E. coli* in lake and river water samples

Water samples collected from two locations, the Baldeney lake and the Ruhr river in Essen, were mixed with Colilert-18® powder and incubated for $2.5\ h$. Headspace gases were then collected from all $20\ ml$ vials (containing $10\ ml$ sample each) which were incubated for $2.5\ h$ and were then analyzed by GC-DMS.

GC-DMS results showed no ONP detected in any of the environmental water samples. The initial cells concentrations in the samples were given in column C of Table 12. It should be noted that the cell concentration values in column C were the concentrations of total cell of

mixed cultures (not necessarily coliforms and *E. coli* cultures because the viewing under Thoma counting chamber neither reveals the identity of the bacteria nor distinguishes the living cells from the dead cells). As can be compared with the value in column D of Table 12, the cell concentrations of the environmental water samples were below the detection limit of the instrument.

Colilert®-18/Quanti-Tray/2000 tests which were subjected on the environmental water samples which were incubated for $18\ h$ showed that coliform and *E. coli* were present in the water samples. The concentration of coliform and *E. coli* in the water samples collected from the Baldeney lake and the Ruhr river were given in column B of Table 12 and the results are presented as *Most Probable Number* (MPN) per $100\ ml$ according to the MPN reading table of the Colilert®-18/Quanti-Tray/2000 method.

Table 12. Detection of coliform and *E. coli* in lake and river water samples by Colilert®-18/Quanti-Tray/2000

A	*B*		*C*	*D*	
Sampling location	Colilert®-18/Quanti-Tray/2000		Thoma cell counting chamber	Detection limit of GC-DMS (from Table 11)	
	Coliform ($\frac{MPN}{100\ ml}$)	*E. coli* ($\frac{MPN}{100\ ml}$)	Initial cells concentration ($cells/ml$)	Positive mode ($cells/ml$)	Negative mode ($cells/ml$)
Baldeney lake	2025.0	258.1	6.15×10^5	3.37×10^7	3.21×10^7
Ruhr river	342.8	68.6	1.10×10^5		

4.4 Conclusions

Determination of cleaving period of ONPG by β-D-galactosidase enzyme based on *E. coli* growth curve profile and the detection of *o*-nitrophenol by GD-DMS was successfully done in this section. It was found that the cleaving period is approximately $2.5\ h$ as indicated by the shift of growth curve from the lag (initial) phase into a log phase (in which the growth rate increased after $2.5\ h$ of incubation of *E. coli*) and as indicated by the detection of *o*-nitrophenol (ONP) by the GC-DMS. Headspace analysis of *E. coli* samples using GC-DMS at RF

Voltage $1100\,V$ gave DMS spectra of *o*-nitrophenol signal at a retention time of $184.9\,s$. Overall, the method permits a total analysis time within just $3\,h$, which is significantly faster than the standard Colilert-18® method. Using DIN 32645 method, detection limits of $45.11\,nanogram$ and $48.85\,nanogram$ were obtained for ONP, each for the positive and the negative channels of the detector, respectively. Under the applied method (in which *E. coli* was incubated for $2.5\,h$ at $36\ ^{o}C$), the aforementioned limits correspond to $3.37 \times 10^{7}$and $3.21 \times 10^{7} cells/ml$, each for the positive and negative ion channels, respectively. Coliform and *E. coli* bacteria in water samples collected from the Baldeney lake and the Ruhr river, Essen, were not able to be detected by GC-DMS because the cells concentrations in the water samples were too low (below the detection limit of the instrument). Further work including whether the method could differentiate *E. coli* and coliform from other bacteria are needed.

5 Differentiation of *E. coli* and coliform bacteria using GC-DMS and GC-MS based on enzymatic approach

5.1 Introduction

In the previous chapter, it has been described that by growing **pure** culture of *E. coli* in Colilert-18®, GC-DMS was able to detect *o*-nitrophenol (ONP) which was produced by the bacteria (with a magnitude of $10^7\ cells/ml$ of initial cells concentration) . However, in most cases of environmental water samples, *E. coli* usually exists as a **mixed** culture, together with other coliform bacteria or also with non-coliform bacteria.

It has been described in the previous chapter that *o*-nitrophenol was produced by *E. coli* grown in an ONPG-rich medium such as Colilert-18® due to the presence or activation of β-galactosidase enzyme in *E. coli*. However, according to the modern coliform taxonomy, this enzyme is not unique just to *E. coli*, but also to other bacteria in the coliform group. This means, the absence of *o*-nitrophenol can confirm the absence of *E. coli,* but the presence of ONP will not necessarily confirm the presence of *E. coli,* or that the whole ONP detected are not produced by *E. coli* alone. Therefore, it is necessary to investigate whether the developed method could distinguish the different bacteria in order to avoid false positive results. It would also be interesting to see if the developed method could differentiate different strains of *E. coli* because not every *E. coli* is pathogenic.

Differentiation of different types of bacteria using **non miniaturized** GC-DMS (conventional GC-DMS) has been reported by several studies. Shnaydermann et al. (2005) demonstrated the differentiation of *E. coli, B. subtilis, B. thuringiensis,* and *M. smegmatis* using headspace technique with GC-DMS [4]. Prasad et al. (2006) demonstrated the differentiation of Gram-negative from Gram-positive bacteria using pyrolysis technique conjugated to GC-DMS (py-GC-DMS) [133]. Krebs et al (2006) and Cheung at al. (2009) also employed py-GC-DMS to discriminate different types of *Bacillus* [118, 138]. In addition to the non miniaturized version of the GC-DMS, most of these works were performed not based on the detection of unique biomarker(s), but rather on the pattern recognition of the detected compounds.

In this work, the performance of the miniaturized GC-DMS in the differentiation of bacteria was assessed through the presence/absence of ONP biomarker. Spectra of *E. coli* metabolites were compared to the spectra of other *E. coli* (with different strains) metabolites; 3 different strains of *E. coli* (*E. coli* DSM 30083, *E. coli* DSM 1576, and *E. coli* RV) were prepared and GC-DMS spectra of their metabolites were compared with each other. The GC-DMS spectra of *E. coli* metabolites were also compared to the metabolites spectra of another coliform bacterium, namely *K. pneumoniae*. *K. pneumoniae* is an opportunistic pathogen often found in water and is associated with pneumonia and urinary tract infections. Spectra of *E. coli* metabolites were then compared to the metabolites spectra of a non-coliform bacterium, namely *P. aeruginosa*. *P. aeruginosa* was chosen due to its health relevance and interference with *E. coli* presence. *P. aerugnosa* is an opportunistic pathogen that is often responsible for lung, urinary tract, and kidney infections and is often found in many natural and artificial water environments such as public swimming pool [173-176]. For each GC-DMS analysis, a validation using GC-MS was also done to confirm the identity of the metabolites compounds.

5.2 Experimental Section

5.2.1 Reagents and Samples

5.2.1.1 Bacteria

Four coliform bacteria (*E. coli* DSM 30083, *E. coli* DSM 1576, *E. coli* RV, and *K. pneumoniae*) and a non-coliform bacterium (*P. aeruginosa*) were used and obtained from the DSMZ (Braunschweig, Germany), except *E. coli* RV (Ring-Versuch) which was obtained from IWW Zentrum Wasser (Muelheim a.d. Ruhr, Germany). Prior to use, all bacteria were grown overnight at $37\ ℃$ on NB agar.

5.2.1.2 Growth Media

Eight packages of Colilert-18® (IDEXX, cat. nr. WPO2OI-18) were used in this experiment. Each package was dissolved in $100\,ml$ of sterile deionized water as per manufacturer instruction.

5.2.2 Instrumentation

5.2.2.1 GC-DMS

The experimental setup consisted of a miniaturized GC-DMS (microAnalyzer™ from the Sionex, USA) connected to a $0.5\ bar$ nitrogen gas supply. The operational principle of the instrument has been described in the previous chapter. The same experimental setup was applied in this work without modifications.

As a summary, in this work, for each analysis, the sample pump ($80\ ml/min$) was run for $30\ s$ to collect $500\ \mu l$ headspace sample and $40\ ml$ nitrogen. A transport flow pump inside the instrument maintained a constant transport gas flow ($300\ ml/min$) through HCRMS (hydrocarbon/moisture trap) molesieve filters. After the $30\ s$ sampling, a 3-way valve was programmed to allow the flow of the transport gas ($1-5\ ml/min$) through the pre-concentration trap and the GC column.

The temperature of the pre-concentration trap during the desorption of the chemical was programmed as follow: the initial temperature was set at $40\ °C$, and then it was increased to $200\ °C$ in $1\ s$, to $300\ °C$ in $4\ s$, and then was held at $300\ °C$ for $100\ s$. The sample was then passed through the GC column to allow a nominal preseparation of analytes. The GC was equipped with a 10-m×0.25-mm×0.25-µm DB-XLB column (Agilent Technologies). The GC column temperature was programmed as follow: the initial temperature was set at $60\ °C$ and held for $60\ s$, increased $1\ °C/s$ to $140\ °C$, and then held at $140\ °C$ for $200\ s$.

The DMS parameters were set as follow: the RF voltage was set at $1100\ V$; the scanning range of the GC-DMS spectra was recorded at the compensation voltage between $-13\ V$ and $+5\ V$ and at the retention time between $0\ s$ and $500\ s$. Response of the ion channels were recorded in both positive and negative modes.

5.2.2.2 GC-MS

For the confirmation of the compounds identity, headspace gases of bacterial samples were analyzed with a GC-17A GC-MS system (Shimadzu) equipped with an Rtx-440 (30-m×0.25-m×0.25-µm) fused silica column at a flow rate of $1.4\ ml/min$ of helium. The oven temperature was programmed as follow: the initial temperature was set at $40\ ℃$ and was

held for $1\ min$, followed by $10\ ℃\ /min$ increase to a final temperature of $250\ ℃$ which was held constant for $5\ min$. The injector and interface temperature were held isothermally at $200\ ℃$ and $250\ ℃$, respectively. The sample ($500\ \mu l$) was injected manually into the column from gas-tight syringe, and the detector was set with a scan interval of $0.15\ s$ and m/z range of $45 - 350$.

5.2.3 Procedures

5.2.3.1 Inoculum Preparation

Two plates of each bacteria colony that were previously grown out of single colonies were inoculated into each RG tube containing $10\ ml$ of deionized water. The suspensions were shaken for $10\ s$ and were then decimally diluted to prepare suspensions with concentrations of 10, 100, and 1000 times lower than the original suspension. The cell concentrations were then counted using the Thoma counting chamber.

5.2.3.2 Detection of Coliform and Non-coliform Bacteria using Miniaturized GC-DMS

To detect and distinguish coliform and non-coliform bacteria based on the presence of *o*-nitrophenol in their headspace, four coliform bacteria (*E. coli* DSM 30083, *E. coli* DSM 1576, *E. coli* RV, and *K. pneumoniae*) and a non-coliform bacterium (*P. aeruginosa*) were all inoculated into Colilert-18® in $20\ ml$ headspace vials individually. The volume of the bacterial suspensions was each $10\ ml$ and the initial concentration was $5 \times 10^7\ cells/\ ml$. The samples were incubated for $3\ h$ and the headspace gases were analyzed with GC-DMS and GC-MS. After the injection of the headspace gases into microAnalyzer and GC-MS, the sample vials were immediately stored at $4\ ℃$ for cells counting. Blank samples without bacteria were also analyzed. All samples were made at least in triplicates.

5.2.3.3 Headspace Sampling and Analysis

Headspace of volatile metabolites of *E. coli* was collected from each sample vial using a $500\ \mu l$ gas-tight syringe (Hamilton, USA). The syringe was injected at a depth of $1\ cm$ above the samples suspension. The volume of each headspace sample was $500\ \mu l$. At the end of the incubation period, the headspace samples were injected into the GC-DMS system for a differential mobility spectra analysis (and into the GC-MS system for the confirmation of the compounds identity),

5.2.4 Data Analysis

5.2.4.1 GC-DMS data

For each analysis, the GC-DMS spectra corresponding to the detected positive and negative ions were recorded using Expert^{TM} and the chromatographic data was automatically stored as Microsoft Office Excel workbook. IGOR Pro 6 was then used to generate the GC-DMS spectra, to process the data, and to generate graphs.

In generating the retention time and compensation voltage graphs, IGOR Pro 6 was used. In some of the graphs, the data were processed using the Gaussian curve fitting functions when necessary. Both the raw data and the processed data are presented in the same frames.

5.2.4.2 GC-MS data

For each analysis, the GC-MS spectra were recorded using GCMS "LabSolutions" Version 2.30 (Shimadzu Corporation) and the chromatographic data was automatically stored as $*.qgd$ data file. The "PostRun" version of the software was then used to analyze the data and to generate graphs.

In identifying peaks, besides applying manual observation (by comparing the visually observed peaks from the blank samples and peaks from the spiked samples), auto-integration was also applied. Fifty highest peaks from each spectrum were auto-integrated and the identified peaks were listed in the fragment table. Using "similarity search" function which is connected to the NIST library database, the peaks were then identified.

In presenting the spectra, each spectrum in the figure was also smoothed. The smoothing was done using the Savitzky-Golay filter.

5.3 Results and Discussion

To distinguish coliform from non-coliform bacteria based on the presence of *o*-nitrophenol in their headspace, four coliform bacteria (*E. coli* DSM 30083, *E. coli* DSM 1576, *E. coli* RV, and *K. pneumoniae*) and a non-coliform bacterium (*P. aeruginosa*) which were incubated individually in Colilert-18® were analyzed using GC-DMS and GC-MS.

The GC-MS and GC-DMS spectra of volatile metabolite compounds released by the bacteria are given in Figure 40 - Figure 45 (for the GC-MS) and Figure 46 - Figure 51 (for the GC-DMS).

5.3.1 GC-MS spectra of the bacterial metabolites

To have a thorough comparison among the GC-MS spectra, the results will be presented in the following forms:

1. At first each of the bacterial metabolites spectra is compared to the blank medium. Figure 40 refers to *E. coli* DSM 30083, Figure 41 refers to *K. pneumoniae,* and Figure 42 refers to *P. aeruginosa*. In every comparison to their blank medium, each figure is divided into 3 frames:
    a. **Top frames** always display plots with retention time between 3.5 and $9\ min$
    b. **Middle frames** always display plots with retention time between 9 and $15\ min$
    c. **Bottom frames** always display plots with retention time between 15 and $21\ min$
2. Spectra of *E. coli* bacteria with different strains are compared to each other (Figure 43). The result is also divided into 3 frames as above.
3. Spectra of *E. coli* DSM 30083 is compared to spectra of *K. Pneumoniae* (Figure 44) and to *P. aeruginosa* (Figure 45). Each figure also consists of 3 frames of retention times.

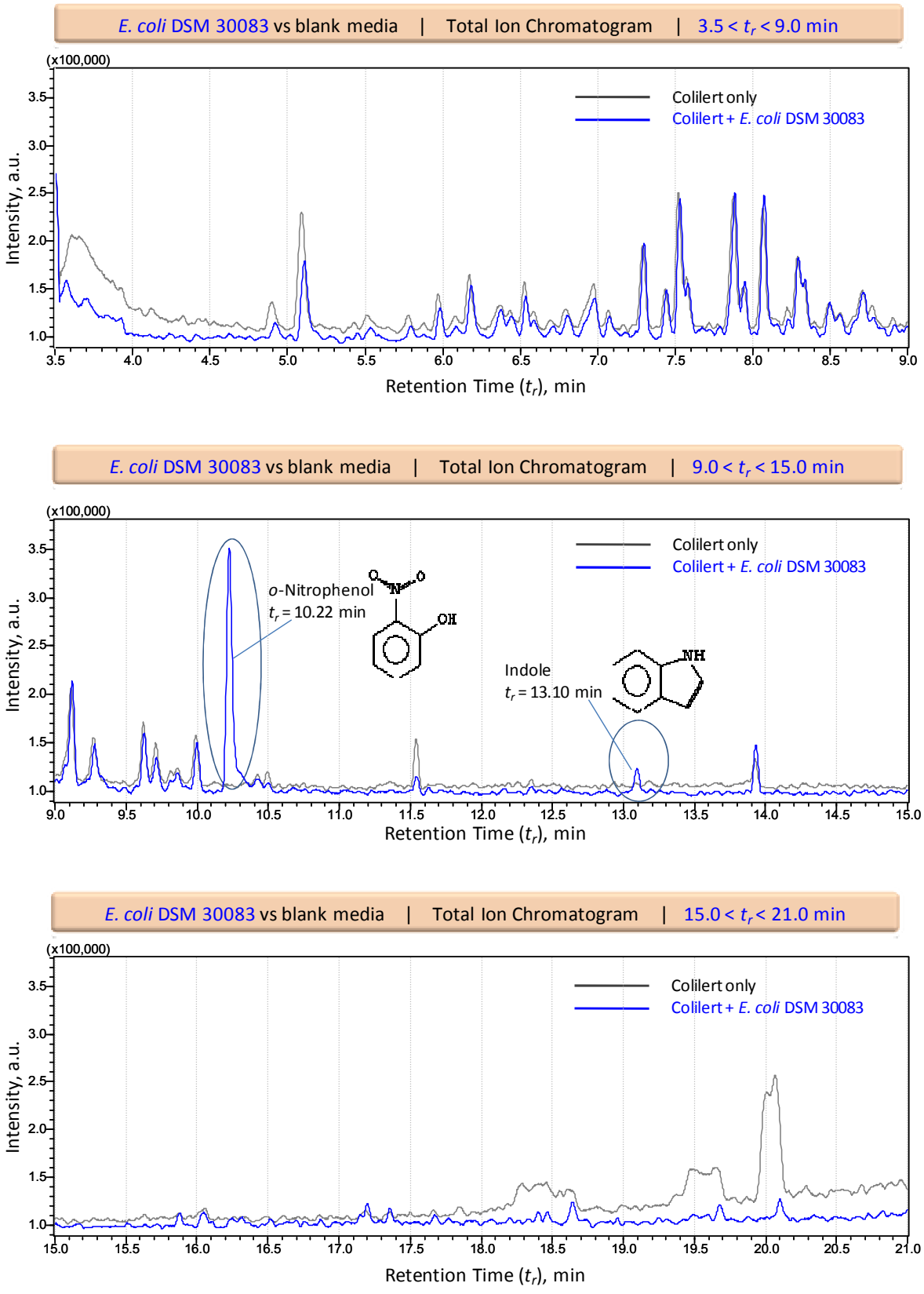

Figure 40. GC-MS spectra of *E. coli* DSM 30083 in compared with the blank media (Colilert-18®)

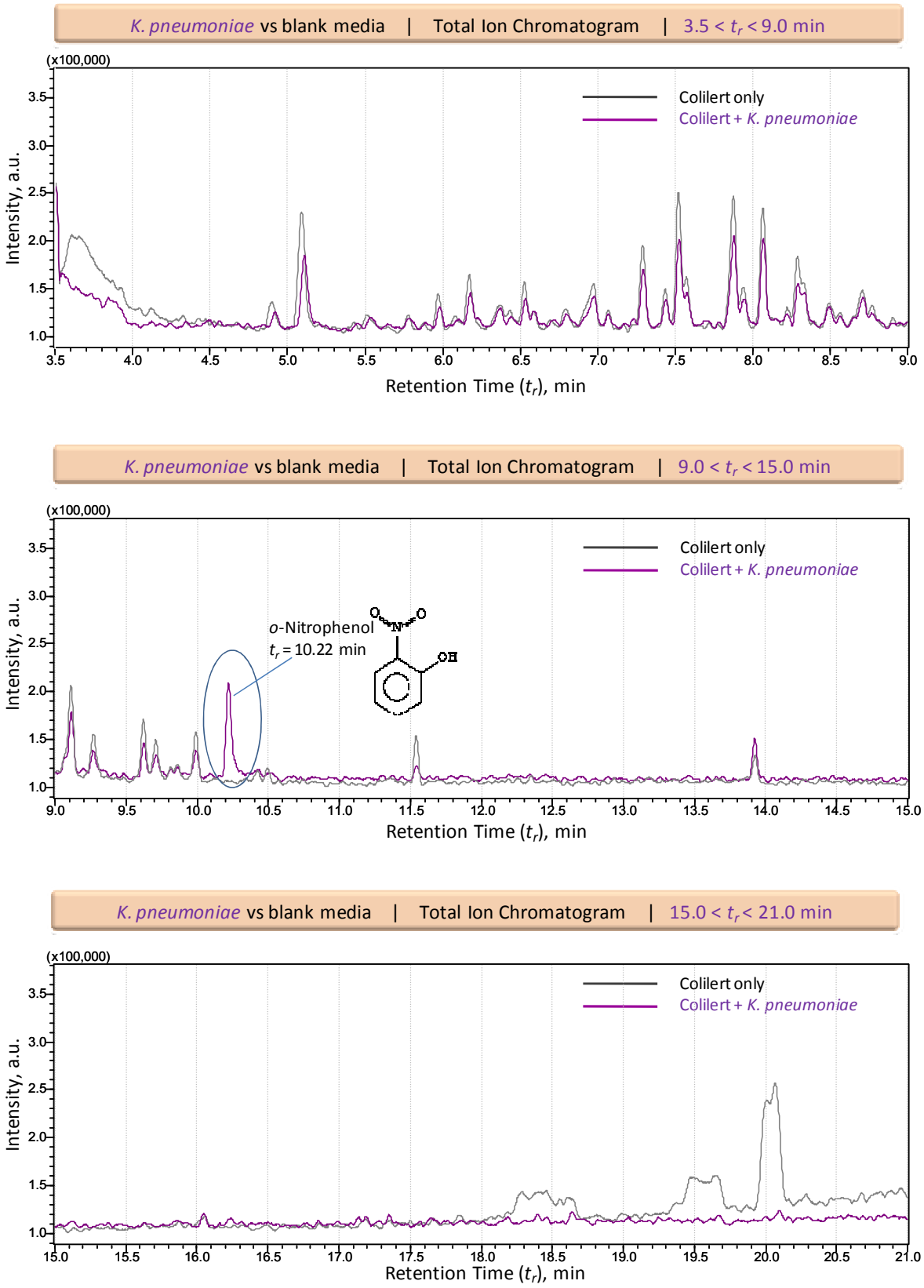

Figure 41. GC-MS spectra of *K. pneumonia* in compared with the blank media (Colilert-18®)

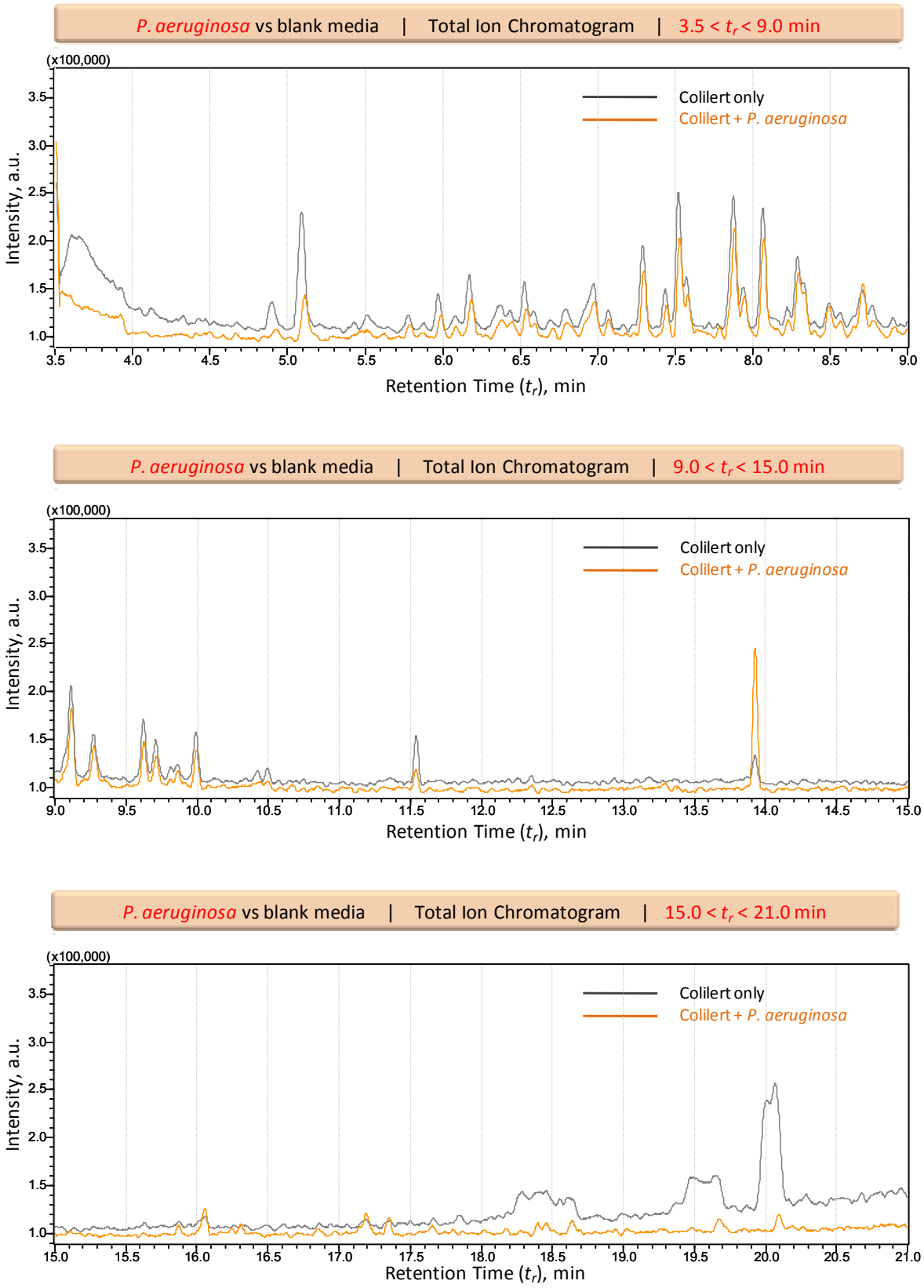

Figure 42. GC-MS spectra of *P. aeruginosa* in compared with the blank media (Colilert-18®)

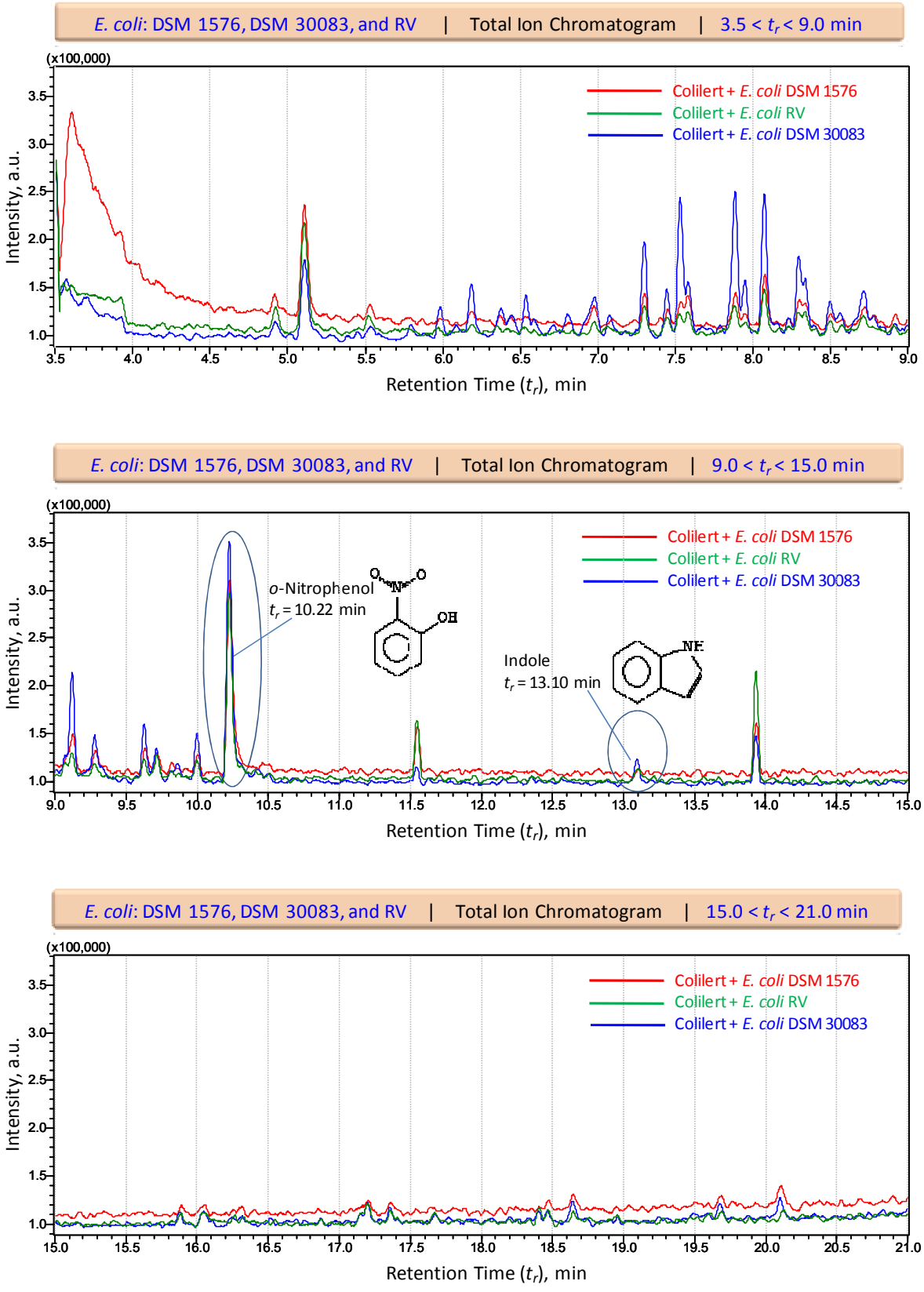

Figure 43. GC-MS spectra of *E. coli* DSM 30083, in compared with other *E. coli* (*E. coli* DSM 1576 and *E. coli* RV metabolites)

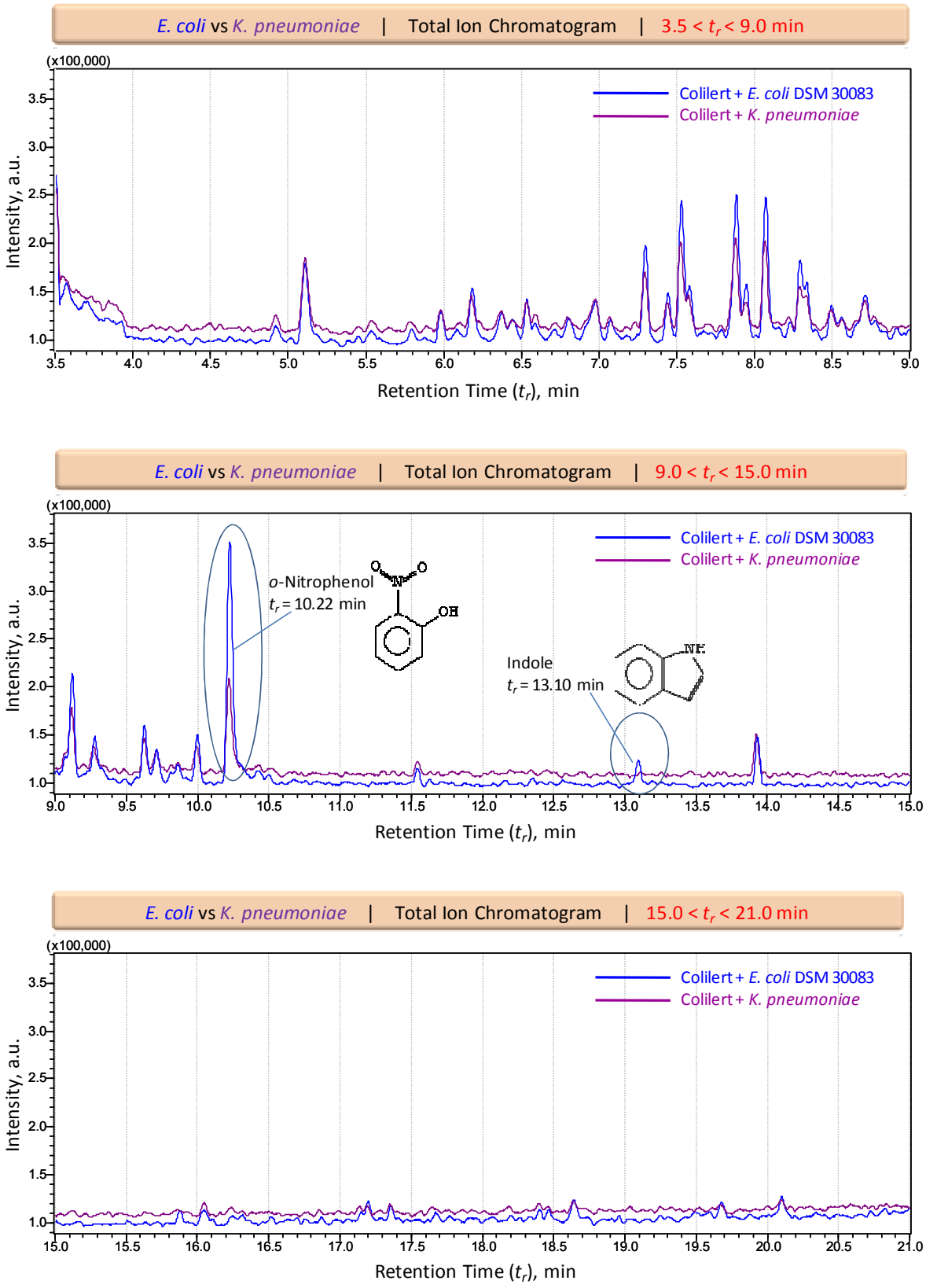

Figure 44. GC-MS spectra of *E. coli* DSM 30083 in compared with *K. pneumoniae*

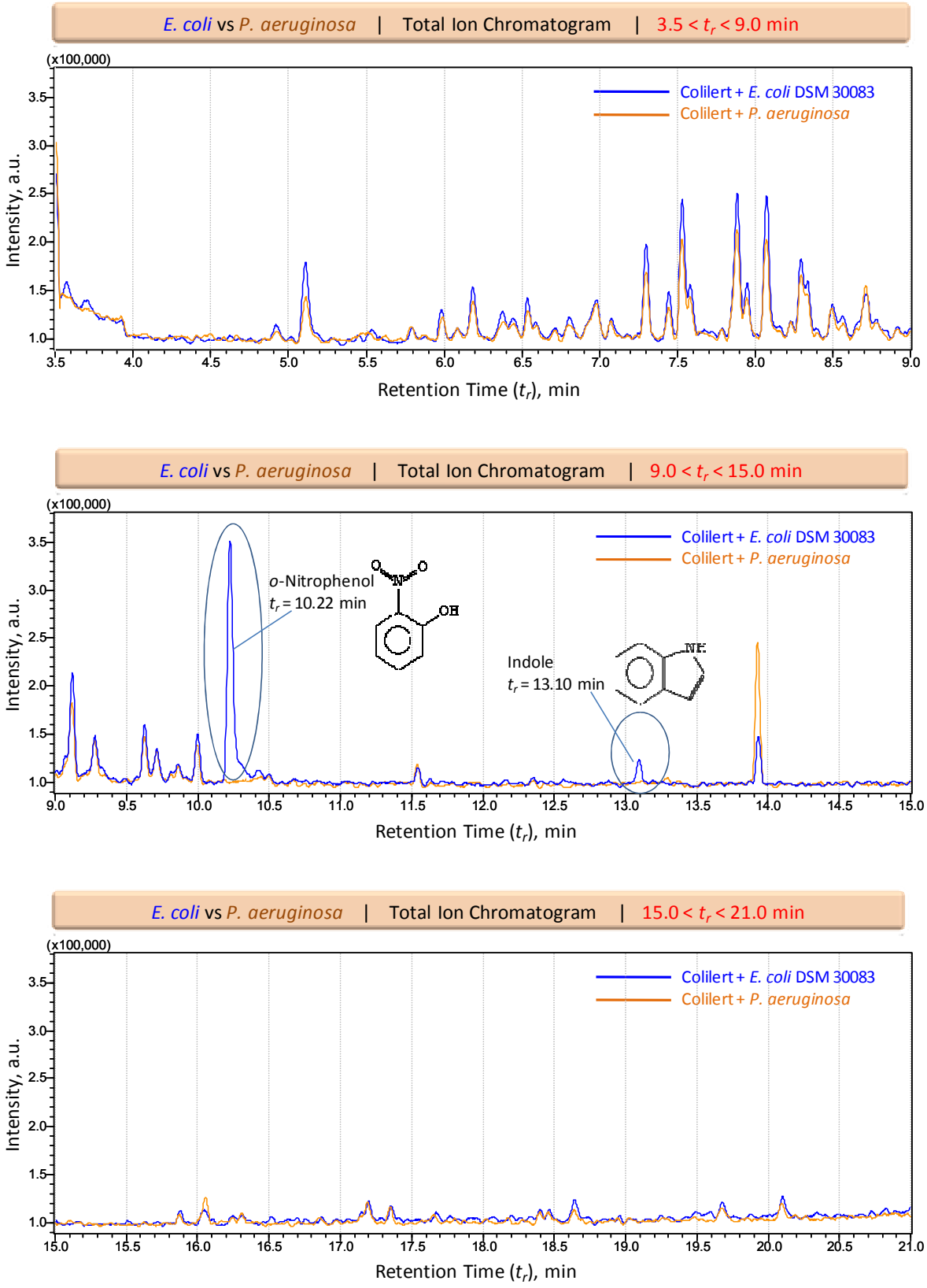

Figure 45. GC-MS spectra of *E. coli* DSM 30083 in compared with *P. aeruginosa*

As can be seen in the above figures (Figure 40 - Figure 45), characteristics of the GC-MS spectra of the bacterial metabolites are as follow:

1) Spectra of the bacteria versus the medium itself (Colilert-18®):

a) *E. coli* culture released many volatile metabolites, but most of them were produced by the medium itself (as shown by Figure 40, middle frame); the peaks that are unique to *E. coli* alone are *o*-nitrophenol ($t_r = 10.22\,min$) and indole ($t_r = 13.10\,min$).

b) As shown by Figure 41 (middle frame), in compared to the medium spectrum, the compound which was uniquely produced by *K. pneumoniae* alone was *o*-nitrophenol ($t_r = 10.22\,min$); indole compound was not observed.

c) *P. aeruginosa* did not produce any biomarker or any compounds which could be distinguished from the compounds produced by Colilert-18® itself (Figure 42).

2) Spectra of different strains of *E. coli*:

Three types of *E. coli* (DSM 1576, DSM 30083, and RV) which were prepared and incubated in the same way and with the same initial cells concentration were analyzed. As shown by Figure 43, all *E. coli* produced *o*-nitrophenol ($t_r = 10.22\,min$) and a relatively smaller amount of indole ($t_r = 13.10\,min$). The GC-MS spectra revealed no other biomarkers produced by the three *E. coli* strains. A more quantitative result on the intensity of *o*-nitrophenol is given in the GC-DMS section.

3) Spectra of coliform bacteria compared with each other:

Spectra of metabolites of *E. coli* and *K. pneumoniae* were compared with each other and given in Figure 44. Both coliforms produced *o*-nitrophenol, but *K. pneumoniae* did not produce indole (Figure 44, middle frame). This means, if headspace gases of a water sample in Colilert-18® were analyzed by GC-MS and *o*-nitrophenol was detected but indole was not, it is quite likely that the water sample contained coliform bacteria which were not *E. coli*. However, if both *o*-nitrophenol and indole were detected, it cannot immediately be said that there are other bacteria besides *E. coli*.

4) Spectra of coliform bacteria in compared with a non-coliform bacteria:

Spectra of metabolites of *E. coli* and *P. aeruginosa* are compared with each other (Figure 45). Unlike *E. coli*, *P. aeruginosa* did not produce any *o*-nitrophenol and indole, or any other unique compounds. This means, using GC-MS spectra data alone, if there are both *E. coli* and *P. aeruginosa* in water sample, only *E. coli* would be detected. The presence or absence of *P. aeruginosa* cannot be confirmed (in case the media is Colilert-18®).

5.3.2 GC-DMS spectra of the bacterial metabolites

GC-DMS spectra of different bacteria (*E. coli* DSM 30083, *E. coli* DSM 1576, *E. coli* RV, *K. pneumoniae,* and *P. aeruginosa*) which were grown in Colilert-18® and GC-DMS spectra of the blank medium itself (Colilert-18® without bacteria) are given in Figure 46 - Figure 51. Each figure consists of:

- **Top frame**: 2D spectra showing the locations of the compensation voltage and retention time of the analyte signal;
- **Middle frame**: Plots of signal intensity against compensation voltage at a specific retention time where signal was detected; the raw plot is given in blue, whereas the Gaussian function fitted to the plot is given in red;
- **Bottom frame**: 3D spectra showing signal intensity of the peak and its location in the compensation voltage and retention time coordinates;

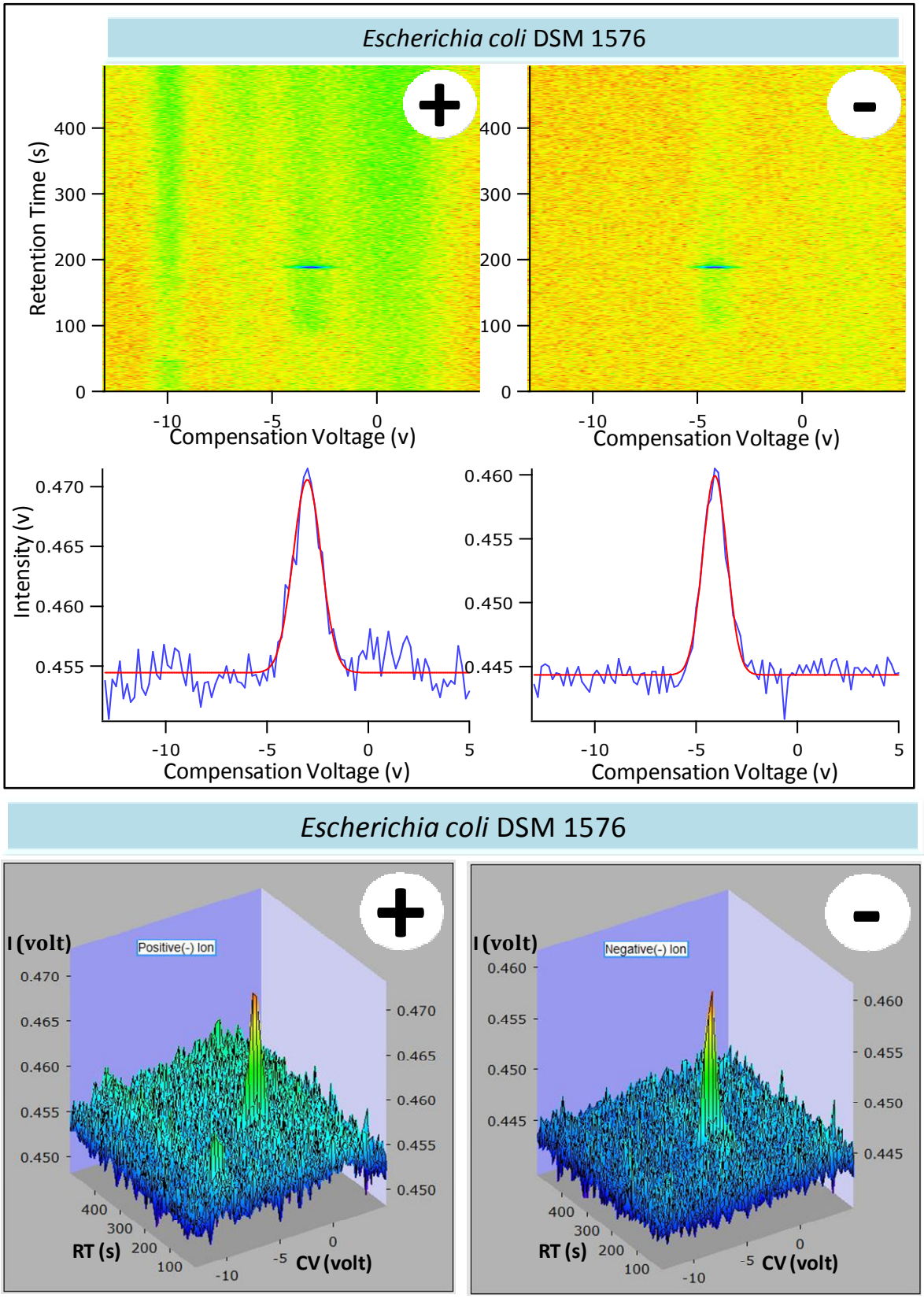

Figure 46. GC-DMS spectra of volatile metabolites released by *E. coli* DSM 1576 showing the presence of *o*-Nitrophenol (ONP) peaks in positive and negative modes

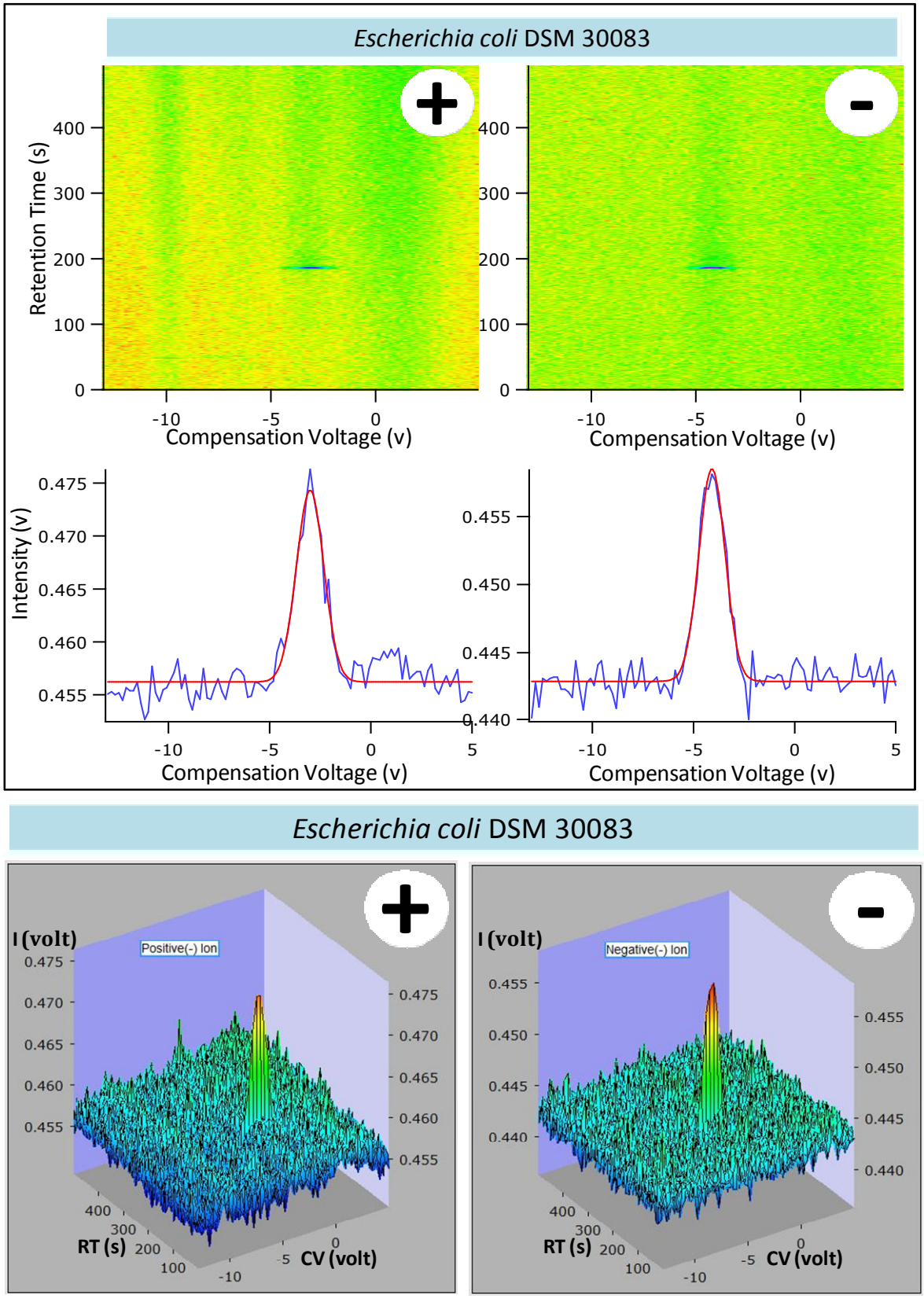

Figure 47. GC-DMS spectra of volatile metabolites released by *E. coli* DSM 30083 showing the presence of *o*-Nitrophenol (ONP) peaks in positive and negative modes

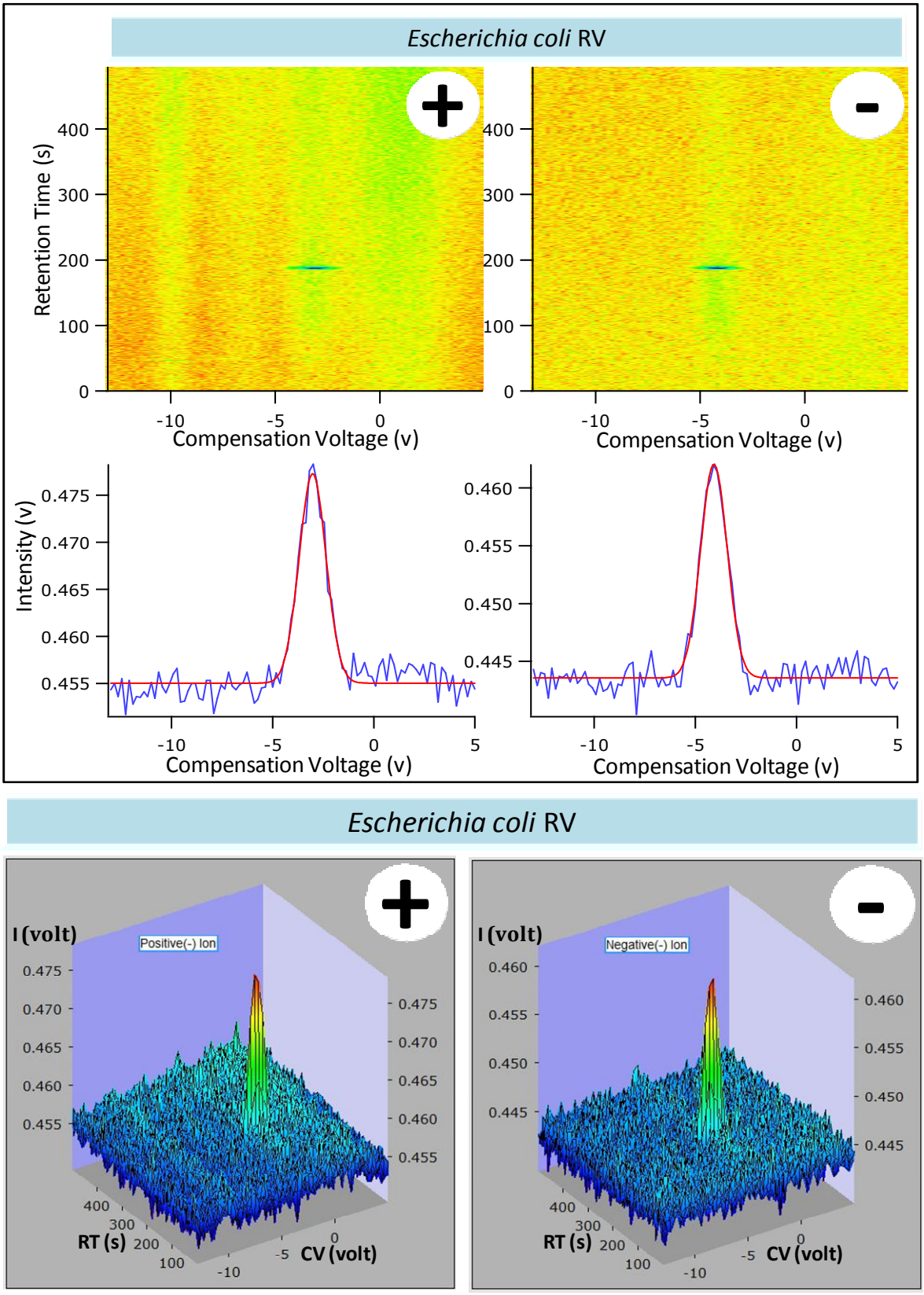

Figure 48. GC-DMS spectra of volatile metabolites released by *E. coli* RV showing the presence of *o*-Nitrophenol (ONP) peaks in positive and negative modes

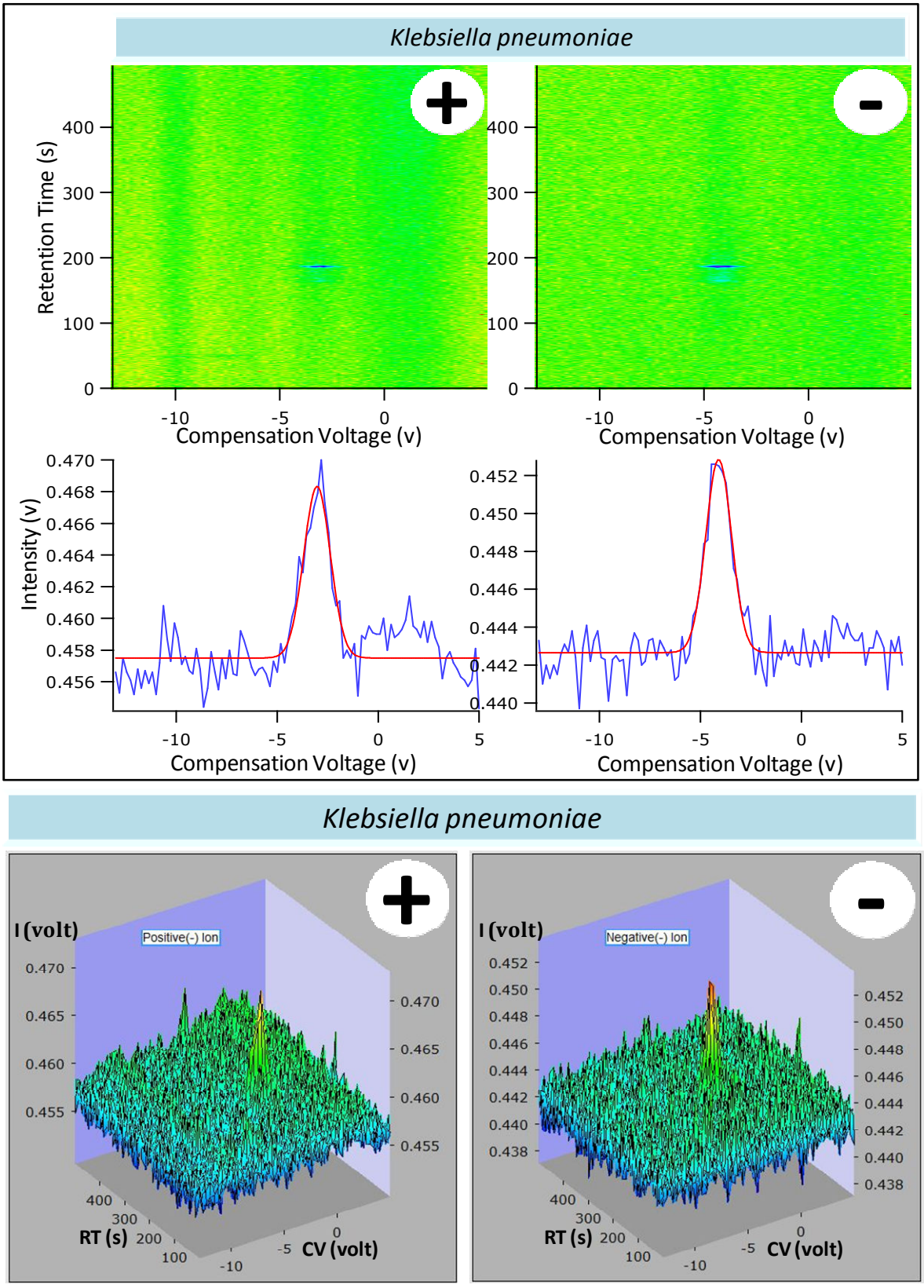

Figure 49. GC-DMS spectra of volatile metabolites released by *K. pneumoniae* showing the presence of *o*-Nitrophenol (ONP) peaks in positive and negative modes

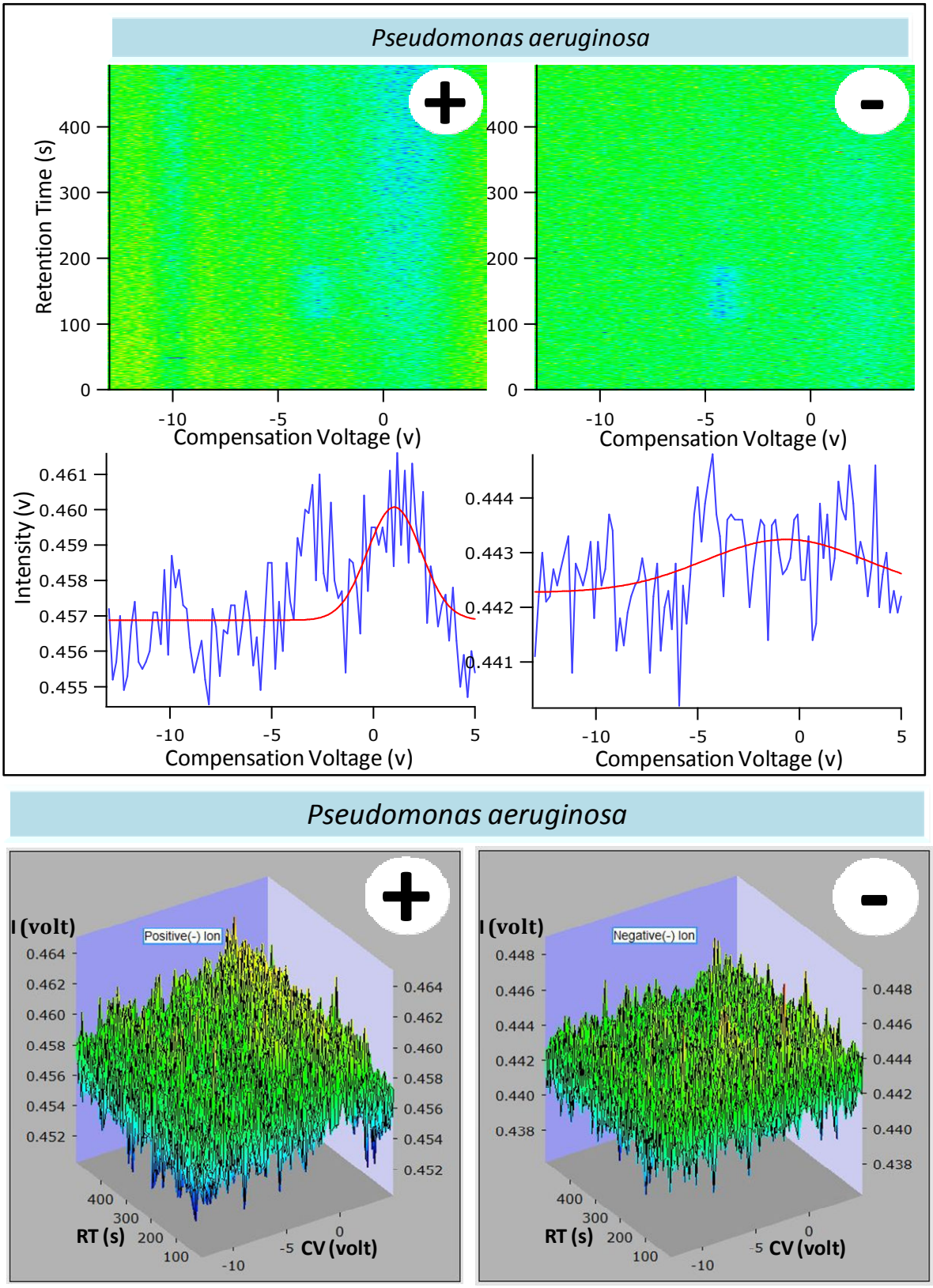

Figure 50. GC-DMS spectra of volatile metabolites released by *P. aeruginosa* showing the absence of *o*-Nitrophenol (ONP) in positive and negative modes

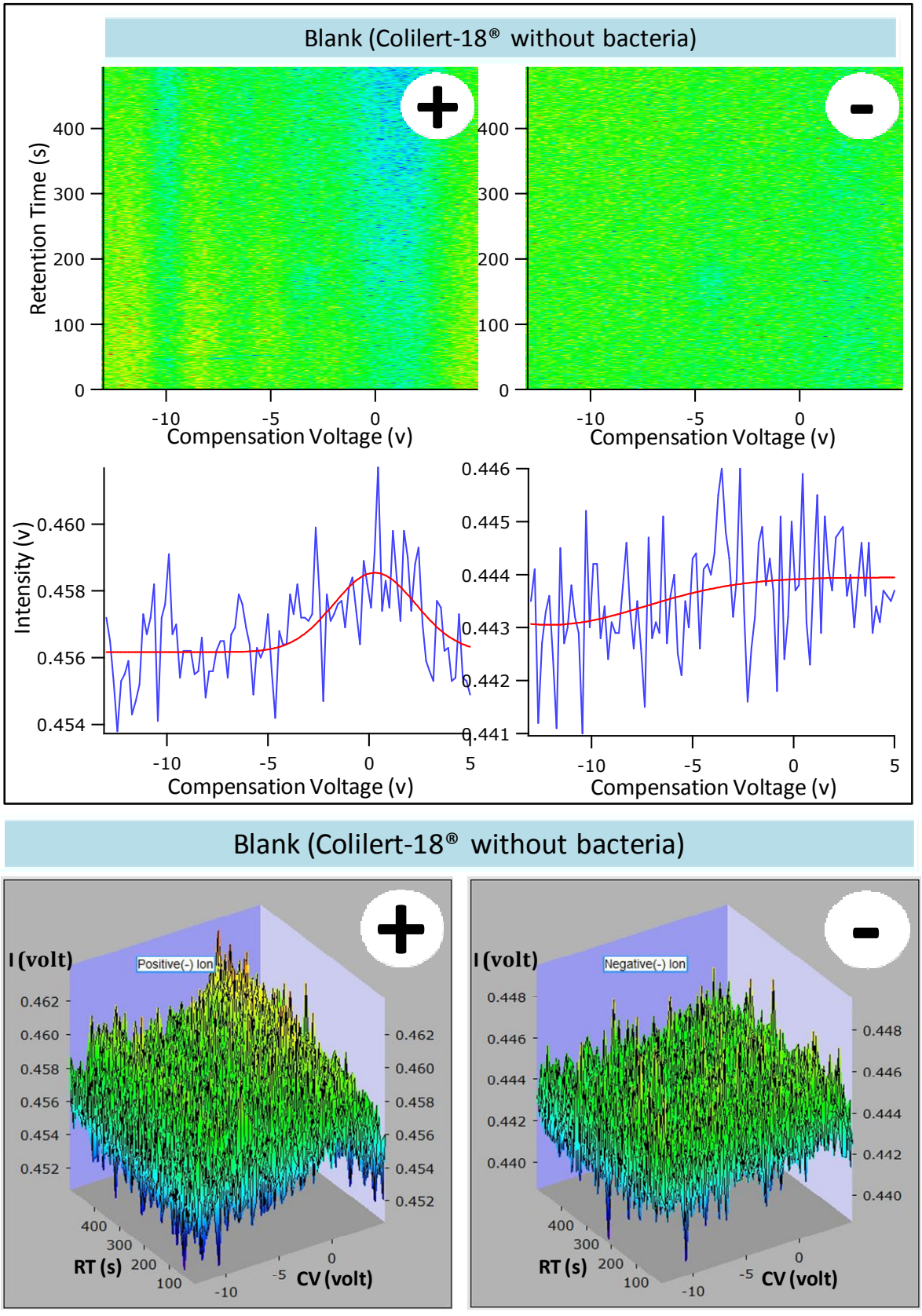

Figure 51. GC-DMS spectra of <u>blank medium (Colilert-18®)</u> showing the <u>absence</u> of *o*-Nitrophenol (ONP) in positive and negative modes

The following phenomena can be observed in the above figures:

- All *Escherichia coli* produced a similar amount of *o*-nitrophenol (ONP) at retention time $185\ s$ and compensation voltage $-2.82\ V$ (in the positive mode) and $-4.09\ V$ (in the negative mode), as shown by Figure 46, Figure 47, and Figure 48
- *Klebsiella pneumoniae* also produced ONP (as shown by Figure 49), but with relatively lower intensity than ONPs produced by *E. coli,* as can be better displayed by the 3D spectra
- *Pseudomonas aeruginosa* did not produce any biomarkers (Figure 50); the GC-DMS spectra of *P. aeruginosa* is similar to that of the blank medium (Figure 51)

These results are comparable to the GC-MS results which were presented in the earlier section, with an exception of the absence of indole signal in the GC-DMS spectra. The absence of indole has been discussed in detailed in Chapter 2.

The presence/ absence of ONP in the above results confirm the activation of β- galactosidase enzyme in *Escherichia* and *Klebsiella* (both belong to the Enterobacteriaceae family) in the presence of ONPG substrate. ONPG substrate allows the growth of favorable organisms and restricts the non-favorable organisms, hence an effective approach in the differentiation of coliform bacteria. Unlike Enterobacteriaceae, *P. aeruginosa* (which belongs to the Pseudomonadaceae family) is characterized by the presence of β-Lactamase enzymes (such as AmpC beta-lactamase, extended spectrum beta-lactamase (ESBL) and metallo beta-lactamase (MBL)) [177, 178].

A closer look at the **final** cells concentration (concentration **after incubation**) also supported the above findings. After $3\ h$ incubation, the final cell concentrations of all coliform bacteria were higher than the initial concentrations (Figure 52 below). The final cell concentration of *P. aeruginosa* was lower than its initial concentration. The values of cells concentration shown in the ordinate are the **logarithmic values** of final cells concentration.

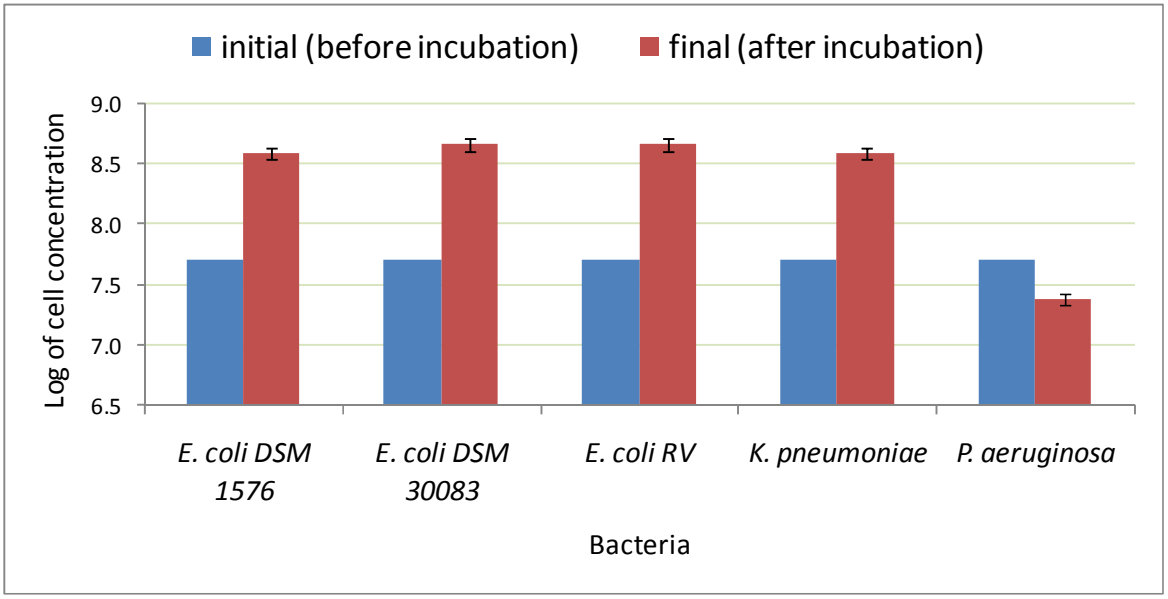

Figure 52. Initial (5×10^7 $cells/ml$) and final cell concentrations of coliform and non-coliform bacteria after $3h$ of incubation at $36\ ^oC$ in Colilert-18®

5.4 Conclusions

The differentiation of coliform and non-coliform bacteria using the proposed method has been successfully applied in this section. The method was able to distinguish *E. coli* DSM 30083, *E. coli* DSM 1576 and *E. coli* RV from *P. aeruginosa* (a non-coliform). After $3\ h$ of incubation in Colilert-18®, all *E. coli* produced *o*-nitrophenol (ONP) which could be detected by the miniaturized GC-DMS; their final cell concentrations were also increased. On the other hand, *P. aeruginosa* did not produce any biomarkers; its final cells concentration was also lower than its initial cells concentration. From this result, it can be concluded that *E. coli* could be distinguished from non-coliform bacterium based on the presence/absence of ONP detected by the GC-DMS and based on their final concentrations.

This work also shows that *E. coli* could not be easily distinguished from *K. pneumoniae* (another coliform). Although signal intensity of ONP produced by *E. coli* is relatively higher than *K. pneumoniae*, they produced the same biomarker and their final concentration is similar. To distinguish *E. coli* from *K. pneumoniae,* GC-MS analysis is recommended, because indole produced by *E. coli* (but not produced by *K. pneumoniae*) could not be detected by GC-DMS, but could be detected by GC-MS.

6 Development of an early warning system for the detection of coliform bacteria using miniaturized GC-DMS

6.1 Introduction

Regular monitoring of fecal contamination in surface water that has direct and indirect relevance to public health is a necessary practice. Many studies have reported that failure in detection of fecal contaminants in a timely manner often causes severe outbreaks of waterborne diseases [1, 10, 179-183]. For this reason, preventive and imperative actions in detecting and identifying the source of fecal contamination are necessary.

To transfer the method outlined in the previous chapters into a practical application, such as to understand the effect of seasonal temperature variation, the effect of incubation temperature is assessed in this chapter. In this work, coliform bacteria were grown at $10, 20$ and $36\ ℃$ in Colilert-18® and the headspace gases were analyzed using the miniaturized GC-DMS. Study by Prasad et al. (2007) has shown an example of effect of bacterial growth temperature on the production of biomarkers. In that study, the authors used pyrolysis-GC-DMS (py-GC-DMS) to analyze *E. coli, P. aeruginosa, S. warneri* and *M. luteus* grown at temperatures of $23, 30,$ and $37\ ℃$. It was found that the temperature dependent components comprised 84% of all peaks in the py-GC-DMS analysis of *E. coli* and were attributed to the pyrolytic decomposition of proteins rather than lipids [132].

The overall result from this chapter and all previous chapters were summarized into an algorithm on how to detect and identify coliform and *E. coli* in water sample using the developed method in a practical application. An example of such algorithm has been introduced by Bastholm et al. (2008). The authors proposed a simple bioluminescence procedure for early warning detection of coliform bacteria in drinking water [184]. The study by Bastholm et al. (2008) claimed an analysis time of 6 to $8\ h$ which is among the fastest reported methods. Unlike in that study, in which isopropyl-β-D-thiogalactopyranoside (IPTG) substrate was used to induce the acitivity of β-D-galactosidase activity in coliform bacteria,

this work was done based on the hydrolysis of Ortho-Nitrophenyl-β-D-galactopyranoside (ONPG) substrate to induce the activity of the same enzyme in coliform.

6.2 Experimental Section

6.2.1 Reagents and Samples

6.2.1.1 Bacteria

E. coli DSM 30083 was purchased from the Deutsche Sammlung von Mikroorganismen und Zellkulturen GmbH (Braunschweig, Germany). Prior to use, the bacteria was grown on 2 plates of NB agar and incubated overnight at $37\ ^{o}C$.

6.2.1.2 Growth Media

One package of Colilert-18® (IDEXX) was used in this experiment. The package was dissolved in $100\ ml$ of sterile deionized water as per manufacturer's instruction.

6.2.2 Instrumentation

The experimental setup consisted of a miniaturized GC-DMS (microAnalyzer™ from the Sionex, USA) connected to a nitrogen gas supply. The operational principle of the microAnalyzer has been described in the earlier chapter. The same experimental setup was applied in this work without modifications.

6.2.3 Procedures

6.2.3.1 Sample Preparation

Into each RG tube containing 10 ml of deionized water, two plates of bacteria colonies which were previously grown out of single colonies were inoculated. The suspensions were shaken for $10\ s$ and out of them a series of dilution ($10, 100$, and 1000 times) were prepared. The cell concentrations were then counted using Thoma counting chamber.

6.2.3.2 Determination of the Effect of Incubation Temperature

To determine the effect of incubation temperature on the micro-DMX signal intensity of the biomarker, the incubation temperature was varied. Samples of *E.* coli in Colilert-18® (each $10\ ml$ with the initial concentration of $5 \times 10^{7}\ cells/ml$) were incubated for $3\ h$ at $10, 20,$

and $36\ ℃$. The samples were then analyzed using miniaturized GC-DMS and were immediately stored at $4\ ℃$ after each incubation, to be prepared for cell counting. For each analysis, the procedure was made in triplicate.

6.2.3.3 Headspace Sampling and Analysis

Headspace of volatile metabolites of *E. coli* inside every sample vial was collected using a $500 \mu l$ gas-tight syringe (Hamilton, USA). The syringe was injected at a depth of $1\ cm$ above the sample suspension. The volume of each headspace sample was $500 \mu l$. The samples were injected into the instrument for a differential mobility spectra analysis and into GC-MS for the confirmation of the compounds identity. The compensation voltages and retention times recorded in the DMS analysis were compared to that of their standard solutions which were calibrated earlier.

6.2.4 Data Analysis

The differential mobility spectra data produced by the miniaturized GC-DMS which were recorded in the positive and negative modes were analyzed using IGOR Pro 6.

6.3 Results and Discussion

6.3.1 Effect of Incubation Temperature

To understand the effect of seasonal variation in practical application, a series of $10\ ml$ of *E. coli* samples which were grown in Colilert-18® with initial concentration of $5 \times 10^7\ cells/ml$ were incubated for $3\ h$ at $10, 20$ and $36\ ℃$ and the headspace gases were analyzed using the miniaturized GC-DMS. It was observed that the incubation at 10 and $20\ ℃$ produced much lower signal intensity of *o*-nitrophenol and much lower final cells concentrations than that incubated at $36\ ℃$ (Figure 53).

This result is especially important in deciding the type of procedure suitable for on-site monitoring. Since the result is greatly affected by temperature variation, it is necessary for the samples to be always preheated (incubated) at $36\ ℃$ prior to GC-DMS analysis.

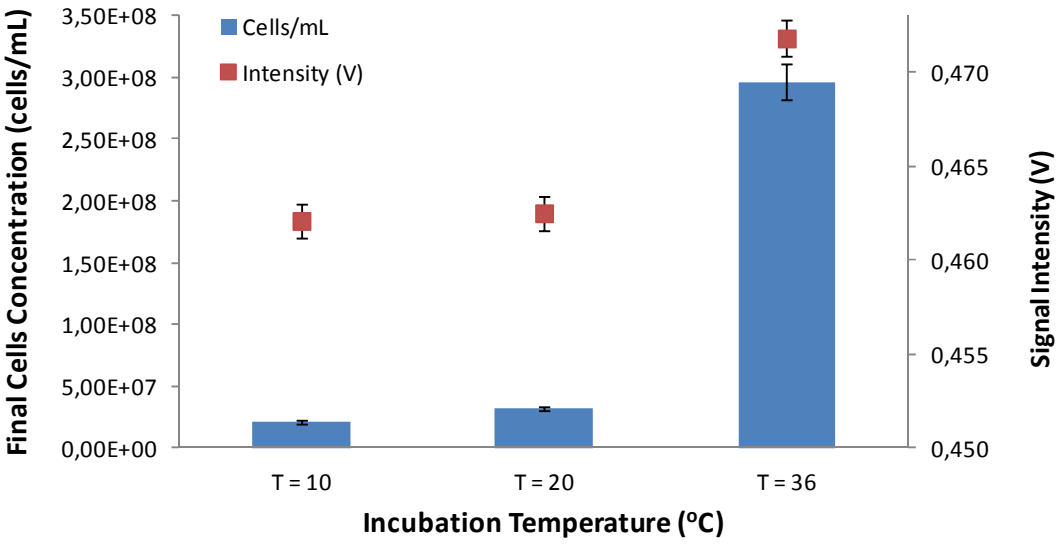

Figure 53. Effect of incubation temperature on cells growth and the correspond signal intensity

6.3.2 Algorithm for an Early Warning Detection of *E. coli* and Coliform in Water

Before formulating a simple algorithm for an early warning detection of the target organisms, a couple of results obtained in the whole research work detailed in the previous chapters will be first highlighted here:

- In reference to the results in **Chapter 4 ~ Section 4.3.6** (*Detection of E. coli in water sample collected from lake and river*), it was found that the developed method could not detect *E. coli* bacteria in the lake and river water samples (due to the concentration of *E. coli* being lower than the detection limit of the instrument). Although the sample collection area were not necessarily polluted (and certainly not experiencing an outbreak), there is a need to improve the detection limit of this method so that it would be at least comparable to the standard method such as Quanti-Tray method which was also used in that work for comparative purpose and was able to detect the presence of the bacteria. As a recommendation here, membrane filtration method (such as that included in the *ISO 9308-1:2012: " Water quality - Enumeration of Escherichia coli and coliform bacteria - Part 1: Membrane filtration method for waters with low bacterial background flora*" [39]) should be combined with the developed method. The objective is to enrich the amount of

bacteria in the water samples (to concentrate the bacteria via membrane filtration) so that the initial concentration of bacteria prior to incubation could be increased, allowing better detection by the GC-DMS. However, mechanical filtration using membrane filter technique has several limitations. As have been summarized in **Chapter 1 ~ Section 1.3.3.1.2** (*Membrane filter technique*), although membrane filter (MF) technique enables the examination of larger volumes of water, which leads to greater sensitivity and reliability, and also relatively simple to do, MF can cause coliform bacteria to be stressed or injured [45, 46]. In this work, it is important for *E. coli* and coliform to be as fit as possible, allowing them to grow optimally and to produce *o*-nitrophenol. Therefore, more studies needed.

- In reference to the results in **Chapter 4 ~ Section 4.3.3** (*Determination of cleavage opening period*), it was found that the cleavage opening period was $2.5\ h$. However, as can be seen in the profile of *E. coli* growth and the amount of ONP released by *E. coli*, ONP produced at $2.5\ h$ after incubation was understandably the minimum amount. Therefore, for a better detection and quantitation, it is recommended that the incubation period is extended, but should be maintained short enough, in order to enable early detection.

Based on the above consideration and the overall results, a simple algorithm for an early warning detection of *E. coli* and coliform in water sample was developed and the result is presented in Figure 54.

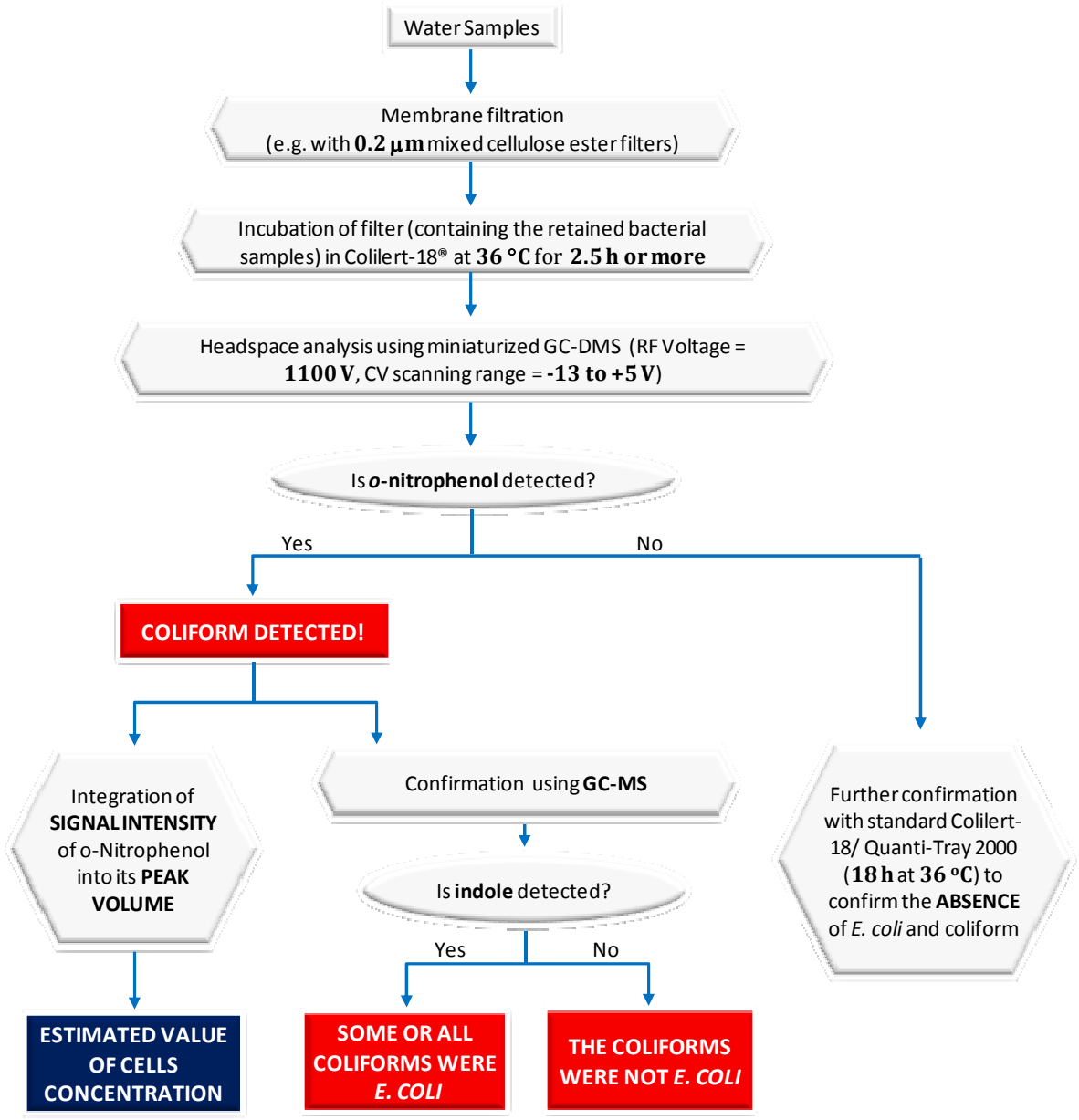

Figure 54. Algorithm for early warning detection and identification of *E. coli* and coliforms using the miniaturized GC-DMS

The developed algorithm outlined in Figure 54 can be explained in more detail as follow:

1. Collect water samples (1 L of samples will give a 100 concentration factor). Prepare for triplicate analysis.

2. Apply membrane filter technique by filtering the water sample through 0.2 μm bacterial filter using a portable membrane filtration system.

3. Place the filter material in a $20\,ml$ headspace vial containing $10\,ml$ Colilert-18® suspension (made from a mix of $100\,ml$ pure water with 1 pack of Colilert-18® powder). Prepare in triplicate.
4. Cap the sample vials and incubate for $2.5\,h$ at $36\,℃$ in a water heater system.
5. Collect $500\,\mu l$ headspace gases using a $500\,\mu l$ gas tight syringe.
6. Inject the headspace gases into the miniaturized GC-DMS system.
7. If a signal is detected at a retention time of approximately $184.9\,s$ and compensation voltages of approximately $-2.92\,V$ and $-4.10\,V$ (in positive and negative modes, respectively), the presence of *o*-nitrophenol, and hence, coliform, is confirmed. This means an early warning should be issued.
8. If no *o*-nitrophenol is detected, return to step #5 every 30 minutes. For an optimum result, the headspace gases should be taken from new sample vials (which are incubated together initially but for a longer period of incubation, and which has not lost any headspace gases).
9. If *o*-nitrophenol is finally detected, integrate the signal intensity into peak volume, and estimate the final cells concentration.
10. To confirm the presence of *E. coli*, validate the coliform identity using GC-MS and confirm the presence/absence of *E. coli* from the presence/absence of indole.
11. If neither *E. coli* nor other coliform detected, confirm the absence using standard Colilert-18®/Quanti-Tray method.

6.4 Conclusions

Seasonal variation such as the difference in ambient temperature was found to affect significantly the bacterial growth and the intensity of the released *o*-nitrophenol, as expected. In this study, it was observed for optimum and controlled growth, the sample should be preheated/ incubated at $36\,℃$ prior to the detection by GC-DMS. This means, in practical application, the instrument must be equipped by a sample preheating device/

incubator. An algorithm for early warning detection and identification of *E. coli* and coliforms using the miniaturized GC-DMS based in the overall research work has been developed.

7 General conclusions and outlook

Detection and identification of coliform and *E. coli* was done successfully by means of enzymatic approach using defined substrate technology in conjugation with headspace analysis of bacterial metabolite using miniaturized GC-DMS. The following results were concluded from the overall work:

1. Upon the GC-DMS analysis of 12 known *E. coli* metabolite compounds which were prepared from standard solutions in water, it was found that detection and identification of *E. coli* is not suitable to be done via "finger-print" recognition of the 12 compounds because 3 of the 12 compounds (2-undecanone, indole, and 2-tridecanone which have relatively low volatility) were not detectable by GC-DMS under the proposed experimental setting.

2. Upon the RF voltage study of the other 9 of the 12 compounds (2,5-dimethyltetrahydrofuran, dimethyl disulfide, 2-heptanone, 2,5-dimethylpyrazine, benzaldehyde, dimethyl trisulfide, 2-nonanone, nonanal, and decanal) it was found that the optimum RF voltage was a trade-off between signals separation and signals intensities. The optimum RF voltage for those compounds was found to be $1200\ V\ (24\ kV/cm)$.

3. In the examination of five types of growth media commonly used to grow *E. coli* (Colilert-18®, glucose broth, M9-medium, tryptic soy broth (TSB) and tryptophan broth), it was found that, unlike in other media, *E. coli* grown in Colilert-18® could produce *o*-nitrophenol (ONP), a unique biomarker which was an indicator of the presence/absence of β- Galactosidase enzyme (which characterizes the presence/absence of coliform bacteria including *E. coli*) and which was detectable by the GC-DMS. For this reason, Colilert-18® was chosen to be a suitable growth media.

4. The developed method was not able to detect the presence/absence of methylumbelliferone, and therefore could not confirm the presence/absence of β-Glucuronidase enzyme, which is specific only to *E. coli* in the coliform group. To confirm the presence/absence of methylumbelliferone, conventional method (the viewing of the samples under a $365\ nm$, $6\ Watt$ fluorescent UV lamp to reveal the

blue fluorescence effect of methylumbelliferone) is necessary. Alternatively, a GC-MS analysis for absence/presence of indole could be done.

5. The developed method in this work permits a very specific and rapid detection of coliform within just $2.5\ h$, approximately $7 - 9$ faster than the analysis time needed by standard Colilert-18® test. This was because after just $2.5\ h$ of incubation, *o*-nitrophenol was already produced and GC-DMS was able to detect a very small amount of *o*-nitrophenol. Using DIN 32645 method, detection limits of $45.11\ nanogram$ and $48.85\ nanogram$ were obtained for *o*-nitrophenol, each for the positive and the negative channels of the detector, respectively.

6. Headspace analysis of *E. coli* samples using GC-DMS at RF Voltage $1100\ V$ gave DMS spectra of *o*-nitrophenol signal at a retention time of $t_r = 184.9\ s$ and compensation voltages of $C_{v,1} = -2.82\ V$ (in the positive mode) and $C_{v,2} = -4.09\ V$ (in the negative mode).

7. Calibration of initial concentration of *E. coli* (concentration level before *E. coli* was incubated for $2.5\ h$ at $36\ {}^{o}C$) against signal intensity and the subsequent calculation of detection limit using DIN 32645 method gave detection limits of $3.37 \times 10^7$and $3.21 \times 10^7 cells/ml$, each for the positive and negative ion channels, respectively.

8. Further work was done to investigate the performance of the miniaturized GC-DMS in differentiation of bacteria. Using 5 different bacteria (*E. coli* DSM 30083, *E. coli* DSM 1576, *E. coli* RV, *K. pneumonia* and *P. aeruginosa*), it was found that the developed method was able to distinguish *E. coli* from *P. aeruginosa* (a non-coliform bacterium), but not easily distinguish *E. coli* from *K. pneumonia* (another coliform bacterium). This is especially important to note because, in practical application, specific and accurate information on types of microbial water contaminants would determine the specific action to be taken by the authority in charge for water quality monitoring or handling outbreaks.

9. Upon the variation of incubation temperatures, it was found that the incubation temperature affected greatly the cells concentration and, hence, the signal intensity of *o*-nitrophenol. Therefore, to anticipate the effect of seasonal variation in practical

application, the sample should be preheated (incubated) at $36\ ^{o}C$ before the headspace is analyzed by the GC-DMS.

10. An algorithm to detect and identify coliform and *E. coli* based on the developed method has been presented.

11. The developed method has a main limitation: as stated earlier, under the current instrumental and operational setting, the detection limits of *E. coli* are in the range of 3.37×10^{7} and $3.21 \times 10^{7} cells/ml$ (for the positive and negative modes, respectively), which are too high compared to standard method such as Quanti-Tray/2000. Such values were obtained for *E. coli* which were incubated for $2.5\ h$. Since the final cells concentration increases with incubation period, the minimum initial cell concentration could be decreased if the incubation period is increased, but this will outweigh the benefit of fast response. An alternative in improving the detection is by enriching the bacteria through membrane filtration technique in combined with the developed method. Another possibility is by employing better sample extraction methods. Such methods, however, should be in accordance with the overall objective of the work, i.e. a fast, efficient, and practical for on-site analysis.

8 Appendix

8.1 List of publications

Papers

1. **Saptalena, L. G.,** Kerpen, K., Kuklya, A., and Telgheder, U. (**2012**), Rapid detection of synthetic biomarkers of *Escherichia coli* in water using microAnalyzer™: a field dependence study. International Journal for Ion Mobility Spectrometry **15**(2):47-53, DOI 10.1007/s12127-011-0087-4

2. Ribbe, L., Kretschmer, N., **Saptalena, L. G.**, Oyarzún, R., Atenas, M., Meza, F., and Salgado, E. (**2008**). Monitoring to Support Water Quality Management in North-Central Chile. In IWRA World Water Congress. p. 13.

Posters

1. **Saptalena, L. G.** and Telgheder, U. (**2012**). Rapid detection of coliform bacteria using differential mobility spectrometry based on the presence of *o*-nitrophenol. Poster presented at the „127. GDNAE-Versammlung: Mobilität, Kommunikation und Interaktion“, Göttingen, September 14-18, 2012

2. **Saptalena, L. G.** and Telgheder, U. (**2012**). Rapid detection of *Escherichia coli* using differential mobility spectrometry based on the presence of *o*-nitrophenol. Poster presented at the „4th EuCheMS Chemistry Congress“, Prague, August 26-30, 2012

3. **Saptalena, L. G.** and Telgheder, U. (**2011**). MicroAnalyzer^{TM} for Characterization of Volatile Metabolites of Fecal Contaminants in Water Sample. Poster presented at the „Jahrestagung der GDCh - Fachgruppe Analytische Chemie - ANAKON 2011“ conference, Zurich, March 22-25, 2011

4. **Saptalena, L. G.**, Telgheder, U., and Schmidt, T. C. (**2011**). Rapid detection of *Escherichia coli* in water samples using microAnalyzer^{TM}. Poster presented at the

„Jahrestagung der Wasserchemischen Gesellschaft - WASSER 2011“ conference, Norderney, May 30 – June 1, 2011 ***(with Award for the Best Poster)***

5. **Saptalena, L. G.** and Telgheder, U. (**2010**). Determination of Volatile Metabolites of Fecal Contaminants in Water Samples by Differential Mobility Spectrometry. Poster presented at the “International Postgraduate Studies in Water Technologies – IPSWaT 2010” annual meeting, Leipzig, July 7-9, 2010

Presentation

1. **Saptalena, L. G.** and Telgheder, U. (**2010**). Determination of Volatile Metabolites of Fecal Contaminants in Water Samples by Differential Mobility Spectrometry. Presentation at the “International Postgraduate Studies in Water Technologies – IPSWaT 2010” annual meeting, Leipzig, July 7-9, 2010

8.2 Curriculum vitae

Name	:	Lena Ganda SAPTALENA
Date of birth	:	December 1978
Place of birth	:	Bandung, Indonesia
Nationality	:	Indonesian
Contact	:	lenasaptalena@gmail.com

Education and Selected (Full-time) Work Experience:

- **Since 03.2009**
  PhD Candidate at *the University of Duisburg-Essen*, Germany
  Major: Instrumental Analytical Chemistry
  Degree to obtain: *Dr. rer. nat*
  Funding: IPSWaT scholarship from BMBF Germany

- **09.2006 – 08.2008**
  Master study at *the Institute for Technology and Resources Management in the Tropics and Subtropics, Cologne University of Applied Sciences*, Germany
  Major: Integrated Water Resource Management
  Degree obtained: Master of Science
  Funding: IPSWaT scholarship from BMBF Germany

- **08.2004 – 06.2006**
  Chemical Process Engineer at *PT Keihin Indonesia*, Bekasi, Indonesia

- **10.2001 – 06.2004**
  Research Staff at *Membrane Research Center – PPAU Bioteknologi ITB*, Bandung, Indonesia

- **07.2001 – 09.2001**
  IT Staff at *PT Pintu Mas Mulia Kimia*, Jakarta, Indonesia

- **08.1996 – 02.2001**
  Bachelor study at *Institut Teknologi Bandung (ITB)*, Bandung, Indonesia
  Major: Chemical Engineering
  Degree obtained: Bachelor of Engineering

8.3 Erklärung

Hiermit versichere ich, dass ich die vorliegende Arbeit mit dem Titel

„Determination of Volatile Metabolites of Fecal Contaminants in Water Samples by Differential Mobility Spectrometry"

selbst verfasst und keine anderen, außer den angegebenen Hilfsmitteln und Quellen benutzt habe, und dass die Arbeit in dieser oder ähnlicher Form noch bei keiner anderen Universität eingereicht wurde.

Essen, 29.01.2014

Lena Ganda SAPTALENA

8.4 References

[1] ECDC. Rapid risk assessment update: Outbreak of Shiga toxin-producing *E. coli* (STEC) O104:H4 2011 in the EU, 8 July 2011. European Centre for Disease Prevention and Control 2011;Technical Report:July 12th.

[2] Rompré A, Servais P, Baudart J, De-Roubin MR, Laurent P. Detection and enumeration of coliforms in drinking water: Current methods and emerging approaches. Journal of Microbiological Methods 2002;49:31.

[3] Schulz S, Dickschat JS. Bacterial volatiles: The smell of small organisms. Natural Product Reports 2007;24:814.

[4] Shnayderman M, Mansfield B, Yip P, Clark HA, Krebs MD, Cohen SJ, Zeskind JE, Ryan ET, Dorkin HL, Callahan MV, Stair TO, Gelfand JA, Gill CJ, Hitt B, Davis CE. Species-specific bacteria identification using differential mobility spectrometry and bioinformatics pattern recognition. Analytical Chemistry 2005;77:5930.

[5] Maddula S, Blank LM, Schmid A, Baumbach JI. Detection of volatile metabolites of Escherichia coli by multi capillary column coupled ion mobility spectrometry. Analytical and Bioanalytical Chemistry 2009;394:791.

[6] Yu K, Hamilton-Kemp TR, Archbold DD, Collins RW, Newman MC. Volatile compounds from Escherichia coli O157:H7 and their absorption by strawberry fruit. Journal of Agricultural and Food Chemistry 2000;48:413.

[7] Zechman JM, Aldinger S, Labows Jr JN. Characterization of pathogenic bacteria by automated headspace concentration-gas chromatography. Journal of Chromatography - Biomedical Applications 1986;VOL. 377:49.

[8] Labows JN, McGinley KJ, Webster GF, Leyden JJ. Headspace analysis of volatile metabolites of Pseudomonas aeruginosa and related species by gas chromatography-mass spectrometry. Journal of Clinical Microbiology 1980;12:521.

[9] Henis Y, Gould JR, Alexander M. Detection and identification of bacteria by gas chromatography. Applied microbiology 1966;14:513.

[10] Saptalena LG, Kerpen K, Kuklya A, Telgheder U. Rapid detection of synthetic biomarkers of Escherichia coli in water using microAnalyzer: A field dependence study. International Journal for Ion Mobility Spectrometry 2012;15:47.

[11] Sionex. Sionex Introduces the microAnalyzer, Trace Chemical Detector System. http://www.sionex.com/products/downloads/SIONEX-Introduces-the-microAnalyzer.pdf. *Accessed 15 Mar 2010* 2008; Technical Literature, Oct. 15, 2008.

[12] Buryakov IA, Krylov EV, Nazarov EG, Rasulev UK. A new method of separation of multi-atomic ions by mobility at atmospheric pressure using a high-frequency amplitude-asymmetric strong electric field. International Journal of Mass Spectrometry and Ion Processes 1993;128:143.

[13] Eiceman GA, Krylov EV, Krylova NS, Nazarov EG, Miller RA. Separation of ions from explosives in differential mobility spectrometry by vapor-modified drift gas. Analytical Chemistry 2004;76:4937.

[14] Lu Y, Chen P, Harrington PB. Comparison of differential mobility spectrometry and mass spectrometry for gas chromatographic detection of ignitable liquids from fire debris using projected difference resolution. Analytical and Bioanalytical Chemistry 2009;394:2061.

[15] Eiceman GA, Krylov EV, Tadjikov B, Ewing RG, Nazarov EG, Miller RA. Differential mobility spectrometry of chlorocarbons with a micro-fabricated drift tube. Analyst 2004;129:297.

[16] Eiceman GA, Nazarov EG, Tadjikov B, Miller RA. Monitoring Volatile Organic Compounds in Ambient Air inside and outside Buildings with the Use of a Radio-Frequency-Based Ion-Mobility Analyzer with a Micromachined Drift Tube. Field Analytical Chemistry and Technology 2000;4:297.

[17] Krebs MD, Zapata AM, Nazarov EG, Miller RA, Costa IS, Sonenshein AL, Davis CE. Detection of biological and chemical agents using Differential Mobility Spectrometry (DMS) technology. IEEE Sensors Journal 2005;5:696.

[18] Nelis H, Van Poucke S. Enzymatic detection of coliforms and Escherichia coli within 4 hours. Water, Air, and Soil Pollution 2000;123:43.

[19] Geldreich EE. Coliforms and *E. coli*. Problem or Solution? . The Royal Society of Chemistry, Cambridge 1997:218.

[20] Allen MA, Edberg SC. Coliforms and *E. coli*. Problem or Solution? . The Royal Society of Chemistry, Cambridge 1997:176.

[21] Edberg SC, Rice EW, Karlin RJ, Allen MJ. Escherichia coli: the best biological drinking water indicator for public health protection. Symposium series (Society for Applied Microbiology) 2000:106S.

[22] Hofstra H, Huis in't Veld JHJ. Methods for the detection and isoltion of Escherichia coli including pathogenic strains. Journal of Applied Bacteriology Symposium Supplement 1988:197S.

[23] APHA, AWWA, AEF. Standard Methods for the Examination of Water and Wastewater, 20th edn. Washington, DC. 1998.

[24] AFNOR. Eaux méthodes d'essais. Recueil de Normes Françaises, 4th edn. la Défense, Paris, 735 pp. 1990.

[25] Bernasconi C, Volponi G, Bonadonna L. Comparison of three different media for the detection of E. coli and coliforms in water. Water Science and Technology 2006;54:141.

[26] Leclerc H, Mossel DA, Edberg SC, Struijk CB. Advances in the bacteriology of the coliform group: their suitability as markers of microbial water safety. Ann. Rev. Microbiol. 2001;55 201.

[27] Al-Turki, El-Ziney MG. Evaluation of Commercial Colilert18-Quantitray® Method by ISO Techniques for Enumeration and Quantification of Total Coliforms and Escherichia coli in Drinking-Water of Buraidah, Saudi Arabia. . Journal of Applied Sciences 2009;9 3357.

[28] Chröst RJ. Microbial Enzymes in Aquatic Environments. Springer-Verlag, New York 1991:317

[29] Feng PCS, Hartman PA. Fluorogenic assays for immediate confirmation of *Escherichia coli*. Applied and Environmental Microbiology 1982;43:1320.

[30] Killian M, Bulow P. Rapid diagnosis of enterobacteriaceae: I. Detection of bacterial glycosidases. Acta Pathologica et Microbiologica Scandinavica - Section B Microbiology and Immunology 1976;84:245.

[31] DVGW. Verordnung zur Novellierung der Trinkwasserverordnung vom 21. Mai 2001. 2003. p.Appendix 2.

[32] US-EPA. Total coliform rule and surface water treatment rules. Federal Regulations. Government Printing Office, Washington, DC. 1990.

[33] WHO. Guidelines for Drinking Water Quality, 2nd edn. World Health Organisation, Geneva. 1994.

[34] UN-Water. World Water Day 2012: Facts and Figures. 2012.

[35] Ayers RS, Westcot DW. Water quality for agriculture. FAO, Irrig Drain Paper 29 Revision 1 1994.

[36] Law LP. Agricultural utilization of sewage effluent and sludge: An annotated bibliography. Federal Water Pollution Control Federation, 1968.

[37] FBR. FBR - Information Sheet H 201: Greywater Recycling Planning fundamentals and operation information. 2005.

[38] DIN. DIN 19650, Ausgabe: 1999-02. Bewässerung - Hygienische Belange von Bewässerungswasser. 1999.

[39] ISO. ISO 9308-1:2012: Water quality - Enumeration of Escherichia coli and coliform bacteria - Part 1: Membrane filtration method for waters with low bacterial background flora. 2012.

[40] ISO. ISO 9308-2:2012: Water quality - Enumeration of Escherichia coli and coliform bacteria - Part 2: Most probable number method. 2012.

[41] Eaton AD, Clesceri LS, Greenberg AE. Standard Methods for the Examination of Water and Wastewater. 2005;American Public Health Association, USA.

[42] McFeters GA, Cameron SC, LeChevallier MW. Influence of diluents, media, and membrane filters on detection of injured waterborne coliform bacteria. Applied and Environmental Microbiology 1982;43:97.

[43] Rice EW, Fox KR, Nash HD, Read EJ, Smith AP. Comparison of media for recovery of total coliform bacteria from chemically treated water. Appl. Environ. Microbiol. 1987;53:1571.

[44] Grabow WOK, du Preez M. Comparison of m-Endo LES, MacConkey, and Teepol media for membrane filtration counting of total coliform bacteria in water. Appl. Environ. Microbiol. 1979;38:351.

[45] Burlingame GA, McElhaney J, Bennett M, Pipes WO. Bacterial interference with coliform colony sheen production on membrane filters. Appl. Environ. Microbiol. 1984;47:56.

[46] Clark JA. The influence of increasing numbers of non-indicator organisms by the membrane filter and presence– absence test. Can. J. Microbiol. 1980;26:827.

[47] LeChevallier MW, Cameron SC, McFeters GA. New medium for improved recovery of coliform bacteria from drinking water. Appl. Environ. Microbiol. 1983;45:484.

[48] Adams JC, Lytle MS, Dickman DG, Foster DH, Connell JP, Bressler WR. Comparison of methods for enumeration of selected coliforms exposed to ozone. Appl. Environ. Microbiol. 1989;55:33.

[49] Sartory DP. Improved recovery of chlorine-stressed coliforms with pyruvate supplemented media. Water Sci. Technol. 1995;31:255.

[50] Calabrese JP, Bissonnette GK. Improved membrane filtration method incorporating catalase and sodium pyruvate for detection of chlorine-stressed coliform bacteria. Appl. Environ. Microbiol. 1990;56:3558.

[51] Kaspar CW, Hartman PA, Benson AK. Coagglutination and enzyme capture tests for detection of *Escherichia coli* β-galactosidase, β-glucuronidase, and glutamate decarboxylase. Applied and Environmental Microbiology 1987;53:1073.

[52] Edberg SC, Kontnick CM. Comparison of β-glucuronidase-based substrate systems for identification of *Escherichia coli*. Journal of Clinical Microbiology 1986;24:368.

[53] Chang GW, Brill J, Lum R. Proportion of β-D-glucuronidase-negative *Escherichia coli* in human fecal samples. Applied and Environmental Microbiology 1989;55:335.

[54] Frampton EW, Restaino L. Methods for Escherichia coli identification in food, water and clinical samples based on beta-glucuronidase detection. Journal of Applied Bacteriology 1993;74:223.

[55] Massanti MF, Scarlata G, Nastasi A. β-Glucuronidase activity in Enterobacteriaceae. Boll. Ist. Sieroter. Milan 1981;60:26.

[56] Manafi M, Kneifel W, Bascomb S. Fluorogenic and chromogenic substrates used in bacterial diagnostics. Microbiological Reviews 1991;55:335.

[57] Dahlen G, Linde A. Screening plate method for detection of bacterial β–glucuronidase. Journal of Applied Microbiology 1973;26:863.

[58] Brenner KP, Rankin CC, Roybal YR, Stelma Jr GN, Scarpino PV, Dufour AP. New medium for the simultaneous detection of total coliforms and Escherichia coli in water. Applied and Environmental Microbiology 1993;59:3534.

[59] Bulte M, Reuter G. Glucuronidase- and indol-capillary test as a reliable rapid identification method for determinatin of *E. coli* in foods - Toxinogenic strains included (Glucuronidase-nachweis und Indol-kapillartest als Zuverlassige Schnellidentifizierungsverfahren zur erfassung von *E. coli* in Lebensmitteln - Toxinogene Stamme eingeschlossen). Zentralbl. Hygiene B 1989;188:284.

[60] Watkins WD, Rippey SR, Clavet CR, Kelley-Reitz DJ, Burkhardt Iii W. Novel compound for identifying Escherichia coli. Applied and Environmental Microbiology 1988;54:1874.

[61] Bürger H. Biochemische leistungen nichtprofilierender mikrooraganismen: II. Nachweis von glycosid-hydrolasen, phosphatasen, esterasen und lipasen. Zentralbl. Bakteriol. Abt. Orig. B 1967;202:97.

[62] Ley A, Barr S, Fredenburgh D, Taylor M, Walker N. Use of 5-bromo-4-chloro-3-indolyl-β-D-galactopyranoside for the isolation of β-galactosidase-positive bacteria from municipal water supplies. Canadian Journal of Microbiology 1993;39:821.

[63] Seong Joo P, Lee EJ, Lee DH, Lee SH, Kim SJ. Spectrofluorometric assay for rapid detection of total and fecal coliforms from surface water. Applied and Environmental Microbiology 1995;61:2027.

[64] Apte SC, Davies CM, Peterson SM. Rapid detection of faecal coliforms in sewage using a colorimetric assay of β-D-galactosidase. Water Research 1995;29:1803.

[65] Standridge JH, Kluender SM, Bernhardt M. Spectrophotometric enhancement of MMO-MUG (Colilert) endpoint determination. Proceedings of AWWA-Water Quality Technology Conference, Toronto, Ontario. American Water Works Association. 1992.

[66] Edberg SC, Edberg MM. A defined substrate technology for the enumeration of microbial indicators of environmental pollution. Yale Journal of Biology and Medicine 1988;61:389.

[67] Rice EW, Allen MJ, Brenner DJ, Edberg SC. Assay for β-glucuronidase in species of the genus Escherichia and its applications for drinking-water analysis. Applied and Environmental Microbiology 1991;57:592.

[68] Rice EW, Allen MJ, Edberg SC. Efficacy of β-glucuronidase assay for identification of Escherichia coli by the defined-substrate technology. Applied and Environmental Microbiology 1990;56:1203.

[69] Clark DL, Milner BB, Stewart MH, Wolfe RL, Olson BH. Comparative study of commercial 4-methylumbelliferyl-β-D-glucuronide preparations with the Standard Methods membrane filtration fecal coliform test for the detection of Escherichia coli in water samples. Applied and Environmental Microbiology 1991;57:1528.

[70] Clark JA, El-Shaarawi AH. Evaluation of commercial presence-absence test kits for detection of total coliforms, Escherichia coli, and other indicator bacteria. Applied and Environmental Microbiology 1993;59:380.

[71] Colquhuon KO, Timms S, Fricker CR. Detection of E. coli in potable water using direct impedance technology J. Appl. Bacteriol. 1995;79:635.

[72] Edberg SC, Allen MJ, Smith DB. Rapid, specific autoanalytical method for the simultaneous detection of total coliforms and E. coli from drinking water. Water Science and Technology 1989;21:173.

[73] Edberg SC, Allen MJ, Smith DB, Kriz NJ. Enumeration of total coliforms and Escherichia coli from source water by the defined substrate technology. Applied and Environmental Microbiology 1990;56:366.

[74] Edberg SC, Allen MJ, Smith DB, LeChevallier M, Kriz N, Callan D, Ward R, Calver D, Jackson W, Uryc M, Storms C, Loriner J, Trok T, Burns M. National field evaluation of a defined substrate method for the simultaneous enumeration of total coliforms and Escherichia coli from drinking water: Comparison with the standard multiple tube fermentation method. Applied and Environmental Microbiology 1988;54:1595.

[75] Fricker EJ, Fricker CR. Use of two presence/absence systems for the detection of E. coli and coliforms from water. Water Res. 1996;30:2226.

[76] McCarty SC, Standridge JH, Stasiak MC. Evaluating a commercially available defined-substrate test for recovery of E. coli. Journal / American Water Works Association 1992;84:91.

[77] McFeters GA, Broadaway SC, Pyle BH, Egozy Y. Distribution of bacteria within operating laboratory water purification systems. Applied and Environmental Microbiology 1993;59:1410.

[78] Olson BH, Clark DL, Milner BB, Stewart MH, Wolfe RL. Total coliform detection in drinking water: Comparison of membrane filtration with Colilert and Coliquik. Applied and Environmental Microbiology 1991;57:1535.

[79] Palmer CJ, Tsai YL, Lang AL, Sangermano LR. Evaluation of Colilert-Marine Water for detection of total coliforms and Escherichia coli in the marine environment. Applied and Environmental Microbiology 1993;59:786.

[80] Fricker EJ, Illingworth KS, Fricker CR. Use of two formulations of Colilert and QuantiTray® for assessment of the bacteriological quality of water. Water Research 1997;31:2495.

[81] Eckner KF. Comparison of membrane filtration and multiple-tube fermentation by the Colilert and Enterolert methods for detection of waterborne coliform bacteria, Escherichia coli, and Enterococci used in drinking and bathing water quality monitoring in southern Sweden. Applied and Environmental Microbiology 1998;64:3079.

[82] McFeters G, Pickett M, Broadaway S, Pyle B. Impact of chlorine injury on reaction kinetics of coliforms and E. Coli in ColisureÂ® and LTB. In: Morris R, Grabow WOK, Jofre J,

editors. Water Science and Technology, vol. 35. Mallorca, Spain: Elsevier Science Ltd, 1997. p.419.

[83] McFeters GA, Broadaway SC, Pyle BH, Pickett M, Egozy Y. Comparative performance of Colisure. Journal / American Water Works Association 1997;89:112.

[84] Brenner KP, Rankin CC, Sivaganesan M, Scarping PV. Comparison of the recoveries of Escherichia coli and total coliforms from drinking water by the MI agar method and the U.S. Environmental Protection Agency-approved membrane filter method. Applied and Environmental Microbiology 1996;62:203.

[85] Ciebin BW, Brodsky MH, Eddington R, Horsnell G, Choney A, Palmateer G, Ley A, Joshi R, Shears G. Comparative evaluation of modified m-FC and m-TEC media for membrane filter enumeration of Escherichia coli in water. Applied and Environmental Microbiology 1995;61:3940.

[86] Gaudet ID, Florence LZ, Coleman RN. Evaluation of test media for routine monitoring of Escherichia coli in nonpotable waters. Applied and Environmental Microbiology 1996;62:4032.

[87] Grant MA. A new membrane filtration medium for simultaneous detection and enumeration of Escherichia coli and total coliforms. Applied and Environmental Microbiology 1997;63:3526.

[88] George I, Petit M, Servais P. Use of enzymatic methods for rapid enumeration of coliforms in freshwaters. Journal of Applied Microbiology 2000;88:404.

[89] Berg JD, Fiksdal L. Rapid detection of total and fecal coliforms in water by enzymatic hydrolysis of 4-methylumbelliferone-beta-D-galactoside. Applied and Environmental Microbiology 1988;54:2118.

[90] Davies CM, Long JAH, Donald M, Ashbolt NJ. Survival of fecal microorganisms in marine and freshwater sediments. Applied and Environmental Microbiology 1995;61:1888.

[91] Lisle JT, Hamilton MA, Willse AR, McFeters GA. Comparison of fluorescence microscopy and solid-phase cytometry methods for counting bacteria in water. Applied and Environmental Microbiology 2004;70:5343.

[92] Lisle JT, Smith JJ, Edwards DD, McFeters GA. Occurrence of microbial indicators and Clostridium perfringens in wastewater, water column samples, sediments, drinking water, and Weddell seal feces collected at McMurdo Station, Antarctica. Applied and Environmental Microbiology 2004;70:7269.

[93] Van Poucke SO, Nelis HJ. Solid phase cytometry-based enzymatic detection of coliforms in drinking water within 4 h. Water Supply 1999;17:67.

[94] Van Poucke SO, Nelis HJ. Rapid detection of fluorescent and chemiluminescent total coliforms and Escherichia coli on membrane filters. Journal of Microbiological Methods 2000;42:233.

[95] Van Poucke SO, Nelis HJ. A 210-min solid phase cytometry test for the enumeration of Escherichia coli in drinking water. Journal of Applied Microbiology 2000;89:390.

[96] Kfir R, Genthe B. Advantages and disadvantages of the use of immunodetection techniques for the enumeration of microorganisms and toxins in water. Water Science and Technology 1993;27:243.

[97] Hanai K, Satake M, Nakanishi H, Venkateswaran K. Comparison of commercially available kits with standard methods for detection of Salmonella strains in foods. Applied and Environmental Microbiology 1997;63:775.

[98] Jin M, Lang J, Shen ZQ, Chen ZL, Qiu ZG, Wang XW, Li JW. A rapid subtractive immunization method to prepare discriminatory monoclonal antibodies for food E. coli o157:H7 contamination. PLoS ONE 2012;7.

[99] Kuo JT, Cheng CY, Huang HH, Tsao CF, Chung YC. A rapid method for the detection of representative coliforms in water samples: Polymerase chain reaction-enzyme-linked immunosorbent assay (PCR-ELISA). Journal of Industrial Microbiology and Biotechnology 2010;37:237.

[100] Levasseur S, Husson MO, Leitz R, Merlin F, Laurent F, Peladan F, Drocourt JL, Leclerc H, Van Hoegaerden M. Rapid detection of members of the family Enterobacteriaceae by a monoclonal antibody. Applied and Environmental Microbiology 1992;58:1524.

[101] Hubner I, Steinmetz I, Obst U, Giebel D, Bitter-Suermann D. Rapid determination of members of the family Enterobacteriaceae in drinking water by an immunological assay using a monoclonal antibody against enterobacterial common antigen. Applied and Environmental Microbiology 1992;58:3187.

[102] Rockabrand D, Austin T, Kaiser R, Blum P. Bacterial growth state distinguished by single-cell protein profiling: Does chlorination kill coliforms in municipal effluent? Applied and Environmental Microbiology 1999;65:4181.

[103] Zaccone R, Crisafi E, Caruso G. Evaluation of fecal pollution in coastal Italian waters by immunofluorescence. Aquatic Microbial Ecology 1995;9:79.

[104] Bej AK, McCarty SC, Atlas RM. Detection of coliform bacteria and Escherichia coli by multiplex polymerase chain reaction: Comparison with defined substrate and plating methods for water quality monitoring. Applied and Environmental Microbiology 1991;57:2429.

[105] Bej AK, Steffan RJ, DiCesare J, Haff L, Atlas RM. Detection of coliform bacteria in water by polymerase chain reaction and gene probes. Applied and Environmental Microbiology 1990;56:307.

[106] Fricker EJ, Fricker CR. Application of the polymerase chain reaction to the identification of Escherichia coli and coliforms in water. Letters in Applied Microbiology 1994;19:44.

[107] Iqbal S, Robinson J, Deere D, Saunders JR, Edwards C, Porter J. Efficiency of the polymerase chain reaction amplification of the fluid gene for detection of Escherichia coli in contaminated water. Letters in Applied Microbiology 1997;24:498.

[108] Juck D, Ingram J, Prévost M, Coallier J, Greer C. Nested PCR protocol for the rapid detection of Escherichia coli in potable water. Canadian Journal of Microbiology 1996;42:862.

[109] Heid CA, Stevens J, Livak KJ, Williams PM. Real time quantitative PCR Genome Res. 1996; 6:1986.

[110] Olsen GJ, Lane DJ, Giovannoni SJ, Pace NR, Stahl DA. Microbial ecology and evolution: a ribosomal RNA approach. Annual Review of Microbiology 1986;40:337.

[111] Maidak BL, Olsen GJ, Larsen N, Overbeek R, McCaughey MJ, Woese CR. The Ribosomal Database Project (RDP). Nucleic Acids Research 1996;24:82.

[112] Benson DA, Boguski MS, Lipman DJ, Ostell J, Ouellette BFF, Rapp BA, Wheeler DL. GenBank. Nucleic Acids Research 1999;27:12.

[113] Richardson KJ, Stewart MH, Wolfe RL. Application of gene probe technology to the water industry. Journal / American Water Works Association 1991;83:71.

[114] Fuchs BM, Wallner G, Beisker W, Schwippl I, Ludwig W, Amann R. Flow cytometric analysis of the in situ accessibility of Escherichia coli 16S rRNA for fluorescently labeled oligonucleotide probes. Applied and Environmental Microbiology 1998;64:4973.

[115] Amann RI, Ludwig W, Schleifer KH. Phylogenetic identification and in situ detection of individual microbial cells without cultivation. Microbiological Reviews 1995;59:143.

[116] Lebaron P, Catala P, Fajon C, Joux F, Baudart J, Bernard L. A new sensitive, whole-cell hybridization technique for detection of bacteria involving a biotinylated oligonucleotide probe targeting rRNA and tyramide signal amplification. Applied and Environmental Microbiology 1997;63:3274.

[117] Schönhuber W, Fuchs B, Juretschko S, Amann R. Improved sensitivity of whole-cell hybridization by the combination of horseradish peroxidase-labeled oligonucleotides and tyramide signal amplification. Applied and Environmental Microbiology 1997;63:3268.

[118] Cheung W, Xu Y, Thomas CLP, Goodacre R. Discrimination of bacteria using pyrolysis-gas chromatography-differential mobility spectrometry (Py-GC-DMS) and chemometrics. Analyst 2009;134:557.

[119] Dworzanski JP, Tripathi A, Snyder AP, Maswdeh WM, Wick CH. Novel biomarkers for Gram-type differentiation of bacteria by pyrolysis-gas chromatography-mass spectrometry. Journal of Analytical and Applied Pyrolysis 2005;73:29.

[120] Ellis DI, Broadhurst D, Kell DB, Rowland JJ, Goodacre R. Rapid and quantitative detection of the microbial spoilage of meat by fourier transform infrared spectroscopy and machine learning. Applied and Environmental Microbiology 2002;68:2822.

[121] Goodacre R, Shann B, Gilbert RJ, Timmins ÃM, McGovern AC, Alsberg BK, Kell DB, Logan NA. Detection of the dipicolinic acid biomarker in Bacillus spores using curie-point pyrolysis mass spectrometry and fourier transform infrared spectroscopy. Analytical Chemistry 2000;72:119.

[122] Jarvis R, Clarke S, Goodacre R. Rapid analysis of microbiological systems using SERS. In: Kneipp K, Kneipp H, Moskovits M, editors. Topics in Applied Physics, vol. 103, 2006. p.397.

[123] Snyder AP, Dworzanski JP, Tripathi A, Maswadeh WM, Wick CH. Correlation of mass spectrometry identified bacterial biomarkers from a fielded pyrolysis-gas chromatography-ion mobility spectrometry biodetector with the microbiological gram stain classification scheme. Analytical Chemistry 2004;76:6492.

[124] Oyama VI. Use of gas chromatography for the detection of life on Mars. Nature 1963;200:1058.

[125] Cundy KV, Willard KE, Valeri LJ, Shanholtzer CJ, Singh J, Peterson LR. Comparison of traditional gas chromatography (GC), headspace GC, and the microbial identification library GC system for the identification of Clostridium difficile. Journal of Clinical Microbiology 1991;29:260.

[126] Koek MM, Muilwijk B, Van Der Werf MJ, Hankemeier T. Microbial metabolomics with gas chromatography/mass spectrometry. Analytical Chemistry 2006;78:1272.

[127] Snyder AP, Shoff DB, Eiceman GA, Blyth DA, Parsons JA. Detection of bacteria by ion mobility spectrometry. Analytical Chemistry 1991;63:526.

[128] Snyder AP, Miller M, Shoff DB, Eiceman GA, Blyth DA, Parsons JA. Enzyme-substrate assay for the qualitative detection of microorganisms by ion mobility spectrometry. Journal of Microbiological Methods 1991;14:21.

[129] Ruzsanyi V, Baumbach JI, Sielemann S, Litterst P, Westhoff M, Freitag L. Detection of human metabolites using multi-capillary columns coupled to ion mobility spectrometers. Journal of Chromatography A 2005;1084:145.

[130] Ruzsanyi V, Sielemann S, Baumbach JI. Detection of sulfur-free odorants in natural gas using ion mobility spectrometry. Journal of Environmental Monitoring 2007;9:61.

[131] Prasad S, Pierce KM, Schmidt H, Rao JV, GÃ¼th R, Synovec RE, Smith GB, Eiceman GA. Constituents with independence from growth temperature for bacteria using pyrolysis-gas chromatography/differential mobility spectrometry with analysis of variance and principal component analysis. Analyst 2008;133:760.

[132] Prasad S, Pierce KM, Schmidt H, Rao JV, Güth R, Bader S, Synovec RE, Smith GB, Eiceman GA. Analysis of bacteria by pyrolysis gas chromatography-differential mobility spectrometry and isolation of chemical components with a dependence on growth temperature. Analyst 2007;132:1031.

[133] Prasad S, Schmidt H, Lampen P, Wang M, Güth R, Rao JV, Smith GB, Eiceman GA. Analysis of bacterial strains with pyrolysis-gas chromatography/ differential mobility spectrometry. Analyst 2006;131:1216.

[134] Rearden P, Harrington PB, Karnes JJ, Bunker CE. Fuzzy rule-building expert system classification of fuel using solid-phase microextraction two-way gas chromatography differential mobility spectrometric data. Analytical Chemistry 2007;79:1485.

[135] Schmidt H, Tadjimukhamedov F, Mohrenz IV, Smith GB, Eiceman GA. Microfabricated differential mobility spectrometry with pyrolysis gas chromatography for chemical characterization of bacteria. Analytical Chemistry 2004;76:5208.

[136] Basanta M, Singh D, Fowler S, Wilson I, Dennis R, Thomas CLP. Increasing analytical space in gas chromatography-differential mobility spectrometry with dispersion field amplitude programming. Journal of Chromatography A 2007;1173:129.

[137] Rearden P. Applications of Solid Phase Microextraction with Ion and Differential Mobility Spectrometry for the Study of Jet Fuels and Organophosphonates. Doctoral dissertation, Ohio State University, Columbus, OH, p. 124-141 2006.

[138] Krebs MD, Mansfield B, Yip P, Cohen SJ, Sonenshein AL, Hitt BA, Davis CE. Novel technology for rapid species-specific detection of Bacillus spores. Biomolecular Engineering 2006;23:119.

[139] Rearden P, Harrington PB. Detection of VOCs using gas chromatography differential mobility spectrometry (GC-DMS). Hyphenated Separations (as published in LabPlus international - February/March 2006) 2006.

[140] Shvartsburg AA. Differential Ion Mobility Spectrometry: Nonlinear Ion Transport and Fundamentals of FAIMS. Florida: CRC Press Taylor & Francis Group, 2009.

[141] Eiceman GA. Ion-mobility spectrometry as a fast monitor of chemical composition. TrAC - Trends in Analytical Chemistry 2002;21:259.

[142] Purves RW, Guevremont R. Electrospray ionization high-field asymmetric waveform ion mobility spectrometry-mass spectrometry. Analytical Chemistry 1999;71:2346.

[143] Eiceman G, Karpas Z. Ion Mobility Spectometry 1994.

[144] Mason EA, McDaniel EW. Transport Properties of Ions in Gases 1988.

[145] Krylov E, Nazarov EG, Miller RA, Tadjikov B, Eiceman GA. Field dependence of mobilities for gas-phase-protonated monomers and proton-bound dimers of ketones by planar field asymmetric waveform ion mobility spectrometer (PFAIMS). Journal of Physical Chemistry A 2002;106:5437.

[146] Borsdorf H, Eiceman GA. Ion mobility spectrometry: Principles and applications. Applied Spectroscopy Reviews 2006;41:323.

[147] Davis W. Faster, More Accurate Detection Through Differential Mobility Spectroscopy. Gases & Instrumentation, March/April 2009.

[148] Good A, Durden DA, Kebarle P. Ion-molecule reactions in pure nitrogen and nitrogen containing traces of water at total pressures 0.5-4 torr. Kinetics of clustering reactions forming H+(H2O)n. The Journal of Chemical Physics 1970;52:206.

[149] Bensch H. The RIP positions in dependence on the moisture. Int. J. Ion Mobility Spectrom. 2002;5:39.

[150] Munro WA, Paul Thomas CL, Langford ML. Characterisation of the ion mobility spectrometric behaviour of a dinitrobutane under varying conditions of temperature and concentration. Analytica Chimica Acta 1998;375:49.

[151] Eiceman GA, Nazarov EG, Rodriguez JE, Bergloff JF. Positive reactant ion chemistry for analytical, high temperature ion mobility spectrometry (IMS): Effects of electric field of the drift tube and moisture, temperature, and flow of the drift gas. Int. J. Ion Mobility Spectrom. 1998;1:28.

[152] Berant Z, Karpas Z, Shahal O. Effects of temperature and clustering on mobility of ions in CO2. Journal of Physical Chemistry 1989;93:7529.

[153] Lubman DM. Temperature dependence of plasma chromatography of aromatic hydrocarbons. Analytical ChemistryÂ® 1984;56:1298.

[154] Watts P. Studies on gas-phase negative ion/molecule reactions of relevance to ion mobility spectrometry: kinetic modelling of the reactions occuring in "clean" air. International Journal of Mass Spectrometry and Ion Processes 1992;121:141.

[155] Hayhurst CJ, Watts P, Wilders A. Studies on gas-phase negative ion/molecule reactions of relevance to ion mobility spectrometry: mass analysis and ion identification of the negative reactant ion peak in "clean" air. International Journal of Mass Spectrometry and Ion Processes 1992;121:127.

[156] Ellis HW, Eisele FL, McDaniel EW. Temperature dependent mobilities of negative ions in N2 and O2. The Journal of Chemical Physics 1978;69:4710.

[157] Spangler GE, Collins CI. Reactant ions in negative ion plasma chromatography. Analytical Chemistry 1975;47:393.

[158] Cravath AM. The rate of formation of negative ions by electron attachment. Physical Review 1929;33:605.

[159] Stach J. Ion mobility spectrometry. Analytiker Taschenbuch 1997;16:119.

[160] Krylova N, Krylov E, Eiceman GA, Stone JA. Effect of moisture on the field dependence of mobility for gas-phase ions of organophosphorus compounds at atmospheric pressure with field asymmetric ion mobility spectrometry. Journal of Physical Chemistry A 2003;107:3648.

[161] Sionex. microAnalyzer™ Series Product Manual S-400039 Revision A. Sionex corporation, USA 2005.

[162] TOXNET. Databases on toxicology, hazardous chemicals, environmental health, and toxic releases. http://toxnet.nlm.nih.gov/ [Retrieved 17.05.2013]. 2013.

[163] Arnold JW, Senter SD. Use of digital aroma technology and SPME GC-MS to compare volatile compounds produced by bacteria isolated from processed poultry. Journal of the Science of Food and Agriculture 1998;78:343.

[164] Marr AG, Ingraham JL, Squires CL. Effect of the temperature of growth of *Escherichia Coli* on the formation of β-Galactosidase. Journal of Bacteriology 1964;87:356.

[165] Arnold RJ, Karty JA, Ellington AD, Reilly JP. Monitoring the growth of a bacteria culture by MALDI-MS of whole cells. Analytical Chemistry 1999;71:1990.

[166] Gutteridge CS, Norris JR. Effect of different growth conditions on the discrimination of three bacteria by pyrolysis gas-liquid chromatography. Applied and Environmental Microbiology 1980;40:462.

[167] Atlas RM. Handbook of Microbiological Media, Fourth Edition, CRC Press , New York, USA. 2010.

[168] Linstrom PJ, Mallard WG. Eds., NIST Chemistry WebBook, NIST Standard Reference Database Number 69, National Institute of Standards and Technology, Gaithersburg MD, 20899, http://webbook.nist.gov, retrieved November 14,. 2012.

[169] Fujikawa H, Kai A, Morozumi S. A new logistic model for Escherichia coli growth at constant and dynamic temperatures. Food Microbiology 2004;21:501.

[170] Miller JH. Experiments in Molecular Genetics. Cold Spring Harbor Laboratory, Cold Spring Harbor, NY, pp. 352–355. 1972.

[171] Thibodeau SA, Fang R, Joung JK. High-throughput beta-galactosidase assay for bacterial cell-based reporter systems. . Biotechniques. 36(3):410-5. 2004.

[172] Stephenson FH. Calculations for Molecular Biology and Biotechnology: A Guide to Mathematics in the Laboratory. Academic Press, 2nd Edition, Elsevier 2010:388.

[173] Amagliani G, Parlani ML, Brandi G, Sebastianelli G, Stocchi V, Schiavano GF. Molecular detection of Pseudomonas aeruginosa in recreational water. International Journal of Environmental Health Research 2012;22:60.

[174] Casanovas-Massana A, Blanch AR. Characterization of microbial populations associated with natural swimming pools. International Journal of Hygiene and Environmental Health 2012.

[175] Lutz JK, Lee J. Prevalence and antimicrobial-resistance of pseudomonas aeruginosa in swimming pools and hot tubs. International Journal of Environmental Research and Public Health 2011;8:554.

[176] Rice SA, Van Den Akker B, Pomati F, Roser D. A risk assessment of Pseudomonas aeruginosa in swimming pools: A review. Journal of Water and Health 2012;10:181.

[177] Jiang X, Zhang Z, Li M, Zhou D, Ruan F, Lu Y. Detection of Extended-Spectrum β-Lactamases in Clinical Isolates of Pseudomonas aeruginosa. Antimicrobial agents and chemotherapy, Sept 2006, p. 2990–2995 Vol. 50, No. 9 2006.

[178] Upadhyay S, Sen MR, Bhattacharjee A. Presence of different beta-lactamase classes among clinical isolates of Pseudomonas aeruginosa expressing AmpC beta-lactamase enzyme. J Infect Dev Ctries 2010; 4(4):239-242 2010.

[179] Wiwanitkit V. Renal failure in the recent 2011 Escherichia coli O104:H4 Outbreak: A summary on up-to-date data. Renal Failure 2012;34:533.

[180] EFSA. Tracing seeds, in particular fenugreek (Trigonella foenum-graecum) seeds, in relation to the Shiga toxin-producing *E. coli* (STEC) O104:H4 2011 Outbreaks in Germany and France. European Food Safety Authority. 2011;Technical Report:July 5th.

[181] Gwack J, Lee KC, Lee HJ, Kwak W, Lee DW, Choi YH, Kim JS, Kang YA. Trends in Water- and Foodborne Disease Outbreaks in Korea, 2007-2009. Osong Public Health and Research Perspectives 2010;1:50.

[182] Guh A, Phan Q, Nelson R, Purviance K, Milardo E, Kinney S, Mshar P, Kasacek W, Cartter M. Outbreak of Escherichia coli O157 associated with raw milk, Connecticut, 2008. Clinical Infectious Diseases 2010;51:1411.

[183] Armstrong GL, Hollingsworth J, Morris Jr JG. *Emerging foodborne pathogens: Escherichia coli O157:H7 as a model of entry of a new pathogen into the food supply of the developed world*. Epidemiologic Reviews 1996;18:29.

[184] Bastholm S, Wahlstrøm L, Bjergbæk LA, Roslev P. A simple bioluminescence procedure for early warning detection of coliform bacteria in drinking water. World Journal of Microbiology and Biotechnology 2008;24:2323.